Development of a Precast Bent Cap System for Seismic Regions

DETAILS

106 pages | | PAPERBACK
ISBN 978-0-309-15533-5 | DOI 10.17226/14484

AUTHORS

Jose I Restrepo; Eric E Matsumoto; Matthew J Tobolski; Transportation Research Board

NATIONAL COOPERATIVE HIGHWAY RESEARCH PROGRAM

NCHRP REPORT 681

Development of a Precast Bent Cap System for Seismic Regions

José I. Restrepo
University of California, San Diego
La Jolla, CA

Matthew J. Tobolski
Tobolski | Watkins Engineering, Inc.
San Diego, CA

Eric E. Matsumoto
California State University, Sacramento
Sacramento, CA

Subscriber Categories
Highways • Bridges and Other Structures

Research sponsored by the American Association of State Highway and Transportation Officials
in cooperation with the Federal Highway Administration

TRANSPORTATION RESEARCH BOARD

WASHINGTON, D.C.
2011
www.TRB.org

NATIONAL COOPERATIVE HIGHWAY RESEARCH PROGRAM

Systematic, well-designed research provides the most effective approach to the solution of many problems facing highway administrators and engineers. Often, highway problems are of local interest and can best be studied by highway departments individually or in cooperation with their state universities and others. However, the accelerating growth of highway transportation develops increasingly complex problems of wide interest to highway authorities. These problems are best studied through a coordinated program of cooperative research.

In recognition of these needs, the highway administrators of the American Association of State Highway and Transportation Officials initiated in 1962 an objective national highway research program employing modern scientific techniques. This program is supported on a continuing basis by funds from participating member states of the Association and it receives the full cooperation and support of the Federal Highway Administration, United States Department of Transportation.

The Transportation Research Board of the National Academies was requested by the Association to administer the research program because of the Board's recognized objectivity and understanding of modern research practices. The Board is uniquely suited for this purpose as it maintains an extensive committee structure from which authorities on any highway transportation subject may be drawn; it possesses avenues of communications and cooperation with federal, state and local governmental agencies, universities, and industry; its relationship to the National Research Council is an insurance of objectivity; it maintains a full-time research correlation staff of specialists in highway transportation matters to bring the findings of research directly to those who are in a position to use them.

The program is developed on the basis of research needs identified by chief administrators of the highway and transportation departments and by committees of AASHTO. Each year, specific areas of research needs to be included in the program are proposed to the National Research Council and the Board by the American Association of State Highway and Transportation Officials. Research projects to fulfill these needs are defined by the Board, and qualified research agencies are selected from those that have submitted proposals. Administration and surveillance of research contracts are the responsibilities of the National Research Council and the Transportation Research Board.

The needs for highway research are many, and the National Cooperative Highway Research Program can make significant contributions to the solution of highway transportation problems of mutual concern to many responsible groups. The program, however, is intended to complement rather than to substitute for or duplicate other highway research programs.

NCHRP REPORT 681

Project 12-74
ISSN 0077-5614
ISBN 978-0-309-15533-5
Library of Congress Control Number 2010943434

COPYRIGHT INFORMATION

NOTICE

The project that is the subject of this report was a part of the National Cooperative Highway Research Program, conducted by the Transportation Research Board with the approval of the Governing Board of the National Research Council.

The members of the technical panel selected to monitor this project and to review this report were chosen for their special competencies and with regard for appropriate balance. The report was reviewed by the technical panel and accepted for publication according to procedures established and overseen by the Transportation Research Board and approved by the Governing Board of the National Research Council.

The opinions and conclusions expressed or implied in this report are those of the researchers who performed the research and are not necessarily those of the Transportation Research Board, the National Research Council, or the program sponsors.

The Transportation Research Board of the National Academies, the National Research Council, and the sponsors of the National Cooperative Highway Research Program do not endorse products or manufacturers. Trade or manufacturers' names appear herein solely because they are considered essential to the object of the report.

Published reports of the

NATIONAL COOPERATIVE HIGHWAY RESEARCH PROGRAM

are available from:

Transportation Research Board
Business Office
500 Fifth Street, NW
Washington, DC 20001

and can be ordered through the Internet at:

http://www.national-academies.org/trb/bookstore

Printed in the United States of America

THE NATIONAL ACADEMIES

Advisers to the Nation on Science, Engineering, and Medicine

The **National Academy of Sciences** is a private, nonprofit, self-perpetuating society of distinguished scholars engaged in scientific and engineering research, dedicated to the furtherance of science and technology and to their use for the general welfare. On the authority of the charter granted to it by the Congress in 1863, the Academy has a mandate that requires it to advise the federal government on scientific and technical matters. Dr. Ralph J. Cicerone is president of the National Academy of Sciences.

The **National Academy of Engineering** was established in 1964, under the charter of the National Academy of Sciences, as a parallel organization of outstanding engineers. It is autonomous in its administration and in the selection of its members, sharing with the National Academy of Sciences the responsibility for advising the federal government. The National Academy of Engineering also sponsors engineering programs aimed at meeting national needs, encourages education and research, and recognizes the superior achievements of engineers. Dr. Charles M. Vest is president of the National Academy of Engineering.

The **Institute of Medicine** was established in 1970 by the National Academy of Sciences to secure the services of eminent members of appropriate professions in the examination of policy matters pertaining to the health of the public. The Institute acts under the responsibility given to the National Academy of Sciences by its congressional charter to be an adviser to the federal government and, on its own initiative, to identify issues of medical care, research, and education. Dr. Harvey V. Fineberg is president of the Institute of Medicine.

The **National Research Council** was organized by the National Academy of Sciences in 1916 to associate the broad community of science and technology with the Academy's purposes of furthering knowledge and advising the federal government. Functioning in accordance with general policies determined by the Academy, the Council has become the principal operating agency of both the National Academy of Sciences and the National Academy of Engineering in providing services to the government, the public, and the scientific and engineering communities. The Council is administered jointly by both the Academies and the Institute of Medicine. Dr. Ralph J. Cicerone and Dr. Charles M. Vest are chair and vice chair, respectively, of the National Research Council.

The **Transportation Research Board** is one of six major divisions of the National Research Council. The mission of the Transportation Research Board is to provide leadership in transportation innovation and progress through research and information exchange, conducted within a setting that is objective, interdisciplinary, and multimodal. The Board's varied activities annually engage about 7,000 engineers, scientists, and other transportation researchers and practitioners from the public and private sectors and academia, all of whom contribute their expertise in the public interest. The program is supported by state transportation departments, federal agencies including the component administrations of the U.S. Department of Transportation, and other organizations and individuals interested in the development of transportation. **www.TRB.org**

www.national-academies.org

CRP STAFF FOR NCHRP REPORT 681

Christopher W. Jenks, *Director, Cooperative Research Programs*
Crawford F. Jencks, *Deputy Director, Cooperative Research Programs*
Waseem Dekelbab, *Senior Program Officer*
Danna Powell, *Senior Program Assistant*
Eileen P. Delaney, *Director of Publications*
Ellen M. Chafee, *Editor*

NCHRP PROJECT 12-74 PANEL
Field of Design—Area of Bridges

Richard A. Pratt, *Alaska DOT and Public Facilities, Juneau, AK* (Chair)
Xiaohua Hannah Cheng, *New Jersey DOT, Trenton, NJ*
Carl J. Fuselier, *Arkansas SHTD, Little Rock, AR*
Jim Ma, *California DOT, Sacramento, CA*
Richard Marchione, *New York State DOT, Albany, NY*
Chuck Prussack, *Central Pre-Mix Prestress Company, Spokane, WA*
Holly Winston, *Oregon DOT, Salem, OR*
Lloyd M. Wolf, *Texas DOT, Austin, TX*
Derrell A. Manceaux, *FHWA Liaison*
Stephen F. Maher, *TRB Liaison*

AUTHOR ACKNOWLEDGMENTS

The research reported herein was performed under NCHRP Project 12-74 by the Department of Structural Engineering at the University of California, San Diego (UCSD). Dr. José I. Restrepo, Professor of Structural Engineering at UCSD, was the Principal Investigator. Dr Eric E. Matsumoto, P.E., from California State University, Sacramento (CSUS), was the Co-Principal Investigator. The other author of this report is Dr. Matthew J. Tobolski, P.E., former graduate researcher at UCSD and current President of Tobolski Watkins Engineering, Inc.

Other invaluable members of the research team include Mary Lou Ralls, P.E., of Ralls Newman, LLC; Steve Mislinski, P.E., of LAN/AECOM; and Dr. M.J. Nigel Priestley and Jon Grafton of Pomeroy Corporation. Additionally, industry oversight was provided by Dr. Reid Castrodale, P.E., of Carolina Stalite; Bill Spence, P.E., of Tidewater Skanska, Inc.; Lucian Bodgan, P.E., of Dywidag Systems International; Robert Gulyas of BASF; Scott Harrigan, P.E., of The Fort Miller Co., Inc.; and Daniel Tassin, P.E., of International Bridge Technologies. As a significant portion of this research relied on experimental testing, the exceptional efforts and dedication of the lab staff of both UCSD and CSUS must be acknowledged.

FOREWORD

By Waseem Dekelbab
Staff Officer
Transportation Research Board

This report develops and validates precast concrete bent cap systems for use throughout the nation's seismic regions. The report also includes a series of recommended updates to the AASHTO *LRFD Bridge Design Specifications, Guide Specification for LRFD Seismic Bridge Design,* and AASHTO *LRFD Bridge Construction Specifications* that will provide safe and reliable seismic resistance in a cost-effective, durable, and constructible manner. The material in this report will be of immediate interest to bridge engineers.

Precast bent cap systems are of increasing utility in highway construction. Precasting moves concrete forming, pouring, and curing operations out of the work zone, making bridge construction safer and more environmentally friendly, and it removes bent cap construction from the critical path, thus accelerating the construction process. Precasting also improves quality and durability because the work is performed in a more controlled environment. The accelerated construction benefits of precast bent cap systems support the philosophy of "get in, get out, stay out." Successful use of precast bent caps relies on proper design, constructibility, and performance of the connections. Early uses of precast bent caps were limited to applications where minimal moment and shear transfer were required at connections. In seismic regions, provisions normally must be made to transfer greater forces through connections.

The research was performed under NCHRP Project 12-74 by the University of California, San Diego, with the assistance of California State University, Sacramento; Tobolski Watkins Engineering, Inc.; and Ralls Newman, LLC. The research presented herein develops and validates design methodologies, recommends design and construction specifications, and provides design examples and example connection details for precast bent cap systems using emulative and hybrid connections for integral and nonintegral systems for all seismic regions throughout the United States.

A number of deliverables are provided as attachments to this report, including design flow charts, design examples, example connection details, specimen drawings, specimen test reports, and an implementation plan from the research agency's final report. These are not published herein but are available on the TRB website at www.trb.org/Main/Blurbs/164089.aspx. These attachments are titled as follows:

- Attachment DS—Design Specifications
- Attachment DE—Design Examples
- Attachment CS—Construction Specifications

- Attachment ECD—Example Connection Details
- Attachment SD —Specimen Drawings
- Attachment TR—Test Reports
- Attachment CPT—Corrugated Pipe Thickness
- Attachment IP—NCHRP 12-74 Implementation Plan

CONTENTS

SUMMARY

Development of a Precast Bent Cap System for Seismic Regions

Accelerated Bridge Construction techniques have been sought to replace or rehabilitate, with minimal traffic interruption, thousands of bridges throughout the United States that are classified as structurally deficient or functionally obsolete. The use of precast concrete bent caps has been identified as one approach with many advantages, such as accelerating construction by removing work from the critical path, reducing environmental impact, increasing quality, and improving safety and overall economy. Considerable research has been conducted to develop constructible details with reliable performance; however, implementation in seismic regions has been limited due primarily to uncertainty in seismic performance of the connections—bent cap to columns and bent cap to superstructure—and a lack of specifications for design and construction.

Precast bent cap systems can be classified as either integral or nonintegral depending on superstructure-to-substructure connectivity. Integral bent cap systems develop longitudinal continuity through girder to bent cap connections. In contrast, nonintegral bent cap systems use bent cap to column connections to provide transverse moment continuity. However, integral precast bent cap systems still require the use of precast bent cap to column connections as well as a superstructure to precast bent cap connection.

Additionally, precast connections are typically described as being either emulative or hybrid. Emulative connections are designed to produce a system performance that is similar to (or "emulates") that achieved by traditional monolithic, cast-in-place (CIP) construction. Bridges using emulative precast bent cap connections are expected to form plastic hinges in the columns and redistribute forces to other members like CIP systems. The lateral force displacement response of an emulative system is expected to exhibit full hysteresis loops and stable energy dissipation. This response is characteristic of significant energy dissipation and hysteretic damping achieved through considerable damage and potential residual deformations as assumed in the underlying seismic design philosophy for CIP bridges. Hybrid systems are designed to provide sufficient energy dissipation through controlled rocking around specially detailed joints at the column ends. In addition to dissipating seismic energy, hybrid systems are intended to provide a significant reduction in damage and residual offsets as compared to CIP and emulative systems.

The primary goal of NCHRP Project 12-74 was to develop and validate design methodologies, design and construction specifications, design examples, and example connection details for precast bent cap systems using emulative and hybrid connections for integral and nonintegral systems for all seismic regions throughout the United States. This goal was achieved through a diverse experimental and analytical program focused on a select set of connection details. As an initial phase of this research, a comprehensive review of existing practice in the use of precast bent cap systems was completed. Based on a review of past implementation of precast bent caps and consideration of other promising connection approaches, a series of

connection details were developed and selected for further review. Initially, each detail was evaluated for past implementation, expected seismic performance, durability, constructability, and cost. The details that were finally selected included two emulative details (grouted duct and cap pocket), three hybrid details (conventional, concrete-filled pipe, and dual steel shell) and one integral detail (discontinuous post-tensioned girders spliced through a bent cap).

This report summarizes the research efforts conducted under NCHRP Project 12-74 and presents key findings and recommendations to facilitate the implementation of precast bent cap systems in seismic regions. A total of seven 42% scale bent cap to column component tests were conducted including a CIP control specimen, a full ductility grouted duct specimen, a cap pocket full ductility specimen, a cap pocket limited ductility specimen, and three hybrid full ductility specimens. Additionally, one 50% scale girder to bent cap component test was conducted on the integral connection detail. A description of the experimental test program is provided in addition to the presentation of results and associated interpretation of findings. Analytical modeling was also conducted on the hybrid systems to investigate the potential impacts this system type may have on the developed level of inelastic seismic displacement demand experienced during strong ground shaking. Based on the results of the analytical and experimental efforts, design and construction specifications, design examples, and example connection details are developed and presented. A significant number of deliverables are provided as attachments to this report—recommended design specifications, design flow charts, design examples, construction specifications, example connection details, specimen drawings, specimen test reports and an implementation plan. These attachments are available online at www.trb.org/Main/Blurbs/164089.aspx.

Based on the observations made during testing, the response of the CIP control specimen was determined to adequately represent the intended response of AASHTO's 2009 *Guide Specifications for LRFD Seismic Bridge Design* (*1*). However, the design and construction of the control specimen and emulative test specimens were based on the 2006 *Recommended LRFD Guidelines for the Seismic Design of Highway Bridges* (*2*). Even though the previous, less conservative code provisions were used to dictate the joint detailing requirements, the CIP and emulative specimens satisfied the intended design objectives. The response of all full ductility emulative specimens was dominated by flexural hinging within the column with controlled joint deformations due to adequate detailing. These specimens all achieved lateral drift capacities in excess of a 5% drift ratio indicating that the provided detailing has sufficient inelastic drift capacity. The use of the stay-in-place corrugated steel pipe serving as joint shear reinforcement provided sufficient joint shear resistance when subjected to column overstrength demands. The cap pocket limited ductility specimen experienced noticeably more joint damage when subjected to lateral loading consistent with column flexural hinging. The damage was due to the relaxation of seismic detailing requirements due to the intended limited ductility performance of this specimen. However, even with the intention of limited ductility response, the specimen was able to undergo lateral displacement in excess of a 5% drift ratio.

The three tested hybrid specimens varied in terms of column design and detailing. The first specimen used conventional spiral reinforcement at the column end in combination with a reduced amount of flexural reinforcement and the presence of unbonded post-tensioning. The second specimen used a full height steel shell with column longitudinal reinforcement only at the end and terminating shortly within the column. The third specimen used a similar external full height steel shell in combination with an inner shell forming a voided column. For the second and third specimens, full length unbonded post-tensioning was used. The first hybrid specimen was able to undergo lateral displacements in excess of a 6% drift ratio with appreciably less damage and residual offset as compared to the CIP and emulative systems. Ultimate failure for all hybrid specimens was caused by the eventual fracture of column longitudinal reinforcement. The second and third hybrid specimens were again able to

undergo lateral displacements on the order of a 6% drift ratio; however, the degradation of the grout bedding layer material resulted in a reduction in the lateral capacity under large deformation cycles. The use of a fiber reinforced grout matrix is expected to greatly enhance the integrity of the joint and thereby minimize the loss in lateral capacity. All hybrid specimens exhibited reductions in damage and residual displacements when compared with the CIP control specimen.

Upon review of the experimental results, the integral system investigated was determined to provide safe and reliable response when subjected to cycled elastic loading and inelastic demands. Capacity design and rational detailing provisions are expected to result in a superstructure system that resists seismically induced demands in an essentially elastic manner. Additionally, service and ultimate level loading should be resisted without major inelastic response in the superstructure. Physical testing indicates that the system studied is capable of resisting cyclic demands in the elastic range without a reduction in stiffness or slip. Large deformation inelastic testing was also performed to consider the potential response to overloading caused by vertical seismic demands and potential seismically induced relative settlements. Testing indicated that the system is capable of resisting inelastic demands in excess of 0.01 radians without a reduction in flexural stiffness. Experimental results indicate that detailing of shear reinforcement at the joint should include provisions to develop the full vertical shear demand in well-anchored reinforcement within a short distance to prevent potential shear slip.

Based on a review of the experimental and analytical efforts conducted under NCHRP Project 12-74, the following conclusions can be drawn:

- The current joint shear design methodology contained in the 2009 *Guide Specifications for LRFD Seismic Bridge Design* (*1*) is appropriate for the design of emulative and hybrid, integral and nonintegral precast bent cap systems with minor modifications.
- For seismic design categories (SDCs) B, C, and D, the principal tensile stress should be calculated and the level of joint shear reinforcement should be based on this stress. For SDCs B, C, and D, if the stress exceeds $0.11\sqrt{f_c'}$ (ksi), joint shear reinforcement should be specifically designed.
- Minimum joint shear reinforcement should be provided for all SDCs.
- Design methodologies and detailing for hybrid systems should be employed to facilitate the implementation of these systems for improving the post-earthquake functionality of the transportation network.
- Properly designed and detailed hybrid systems can produce substantially fewer residual deformations and less damage compared to CIP and emulative systems.
- In hybrid systems, the contribution of flexural reinforcement should be limited to produce the intended response. In addition, the neutral axis depth should be limited to minimize the magnitude of compressive strains within the section.
- Design and detailing of the unbonded post-tensioning and longitudinal reinforcement in a hybrid system should be performed to ensure premature fracture does not occur.
- Provisions of the 2009 *Guide Specifications for LRFD Seismic Bridge Design* (*1*) for the design of multicolumn integral connections should be updated for consistency with the design of multicolumn nonintegral connections.
- For the cap pocket connections, the use of a supplementary hoop at the top and bottom of the corrugated pipe should be employed.
- Proposed equations for anchorage of reinforcement within grouted ducts and the cap pocket connection should be implemented.
- Future provisions of seismic design and detailing requirements should be developed for knee joints for both CIP and precast bent caps.

- Alternate connection details are provided for structures located in SDC A with S_{D1} less than 0.10. However, a minimum of vertical stirrups in the joint are recommended, as well as the extension of column longitudinal reinforcement as close as practical to the top of the bent cap.
- Grouted joints for use in seismic applications should be limited to 3 in. in thickness and should be reinforced with hoops to maintain the spacing of lateral reinforcement within the plastic hinge region.
- For hybrid columns and integral closure joints, grouted connections should employ a 3 lb per cubic yard fraction of polypropylene fibers to enhance the integrity of the joint.
- The studied integral bridge connection provides sufficient strength, stiffness, and safety for implementation throughout the nation's seismic regions and is capable of resisting substantial inelastic demands made by vertical motion or seismically induced foundation movements.
- To provide reliable inelastic behavior, the integral system should be specially detailed at the girder end, including bottom flange confinement and well-anchored shear stirrups.
- Open soffit, integral precast bent caps should be designed considering an appropriate torsional resistance mechanism to distribute column overstrength actions into the superstructure girders.

Based on these recommendations, a series of recommended updates to the AASHTO *LRFD Bridge Design Specifications* (*3*), 2009 *Guide Specifications for LRFD Seismic Bridge Design* (*1*) and *LRFD Bridge Construction Specifications* (*4*) were developed. These updates are available online as attachments at www.trb.org/Main/Blurbs/164089.aspx.

CHAPTER 1

Introduction

1.1 Background

Thousands of bridges throughout the United States have been classified as structurally deficient or functionally obsolete, and many are in need of immediate repair or replacement. A great number of bridges rated as structurally deficient or functionally obsolete combined with the seismic design category (SDC) for Site Class D soil are located in regions subjected to seismic actions (*5*). To replace or rehabilitate these structures with minimal traffic interruption, Accelerated Bridge Construction (ABC) techniques have been sought. The use of precast concrete bent caps is one approach to accelerating construction, as it removes much of the work from the critical path. Other advantages of precast bent caps include reduction in environmental impact due to decreased on-site construction time and removal of environmentally hazardous operations to less intrusive locations; increased quality as bent caps are fabricated in a more controlled environment; improved safety for construction workers and the traveling public due to reduced exposure to hazardous conditions; and improved overall economy (*6*).

Precast bent caps such as those shown in Figure 1.1 have been used to meet a variety of project objectives. Considerable research has been conducted to develop constructible details with reliable performance (*7, 8, 9*). However, implementation in seismic regions has been limited because of (1) uncertainty about the performance of connections—bent cap to columns (or piles) and bent cap to superstructure—especially in assuring adequate ductility, strength, and stiffness; (2) a lack of specifications for design and construction; and (3) potential congestion of connections for higher seismic regions (*10*).

Precast bent cap systems can be classified as either integral or nonintegral depending on superstructure-to-substructure connectivity. When the superstructure is connected to the supporting bent cap by a cast-in-place (CIP) pour, closure pour, post-tensioning, and/or other means, longitudinal moment continuity can be developed. This integral connection creates longitudinal framing action and thereby provides redundancy in the load path, and, in some cases, can reduce the displacement demand and demand on the foundation. Nonintegral connections are typically produced by supporting the superstructure on bearings at the top of the bent cap. The bent cap to column connection provides a moment connection in the transverse direction, but moment transfer does not develop between the superstructure and substructure in the longitudinal direction. Thus, the longitudinal strength and stiffness of the bridge are based on the cantilever response of the supporting columns and soil-structure interaction at the abutments. Figure 1.2 shows plastic hinging for these conditions (*11*). Because of their simplicity, nonintegral bent cap systems are expected to be more widely implemented than integral systems, especially in regions of low to moderate seismicity, where such a system can provide suitable performance. For higher seismicities, nonintegral systems may still provide an economical solution for shorter span bridges, although provisions such as CIP diaphragms and additional seat width should be incorporated into the design. It should be noted that integral precast bent cap systems still require the use of precast bent cap to column connections, such as those used in nonintegral systems, in addition to a superstructure to precast bent cap connection.

Precast connections are typically described as being either emulative or hybrid, depending on the use of "wet" or "dry" connections, respectively. Wet connections use CIP concrete or grout to connect precast elements, whereas dry connections often employ mechanical devices for connection. Many seismic regions around the world such as the United States, Japan, and New Zealand have used emulative connections, which are designed to produce a system performance that is similar to (or "emulates") that developed by monolithic, CIP construction. As shown in Figure 1.3, the San Mateo-Hayward Bridge widening used partially precast construction and limited on-site concrete pours to produce emulative response, increase the speed of erection, and lower cost (*12*).

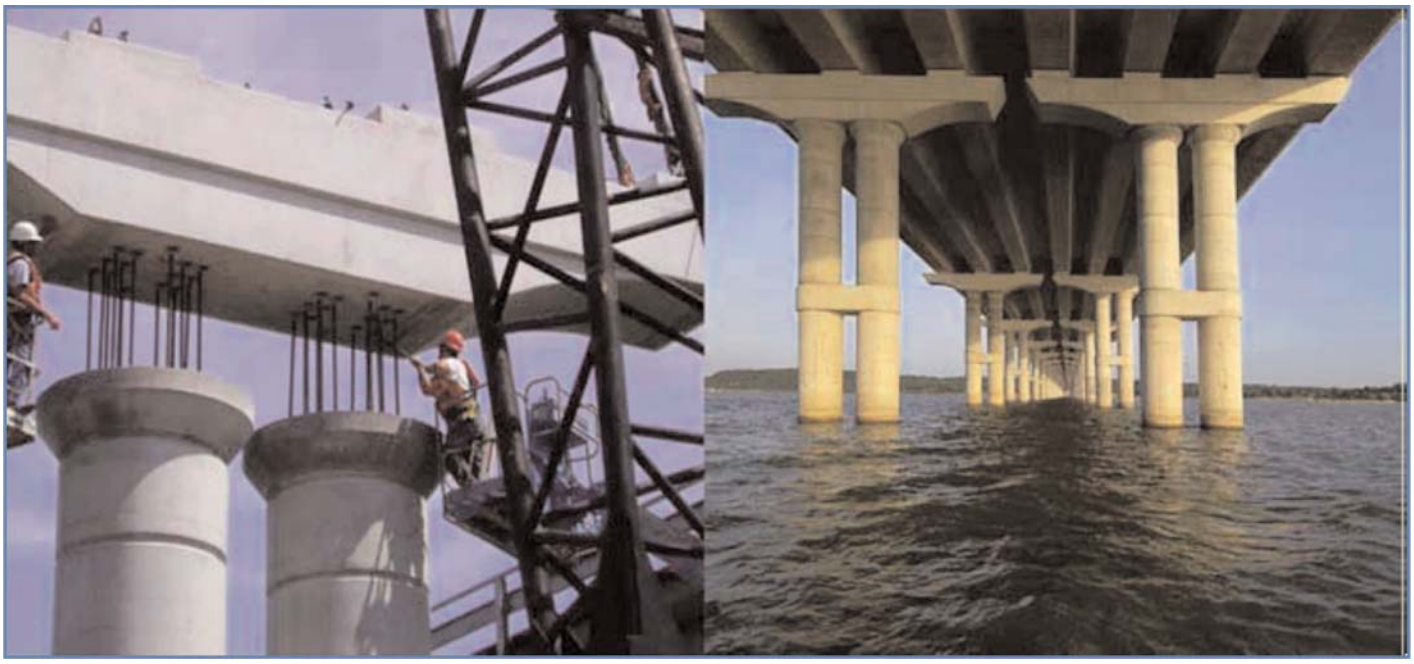

Figure 1.1. Precast concrete bent cap system used in crossing of State Highway 36 over Lake Belton, TX (7).

Bridges using emulative precast bent cap connections facilitate nonlinear response through the distribution of inelastic actions some distance into the column, termed the spread of plasticity (*13*). The lateral force displacement response of an emulative system is expected to exhibit full hysteresis loops and stable energy dissipation as shown in Figure 1.4. This response is characteristic of the significant energy dissipation assumed in the underlying seismic design philosophy for CIP bridges, and it helps ensure life safety. Emulative performance is commonly used in seismic regions despite the potential for large inelastic deformations that can lead to significant residual displacements and regions of severe, and sometimes irreparable, post-earthquake damage (*10*). Significant improvements in the seismic performance can be realized through modification of conventional design and performance approaches. The use of controlled rocking in bridge piers can serve to reduce seismically induced residual displacements while also reducing the damage experienced (*14*). Combining the use of unbonded post-tensioning and reinforcement, systems can exhibit appreciable energy dissipation, reduced residual displacements, and

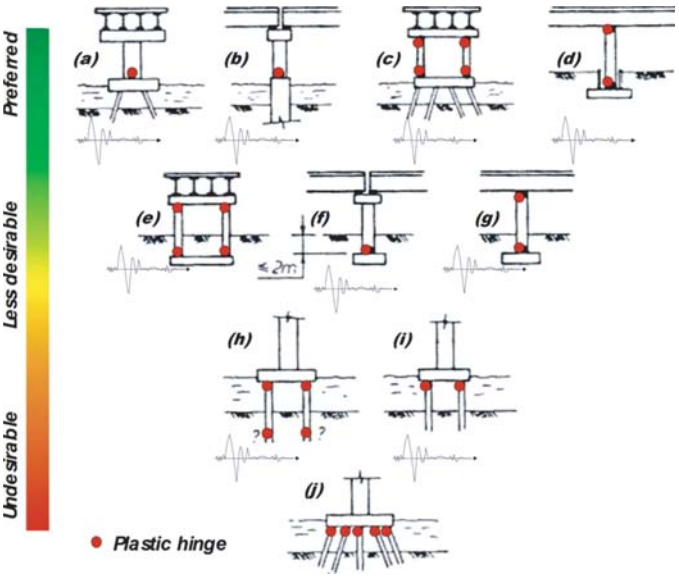

Figure 1.2. Potential plastic hinge locations (11).

Figure 1.3. San Mateo-Hayward Bridge widening project (12).

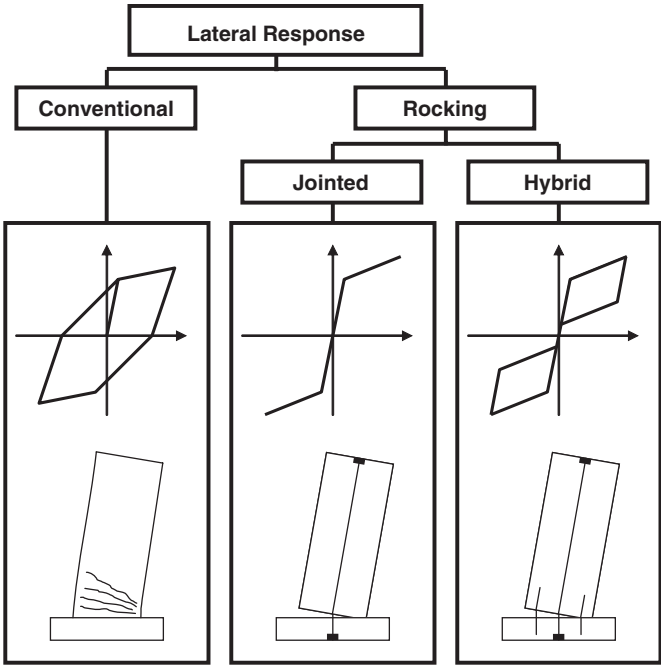

Figure 1.4. An overview of idealized lateral response for various column systems (5).

reduced structural damage when designed using a rationally founded approach (*5*). The combination of unbonded post-tensioning and mild reinforcement is termed "hybrid systems" throughout this report and is depicted in Figure 1.4. Tobolski (*5*) provides detailed information regarding the design and performance of hybrid systems for bridge applications.

1.2 Implications for Bridge Design and Construction

The results published in this report summarize a comprehensive research program that was aimed at the ultimate implementation of precast bent cap systems throughout U.S. seismic regions. The analytical and experimental program conducted served to validate the expected performance of a variety of precast bent cap details when subjected to seismic loadings. The results presented herein facilitate an understanding of the design and construction efforts required for safe and economical implementation of precast bent cap systems throughout the United States. Symbols and variables used throughout this document follow standard AASHTO convention.

1.3 Key Results from Initial Report

The first step in the research program was to develop promising precast bent cap connection and system details for use throughout the United State's seismic regions (*10*). To perform this task, a significant review and survey of state departments of transportation (DOTs) and engineers was conducted to identify prior uses of precast bent caps throughout the world. During this survey, more than 60 projects that used precast bent caps for all levels of seismicity were identified in 23 U.S. states, Puerto Rico, New Zealand, Europe, and Saudi Arabia. However, the majority of these previous applications were in regions subjected to minimal seismic actions, and almost all details were for nonintegral applications.

In addition to gathering information regarding prior implementation, the survey was aimed at obtaining insight into why these details have not been widely used. Engineers and agencies expressed reservations about using precast bent caps in seismic regions because of the lack of prior research and performance data for these systems. Many state DOT officials indicated that they would not allow the use of precast bent caps for higher seismic regions without validated design methodologies. Various other concerns were voiced regarding potential fabrication complexities as seismic demand increased due to heavy congestion at connection regions. Many fabricators did indicate that the use of post-tensioning would be a potentially advantageous way to reduce this congestion and provide a more constructible system. From a construction standpoint, many contractors indicated that they have reservations due to the potentially small tolerances that would be required to erect these precast systems. Many persons indicated that the required tolerances are achievable, but require increased care during construction that would in turn result in construction cost increases.

Based on the review of previous details and seismic research along with the input from industry, a variety of connection concepts were developed and evaluated for expected seismic performance, constructability, durability, advantages, and disadvantages. During this effort, the following nonintegral connection types were developed, as described in Tobolski et al. (*10*):

- Grouted duct connection
- Bolted connection
- Grouted sleeve coupler connection
- Cap pocket connection
- Welded connection
- Partially precast shell connection
- Conventional hybrid connection
- Concrete filled pipe hybrid connection
- Hollow dual shell hybrid connection

Additionally, a variety of precast, integral bent cap systems were presented. However, based on significant interaction with the NCHRP Project 12-74 panel, a future integral connection

detail was developed and tested. Review of some connection details resulted in recommended details that were ready for implementation for limited ductility connection applications. These limited ductility details were the grouted duct connection, grouted sleeve coupler connection, and partially precast shell connection. The proposed connections for testing and validation were presented as well as a rigorous experimental and analytical program for performing the required validation studies.

1.4 Summary of Experimental Specimens

During the course of this research program, a number of promising precast bent cap details were investigated through experimental testing. These specimens were developed to meet a variety of performance objectives for sites located throughout U.S. seismic regions. A summary of these specimens is provided in Table 1.1.

Table 1.1. Summary of experimental specimens.

Code	Specimen Name	Specimen Type	Specimen Purpose
CIP	Cast-in-place control specimen	Beam-to-column emulative	Control specimen detailed in accordance with *Recommended LRFD Guidelines for the Seismic Design of Highway Bridges* (*2*) for high seismic applications.
GD	Grouted duct specimen	Beam-to-column emulative	Grouted duct specimen designed to provide high ductility response with similar response to CIP specimen.
CPFD	Cap pocket full ductility specimen	Beam-to-column emulative	Cap pocket specimen designed to provide high ductility response with similar response to CIP specimen. Detail uses a corrugated metal pipe to provide stay-in-place form and joint shear reinforcement.
CPLD	Cap pocket limited ductility specimen	Beam-to-column emulative	Cap pocket specimen design with alleviated seismic detailing intended to provide limited ductility for regions of low to moderate seismicity. Detail uses similar corrugated metal pipe detail to CPFD.
HYB1	Conventional hybrid specimen	Beam-to-column hybrid	Hybrid specimen detailed with conventional spiral confinement reinforcement and full-length mild reinforcement. Detail is intended to be a hybrid detail most similar to traditional CIP construction.
HYB2	Concrete filled pipe hybrid specimen	Beam-to-column hybrid	Hybrid specimen using full length steel shell acting as confinement and shear reinforcement. Mild reinforcement used only at joint to provide energy dissipation and terminated into the column.
HYB3	Dual steel shell hybrid specimen	Beam-to-column hybrid	Hybrid specimen using two full length shells (outer steel and inner corrugated metal pipe) acting as confinement and shear reinforcement. Mild reinforcement utilized only at joint. Dual shell detail intended to reduce weight of column section for precasting.
INT	Post-tensioned integral specimen	Girder-to-beam emulative	Integral specimen using precast post-tensioned girders spliced through the precast bent cap. Girders are discontinuous at bent cap leaving a cold joint between the members. Intended to provide a constructible precast option for high seismic regions requiring integral response.

CHAPTER 2

Findings

2.1 Introduction

This chapter provides a synopsis of key findings of the experimental and analytical research program. This research program investigated the following:

- Emulative, nonintegral details
  - Grouted duct connection
  - Cap pocket connection
- Hybrid, nonintegral details
  - Conventional system
  - Concrete filled pipe system
  - Dual steel shell system
- Integral detail
  - Post-tensioned girder system detail

Findings include a description of the experimental test program—including specimen design, fabrication, and testing protocol—and response of the specimens. Detailed findings can be found in the attachments to this report, available online at www.trb.org/Main/Blurbs/164089.aspx.

2.2 Description of Experimental Test Program

This section describes the general development of the testing program and associated experimental specimens. Detailed drawings are provided in the attachments to this report.

2.2.1 Design of Nonintegral Prototype Bridge and Specimens

In coordination with the NCHRP Project 12-74 panel, the prototype structure was selected as a two-span, nonintegral bridge with a three-column CIP bent cap supporting precast, prestressed girders, intended to represent a typical highway overcrossing located in an urban area. Design of the component specimens is based on a representative portion of the center column and bent cap of the bridge, as shown in Figure 2.1. The full design of the prototype and specimen are reported in Matsumoto et al. (*15*). This section summarizes key design features of the CIP prototype bridge and CIP specimen.

The CIP prototype bridge and full ductility component specimens were designed in accordance with AASHTO *LRFD Bridge Design Specifications (Third Edition with 2006 Interims)* (2006 LRFD BDS) and *Recommended LRFD Guidelines for the Seismic Design of Highway Bridges* (2006) (2006 LRFD RSGS) prepared as part of NCHRP Project 20-07/Task 193 and provided to the research team (*16, 2*). It is important to note that the 2006 LRFD RSGS was superseded by the *Proposed AASHTO Guide Specifications for LRFD Seismic Bridge Design* (2007 LRFD PSGS) and later updated to the current 2009 *AASHTO Guide Specifications for LRFD Seismic Bridge Design* (2009 LRFD SGS) (*17, 1*). In addition, the 2006 LRFD RSGS contains different—and in some aspects more liberal (i.e., less conservative)—joint reinforcement requirements than the current 2009 LRFD SGS. For example, in contrast the 2006 LRFD RSGS, the 2009 LRFD SGS specifies vertical joint stirrups both inside and outside the joint region, a larger total area of joint stirrups, and a significant increase in bent cap longitudinal reinforcement. These provisions are compared in Chapter 3.

For a major seismic event, the CIP prototype bridge was designed and detailed to exhibit ductile plastic hinging in the column adjacent to the bent cap (and footing). Prototype bridge drawings are shown in the attachments. Initial member sizing was based on input from design engineers and refined through application of the 2006 LRFD BDS (*16*). Seismic analysis and design were performed to finalize column and cap beam sections. The prototype structure was considered nonessential and designed for the associated life-safety performance objectives defined in the 2006 LRFD RSGS (*2*). Because the system is nonintegral, the specified earthquake resisting system in the longitudinal direction consisted of cantilever response of the

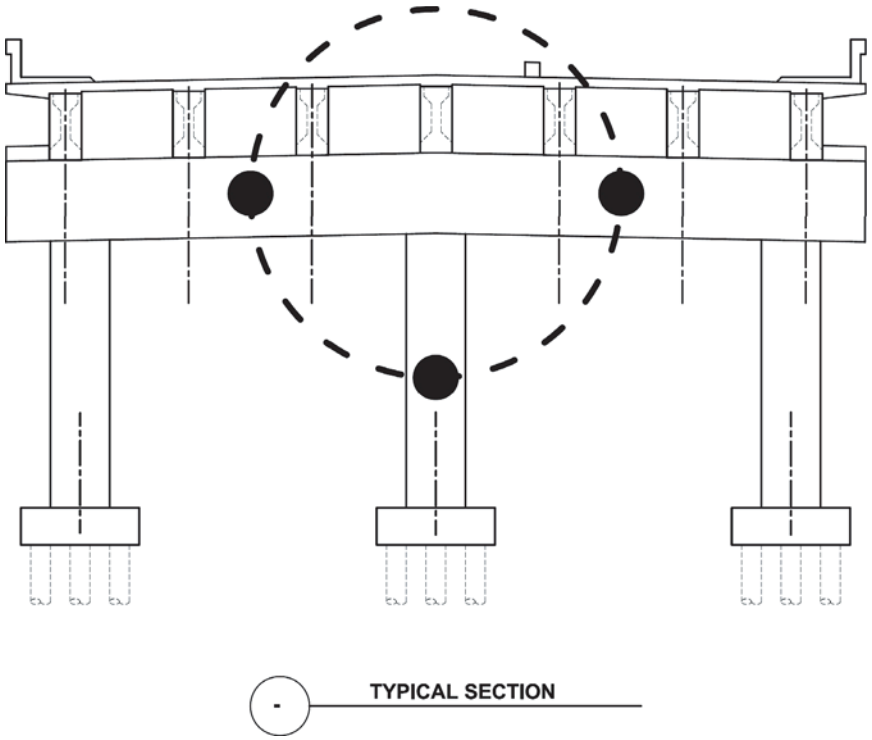

Figure 2.1. Portion of prototype used for specimen design.

columns with plastic hinge formation at the base of columns. One-way soil springs were used to account for the seismic resistance of the abutment backfill. Transverse earthquake resistance was provided by the three-column bent cap with plastic hinge formation occurring at both the top and bottom of the columns. The design acceleration response spectrum (ARS) curve incorporated 5% damping and was developed using a 1.0-sec acceleration of 0.8 g, a 0.2-sec acceleration of 1.5 g, and coefficients for Site Class D soil. The resulting peak rock acceleration was 0.6 g. The ARS curve is representative of a site located in a high seismic region such as Southern California. If the design earthquake response spectral acceleration coefficient at a 1.0-sec period, S_{D1}, was larger than 0.50, the structure was classified as SDC D. This category required a demand analysis, displacement capacity pushover analysis, capacity design, and SDC D detailing.

Elastic dynamic analysis was performed according to the 2006 LRFD RSGS to estimate seismic displacement demands (*2*). The columns were assumed to be fixed at the base, and foundation design was not performed. Moment-curvature analysis was conducted to estimate the effective stiffness of the columns. Seismic demands were determined using the SEISAB program (*18*). Results from the seismic analysis indicated a first mode (longitudinal) period of 1.27 sec and associated displacement demand of 15.1 in. The second mode (transverse) period was 0.58 sec, with a displacement demand of 5.3 in, including magnification to account for demand underestimation for shorter period structures. Shear keys at the abutments were designed to fail during the design seismic event.

In the longitudinal direction, the displacement demand to capacity ratio, *D/C,* was 0.85. For determining transverse capacity, overturning effects were considered using an iterative procedure to refine the estimated column plastic moment capacities based on column axial loads obtained from the pushover analysis. XSection was used to perform moment-curvature analysis, and WFrame was used for pushover analysis, including overturning effects and bent cap flexibility (*19, 20*). The transverse displacement *D/C* ratio was 0.57. Ductility demand ratios were approximately 5.0 for both the longitudinal and transverse directions, well below the limit of 8.0 (multicolumn bent caps). The prototype structure thus satisfied the requirements for displacement and ductility. P-delta effects were checked in accordance with the 2006 LRFD RSGS (*2*).

Capacity protection design principles were also applied. Flexural and shear demands on the bent cap were based on force levels associated with the columns reaching their overstrength capacity. The bent cap design considered axial load effects due to transverse response in combination with gravity loads and overstrength demands imposed by columns. According to the 2006 LRFD RSGS, the bent cap was required to remain "nominally elastic" (*2*). Bent cap transverse reinforcement outside of the joint region was designed according to the 2006 LRFD BDS (*16*) using modified compression field theory and considered seismic plus gravity loading. Column transverse reinforcement was designed to resist overstrength demands due to transverse response.

The joint region of the bent cap was designed based on transverse response using the external force transfer mecha-

nism assumed in the 2006 LRFD RSGS (*2*). Joint design included vertical stirrups with horizontal cross ties in the region adjacent to the column (not within the joint), joint transverse reinforcement (hoops), extension of column bars close to the top of the bent cap, and side face reinforcement. In addition, two 2-leg construction stirrups were used within the joint region, as explained by Matsumoto (*21*). However, the prototype bridge did not incorporate the more conservative joint reinforcement requirements of the 2009 LRFD SGS (*1*), such as placement of the required area of stirrups inside the joint or the additional area of longitudinal bent cap reinforcement.

The CIP test specimen was designed using a 42% scale of the central portion of the prototype bridge (see Figure 2.1). As the prototype bridge would be expected to exhibit ductile plastic hinging in the column region adjacent to the bent cap due to transverse response, the scaled CIP control specimen—loaded in the transverse direction under quasi-static force control and displacement control sequences—was expected to perform similarly. Dead load plus seismic load governed the bent cap flexural reinforcement in the prototype. This reinforcement was scaled for use in the bent cap. Bent cap transverse reinforcement was designed per the 2006 LRFD BDS (*16*). The additional joint shear reinforcement was required per 2006 LRFD RSGS, although a larger principal tensile stress was found for the specimen than the prototype due to the relatively smaller column load, larger cap and column tension, and imperfect scaling of dimensions (*2*). However, this was more desirable for examining joint behavior. Matsumoto (*21*) provides a detailed comparison of column, bent cap, and joint reinforcement for the prototype bridge and CIP specimen.

Full Ductility Emulative Specimens

The GD (grouted duct) and CPFD (cap pocket full ductility) specimens used the same full-ductility design basis as the CIP specimen (*22, 23*). The GD and CPFD specimens were intended to be directly compared with the CIP control specimen. Design of both precast specimens assumed emulative response would be achieved despite the following differences between these specimens and the CIP specimen: (1) separate precast elements, including the bent cap and column, and (2) use of a 1.5-in bedding layer between the bent cap soffit and column to accommodate tolerances.

In addition, the GD specimen used closely spaced, 1.75-in diameter, 22-gage corrugated ducts in the bent cap and high-strength, non-shrink, cementitious grout to anchor the column longitudinal reinforcement. Joint reinforcement matched that used for the CIP specimen, including two 2-leg construction stirrups within the joint region. CIP and GD specimen assembly details and bent cap reinforcement details are shown in the attachments.

The CPFD specimen used a single 18-in nominal diameter, 16-gage steel pipe in the bent cap to house the column bars and serve as a stay-in-place form as well as equivalent joint hoop reinforcement. Normal-weight concrete was placed in the bent cap void and bedding layer to anchor the column bars. The CPFD bent cap reinforcement details are shown in the attachments. Matsumoto (*23*) summarizes the approach used for selecting the readily available lock seam, helical corrugated steel pipe per ASTM A760, Standard Specification for Corrugated Steel Pipe, Metallic-Coated for Sewers and Drains (*24*). Figure 2.2 shows the corrugation and lock seam details for the pipe used in the specimen, and select joint details are summarized in Table 2.1.

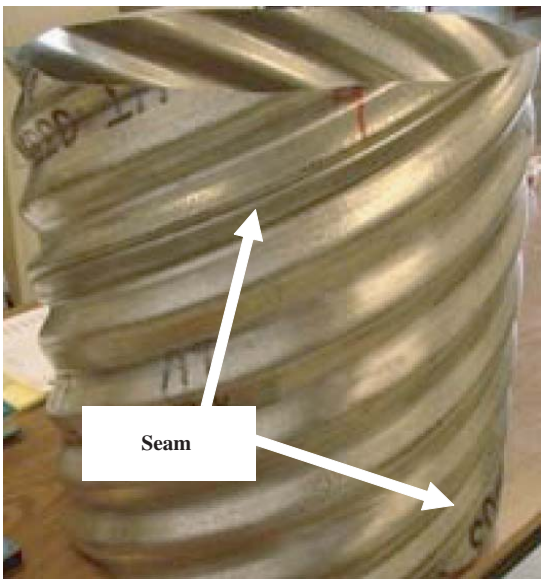

(a) Corrugation and Lock Seam

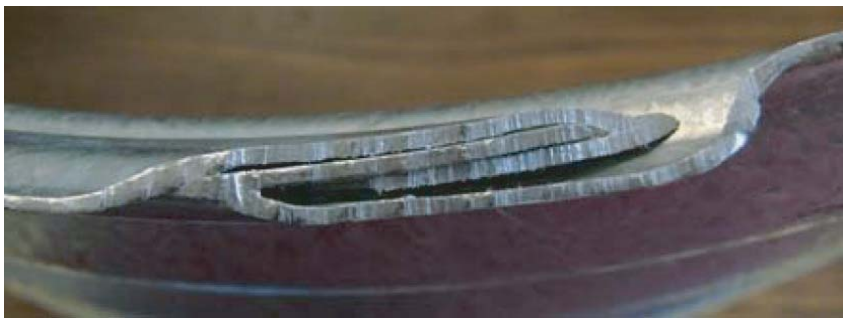

(b) Close–up of Lock Seam

Figure 2.2. Corrugation and lock seam details for cap pocket specimen.

Pipe thickness was a specific design parameter, calculated to provide the same nominal circumferential hoop force in the joint as that required for the CIP specimen per 2006 LRFD RSGS (*2*). Hoop force calculations assumed pipe nominal tensile yield strength of 30 ksi and used the horizontal component of the helical pipe. Subsequent tensile coupon tests conducted on the pipe material indicated a tensile yield strength of approximately 58 ksi. Nevertheless, calculations using the assumed 30 ksi yield strength resulted in a pipe thickness that matched the thinnest readily available pipe (16 gage). In addition, a #3 hoop, matching the column hoop size, was placed approximately 1 in from each end of the pipe to reinforce the pipe and limit dilation and potential unraveling (see Figure 2.3). This was considered a reasonably simple yet conservative measure, given the limited number of specimen tests and unknown performance of this innovative detail. Table 2.1 shows a hoop force ratio (pipe/hoop) of 1.03 when supplementary hoops are neglected, and 1.38 when accounting for the hoops.

Joint reinforcement for the CPFD specimen did not include the horizontal J-bars used for the CIP specimen, although two 2-leg construction stirrups were placed within the joint region. *Emulative Precast Bent Cap Connections for Seismic Regions: Component Test Report-Grouted Duct Specimen (Unit 2)* (*22*) and *Emulative Precast Bent Cap Connections for Seismic Regions: Component Tests-Cap Pocket Full Ductility Specimen (Unit 3)* (*23*) provide detailed comparisons of column, bent cap, and joint reinforcement for the prototype bridge and full ductility specimens.

Limited Ductility Emulative Specimen

The cap pocket limited ductility (CPLD) specimen (*26*) was intended to aid investigation of the response of a precast cap pocket connection designed according to the principles of limited ductility per the 2006 LRFD RSGS rather than the principles of full ductility used for the other specimens (*2*). For direct comparison, the CPLD specimen used the CPFD design as its initial basis. Emulative performance of the CPLD specimen was to be examined, especially through a displacement ductility of 2.0, even though a limited ductility CIP

Table 2.1. Comparison of specimen details—CPLD versus CPFD.

	Item	CPLD	CPFD	Notes
Joint	Helical Pipe: (*24, 25*) Pipe Diameter (nom) Pipe Thickness (gage) Corrugation Angle Corrugation Dimensions Lock Seam Strength Steel Yield Strength	18 in 0.065 in (16) 20 deg 2.67 in × 0.50 in 240 lb/in 57.5 ksi	18 in 0.065 in (16) 20 deg 2.67 in × 0.50 in 240 lb/in 57.9 ksi	Same basis allowed direct comparison of specimens
	Hoop Force Ratio: CPFD Pipe / Design (#3 hoops)	1.03 (no end hoops)	1.38 (extra end hoops) 1.03 (no end hoops)	Potential benefit of end hoops eliminated for CPLD
	Vertical Stirrups, Horizontal Cross Ties	None	External to Joint Only (2006 LRFD RSGS) (*2*)	No joint reinforcement used for CPLD
	Other Reinforcement	None	Two 2-leg construction stirrups placed in joint	Potential benefit of construction stirrups eliminated for CPLD
Column	Longitudinal Reinforcement	16#5 (1.58%, Specimen/ Prototype ratio = 1.14)	16#5 (1.58%, Specimen/ Prototype ratio = 1.14)	No note
	Transverse Reinforcement	#3 hoops @ 2 in	#3 hoops @ 2 in	Same basis allows CPLD joint to potentially be challenged to greater extent
Bent Cap	Longitudinal Reinforcement	8#5 and 2#4 top and bottom (0.50%, Specimen/ Prototype ratio = 0.99)	12#5 top and bottom (0.65%, Specimen/ Prototype ratio = 1.27)	Potential benefit of flexural reinforcement reduced for CPLD
	Transverse Reinforcement	2-leg #3 stirrups @ 8 in	2-leg #3 stirrups @ 6 in	CPLD stirrups reduced to minimum requirement

Figure 2.3. Rebar cage with corrugated pipe and supplementary hoops—CPFD.

specimen was not tested for direct comparison. The CPLD bent cap reinforcement details are shown in drawings provided in the attachments.

Table 2.1 summarizes select joint details for the CPLD specimen, including the specifications for the helical corrugated pipe with lock seams, which were the same as the CPFD specimen. A comparison of the overall CPLD and CPFD specimen details is also presented in Table 2.1. Table 2.2 summarizes the significant differences in SDC D and SDC B design and detailing provisions. Significant joint reinforcement, including transverse (hoop) reinforcement, is required for SDC D but not for SDC B (*17*). The same pipe size and thickness were used for the CPLD and CPFD specimens to allow a direct comparison of specimens. The pipe thickness was not considered excessive and was the minimum size readily available for construction.

Table 2.1 reveals important differences that were intentionally incorporated into the CPLD joint detailing to severely challenge the limited ductility specimen, in accordance with the intent and provisions of the 2006 LRFD RSGS for SDC B: (1) elimination of the construction stirrups within the joint region, (2) elimination of all joint-related stirrups and horizontal ties (A_s^{jh}, A_s^{jv}) placed external to the CPFD joint, and (3) elimination of the extra hoop at each end of the pipe (*2*). Table 2.1 also reveals that bent cap flexural reinforcement was reduced to eliminate potential strengthening of the joint due to higher bent cap flexural strength (and thus to allow potential yielding of flexural reinforcement adjacent to and within the joint) and to provide more accurate prototype scaling. In addition, bent cap transverse reinforcement, including that adjacent to the joint, was based on shear developed within the bent cap due to forces associated with plastic hinging of the column, not a joint force transfer mechanism. These modifications were implemented despite the possibility that principal tensile stresses in the joint could exceed the 2006 LRFD RSGS limit of $3.5\sqrt{f_c'}$, at which the additional joint reinforcement is required (*2*). Thus, these measures were deemed conservative for testing to examine potential failure modes, and it was understood that more stringent detailing could be adopted for design as required.

In addition, CPLD column reinforcement (including confining reinforcement) was not reduced but designed to match the SDC D-based requirements of the CPFD design. This was intended to help ensure that the column would not prematurely become a weak link in the system, but impose as large of a demand and as many cycles as possible on the joint so that potential failure modes associated with the joint could be fully investigated. Matsumoto (*26*) provides a detailed comparison of column, bent cap, and joint reinforcement for the prototype bridge and CPLD specimen.

These measures were deemed reasonably conservative for testing to examine limited ductility performance and potential failure modes. The impact of these measures was unknown. However, it was anticipated that more extensive joint damage would be exhibited than for the CPFD as the specimen displacement ductility approached μ2 and could possibly result in joint failure at larger ductility levels. It was understood that more stringent detailing could be adopted for SDC B design as required.

Hybrid Specimens

Lateral performance of hybrid systems differs from CIP and emulative systems due to the presence of unbonded post-tensioning and reinforcement. The prototype bridge served as the basis for the design of the CIP and emulative systems; however, differences in the design were required for the hybrid systems. To achieve a somewhat comparable lateral response, the hybrid specimens were designed to have similar lateral force resistance when compared to the CIP specimen at a 1.0% drift ratio. However, during the erection of the conventional hybrid specimen, the actual anchor set losses for the post-tensioning were significantly less than expected, resulting in a greater effective post-tensioning force. This increase in effective post-tensioning resulted in an appreciably greater lateral resistance as compared to the CIP and emulative specimens.

Detailed descriptions of the performance objectives, design methodology theory, and specimen designs for all three specimens are highlighted in the attachments to this report as well as by Tobolski (*5*). Complete design drawings for the hybrid specimens are provided as an attachment to this report. Each hybrid detail uses half of the conventional reinforcement as compared to the CIP and emulative specimens connected to the bent cap using a grouted duct connection with a grouted bedding layer joint dimension of 1 in.

The conventional hybrid specimen used closely spaced spiral reinforcement at the column end to provide lateral confinement of the concrete compression toe. The flexural reinforcement in the column extended full height and was

Table 2.2. Design and detailing provisions—SDC D versus SDC B.

NCHRP Project 20-7/Task 193 Criteria	SDC D (Full Ductility)	SDC B (Limited Ductility)
Force Demands (8.3.2, 8.3.3)	Based on forces resulting from the overstrength plastic hinging moment capacity or the maximum connection capacity following the capacity design principles specified in Article 4.11.*	The lesser of the forces resulting from the overstrength plastic hinging moment capacity or unreduced elastic seismic forces in columns or pier walls.
Ductility Demands (8.3.4)	The local displacement ductility demands, μ_D, of members shall be determined based on the analysis method adopted in Section 5. The local displacement ductility demand shall not exceed the maximum allowable displacement ductilities established in Article 4.9.	N/A
Column Shear Demand, V_u (8.6.1)	Based on the force, V_{po}, associated with the overstrength moment, M_{po}, defined in Article 8.5 and outlined in Article 4.11.	Based on the lesser of (1) force obtained from an elastic linear analysis and (2) force, V_{po}, for plastic hinging of the column including an overstrength factor
Concrete Shear Capacity (8.6.2)	Using concrete shear stress for circular columns with hoops, modified by: $\alpha' = \frac{0.03}{\mu_D}\rho_s f_{yh}$ where μ_D is 6 (multicolumn bent) or lower inside plastic hinging region, per Eq. 4.9-5	Using concrete shear stress for circular columns with hoops, modified by: $\alpha' = \frac{0.03}{\mu_D}\rho_s f_{yh}$ where μ_D is 2
Minimum Column Shear Reinforcement (Spiral) (8.6.5)	$\rho_s \geq 0.005$	$\rho_s \geq 0.003$
Minimum Longitudinal Reinforcement (8.8.2)	$A_l \geq 0.010A_g$, Columns	$A_l \geq 0.007A_g$, Columns
Splicing of Longitudinal Reinforcement in Columns (8.8.2)	$A_l \geq 0.010A_g$, Columns	$A_l \geq 0.007A_g$, Columns
Minimum Longitudinal Reinforcement (8.8.3)	Outside plastic hinging region	N/A
Minimum Development Length into Cap Beams (8.8.4)	$l_{ac} = \frac{0.79 d_b f_{ye}}{\sqrt{f'_c}}$, not to be reduced; extended as close as practically possible to opposite face	N/A**
Anchorage of Bundled Bars into Cap Beams (8.8.5)	Increased by 20% for a two-bar bundle and 50% for a three-bar bundle. Four-bar bundles are not permitted in ductile elements.	N/A
Maximum Bar Diameter (8.8.6)	$d_{bl} = \frac{0.79\sqrt{f'_c}(L - 0.5D_c)}{f_{ye}}$	N/A
Lateral Reinforcement Inside Plastic Hinge Region (8.8.7)	Butt-welded hoops or spirals	N/A
Lateral Reinforcement Outside Plastic Hinge Region (8.8.8)	Volumetric ratio shall not be less than 50% of that determined in 8.8.7 and 8.6. Reinforcement shall be of the same type. Lateral reinforcement shall extend into bent caps a distance that is as far as is practical and adequate to develop the reinforcement for development of plastic hinge mechanisms.	N/A

Table 2.2. (Continued).

NCHRP Project 20-7/Task 193 Criteria	SDC D (Full Ductility)	SDC B (Limited Ductility)
Requirements for Lateral Reinforcement (8.8.9)	Various detailing requirements.	N/A
Capacity Protection Requirements (8.9)	Capacity-protected members such as bent caps shall be designed to remain essentially elastic when the plastic hinge reaches its overstrength moment capacity, M_{po}. The expected nominal capacity is used in establishing the capacity of essentially elastic members.	N/A
Superstructure Capacity Design (8.10, 8.11)	For longitudinal direction, the superstructure shall be designed as a capacity-protected member. For transverse direction, integral bent caps shall be designed as an essentially elastic member. Longitudinal flexural bent cap beam reinforcement shall be continuous. Splicing of reinforcement shall, at a minimum, be accomplished using mechanical couplers capable of developing 125% of the expected yield strength, f_{ye}, of the reinforcing bars.	N/A
Superstructure Design for Non-Integral Bent Cap (8.12)	For superstructure to substructure connections not intended to fuse, provide a lateral force transfer mechanism at the interface. For connections intended to fuse, minimum lateral force at interface shall be 0.40 times the dead load reaction plus the overstrength shear key(s) capacity. Non-integral cap beams supporting superstructures with expansion joints at the cap shall have sufficient support length to prevent unseating.	N/A
Joint Design (8.13)	Major joint design and detailing provisions, such as bent cap width, joint shear reinforcement (vertical stirrups inside and outside the joint, and horizontal cross ties/J-bars), transverse joint reinforcement, additional bent cap longitudinal reinforcement, and side face reinforcement.	N/A

*Articles, sections, and equation numbers cited in Table 2.2 refer to 2007 LRFD PSGS (*17*).
**AASHTO *LRFD Bridge Design Specifications* (*3*) provisions (i.e., 5.10.11.4.3), in contrast to NCHRP Project 20-7/Task 193 provisions, require even longer lengths for column bar extension into joint.

locally debonded across the bedding layer to facilitate distributed straining of the reinforcement.

The concrete filled pipe hybrid specimen used a full height, steel shell that provided enhanced confinement at the column end. The flexural reinforcement extending from the bent cap into the column terminated after a given distance required for development in the column. After the termination of the reinforcement, the shell, concrete, and unbonded post-tensioning were the only elements in the column. Similar to the conventional specimen, the reinforcement was locally debonded across the joint to prevent premature reinforcement fracture.

The dual shell hybrid specimen used a full height exterior steel shell that provided confinement at the column end. To form the interior void, a corrugated metal pipe that was in conformance with ASTM A760 was used (*24*). This interior pipe was intended to act as a stay-in-place form during fabrication as well as to prevent the potential implosion of the concrete section during large compressive strains associated with lateral response. Similar to the concrete filled pipe specimen, the reinforcement extending from the bent cap into the column was terminated following adequate development.

The three bent caps for the hybrid specimens were identical and were designed in accordance with the 2006 LRFD RSGS (*2*). This design and detailing considered the various increases in reinforcement required in the joint as well as the flexural reinforcement in the bent cap. Joint shear design was performed considering only the area of flexural steel when determining the required joint shear reinforcement.

During early discussions with the NCHRP Project 12-74 panel, the decision was made to use stainless steel reinforcement

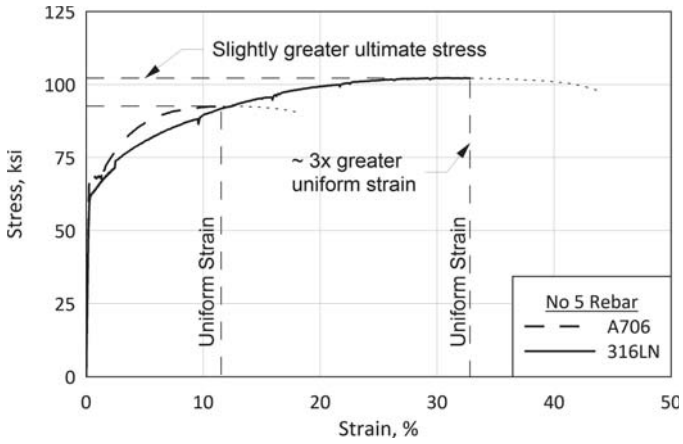

Figure 2.4. Comparison of A706 and 316LN uniaxial tension response (5).

across the joint for the experimental specimens. The reasoning for this decision relates to the localized crack in the hybrid system at nominal yield as opposed to the distributed cracking in a conventional CIP column. The extent of cracking at the bedding layer is highly localized due to the intention debonding across the joint. This will result in slightly larger crack widths at the nominal yield point. The use of stainless steel reinforcement locally across the joint serves to provide added comfort in the durability of these systems during their expected service life. To consider the potential influence of stainless steel reinforcement, a variety of material tests were conducted. Figure 2.4 provides a summary of a series of uniaxial tension tests conducted on No. 5 reinforcement for A706 steel and 316LN stainless steel. These results indicate that the stainless steel reinforcement has more than three times the uniform strain capacity as A706 steel, indicating significantly greater material ductility and energy dissipation capacity. The effective yield for the two steel grades was similar with a slightly greater ultimate tension capacity observed for the 316LN steel.

In addition to uniaxial tension testing, a series of cyclic rebar tests were conducted. Figure 2.5a depicts the cyclic response of the two rebar specimens that were tested with an unbraced length equal to six times the bar diameter. The bars were loaded to a compression strain equal to approximately one-third of the previously reached tension strain. From Figure 2.5, it is apparent that the A706 and 316LN reinforcing bars have similar cyclic response for realistic free lengths. This indicates that commonly accepted relationships for steel reinforcement may be acceptable for the use of stainless steel reinforcement. Further study is needed to fully investigate the potential seismic implications of using stainless steel reinforcement.

Figure 2.5b provides the complete cyclic stress-strain response of the two reinforcing bars. From this figure, it is apparent that the 316LN reinforcing bar has significantly greater ultimate tension strain capacity. The recording of strain was terminated at the last point on the 316LN plot due to the limits of the recording instrumentation.

2.2.2 Fabrication and Assembly of Nonintegral Specimens

All nonintegral emulative specimens were fabricated at the precast yard of Clark Pacific (West Sacramento, California). Precast bent cap and column segments were then assembled at California State University—Sacramento (CSUS). The fabrication and assembly of the precast specimens replicated as much

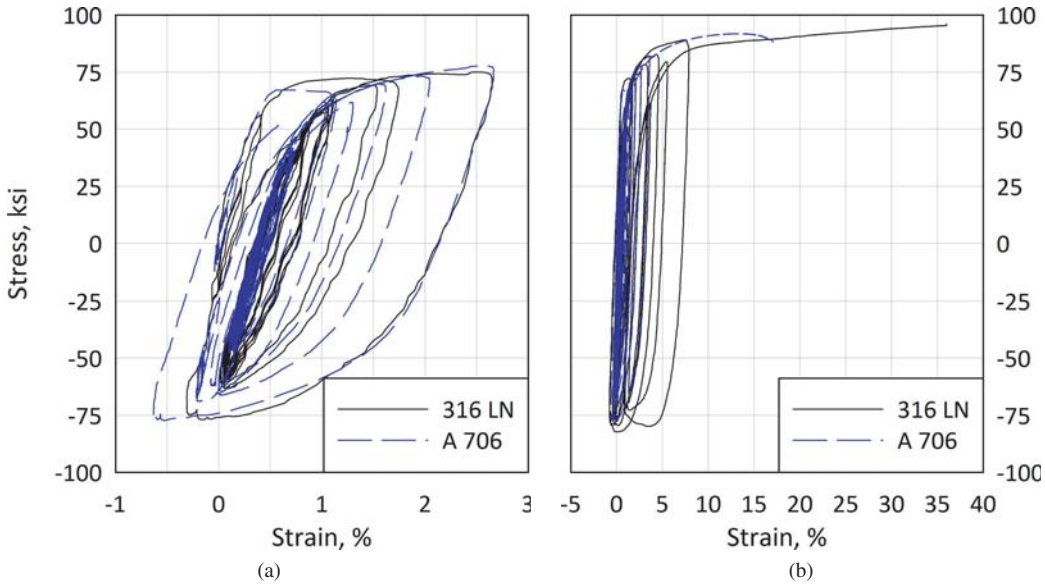

Figure 2.5. Comparison of A706 and 316LN cyclic stress-strain to (a) 3% strain and (b) failure (5).

Figure 2.6. Lowering bent cap rebar cage into elevated formwork—CIP.

as possible the expected field process so constructability issues could be examined. The construction sequence for precast specimens included the following:

1. Fabricate rebar cages for the bent cap and column at CSUS.
2. Transport rebar cages to Clark Pacific, prepare bent cap and column forms, and cast bent cap and column concrete.
3. Transport precast cap and column to CSUS.
4. Prepare column and bent cap for assembly and conduct cap setting operation in upright position.
5. Prepare connection. For grouted duct connection, pump grout into the bedding layer to fill the bedding layer and ducts. For cap pocket connections, fill pocket and bedding layer with concrete from top of cap.
6. Invert specimen and install in test area.

The following sections provide a brief summary and select photos of the specimen fabrication. Further details are provided by Matsumoto (*21, 22, 23, 26*).

Cast-in-Place Specimen

Fabrication of the CIP specimen required building special elevated forms for casting the bent cap on top of the column (see Figure 2.6 and Figure 2.7), as well as inverting the entire T-shaped specimen in the yard for transportation. The specimen was fabricated accurately according to the drawings.

Grouted Duct Specimen

Figures 2.8 through 2.12 show the bent cap rebar cage, cap setting operation, and grouting of the GD specimen. Grout compressive strength was designed to exceed that of the bent

Figure 2.7. Bent cap rebar cage in form during fabrication—CIP.

cap by at least 500 psi to ensure the connection grout was not a weak link in the system. A hand pump system and collar were used for grouting the bedding layer and ducts. Grout was pumped from the bottom of the bedding layer up into the ducts, and an air vent system at the top of the bedding layer helped prevent air entrapment within the connection. Fluidity of grout was determined before grouting using a flow cone test in accordance with ASTM C939-02 (*27*). After the bedding layer form was attached and sealed, the bedding layer

Figure 2.8. Bent cap rebar cage in form during fabrication—GD.

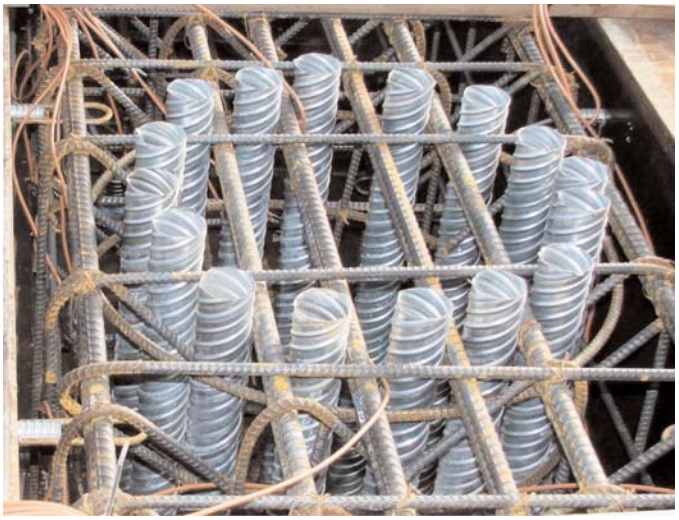

Figure 2.9. Joint region of bent cap during fabrication—GD.

was prewatered to ensure sealing and prevent loss of moisture from the grout. After mixing the grout using a paddle-type mortar mixer, grout with a flow cone efflux time of 20 to 30 sec was pumped into the connection. After grout flowed through air vents in the bedding layer, the vents were sealed. Grout was added manually to top off each duct. After the grout cured several days, the bedding layer form was removed and the bedding layer and the top of the ducts were inspected.

Cap Pocket Specimen

Figure 2.13 compares the bent cap rebar cage for the CPFD and CPLD specimens. The significant reduction of joint reinforcement for the CPLD specimen is evident. A Sonotube dam at the top and bottom of the corrugated pipe and a column bar template were useful to form the cap pocket void full height of the bent cap, as the pipe is placed only between the top and bottom of the longitudinal rebar (see Figure 2.13b). Figure 2.14 shows concreting of the CPFD pocket. Fabrication and assembly operations for the CPLD and CPFD were the same.

Concrete was placed in the pocket and bedding layer using a bucket at the top of the pocket. Concrete was cast into the pocket around the bent cap longitudinal reinforcement from above, and a collar with an air vent system was used to help remove entrapped air at the bedding layer. The concrete mix was selected to be close to that used for the bent cap and column, with the intention of achieving a strength and stiffness at least 500 psi greater than that of the bent cap, ensuring that the connection would not be the weak link in the system. After the bedding layer form was attached and sealed (see Figure 2.15), the bedding layer was prewatered to ensure sealing and to prevent loss of moisture from the pocket concrete. Buckets were used to fill the pocket with concrete in several layers with vibration. Once concrete flowed through the air vents in the bedding layer, the vents were sealed. After hardening, curing compound was applied to the top surface. After the bedding layer form was removed, the bedding layer and top of the pipe were inspected.

The first column hoop below the top of the CPFD column was placed approximately 2 in below its intended location during fabrication. This reduced the overall drift to some extent, but did not affect the maximum load induced in the joint.

Conventional Hybrid Specimen

Figures 2.16 through 2.19 show the rebar cage, cap setting operation, grouting, and post-tensioning of the con-

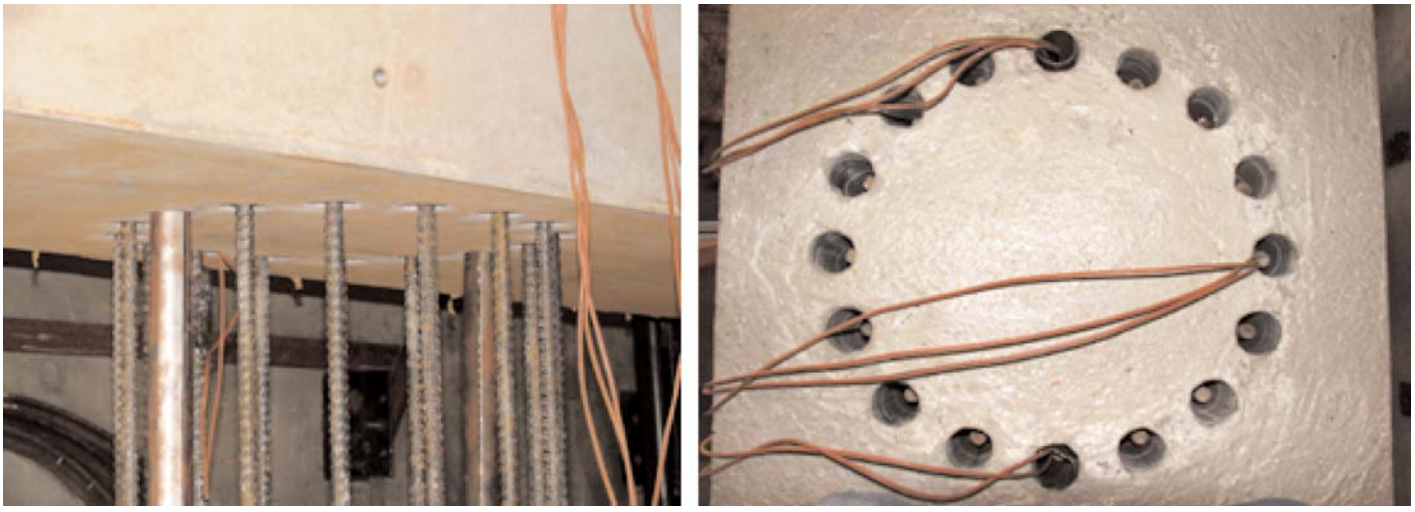

Figure 2.10. Cap placement during and after cap setting operation—GD.

Figure 2.11. Mixing and pumping of grout—GD.

Figure 2.12. Topping off ducts with grout and cap top post-grouting—GD.

ventional hybrid specimen. Unlike the emulative grouted duct specimen, the grouting of the bedding layer and ducts for this specimen were performed by pumping the grout in from the top. The grout tube was inserted into a corrugated duct extending near the bottom of the bedding layer. As the grout filled the bedding layer, the grout tube was slowly extracted from the corrugated duct. The hydraulic head pressure of the column of grout in the one duct was used to fill the remaining ducts with some head loss. Similar to the grouted duct connection, each duct was then topped off in a way similar to what is shown in Figure 2.12. Once grout had adequate time to cure, the column and bent cap assembly was post-tensioned, inverted, and installed in the testing frame.

Concrete Filled Pipe Hybrid Specimen

The reinforcing cage and details of the bent cap for the concrete filled pipe and dual shell specimens are the same as those presented in Figure 2.16 for the conventional hybrid specimen. A view down the inside of the column prior to casting is shown in Figure 2.20. In this figure, the installed curvature gages are apparent. Also in this photo, weld beads on the inside of the column can be observed. These weld beads were placed inside the column shell to promote reliable transfer of reinforcement tensile forces into the shell. The erection of this specimen was the same as the erection of the conventional specimen. The bedding layer form used during casting can be seen in Figure 2.21. During the casting of the bedding layer for this specimen, minor

(a) CPLD

(b) CPFD

(c) CPLD (West Face)

(d) CPFD (West Face)

Figure 2.13. Comparison of cap pocket bent cap rebar cages during fabrication.

(a) Bucketing Concrete into Pocket

(b) Vibrating Concrete in Pocket

Figure 2.14. Concreting of cap pocket connection—CPFD.

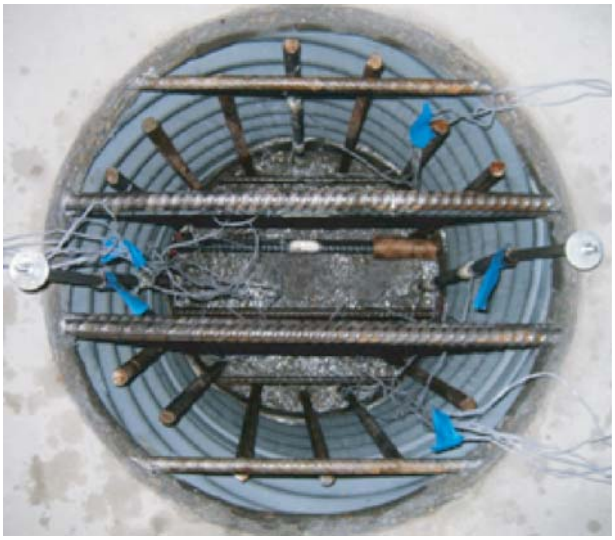

(a) Plan View of Pocket

(b) Bedding Layer

Figure 2.15. Pocket and bedding layer before concreting—CPLD.

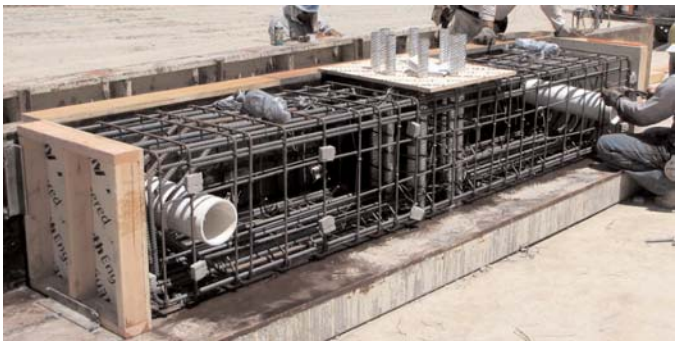

Figure 2.16. Reinforcing cage installed in form—HYB1.

bleeding of the bedding layer grout was observed. Following the removal of the formwork, no defects were noted in the bedding layer as only minor bleeding was seen.

Dual Steel Shell Hybrid Specimen

A view down the region between the internal and external shell for the dual shell specimen can be seen in Figure 2.22. Similar to the concrete filled pipe specimen, in this column detail weld beads were placed on the inside of the column to promote the transfer of forces from the reinforcing bar to the shell. In Figure 2.22, the debonding material on the rebar can also be seen, along with the termination of the bar within the

Figure 2.17. Bent cap setting operation—HYB1.

column. A top view of the column after casting is shown in Figure 2.23. From this figure, the internal corrugated metal pipe is observed with a polyvinyl chloride (PVC) pipe in the center for threading of column post-tensioning. This PVC pipe was used to ensure the easy threading of tendons from anchorage to anchorage. For corrosion purposes, this PVC pipe can be grouted following stressing to prevent moisture from reaching the tendon during its service life. This grouting will not affect the unbonded nature of the tendon because the bond between the grout and PVC will break easily.

2.2.3 Nonintegral Testing Protocol and Instrumentation

Emulative Specimens

The specimen test setup, shown in Figure 2.24, included a simply supported inverted bent cap that allowed accurate

Figure 2.18. Bedding layer and corrugated duct grouting operation—HYB1.

Figure 2.19. Post-tensioning operation—HYB1.

Figure 2.20. View inside steel shell showing weld beads—HYB2.

Figure 2.21. Bedding layer form—HYB2.

establishment of specimen forces. The test setup ensured accurate conditions at each end of the joint so that the force transfer mechanism in the joint could be investigated (*15, 28*). The specimen was tested in inverted position with a column stub that allowed biaxial loading of the specimen using a vertical hydraulic actuator to apply scaled gravity load and a horizontal hydraulic actuator to induce seismic response. As required, different axial force conditions in the bent cap were produced for the push and pull directions.

Force control and displacement control sequences were applied to all specimens, similar to the force and control sequences shown in Figure 2.25 and Figure 2.26. Force control loading was used for an approximate determination of first yield of column longitudinal bars in the push and pull directions, establishment of effective yield, and application of the displacement control sequence including quasi-static displacement in three cycles. Nominal displacement ductility demand, as multiples of system effective yield displacement, was applied at the following levels, or until the residual capacity of the specimen dropped below 30% of the maximum load: μ1, μ1.5, μ2, μ3, μ4, μ6, μ8, and μ10.

Figure 2.22. View down dual shell prior to casting with rebar—HYB3.

Figure 2.23. Top view of column after casting—HYB3.

Figure 2.24b shows the external gages, including linear and string potentiometers and linear variable differential transformers (LVDTs), mounted on the column, joint, and bent cap. Internal strain gages were placed on bent cap, joint, and column reinforcing bars, as well as on corrugated ducts or pipe. In addition to the approximately 100 channels of data, specimen response was also monitored using digital photos, crack markings and measurements, video recording, and notes.

Hybrid Specimens

The test setup for the hybrid specimens is shown in Figure 2.27. As shown in previous images, the hybrid specimens were constructed in an upright condition and then inverted for installation in the test setup. The vertical actuator was set to apply a constant load during testing to simulate gravity loading. This force varied between hybrid specimens in order to try and match the lateral response of the three hybrid tests. The horizontal actuator was actively controlled to apply specified forces or displacements during testing.

The initial stage of loading consisted of force controlled loading protocols, which apply positive and negative lateral forces of increasing magnitude until the first yield of the extreme mild reinforcing bar is reached. This force control protocol is shown in Figure 2.28. Each force loading cycle was repeated three times in both directions. Following the first yield of the system, the lateral loading was applied to a specified lateral drift ratio. The basic loading protocol is shown in Figure 2.29. At each cycle to a given drift ratio, the column was subjected to two cycles in both directions followed by one cycle to the previous lateral drift. This protocol was developed to help accurately calibrate nonlinear models of the system.

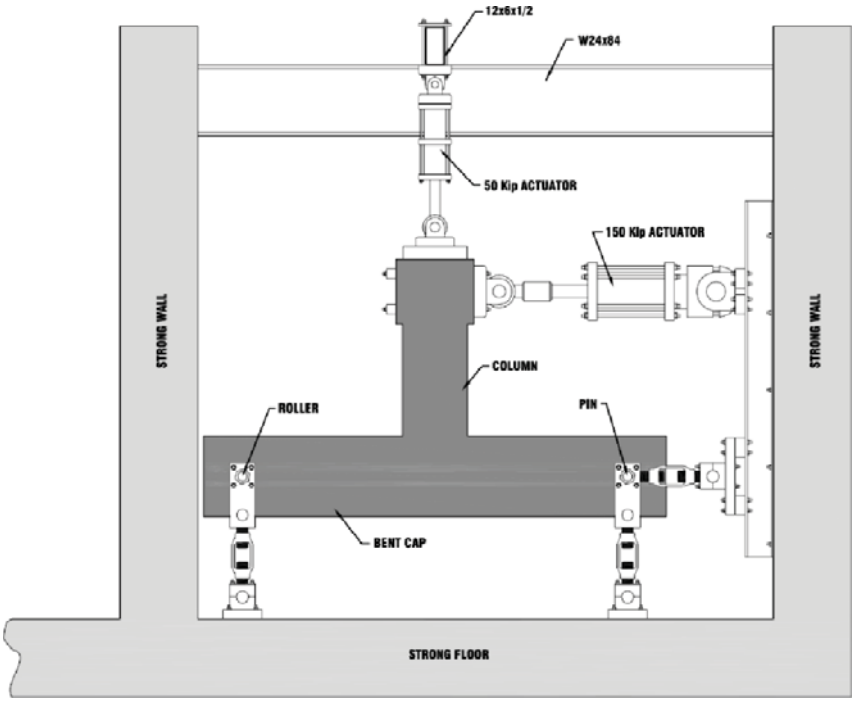

(a) Schematic

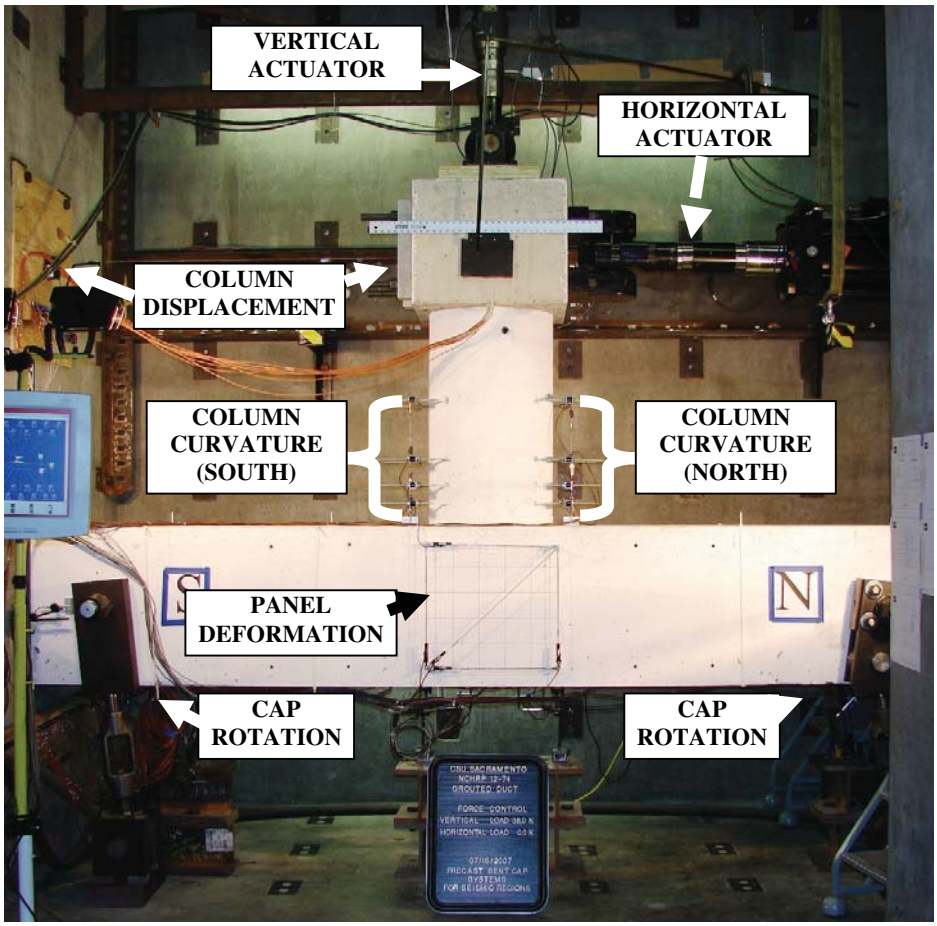

(b) Specimen in Test Bay with External Instrumentation Shown—GD

Figure 2.24. Test setup for emulative specimens.

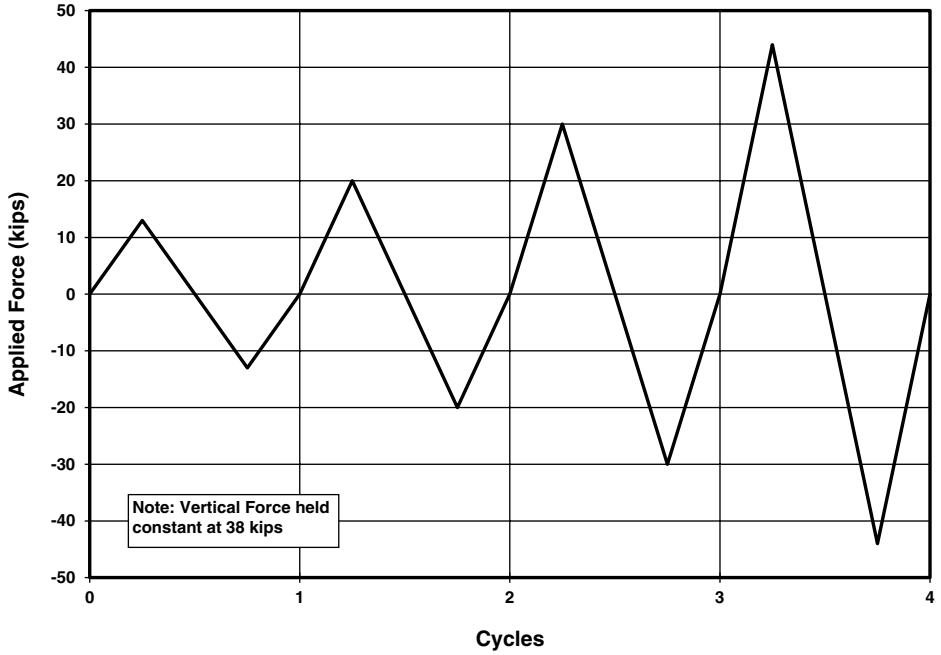

Figure 2.25. Representative force controlled sequence for emulative specimens.

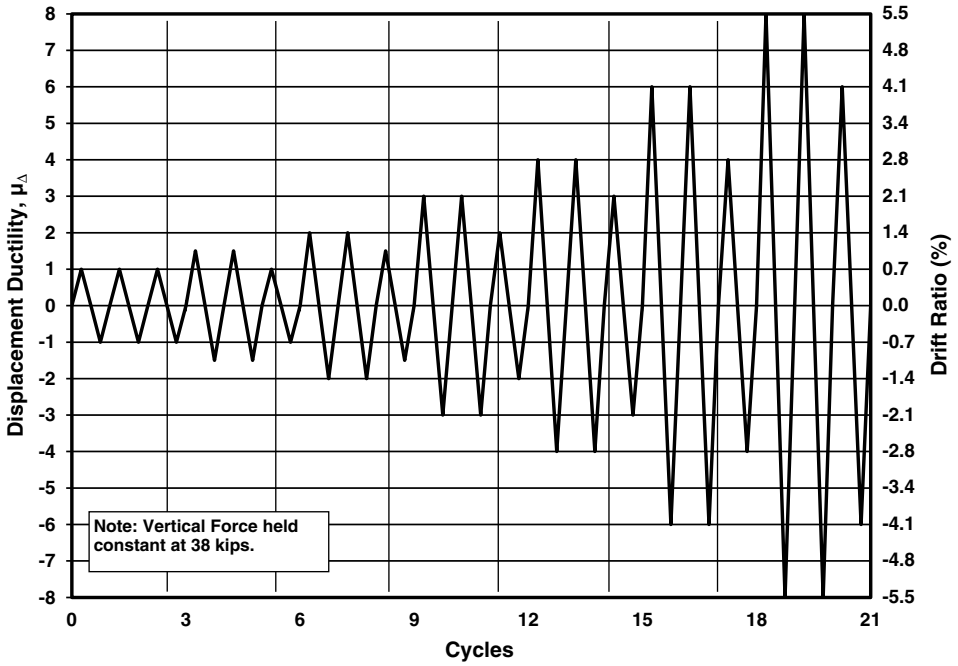

Figure 2.26. Representative displacement controlled sequence for emulative specimens.

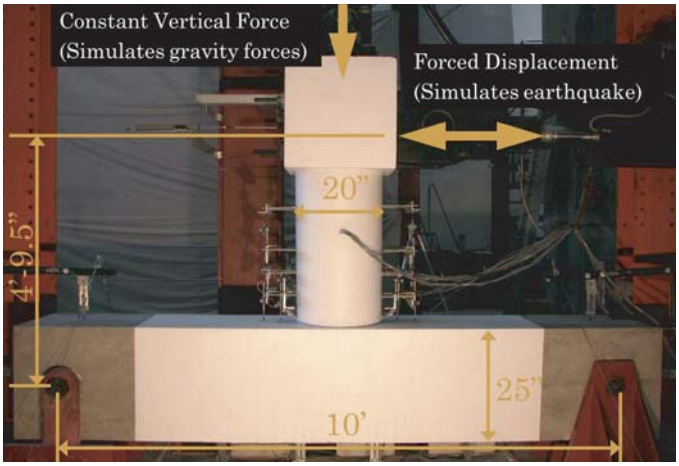

Figure 2.27. Test setup for hybrid specimens.

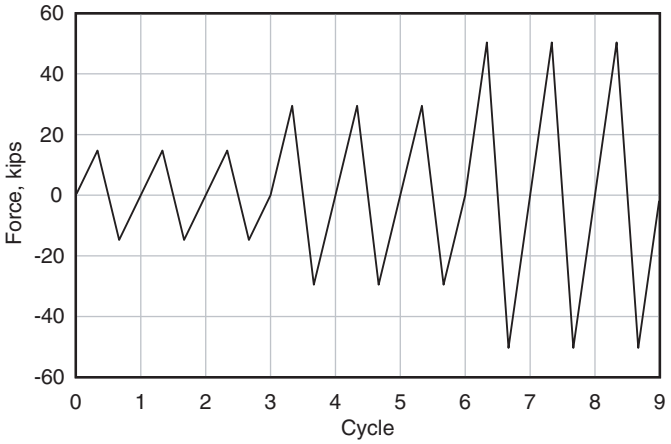

Figure 2.28. Representative hybrid force controlled loading protocol.

External instrumentation mounted on the specimens is shown in Figure 2.30. Instrumentation consisted of linear potentiometers and inclinometers for measuring and isolating various modes of deformation in the member. In addition to the external instrumentation, many internal strain gages were employed to capture the local response of materials.

2.2.4 Design of Integral Prototype Bridge and Specimen

An overall elevation of the prototype bridge is shown in Figure 2.31 with the connection detail shown in Figure 2.32. The design of the prototype bridge was completed in accordance with the AASHTO *LRFD Bridge Design Specifications* (*29*) and the 2009 LRFD SGS (*1*).

The selection of initial member sizing was based on conventional design practices and span range tables for girder systems used. The 74-in deep Washington DOT post-tensioning beam was selected using recommended span limits published for these girders. This girder section was selected over a bulb-tee due to the increased bottom flange area desirable for negative flexural demands at the bent cap. The design was refined through the application of LRFD design requirements, as needed. To minimize the neutral axis depth, a design 28-day compressive strength of 9 ksi was used for the prototype structure.

Post-tensioning in the girders was designed so that the ultimate, extreme event and service limit states were satisfied. The design of the post-tensioning was governed by the Strength I limit state with the seismic demands of a similar magnitude. Two stages of post-tensioning were specified, with the first stage occurring prior to the deck casting and the second stage occurring after the deck casting. Service level performance of the structure was considered in the prototype design through

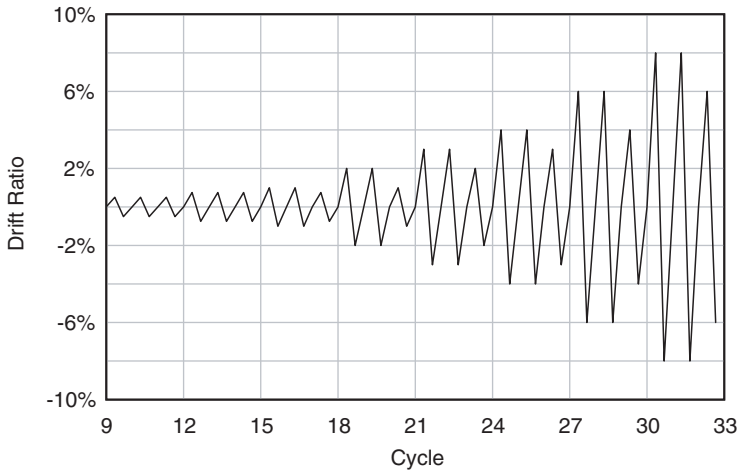

Figure 2.29. Representative hybrid displacement controlled loading protocol.

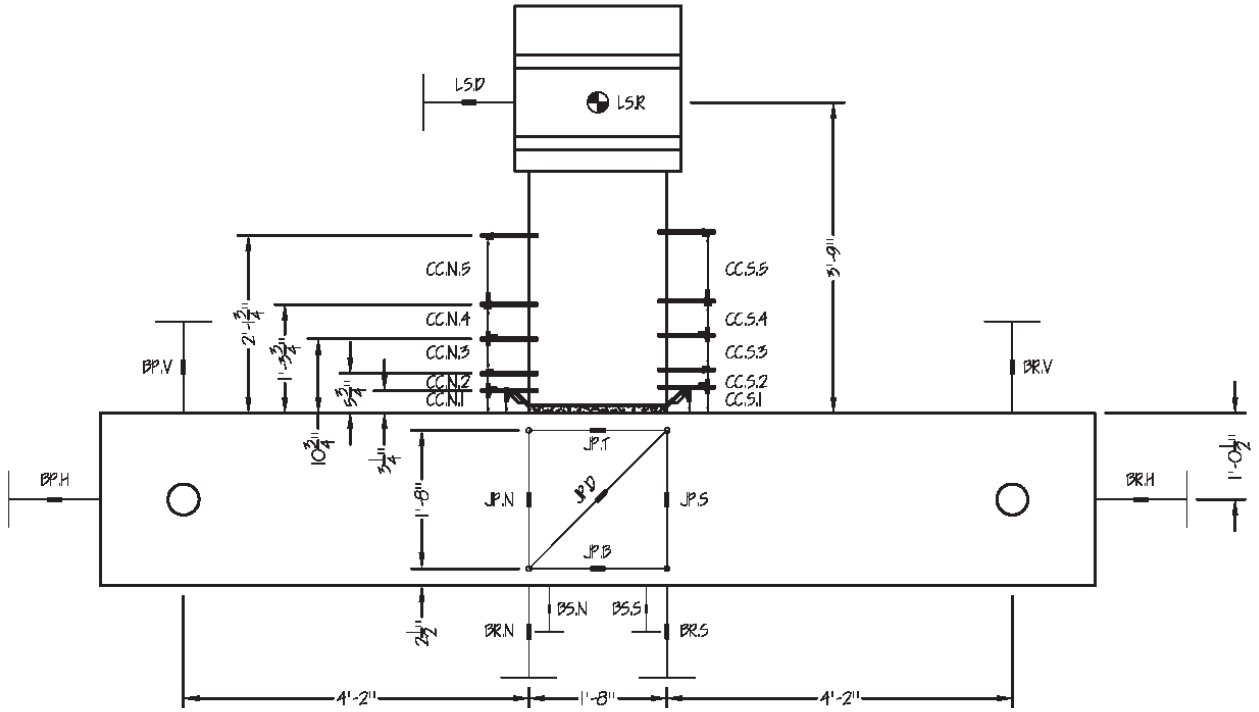

Figure 2.30. Representative hybrid external instrumentation (HYB1 shown).

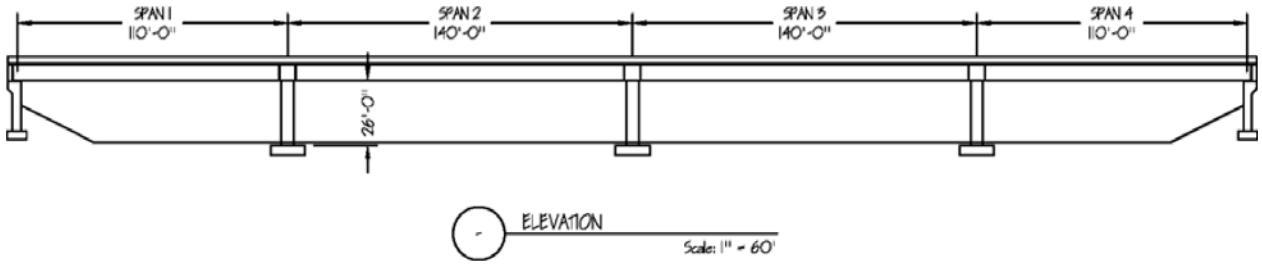

Figure 2.31. Portion of integral prototype bridge.

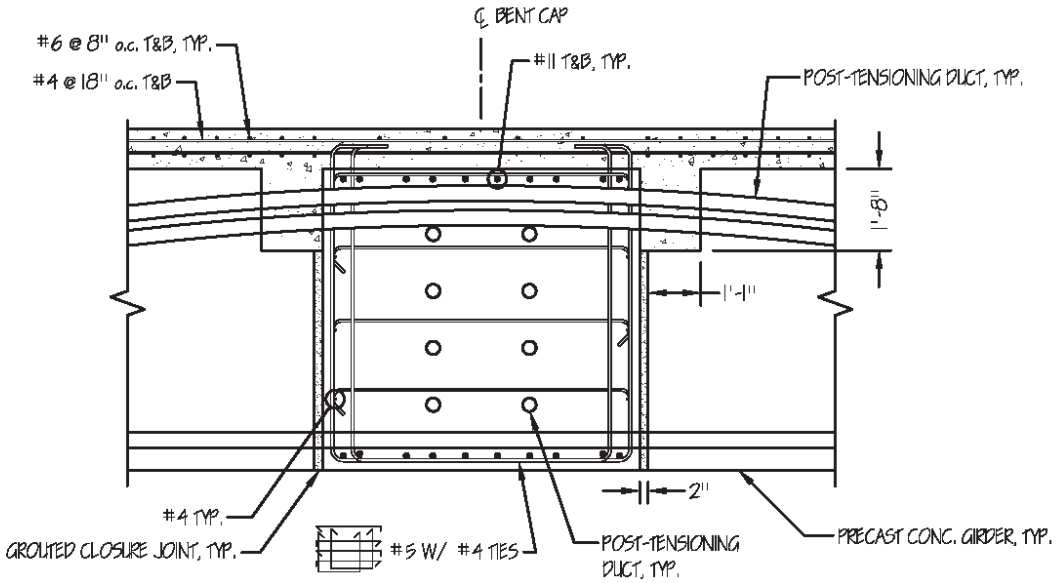

Figure 2.32. Girder to bent cap prototype connection detail.

a construction staging analysis explicitly considering the development of stresses in the system at various stages.

For seismic design, the prototype bridge was considered nonessential and designed to meet life safety requirements as defined by the 2009 LRFD SGS (*1*). The specified mechanism of inelastic deformation in the longitudinal direction consists of flexural plastic hinge formation at both the tops and bottoms of columns and knock off backwalls. Additionally, the superstructure to bent cap joint was allowed to open during seismic excitations as long as the response was essentially elastic. The transverse mechanism involved the development of flexural plastic hinging at both the tops and bottoms of columns and shearing of sacrificial shear keys at the abutments.

The design ARS was developed in accordance with the 2006 LRFD RSGS (*2*). The ARS curve incorporated 5% damping and was developed using a 1-sec acceleration of 0.80 g, a 0.2-sec acceleration of 1.50 g, and site coefficients for Site Class D soil. The resulting peak rock acceleration for the prototype design for the study site was 0.60 g. The input seismic demand and site classification resulted in a bridge subject to SDC D requirements. This ARS curve is representative of a site located in a high seismic region such as Southern California. The imposed demand levels required a seismic demand analysis, displacement capacity analysis with pushover, capacity design provisions, and SDC D detailing. Due to the assumed site location, the bridge was considered located within 6 miles of a fault. Therefore, vertical ground motion with a magnitude of 0.80 g of vertical excitation was considered.

The structural system was modeled in the computer analysis program SAP2000 for service, strength, and seismic design. Modeling procedures for seismic analysis were performed based on provisions of the 2009 LRFD SGS (*1*). Effective section properties were modeled to accommodate the expected dynamic behavior of the bridge system, including column inelasticity. Dynamic analyses indicated that the dominant transverse period of vibration is equal to 0.73 sec and the dominant longitudinal period of vibration is equal to 0.69 sec. The longitudinal analysis considered the effects of the backwall stiffness in accordance with the provisions of the 2009 LRFD SGS. The resulting displacement demands in the longitudinal and transverse directions were 6.8 in and 7.5 in, respectively.

In order to determine the displacement capacity of the system, an inertial pushover analysis was conducted in both the longitudinal and transverse directions. In the longitudinal direction, the bent cap to girder joint was allowed to open during seismic excitation. This decision was made based on extensive discussions with the research team and project panel. It was decided that allowing the bridge to flex and open at the joint was acceptable as long as the joint responded in an essentially elastic manner.

To consider the potential joint opening, a superstructure moment-rotation hinge was modeled at the face of the bent cap. For the prototype design, these hinges were based on moment-curvature analyses of the superstructure and an assumed equivalent plastic hinge length. The original design considered an effective hinge length to be 1 ft; however, a more realistic length is approximately one-half of the structure depth. It is expected that allowing the superstructure joint to hinge will result in a redistribution of seismic moment demand due to the reduction in stiffness following hinging. The prototype design resulted in seismic moment redistribution of approximately 20%. The observed response from analysis indicated that the system is expected to respond in an essentially elastic manner.

In the longitudinal direction, the displacement capacity determined via pushover analysis is 11.0 in, which results in a demand-to-capacity ratio of 0.62. The results of the longitudinal pushover analysis indicated that positive joint opening is expected, but without appreciable rotation demand. The response of the joint is classified as essentially elastic because the calculated rotations are only slightly greater than the elastic rotation. For the transverse displacement capacity, overturning effects were considered in determining the column inelastic response. The transverse displacement capacity determined via pushover analysis was 10.6 in, which results in a demand-to-capacity ratio of 0.71. Ductility demands for both directions were approximately 5, well below the limit of 8 for multicolumn bent caps.

Capacity design principles were applied to the design of the superstructure to ensure that the seismic overstrength demands could be resisted in a nominally elastic manner. Column transverse reinforcement was designed based on overstrength demands imposed by transverse response. Flexural and shear demands on the cap beam were based on the demands developed with flexural hinging of the columns at overstrength demands. Design of bent cap reinforcement was based on overstrength demands in addition to the longitudinal and transverse force-transfer mechanisms assumed in the AASHTO *LRFD Bridge Design Specifications* (*3*).

The main goal of the experimental effort was to determine the response of the girder to bent cap joint when subjected to simulated seismic demands. To satisfy this goal, a portion of the prototype structure was extracted for experimental testing. The test specimen selected for testing consisted of a girder, deck, and reaction block. This specimen was based on an extracted portion of the prototype bridge, as shown in Figure 2.33. The scaled length of the girder used in the experimental program was 31 ft, which is representative of 0.46 times the central span length.

The bent cap was represented by a large reaction block in the testing of the specimen. The flexibility of the bent cap can be neglected in experimental efforts as the deformation from this member can be considered in analytical modeling. The extracted portion of the prototype bridge provides sufficient

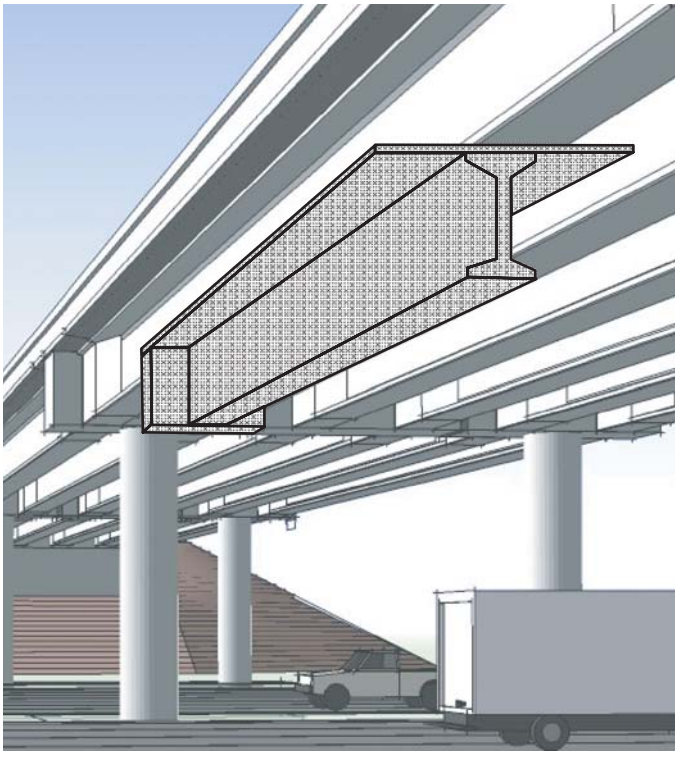

Figure 2.33. Test specimen representation—post-tensioned integral specimen (INT).

information regarding the moment-rotation response of the joint and shear transfer across the joint. These two items are the major unknowns in the performance of this integral bridge detail.

2.2.5 Fabrication and Assembly of Integral Specimen

The integral test specimen was fabricated and constructed at the University of California—San Diego (UCSD) Charles Lee Powell Structural Systems Laboratory. Labor for construction activities was provided by a combination of subcontracted construction firms and lab staff. A local steel fabrication company performed the majority of construction activities related to fabrication of the steel reinforcement cages. A local construction company experienced in bridge construction performed the majority of construction activities related to building formwork. All post-tensioning activities were performed by a post-tensioning manufacturer and contractor. Lab staff performed the casting of concrete and all activities related to erection of members.

The first stage of fabrication consisted of the construction of the reinforcing cages for the girder and reaction block. The girder reinforcing cage can be seen in Figure 2.34 with the post-tensioning ducts installed and the cage installed in the formwork. The scaling of this specimen did not provide significant access for pencil vibrators in the duct. To ensure that adequate consolidation would be achieved during fabrication, a form vibrator was used in regions with limited pencil vibrator access. In addition, a superplasticized concrete mix was used to enhance flowability during casting.

Figure 2.34. Girder reinforcing cage.

Concrete for the girder and reaction block was cast using a bucket attached to the overhead crane in the laboratory. The girder was cast first to ensure that the maximum flowability of the concrete mixture was obtained during the casting of the member with limited vibrator access. During casting of the girder, an external form vibrator was attached to the formwork near the location at which concrete was being poured. This vibrator was moved around the formwork as concrete was placed in different locations and was used on both sides of the formwork. At the end regions, where more sufficient vibrator access was provided, traditional pencil vibrators were used.

The girder and reaction block were cast and allowed to harden until the girder had strength greater than 3 ksi. Inspection of the girder after form removal indicated only one region of minor concrete segregation over a small portion of the bottom flange of the girder (approximately 4 in. in length). This region was patched by lab staff following placement on temporary supports. The girder was moved away from the reaction block to facilitate the construction of two temporary support towers. Following the completion of these towers, the girder was lifted and placed on the towers in line with the reaction block (see Figure 2.35). The girder was leveled on the temporary supports and subsequently secured using chains to provide stability during construction activities.

The girder was placed to maintain an approximate 1-in closure joint between the reaction block and girder. This joint can be seen in Figure 2.36. Additionally, the alignment was checked to ensure the post-tensioning ducts were properly aligned. The careful activities carried out during the placement of the

Figure 2.35. Girder on falsework prior to grouting closure joint.

girder resulted in a system in which the post-tensioning ducts and closure joint were properly aligned with no noticeable variations. The post-tensioning ducts were then jointed using industrial adhesive tape, which was applied by hand. The scaled specimen made the joining of these ducts slightly cumbersome, as hand access was tight. However, the splicing of these ducts was performed without any major complications.

The girder formwork was modified and reused as the closure joint formwork by drilling new holes in the form and reusing the original form tie holes in the girder. After installation of the side forms, the bottom of the joint was closed using a single piece of plywood. A drain hole was placed in the bottom of the form to allow for draining of excess water (water is used to moisten the faces of the reaction block and girder prior to grouting). The edges of the formwork were sealed using a commercially available sealant and allowed to set prior to grouting. Grout material was mixed on the laboratory floor and lifted onto the top of the specimen. The grout was then gravity fed into the closure joint, as shown in Figure 2.37. The grout material was Masterflow 928 high-strength, non-shrink grout containing a 0.2% volume fraction of polypropylene fibers. This grout matrix was mixed to be flowable based on manufacturer's recommended water content and considering the presence of the fibers. The relatively low volume fraction of fibers did not greatly affect the flowability of the matrix. No noticeable leakage was observed during the grouting activities. The grouting activities were completed without any observed complications.

Formwork was removed from the girder the following day. Observations after removal of the formwork indicated no observable voids in the closure joint and overall a very successful grouting operation. The grout was allowed to cure for 3 days prior to the first stage post-tensioning. The first portion of the post-tensioning operation consisted of setting the wedges for the bottom tendons. Each strand was stressed to approximately 5% guaranteed ultimate tensile strength (GUTS) to allow for sufficient seating of the wedge on the live end. The middle tendon was then stressed to a target stress of 75% GUTS. Each strand was individually stressed using a monostrand jack. Both the bottom and middle ducts were then grouted using SikaGrout 300PT. Following 2 days of curing in the post-

(a) (b)

Figure 2.36. Girder post-tensioning duct (a) prior to splicing and (b) after splicing.

Figure 2.37. Grouting of girder to reaction block closure joint.

tensioning grout, the temporary support near the reaction block was removed, simulating the removal of the strong back in the prototype structure. The post-tensioning force in the middle tendon at this stage provides a sufficient shear friction mechanism in the system for casting of the deck and associated construction activities.

Formwork for the reinforced concrete deck was constructed to react off the girder, as is customary in precast concrete bridge construction (see Figure 2.38). The construction of the deck formwork utilized the existing holes in the girder from the form ties to secure the forms in place. With the formwork in place, the deck reinforcing cage was fabricated. Similar to casting of the deck and reaction block, the deck was cast using a bucket attached to the overhead crane. The deck formwork was removed after the minimum uniaxial compressive strength of the deck concrete was 3 ksi.

Figure 2.38. Construction of concrete deck reacting off girder.

The top post-tensioning tendon was stressed following the casting and curing of the deck. This tendon was stressed to 75% GUTS, similar to the middle tendon. Additionally, each strand in the tendon was individually stressed using a monostrand jack. Following post-tensioning, the duct was grouted using SikaGrout 300PT and allowed to cure. The specimen was then painted white to aid in the identification of cracking during testing. Loading frames and external instrumentation were subsequently installed on the specimen, in addition to the installation of vertical actuators in preparation of testing.

2.2.6 Integral Specimen Testing Protocol and Instrumentation

The general testing system is shown in Figure 2.39. From this figure, the nomenclature for actuator reference and plan location reference can be observed.

For the integral testing protocol, the first stage of loading consisted of relieving the reaction from the temporary support installed between Actuator 1 and Actuator 2. The goal of this stage was to relieve the reaction while minimizing the associated displacement. Actuators 2 and 3 were set to force control with zero force. Actuator 1 was controlled in manual displacement control and applied upward displacements until the load on the temporary support tower was relieved.

The next stage of loading was designed to apply the simulated dead loading. Actuator 1 was controlled in displacement control and applied upward displacements until a specified force was reached. Actuators 2 and 3 were slaved to Actuator 1 in force control to apply moment and shear profiles as shown in the prototype specimen section.

For all additional stages, Actuator 1 was controlled in displacement until either a specified force or joint rotation limit was reached. A modified equation relating the force in Actuators 2 and 3 to the force in Actuator 1 was used. This new

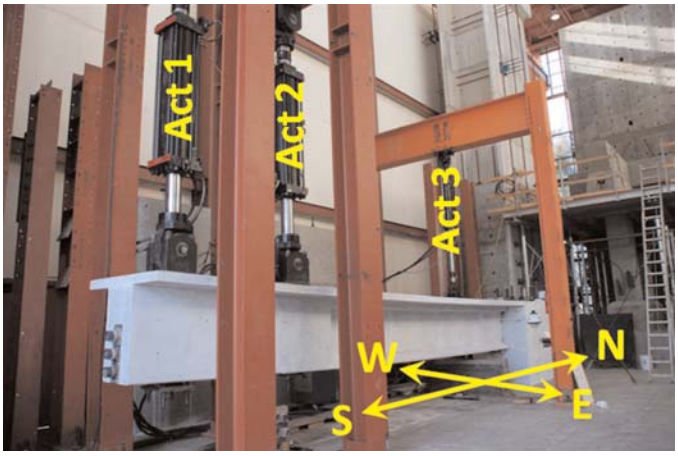

Figure 2.39. Integral specimen loading system.

loading equation is based on the seismic flexural and shear demand profiles determined via lateral analysis of the prototype structure.

Following the application of the simulated dead loading, 100 cycles of essentially elastic loading were imposed on the system primarily in the negative flexural direction. This loading was meant to allow investigation of the potential response of the system in service and ultimate loading. The system was loaded initially in the negative flexural direction until the system was nearing the expected limit of proportionality. Following this, the system was loaded to 90% of the initial dead load demand. This was repeated for 100 cycles in continuous operation.

The next stage of loading was simulated seismic demands. The loading demands generated for the seismic stage were based on a combination of lateral seismic load demands and vertical seismic shear demand. The vertical seismic shear demand was held constant during all phases, with constant loading applied at the actuator nearest the joint. Flexural moment and shear demands were based on scaled flexural demands caused by simulated column overstrength demands. The simulated flexural demands impose flexural moments at the girder to reaction block interface that are applicable to vertical, lateral, or seismic settlement demands. The cyclic loading is conservative for loadings generated by seismically induced settlement. Additionally, the additional shear demand applied at the joint is conservative for lateral loading scenarios. This loading program was developed to conservatively encompass the various potential loading cases.

The loading was controlled while operating Actuator 1 in displacement control set to hold when a specified joint rotation limit was reached. The rotation targets were initially specified using the linear potentiometers at the joint. However, it became apparent during testing that these calculated rotations were not correct during increasing displacements due to cracking at potentiometer target supports and spalling of concrete. The actual achieved rotations were reassessed based on more reliable inclinometer readings, which better match the observed rotations during testing. The actual loading protocol used during the seismic cycle is shown in Figure 2.40. As a main goal of large joint rotation cycles is to determine the overall rotation capacity of the connection due to relative settlement potential, a reversed cyclic loading protocol, which produces a highly sever case, was used. This is because relative settlement demands on the connection will only occur in one loading direction and not the reverse. This protocol probably caused a reduction in the actual ultimate rotation capacity when subjected to loading in a single direction. Another driving factor in the development of this testing protocol was the desire to determine the inelastic rotation response in the event of superstructure inelasticity.

The test specimen was instrumented to capture the major response characteristics of the specimen when subjected to applied loadings. This instrumentation includes strain gages mounted on rebar and post-tensioning and external gages mounted onto the specimen.

External instrumentation consists of linear potentiometers, string potentiometers, and inclinometers mounted on the exterior of the specimen. A summary of external instrumentation is shown in Figure 2.41. Linear potentiometers are placed to capture opening of the joint, slip between the girder and reaction block, and estimated rotation of the girder at the joint. String potentiometers are installed to capture the displacement of the specimen at the actuator locations. Inclinometers are installed to capture the rotation of the reaction block and girder at the joint. Strain gages were installed on deck longitudinal

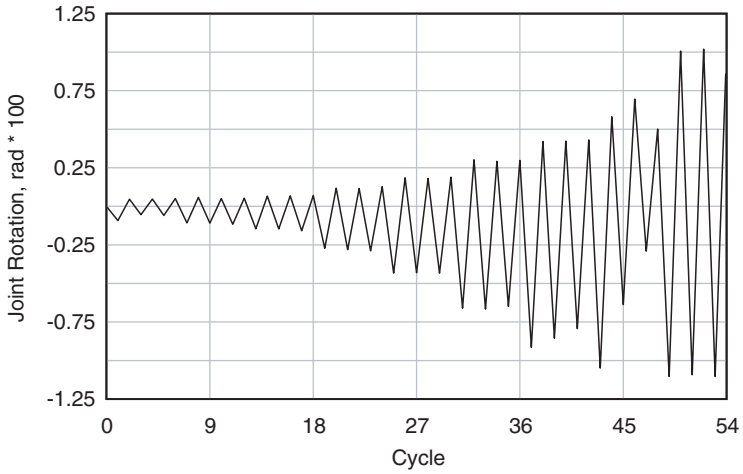

Figure 2.40. Integral specimen realized loading protocol.

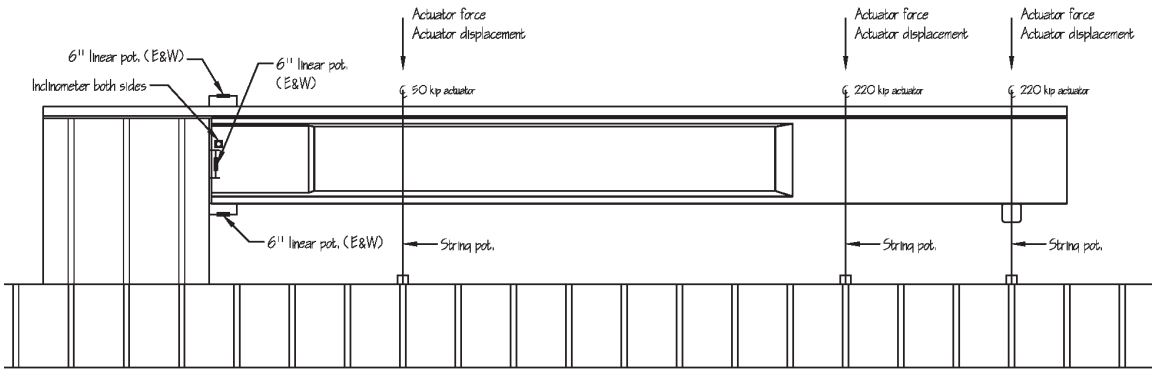

Figure 2.41. Integral specimen external instrumentation plan.

reinforcement, girder longitudinal reinforcement at the base, and girder shear reinforcement.

2.3 Test Results

This section summarizes key aspects of specimen response for the emulative, hybrid and integral experimental tests. Detailed results are provided by Matsumoto (*30, 21, 22, 23, 26*) and Tobolski (*5*).

In reporting specimen response, displacement ductility (μ) and drift ratio are both used. The drift ratio is the column displacement divided by the column height and is reported as a percentage. This is a more consistent basis for comparison of specimen response than displacement ductility. However, system ductility levels are also reported, although these values should be considered nominal (i.e., approximate) due to the approximate determination of first yield. The terms "drift" and "drift ratio," are used interchangeably.

2.3.1 Nonintegral Emulative Connections

This section summarizes primary aspects of specimen response, including column hysteretic response (lateral force displacement), displacement decomposition, and joint response. Comparisons are made between the CIP and precast connections, as well as between the full and limited ductility specimens.

The lateral force displacement (hysteretic) response of the column is used to characterize the fundamental performance of the specimen. Displacement decomposition refers to the separation of the column displacement into the components that contribute to the overall lateral displacement of the column (column flexure, fixed end rotation due to plastic hinging and bar slip, bent cap flexibility, and joint shear). Comparisons are made between decomposition for analytical predictions and experimental measurements. Joint response includes a summary of joint cracking, principal stresses, joint deformation, and strain records.

Cast-in-Place Specimen

CIP specimen response was dominated by plastic hinging of the column adjacent to the bent cap, as shown in Figure 2.42 and Figure 2.43. The specimen exhibited excellent ductility to a large drift of 5.9% (nominal displacement ductility of 10), and the load-displacement response indicated stable hysteretic behavior without appreciable strength degradation. Post-test inspection revealed that the core remained primarily intact with several column bars buckling and fracturing at ultimate. Initial spalling of the column occurred at 1.8% drift (μ3), with progressive spalling at higher drifts. In contrast to significant

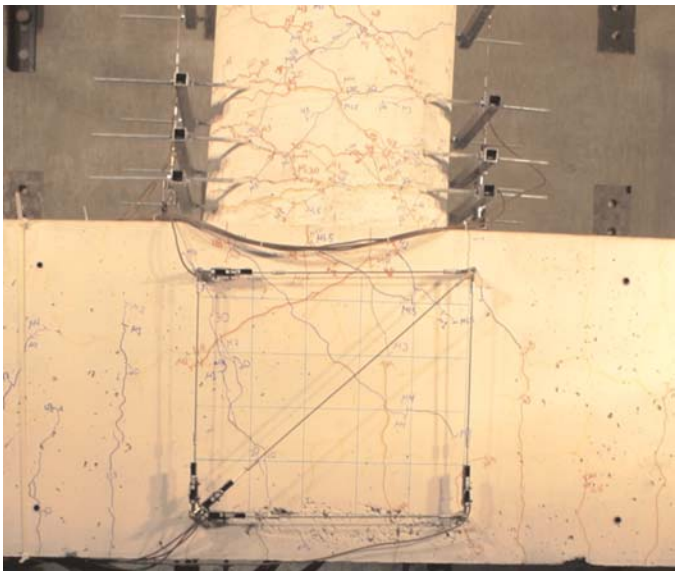

Figure 2.42. Specimen response at a 2.3% drift ratio (μ4)—CIP.

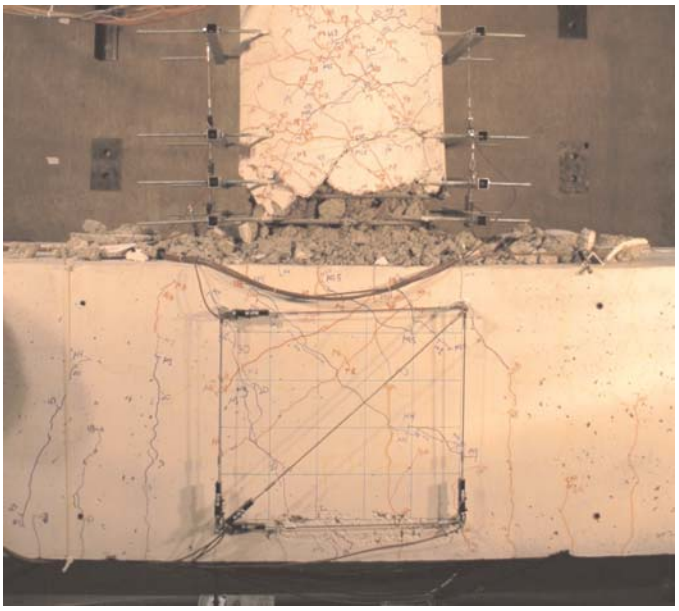

Figure 2.43. Specimen response at a 5.9% drift ratio (μ10)—CIP.

column flexural and shear cracks and spalling associated with increasing lateral force, relatively minor cracking occurred in the joint region (0.025 in maximum) without spalling. This corresponded to stiff joint shear response and limited softening, with the contribution of joint shear to column displacement averaging 3.4%. Principal tensile stresses significantly exceeded 3.5 $\sqrt{f_c'}$ psi and justified the use of additional joint reinforcement required for development of a force transfer mechanism. Bent cap longitudinal bars reached only 46% of yield. However, the north construction stirrup within the joint yielded, indicating its contribution to the stable joint performance.

Column Lateral Force versus Lateral Displacement. The lateral force displacement (hysteretic) response of the column, shown in Figure 2.44, indicates stable hysteretic behavior with loops of increasing area without appreciable strength degradation. A comparison of the load-displacement envelope to the predicted envelope showed a good correlation. The hysteretic response also portrayed appropriate stiffness, strength, ductility, and features such as crack distribution and width representative of appropriate response for a CIP beam-column connection. The dominance of ductile plastic hinging in the column and minimal damage in the capacity-protected joint and bent cap satisfied the performance goal for the CIP control specimen. Thus, the specimen provided an appropriate baseline for comparison with the precast specimens.

Column Displacement Decomposition. Column displacement decomposition, summarized in Figure 2.45, confirmed the dominance of plastic hinging and showed that displacement components were reasonably determined and predictions were reasonably made. The joint shear displacement was minor, contributing only 3.4% on average to the overall column displacement, and was consistent with visual observations of minor joint cracking. Splitting cracks formed

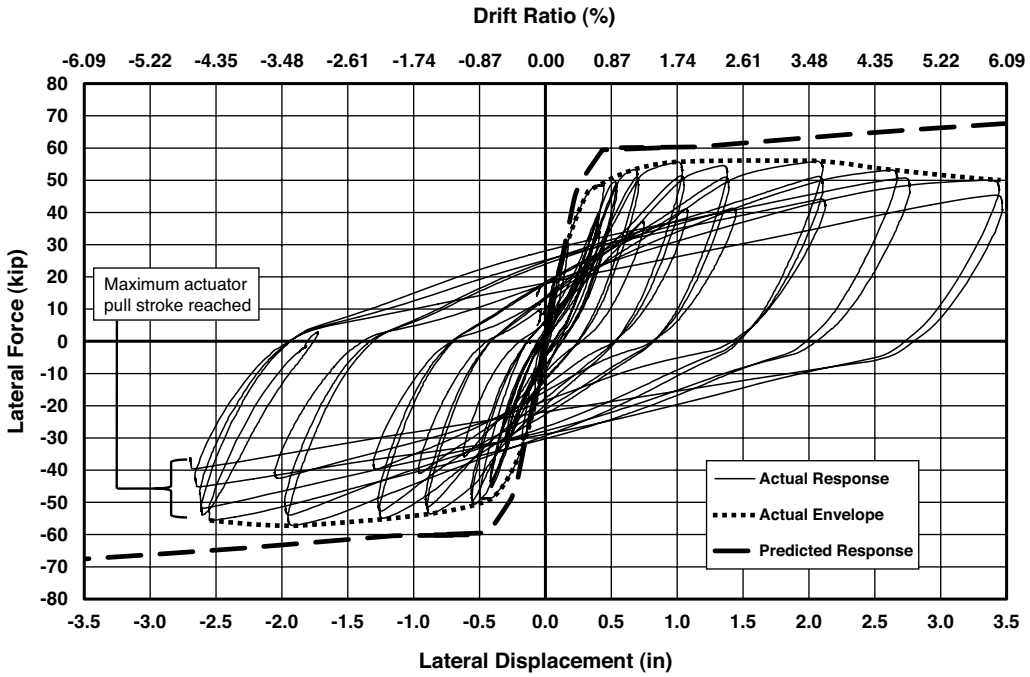

Figure 2.44. Lateral force versus lateral displacement—CIP.

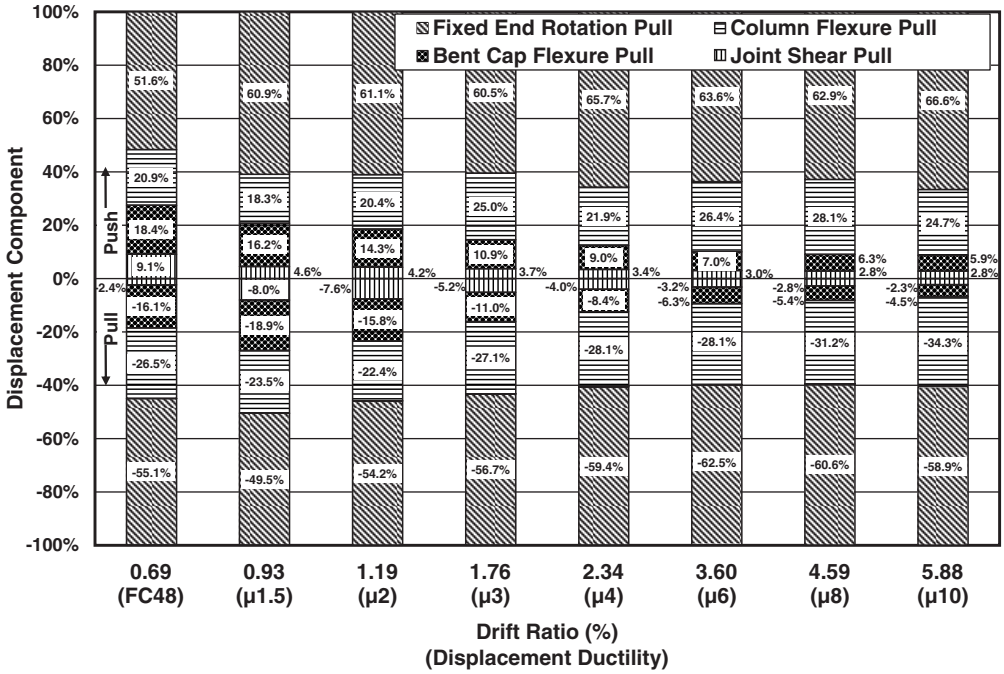

Figure 2.45. Displacement decomposition component percentages—CIP.

in the bent cap and column, and the top surface of the bent cap (as tested) exhibited splitting cracks and local spalling; however, column bars were well anchored within the joint, with bar slip contributing less than 4% on average to fixed end rotation.

Joint Response. As shown in Table 2.3, CIP joint distress was limited. Analysis of the joint indicated that the principal tensile stress was limited to 5.4 $\sqrt{f_c'}$ psi, less than half of the 2006 LRFD RSGS (*2*) limit of 12 $\sqrt{f_c'}$ psi, but about 50% larger than 3.5$\sqrt{f_c'}$ psi, the level at which more extensive (additional) joint reinforcement is required for development of the assumed force transfer mechanism. Principal compressive stresses did not exceed 0.09f_c', less than a third of the 2006 LRFD RSGS limit of 0.25f_c'. These values correspond well with the intentions of the design and the observed joint performance. The joint shear stress-strain response was appropriately stiff and exhibited minor softening at increasing drift (see envelope in Figure 2.46). This correlated well with the maximum surface crack width in the joint region that was limited to 0.025 in (with no surface spalling), as shown in Figure 2.47, as well as displacement decomposition results. Joint deformation was very small, with maximum change in panel area limited to less than 0.2%. Bent cap longitudinal bars did not yield, reaching only 46% of yield, even though additional bent cap longitudinal reinforcement (0.245A_{st}) required by 2009 LRFD SGS was not included (*1*). Stirrup strain outside the joint remained well

Table 2.3. Maximum joint response—all specimens.

Parameter		CIP	GD	CPFD	CPLD
Joint Shear Stress	(psi)	328 (4.86$\sqrt{f_c'}$)	312 (4.62$\sqrt{f_c'}$)	323 (4.31$\sqrt{f_c'}$)	371 (6.32$\sqrt{f_c'}$)
Principal Tensile Stress	(psi)	363 (5.38$\sqrt{f_c'}$)	343 (5.09$\sqrt{f_c'}$)	356 (4.75$\sqrt{f_c'}$)	411 (6.99$\sqrt{f_c'}$)
Principal Compressive Stress	(psi)	401 (0.088f_c')	370 (0.081f_c')	398 (0.071f_c')	460 (0.13f_c')
Angle of Principal Plane	(deg)	45.0	45.0	44.2	44.8
Joint Rotation	(rad)	1.95×10^{-3}	2.25×10^{-3}	1.73×10^{-3}	2.87×10^{-3}
Change in Panel Area	(%)	0.16	0.19	0.13	0.46

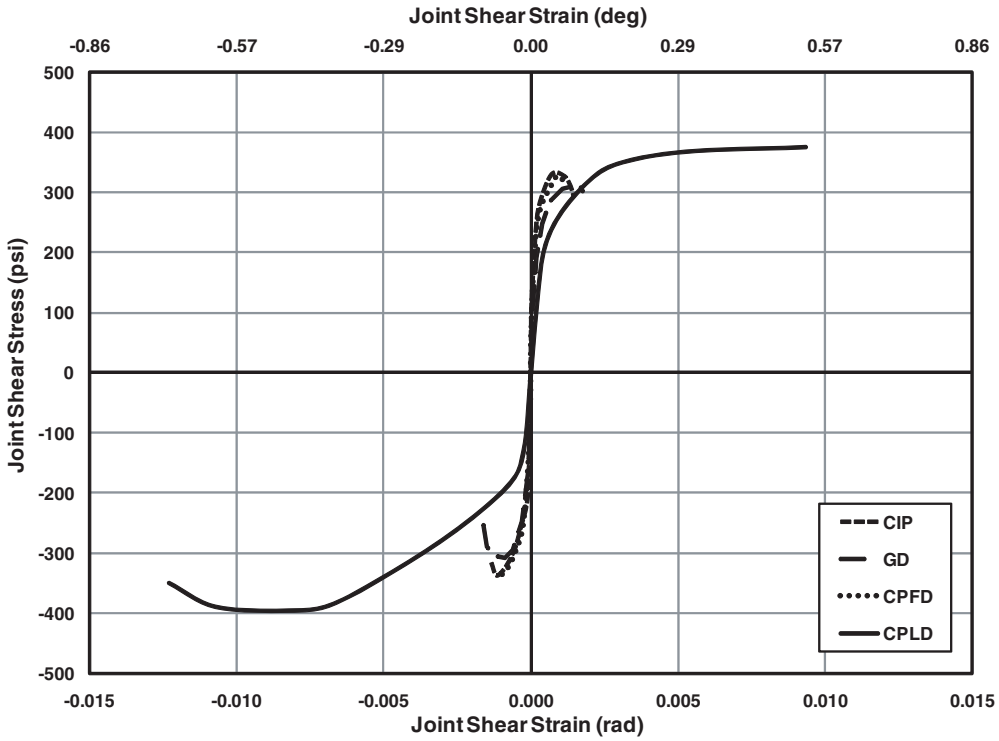

Figure 2.46. Joint shear stress versus joint shear strain envelopes—all specimens.

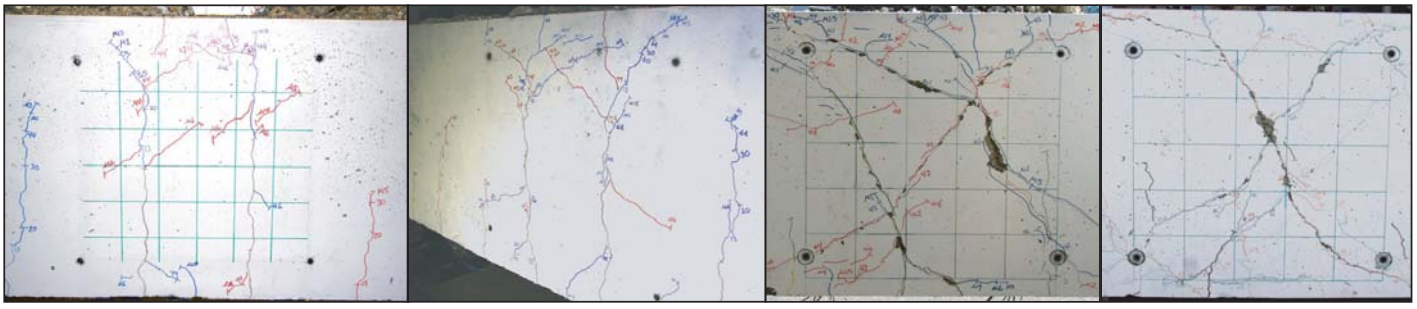

(a) East Side—CPFD (b) West Side—CPFD (c) East Side—CPLD (d) West Side—CPLD

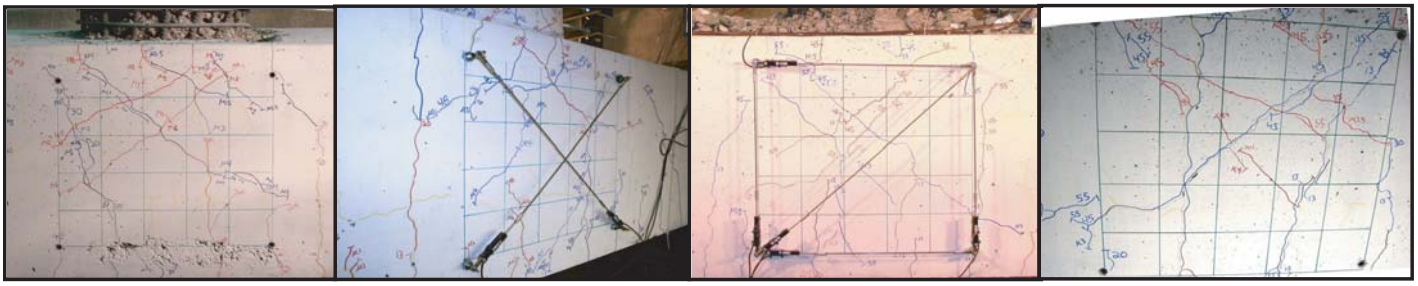

(e) East Side—CIP (f) West Side—CIP (g) East Side—GD (h) West Side—GD

Figure 2.47. Joint region cracking post test—emulative specimens.

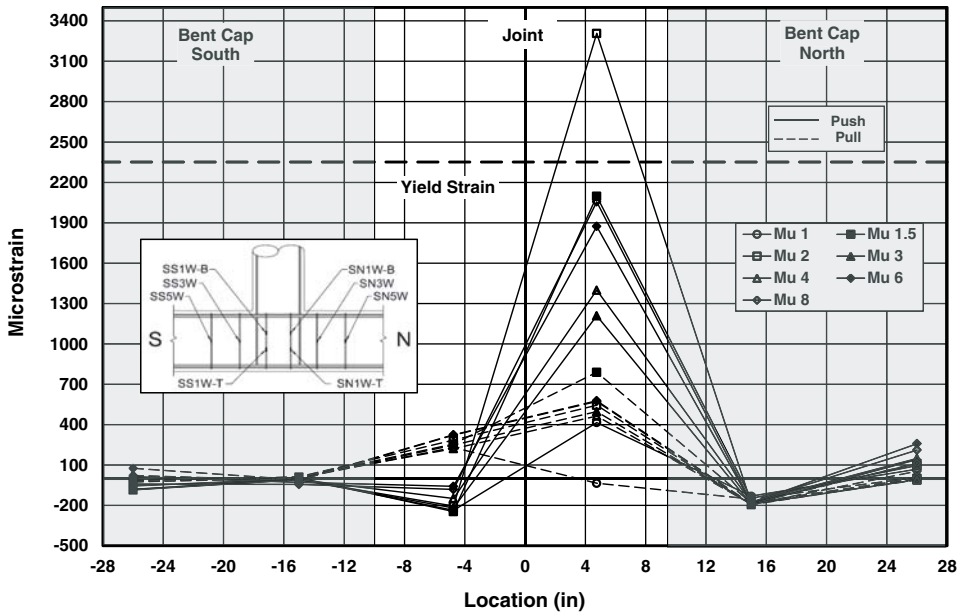

Figure 2.48. Strain profile—stirrups in bent cap (midheight) and joint (bottom), displacement control—CIP.

below yield, but the north construction stirrup within the joint yielded, as shown in Figure 2.48, indicating its contribution to the stable joint performance.

Grouted Duct Specimen

GD specimen response was dominated by plastic hinging of the column adjacent to the bent cap (Figure 2.49 and Figure 2.50), as intended by the emulative assumption in the design. Similar to the CIP specimen, the GD specimen exhibited excellent ductility to a large drift of 5.2% (nominal displacement ductility of 8), and load-displacement response indicated stable hysteretic behavior without appreciable strength degradation. Post-test inspection revealed that the core and bedding layer remained primarily intact with several column bars buckling and two bars fracturing at ultimate. Initial spalling of the column developed at the column-bedding layer interface at 1.2% drift (μ1.5), with progressive spalling at higher drifts. As for the CIP specimen, significant column flexural and shear cracks and spalling developed, but relatively minor cracking occurred in the joint region (0.040 in maximum). This corresponded to stiff joint shear response and limited softening, with the contribution of joint shear to column displacement averaging 4.9%. Column bars were well anchored within the ducts, with only minor bar slip evident.

Principal tensile stresses significantly exceeded $3.5\sqrt{f_c'}$ and justified the use of additional joint reinforcement required for development of a force transfer mechanism. Similar to the CIP specimen, bent cap longitudinal bars reached only 53% of yield. The south construction stirrup reached 75% of yield, indicating its contribution to the stable joint performance.

Column Lateral Force versus Lateral Displacement. The lateral force displacement (hysteretic) response of the GD column, shown in Figure 2.51, indicates stable hysteretic behavior with loops of increasing area without appreciable strength degradation, as well as stiffness, strength, ductility, and features such as crack distribution anticipated for an emulative

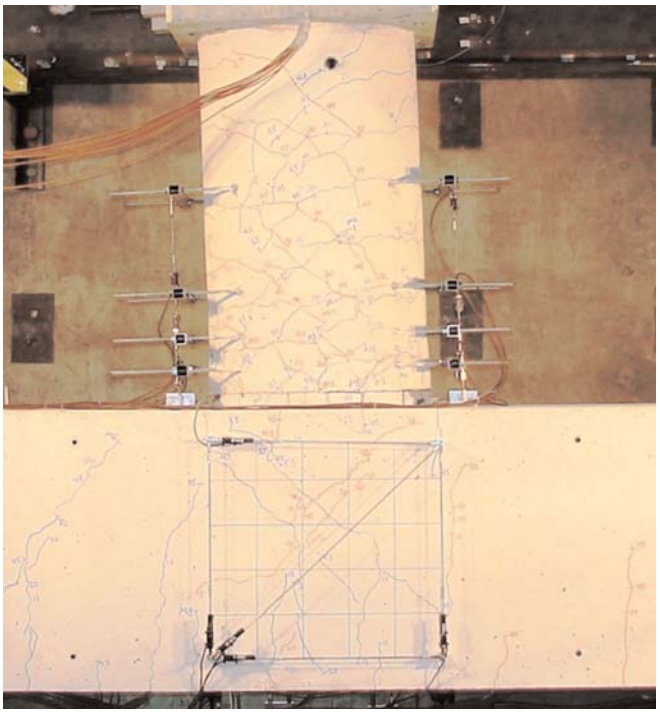

Figure 2.49. Specimen response at a 2.6% drift ratio (μ4)—GD.

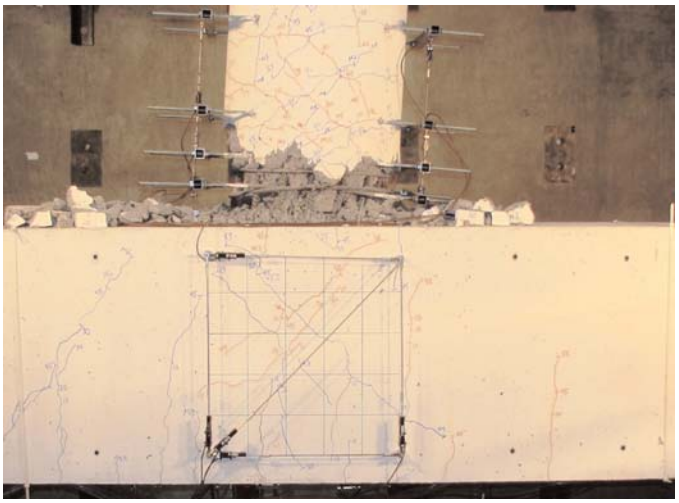

Figure 2.50. Specimen response at a 5.1% drift ratio (μ8)—GD.

beam-column connection test. A comparison of the load-displacement envelope to the predicted envelope showed a good correlation. In addition, Figure 2.52 reveals a very similar load-displacement response for the GD and CIP specimens. The dominance of ductile plastic hinging in the column and minimal damage in the capacity-protected joint and bent cap satisfied the emulation performance goal for the GD specimen.

Column Displacement Decomposition. GD column displacement decomposition, summarized in Figure 2.53, confirmed the dominance of plastic hinging and showed that displacement components were reasonably determined and predictions were reasonably made. The joint shear displacement was minor, contributing 4.9% on average to the overall column displacement, and was consistent with visual observations of minor joint cracking. Column bars were well anchored within the ducts, and although splitting cracks developed between ducts (at the top and bottom of the bent cap as tested), there was no evidence of grout splitting within ducts, initiation of pullout failure, significant bar slip or duct slip. Displacement component magnitudes and percentages for the GD and CIP specimens compared very favorably.

Joint Response. As shown in Table 2.3 and Table 2.4, GD joint distress was limited and joint behavior compared very favorably with the CIP specimen. Analysis of the joint indicated that the principal tensile stress was limited to $5.1\sqrt{f_c'}$, less than half of the 2006 LRFD RSGS (*2*) limit of $12\sqrt{f_c'}$, but about 50% larger than $3.5\sqrt{f_c'}$, the level at which more extensive (additional) joint reinforcement is required for development of the assumed force transfer mechanism. Principal compressive stresses did not exceed $0.08f_c'$, less than a third of the 2006 LRFD RSGS limit of $0.25f_c'$. These values correspond well with the intentions of the design and the observed joint performance. The joint shear stress-strain response compared closely with the CIP, with limited joint softening evident at increasing drift ratios (see Figure 2.46). This correlated well with the max-

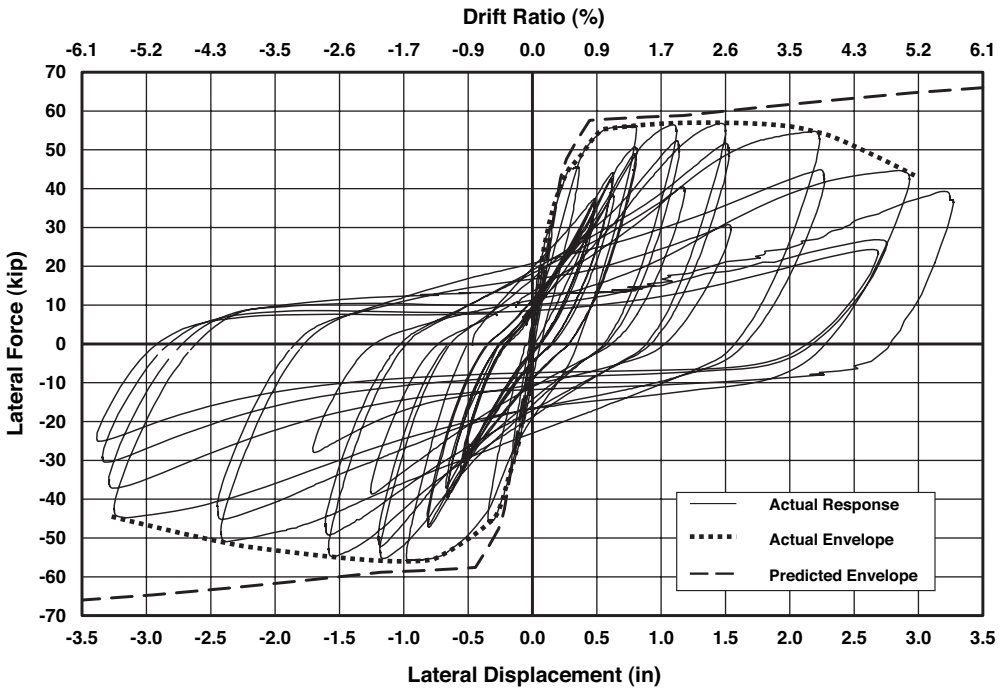

Figure 2.51. Lateral force versus lateral displacement—GD.

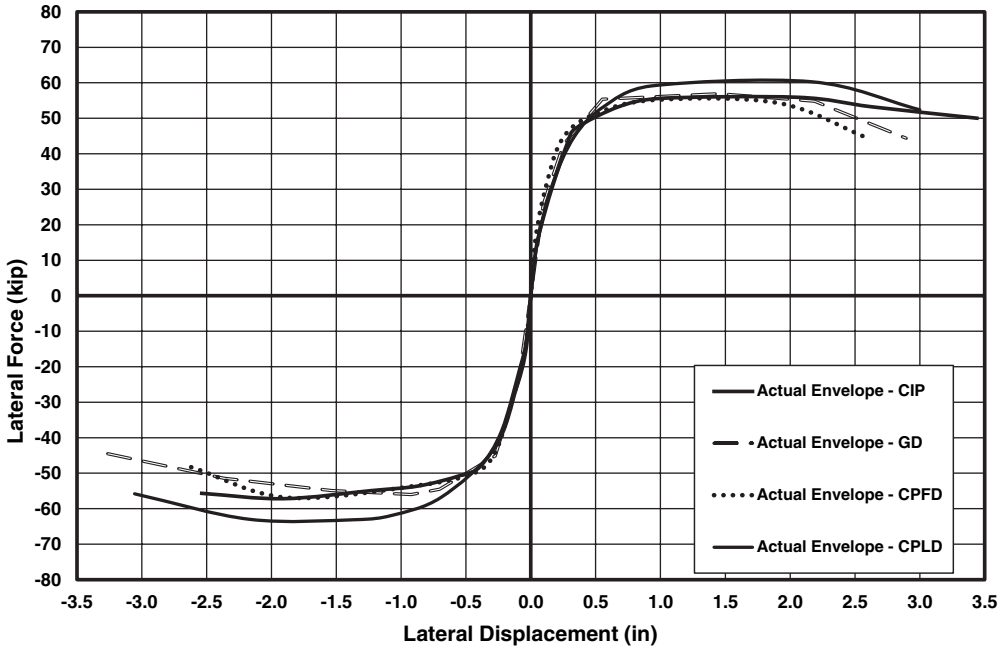

Figure 2.52. Applied lateral force versus lateral displacement envelopes—all specimens.

imum surface crack width in the joint region that was limited to 0.040 in, as shown in Figure 2.47, as well as displacement decomposition results.

Diagonal joint crack patterns were reasonably consistent for the GD and CIP specimens, as were flexural crack patterns. Although maximum joint crack widths for the GD specimen were somewhat larger (0.040 in versus 0.025 in), they were consistent with the level of joint stresses. Minor surface spalling developed on the east face of the bent cap for GD, whereas no spalling developed for CIP. Joint deformation was very small, with maximum change in panel area limited to less than 0.2%. The GD bedding layer performed integrally with

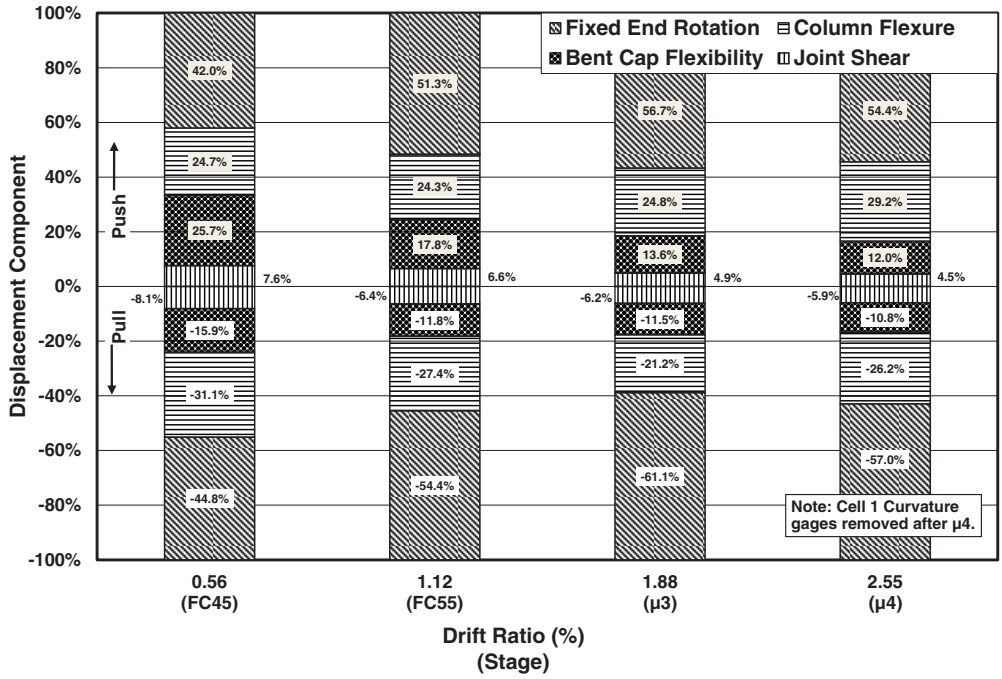

Figure 2.53. Displacement decomposition component percentages—GD.

Table 2.4. Maximum joint response—comparison ratios for all specimens.

Parameter	GD/CIP	CPFD/CIP	CPLD/CIP	CPLD/CPFD
Joint Shear Stress	0.95	0.89	1.30	1.47
Principal Tensile Stress	0.94	0.88	1.30	1.47
Principal Compressive Stress	0.92	0.81	1.48	1.86
Angle of Principal Plane	1.00	0.98	1.00	1.01
Joint Rotation	1.15	0.89	1.47	1.66
Change in Panel Area	1.19	0.81	2.82	3.26

the column, and crushing of the column concrete above the bedding layer confirmed the preferable condition that grout was not a weak link in the system. Similar to the CIP specimen, bent cap longitudinal bars reached only 53% of yield, even though the additional bent cap longitudinal reinforcement ($0.245A_{st}$) required by 2009 LRFD SGS was not included (*1*). Stirrup strain outside the joint reached 68% of yield, and, although the construction stirrups within the joint did not yield, the south construction stirrup reached 75% of yield (see Figure 2.54), indicating its contribution to the stable joint performance. The CIP specimen exhibited a similar trend of large stirrup strains (exceeding yield) within the joint.

Cap Pocket Full Ductility Specimen

CPFD specimen response was dominated by plastic hinging of the column adjacent to the bent cap (see Figure 2.55 and Figure 2.56), as intended by the emulative assumption in the design. Similar to the CIP specimen, the CPFD specimen exhibited excellent ductility to a large drift of 4.3% (nominal displacement ductility of 8), and load-displacement response indicated stable hysteretic behavior without appreciable strength degradation. Post-test inspection revealed that two column bars fractured after buckling at ultimate. Initial spalling of the column just above the bedding layer formed at a drift of

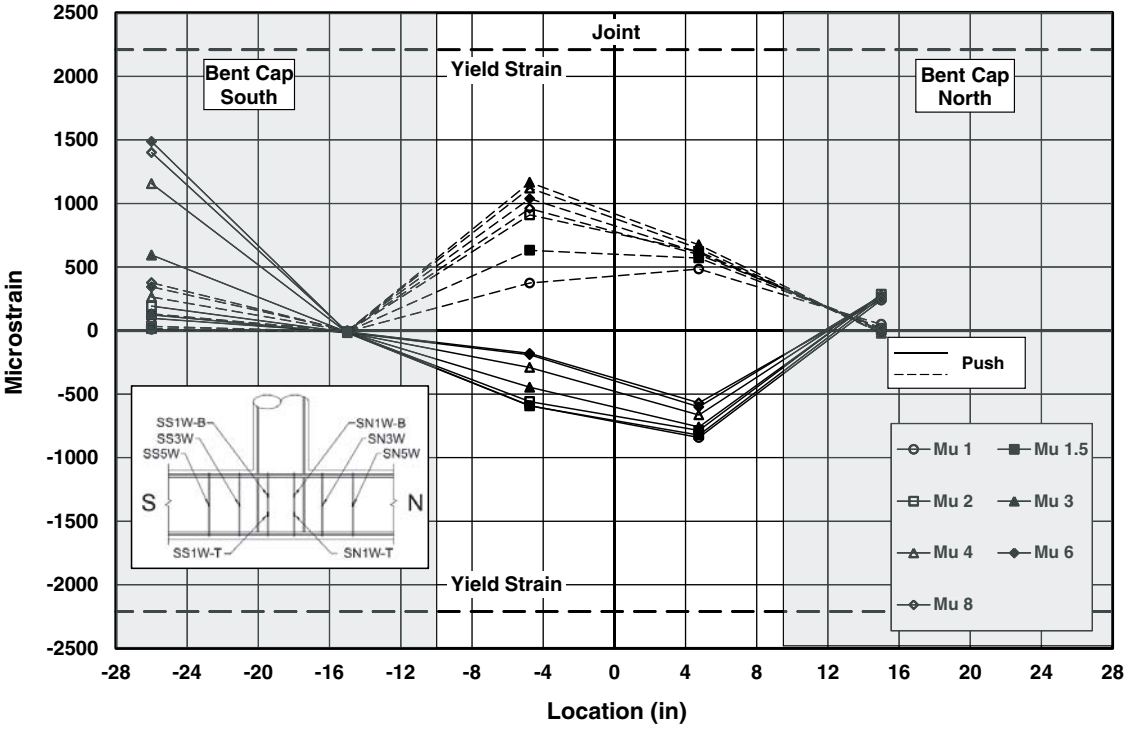

Figure 2.54. Strain profile—stirrups in bent cap (midheight) and joint (bottom), displacement control—GD.

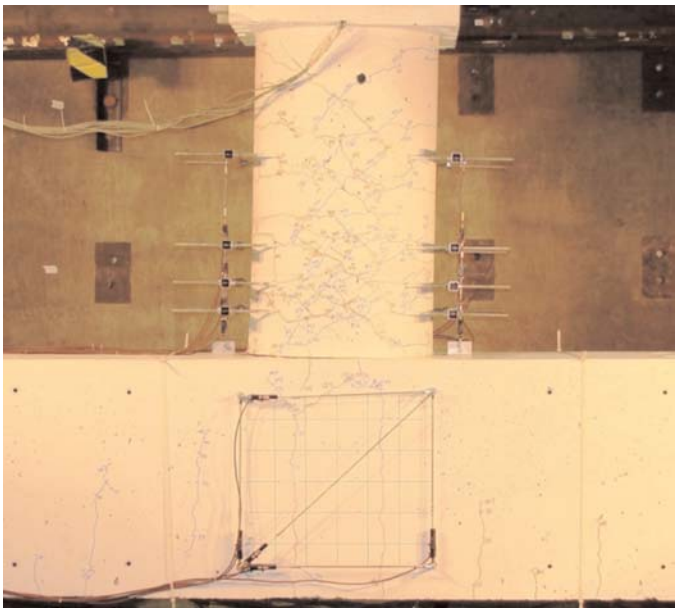

Figure 2.55. Specimen response at a 2.1% drift ratio (μ4)—CPFD.

0.9% (μ1.5), with spalling much more evident at a drift of 3.2% (μ6). Significant column flexural and shear cracks and spalling developed; however, a distinctive crack pattern in the joint developed, different from that observed for the CIP specimen. Diagonal cracks formed above and below the corrugated pipe through a drift of 3.1% (μ6, pull), at which stage diagonal cracks (limited to 0.009 in) passed through the central portion of the joint. Joint shear contributed only 5% to column displacement, and joint shear stiffness compared closely to that of the CIP, with limited joint softening evident at increasing drift ratios. Column bars were well anchored within the pipe, with only minor bar slip. Principal tensile stresses significantly exceeded $3.5\sqrt{f_c'}$ and justified the use of additional joint reinforcement, including the pipe, for development of a force transfer mechanism.

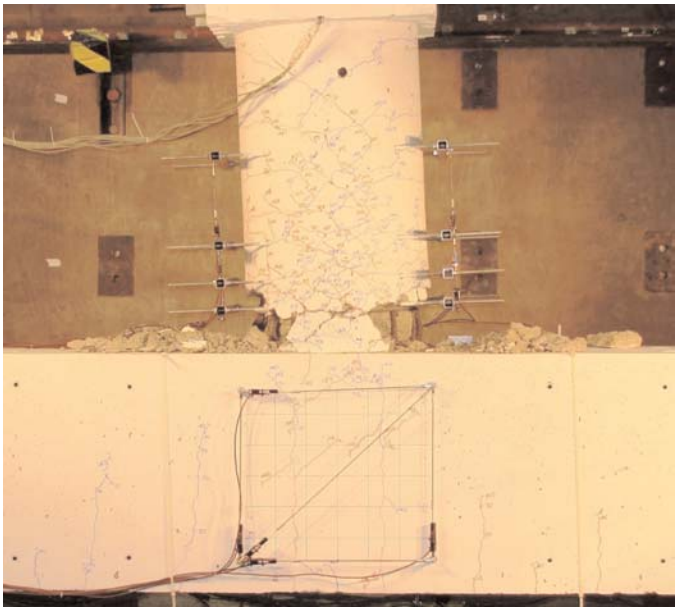

Figure 2.56. Specimen response at a 4.2% drift ratio (μ8)—CPFD.

Stirrup strains within the joint reached only 25% of yield for the CPFD, but yielded for the CIP. Bent cap longitudinal bar strains exhibited a pattern similar to the CIP bottom bar, but the CPFD longitudinal bars yielded within the joint. In addition, supplementary hoops that were placed at the ends of the pipe to reinforce the pipe and limit dilation and potential unraveling reached up to 52% of yield, indicating their contribution to joint performance. Pipe strains were limited to 37% of yield. The bedding layer appeared to perform integrally with the column, did not produce unusual behavior in the joint or specimen, and was not a weak link in the system. In addition, integral behavior between the pocket concrete, pipe, and surrounding concrete was evident.

Column Lateral Force versus Lateral Displacement. The lateral force displacement (hysteretic) response of the CPFD column, shown in Figure 2.57, indicates stable hysteretic behavior with loops of increasing area without appreciable strength degradation, as well as stiffness, strength, ductility, and features such as crack distribution anticipated for an emulative beam-column connection test. A comparison of the load-displacement envelope to the predicted envelope showed a good correlation. In addition, Figure 2.52 reveals a very similar load-displacement response for the CPFD and CIP specimens. The dominance of ductile plastic hinging in the column and minimal damage in the capacity-protected joint and bent cap satisfied the emulation performance goal for the CPFD specimen.

Column Displacement Decomposition. CPFD column displacement decomposition, summarized in Figure 2.58, confirmed the dominance of plastic hinging and showed that displacement components were reasonably determined and predictions were reasonably made. The joint shear displacement was minor, contributing only 4.1% to the overall column displacement, and was consistent with visual observations of minor joint cracking. Column bars were well anchored within the pipe, contributing less than 7% to fixed end rotation. Although two flexural cracks extended across the pipe, there was no evidence of concrete splitting within the pipe, initiation of pullout failure, or significant bar slip or pipe slip. Displacement component magnitudes and percentages for the CPFD and CIP specimens compared very favorably.

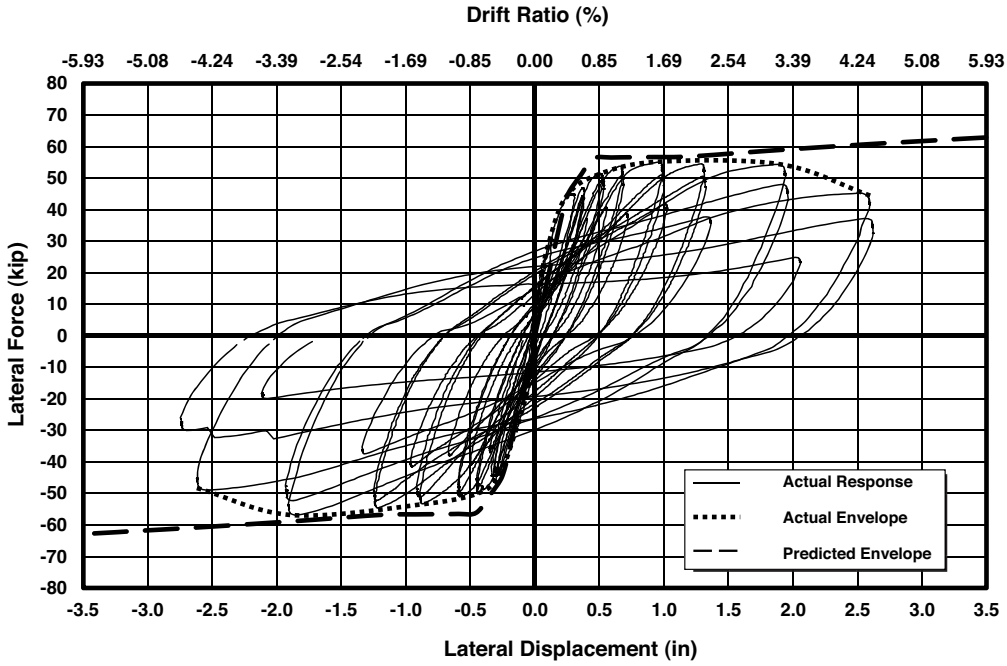

Figure 2.57. Lateral force versus lateral displacement—CPFD.

Joint Response. As shown in Table 2.3 and Table 2.4, CPFD joint distress was limited and joint behavior compared very favorably with the CIP specimen. Analysis of the joint indicated that the principal tensile stress was limited to $4.4\sqrt{f_c'}$, less than half of the 2006 LRFD RSGS (*2*) limit of $12\sqrt{f_c'}$, but 37% larger than $3.5\sqrt{f_c'}$, the level at which more extensive (additional) joint reinforcement is required according to the 2006 LRFD RSGS. Principal compressive stresses did not exceed $0.07f_c'$, less than a third of the 2006 LRFD RSGS limit of $0.25f_c'$. These values correspond well with the intentions of the design and the observed joint performance. Accounting for the different concrete strengths, the CPFD stresses were 11% to 19% smaller than those for CIP. The joint shear stress-strain

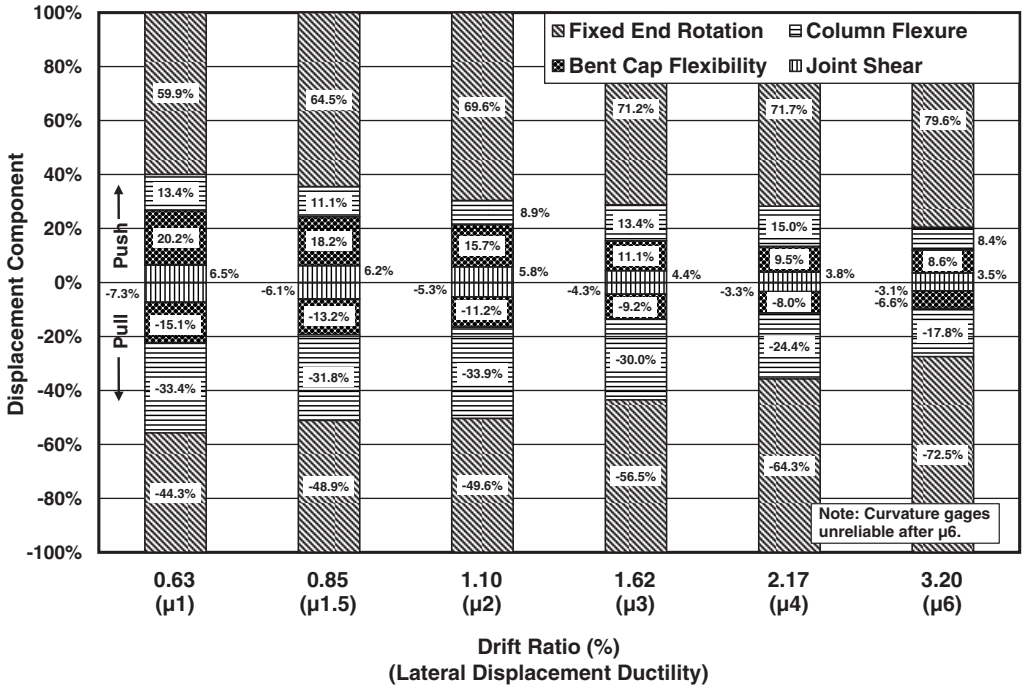

Figure 2.58. Displacement decomposition component percentages—CPFD.

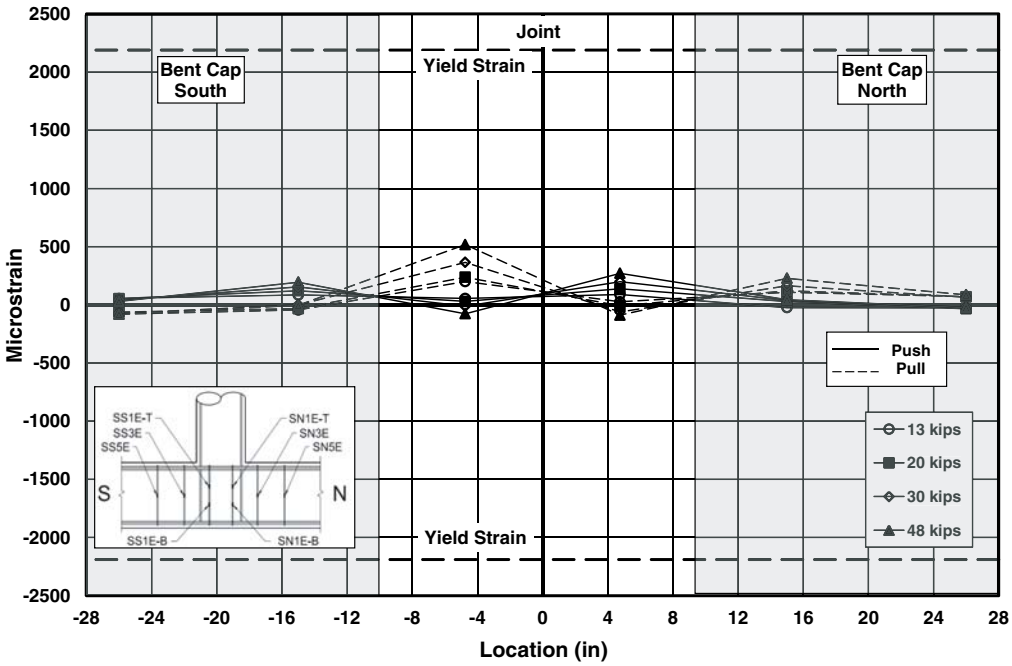

Figure 2.59. Strain profile—stirrups in bent cap (midheight) and joint (bottom), force control—CPFD.

response compared closely to the CIP, with limited joint softening evident at increasing drift ratios (see Figure 2.46).

The maximum change in the CPFD panel area was approximately 20% less than that for the CIP specimen, corresponding with fewer diagonal cracks in the CPFD joint region and a significantly smaller maximum diagonal crack width (0.009 in) compared to the CIP joint (0.025 in). In addition, only at a 3.2% drift (μ6, pull) did diagonal cracks pass through the central portion of the CPFD joint itself. The CIP joint exhibited a more extensive pattern of diagonal cracks through the joint region for both push and pull loading. The different CPFD crack pattern and widths and strain distribution suggest a somewhat different load path in the joint region due to the presence of the corrugated pipe.

Differences in joint behavior were also evident in strain distributions. Stirrup strains within the joint reached only 25% of yield for the CPFD (see Figure 2.59), but yielded for the CIP. Bent cap longitudinal bar strains exhibited a pattern similar to the CIP bottom bar, but the CPFD longitudinal bars yielded within the joint. In addition, supplementary hoops that were placed at the ends of the pipe to reinforce the pipe and limit dilation and potential unraveling reached up to 52% of yield, indicating their contribution to joint performance. Pipe strains were largest at midheight, where principal strains were limited to 37% of yield.

Cap Pocket Limited Ductility Specimen

CPLD specimen response was characterized by a combination of plastic hinging of the column adjacent to the bent cap and joint shear cracking and deformation (see Figure 2.60, Figure 2.61, Figure 2.47, and Figure 2.46). However, the system achieved an unexpectedly large drift ratio of 5.1% (nominal displacement ductility of 8), and load-displacement response indicated stable hysteretic behavior without appreciable strength degradation. Failure was due to buckling and fracture of two column bars rather than joint failure. These characteristics were similar to the full ductility specimens.

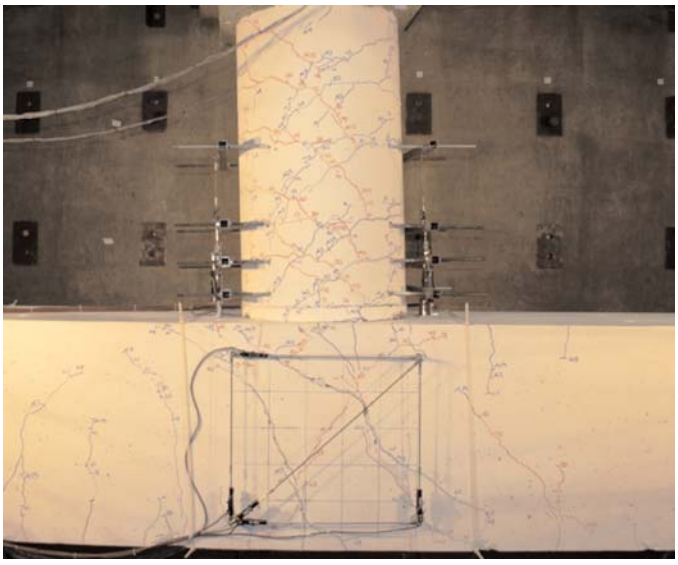

Figure 2.60. Specimen response at a 2.5% drift ratio (μ4)—CPLD.

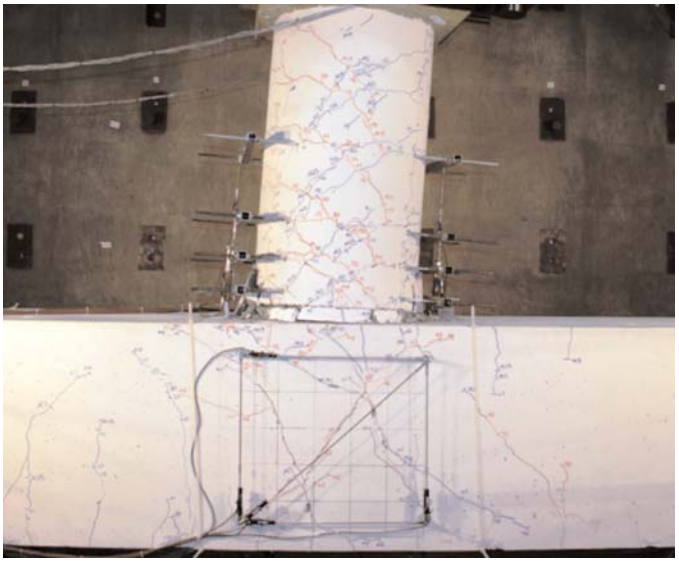

Figure 2.61. Specimen response at a 5.0% drift ratio (μ8)—CPLD.

Nevertheless, significant effects of joint shear associated with the SDC B limited ductility design developed, including the following:

- More severe joint distress including crack widths as large as 0.080 in (with minor joint spalling);
- Much softer joint shear response and large joint shear strains after an initial stiff response;
- Similar initial spalling of the column at a drift of 1.2% (μ2) but delay of significant spalling and plastic hinging to a much larger drift (3.7%, μ6) due to the initial dominance of joint shear;
- A flexure/shear displacement component ratio that averaged 2.2, nearly an order of magnitude smaller than that for the CPFD and CIP specimens (16.5 and 20.0, respectively); and
- Much larger bar slip, but without loss of anchorage.

Principal tensile stresses significantly exceeded $3.5\sqrt{f_c'}$, justifying the use of joint reinforcement. However, joint reinforcement other than the corrugated pipe was not used, thus allowing joint shear cracks to open and grow without restraint. Joint crack patterns were more similar to the CIP specimen than to the CPFD specimen. Although column longitudinal bars remained anchored within the pipe, significant bar slip developed. Bottom bent cap longitudinal reinforcement exhibited a pattern similar to the CPFD, reaching yield, but pipe strains were larger for the CPLD.

Column Lateral Force versus Lateral Displacement. The lateral force-lateral displacement (hysteretic) response of the CPLD column, shown in Figure 2.62, indicates stable hysteretic behavior with loops of increasing area without appreciable strength degradation, as well as stiffness and strength anticipated for an emulative beam-column connection test. The level of ductility exceeds that expected for a limited ductility connection. A comparison of the load-displacement envelope to the predicted envelope—which assumed full flexural capacity without any limitation based on limited ductility performance—showed a good correlation. In addition,

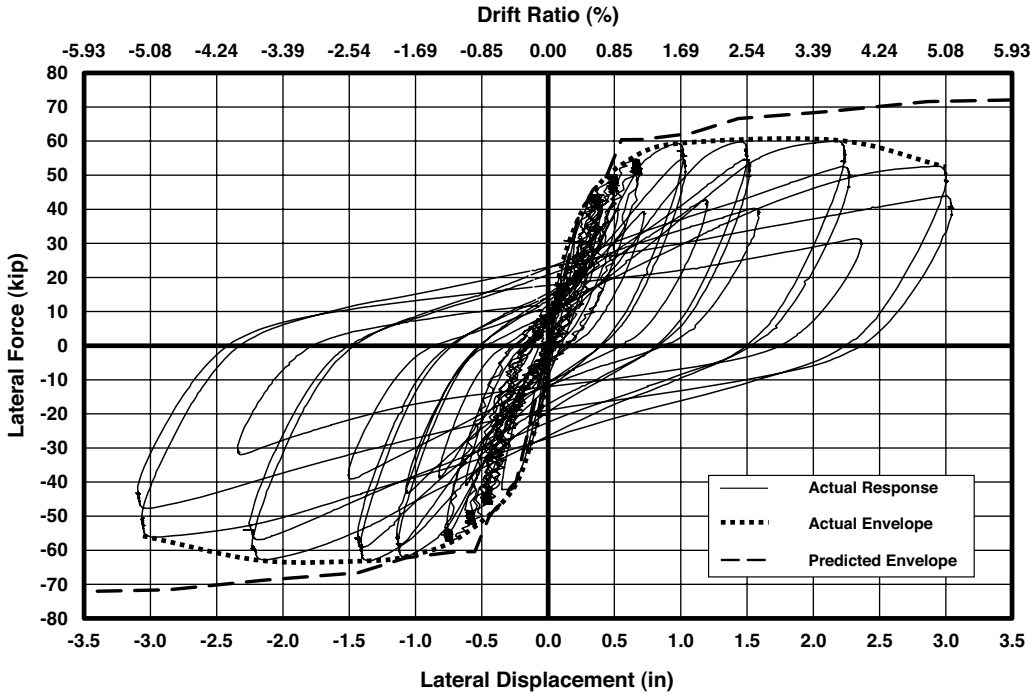

Figure 2.62. Lateral force versus lateral displacement—CPLD.

Figure 2.52 reveals a very similar overall load-displacement response for the CPLD, CPFD, and CIP specimens. The eventual dominance of ductile plastic hinging in the column satisfied the performance goal for the limited ductility specimen.

Column Displacement Decomposition. Limited ductility emulative bridge bent caps are expected to exhibit flexural plastic hinging, but also are expected to achieve a significantly lower displacement ductility capacity (in the range of μ2) due to less stringent joint and column detailing requirements (*2, 1*). The CPLD column detailing matched that of the CPFD design, allowing the CPLD to develop plastic hinging and exhibit large flexural displacement components at increasing drift levels. However, the less stringent SDC B joint detailing permitted more extensive joint damage to occur; thus, joint shear components were expected to contribute significantly.

In agreement with visual observations (see Figure 2.47), the CPLD displacement decomposition summarized in Figure 2.63 demonstrated that the column displacement due to joint shear was nearly an order of magnitude larger than and the flexural component averaged approximately 25% less than that for the full ductility specimens (see Figure 2.64). The CPLD flexure/shear ratio (2.2 average) was also nearly an order of magnitude smaller than for CPFD and CIP (16.5 and 20.0, respectively).

In addition, the CPLD bar slip component of column displacement was approximately 11 times larger than the bar slip component for the CIP and CPFD specimens. A significant increase in CPLD slip toward ultimate was observed, even as the load decreased. Although this may indicate bar pullout was impending, pullout did not mobilize before column bar buckling failure occurred.

Joint Response. As shown in Figure 2.47 and Table 2.3, the joint region for the CPLD specimen exhibited a significant level of distress that increased throughout the test. The CPLD specimen did not include 2006 LRFD RSGS (*2*) joint reinforcement (for full ductility specimens) or supplemental construction stirrups in the joint. Analysis of the joint indicated that the principal tensile stress reached was $7.0\sqrt{f_c'}$, twice the $3.5\sqrt{f_c'}$ limit at which extensive (additional) joint reinforcement is required according to the 2006 LRFD RSGS. Table 2.4 shows significantly larger joint stresses and deformation for CPLD specimens compared to the full ductility specimens. However, no joint reinforcement other than the corrugated pipe was used, which allowed joint shear cracks to open and grow without restraint. Principal compressive stresses reached $0.13f_c'$, approximately half the limit of $0.25f_c'$. The joint shear stress-strain response shown in Figure 2.46 shows much softer joint shear response and larger joint shear strains for CPLD specimens compared to other specimens, after initially stiff response.

CPLD diagonal cracks were as wide as 0.050 in at μ2 (push, both faces), and although cracks increased to large widths at ultimate (0.070 in, east face; 0.080 in, west face), joint failure did not occur. Joint stirrups were not used for the CPLD; however, CIP analysis demonstrated that construction stirrups were highly effective, reaching yield, and contributed to resisting joint stresses and limiting crack opening. These stirrups were less effective for the CPFD specimen, which exhibited

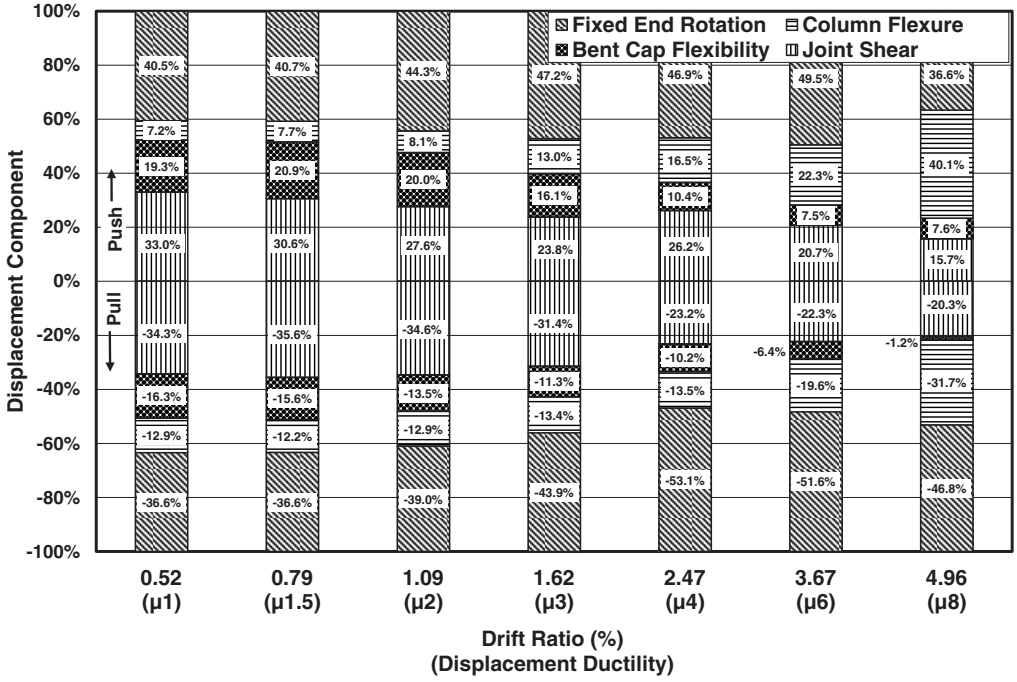

Figure 2.63. Displacement decomposition component percentages—CPLD.

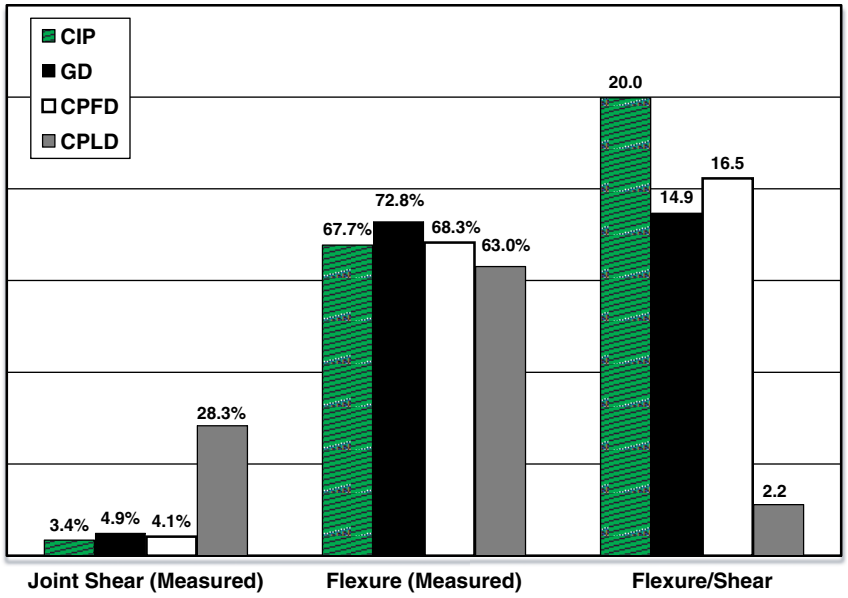

Figure 2.64. Comparison of flexural and joint shear displacement components—all specimens.

more limited cracking. Although different joint crack patterns correspond to different load paths, the most important effect of the joint cracking on overall specimen response was the significant increase in joint shear displacements due to softening of the CPLD joint.

Larger corrugated pipe strains developed for the CPLD, up to 70% of yield, compared to the CPFD (37% of yield), and strain distributions also differed. Strain patterns for the bent cap longitudinal bars were reasonably consistent among specimens, especially for the bottom bars, with both CPLD and CPFD bars yielding at the centerline. Although column longitudinal bars remained anchored within the pipe, the bar slip component of column displacement was approximately 11 times that of the CIP and CPFD specimens. However, a bar anchorage equation from prior research on grout pockets indicated a larger development length for the CPLD column bars (beyond that required by 2006 LRFD RSGS) and may have helped reduce slip (*7, 2*).

The bedding layer appeared to perform integrally with the column, did not produce unusual behavior in the joint or specimen, and was not a weak link in the system.

2.3.2 Nonintegral Hybrid Connections

This section summarizes primary aspects of specimen response, including column hysteretic response (lateral force-displacement), displacement decomposition, and joint response. Comparisons are made between the CIP and precast connections, as well as between the full and limited ductility specimens.

Conventional Hybrid Specimen

For the conventional hybrid specimen (HYB1), the primary lateral response was dominated by the localized joint rotation occurring at the bedding layer, as shown in Figure 2.65 and Figure 2.66. This specimen achieved drift ratios in excess of 6.0% with no noticeable reduction in lateral capacity. Localized spalling of concrete within the compression toe was observed related to the large strains expected with large drift ratios. Fracture of the first reinforcing bar was noted by auditory observation following two loading cycles reaching a 6.0% drift ratio. Review of the specimen indicated that appreciable buckling of the longitudinal reinforcement occurs within the compression region followed by premature fracture on the following tension cycle. Minimal damage to the column was observed outside of the base of the column with only a few minor flexural and tension cracks noted. The overall performance of the bent cap joint indicated only minor flexural cracking, and small crack widths indicated that a reliable joint design methodology was used.

Column Lateral Force versus Lateral Displacement. The complete force-displacement curve obtained for this specimen is shown in Figure 2.67. The lateral force presented is the actual lateral force considering the effects of system deformation during testing. Stable lateral response is observed up to and including drift levels of 6.0%. For the loading cycles reaching 8.0% drift, a considerable drop in the lateral force resistance is observed. During testing, it was noted by auditory observation that the first reinforcing bar fractured during the push cycle to 4.0% drift ratio following the two cycles to 6.0% drift ratio. This

(a) (b)

Figure 2.65. Specimen response at 2% drift (a) column base and (b) joint—HYB1.

can be observed in the experimental data, which show the sudden short drop in lateral force just prior to reaching a 4.0% drift ratio in the push direction. The nominal capacity calculated using the simplified analysis technique and the complete force-displacement prediction is also provided. Review of Figure 2.67 indicates that the nominal capacity predicted using the simplified procedure provides a reasonable estimate of the nominal lateral capacity of the specimen. Additionally, the complete force-displacement prediction matches very well with the recorded response. The predicted failure of the section was underpredicted, indicating appreciable conservatism in the ultimate displacement capacity prediction.

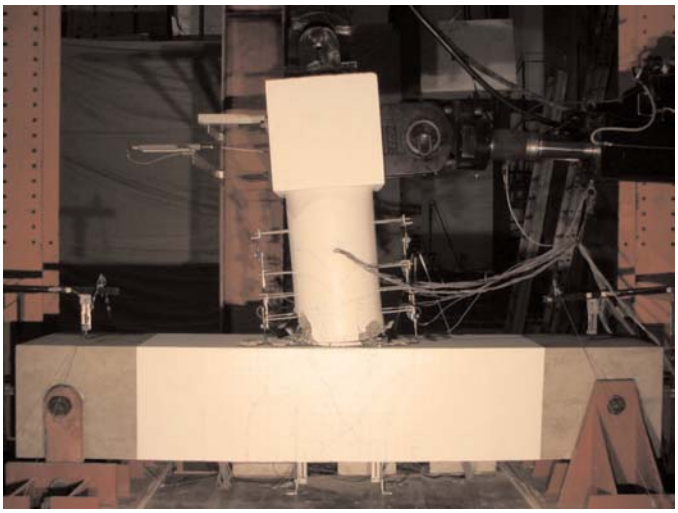

Figure 2.66. Specimen response at 6% drift—HYB1.

The force-displacement envelopes for all three hybrid specimens along with the CIP specimen are shown in Figure 2.68. It is apparent that all hybrid specimens have greater lateral capacity than the CIP control specimen. The larger-than-anticipated effective post-tensioning force in the conventional hybrid specimen resulted in this increase, and the other hybrid specimens were designed to be similar to the conventional hybrid specimen.

Column Displacement Decomposition. Figure 2.69 provides a graphical breakdown of the key components of the lateral deformation captured with instrumentation during testing. This plot provides a summary of the relative contribution of a given mode of deformation as compared to the total displacement recorded at the same instant of time. This plot shows that with increasing lateral deformation, the relative contribution of end rotations increases and the relative contributions of column flexure and beam rotation decrease. This trend is expected as the system facilitates larger deformations through concentrated end rotations. The reduction in total displacement modes recorded at larger drift ratios indicates the presence of additional modes of response occurring at large drift ratios. The difference between the sum of the relative contributions and 100% is due to additional system deformations not explicitly isolated with instrumentation during testing.

Joint Response. Observed bent cap joint damage following the testing is shown in Figure 2.70 for all hybrid specimens. Figure 2.70a shows that only minor damage occurred within the joint during the entirety of the testing. The diagonal cracking patterns indicate that joint shear cracking occurred but that

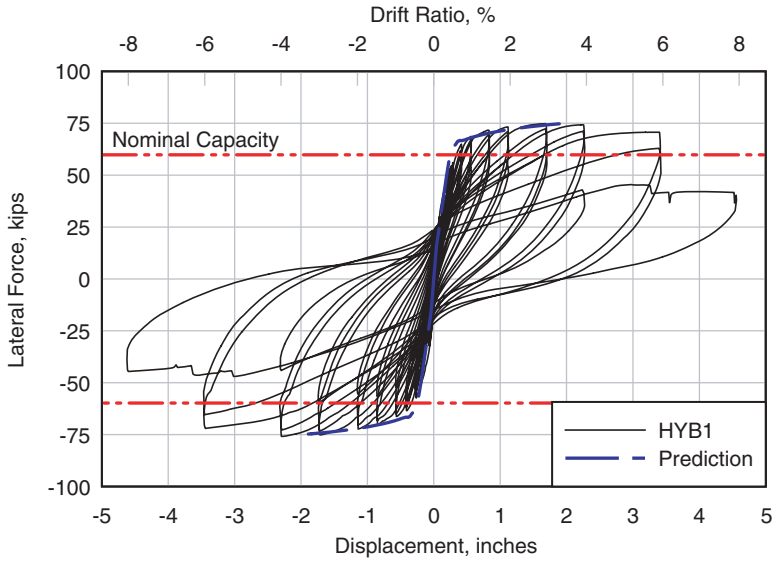

Figure 2.67. Lateral force versus lateral displacement—HYB1.

the joint reinforcement design was adequate to resist extensive crack growth and subsequent joint damage.

Column Compression Strain Profile. Small-diameter, No. 2 reinforcing bars were embedded within the confined concrete core near the spiral reinforcement to try and capture the maximum confined concrete strains in the section. These bars were aimed at determining (1) the level of straining in the concrete compared to the expected failure strain and (2) the vertical distribution of strains. Results from these strain gages are shown in Figure 2.71, which shows that the maximum recorded compression strain is less than the predicted ultimate compression strain of the confined concrete core as predicted by Mander, Priestley, and Park (1988) (*31*). Additionally, the spread of the compression strain within the column is slightly less than the assumed distance equal to the neutral axis depth. The recorded resulting strains were less than the expected strain, which indicates that there is sectional nonlinearity at the column base, which results in a reduction in the experienced maximum straining. The assumptions presented in *Improving the Design and Performance of Concrete Bridges in Seismic Regions* (*5*) are conservative and reasonable for design but may be subject to future improvements.

Residual Drift. One of the major aims of hybrid bridge systems is the reduction of residual displacements. Figure 2.72 provides a plot of the ratio of recorded residual drift to maximum drift during that cycle. This plot includes data for the

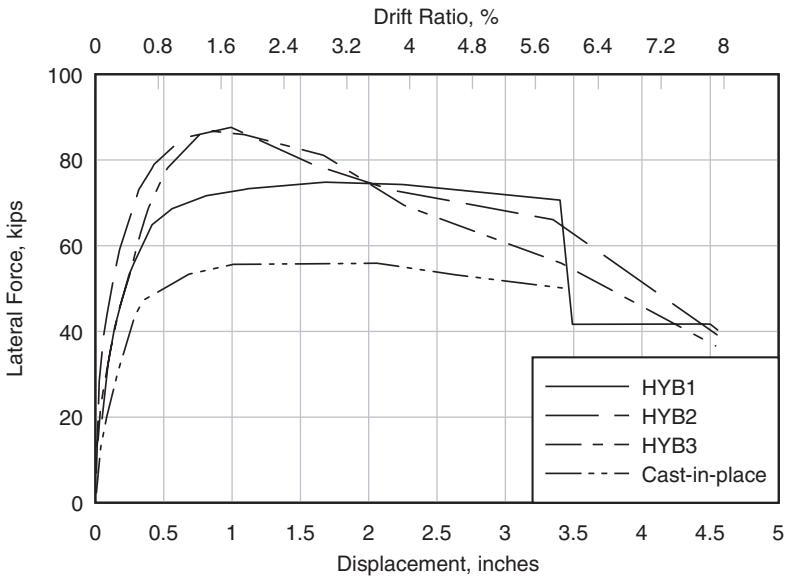

Figure 2.68. Lateral force versus lateral displacement envelopes—hybrids and CIP.

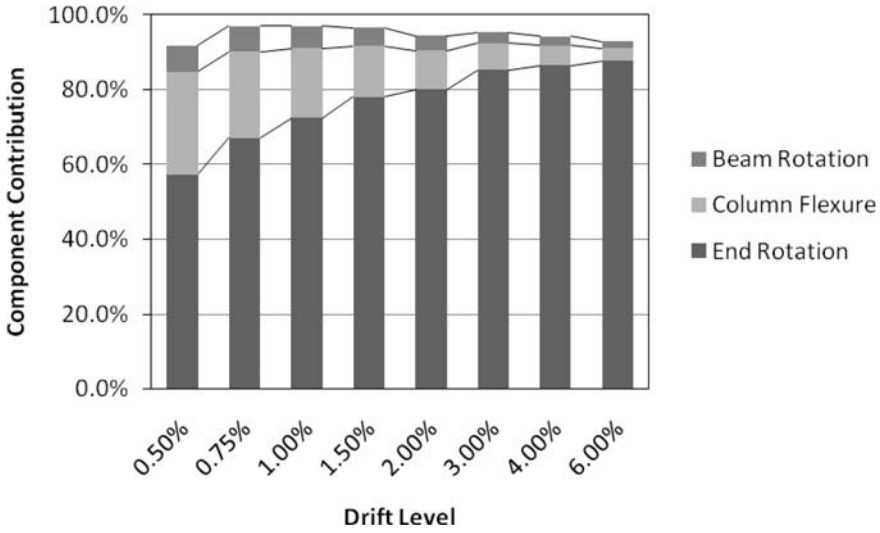

Figure 2.69. Lateral displacement decomposition—HYB1.

(a) HYB1 (b) HYB2 (c) HYB3

Figure 2.70. Joint region cracking post test—hybrid specimens.

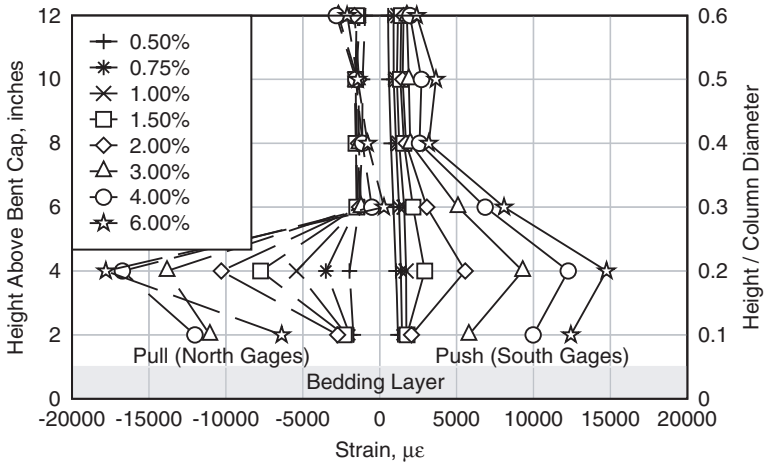

Figure 2.71. Compression strain distribution—HYB1.

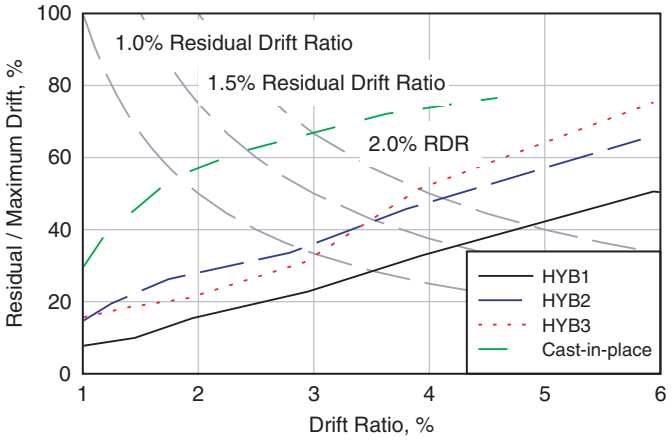

Figure 2.72. Residual drift ratio versus applied drift ratio—three hybrid systems.

three hybrid specimens as well as the CIP control specimen. Only the first cycle residual drift ratios are shown; however, the second cycle exhibited only slightly greater residual drifts. In general, for the conventional hybrid specimen the residual drift ratio increases with the applied lateral drift. However, the recorded residual drift is significantly less in comparison to the CIP specimen, indicating an overall improvement in the post-earthquake performance of the system.

Concrete Filled Pipe Hybrid Specimen

Similar to the conventional hybrid specimen, the primary lateral response of the concrete filled pipe specimen (HYB2) is dominated by the localized end rotations at the bedding layer, as shown in Figure 2.73 and Figure 2.74. Up to the 2.0% drift level, the overall response of the system was as anticipated. However, following the drift cycles to 2.0%, noticeable degradation of the grout bedding layer was observed. Deterioration continued with increasing lateral drifts. The degradation in the bedding layer resulted in a continual loss of lateral strength due to a reduction in the effective column dimension. No damage was observed in the column outside of the bedding layer. Fracture of the reinforcement was noted on 6.0% drift ratio cycles with similar observed buckling leading to fracture. The bent cap responded as anticipated and similarly to the conventional hybrid specimen even with the increase in lateral demand recorded. The overall performance of the bent cap joint indicated only minor flexural cracking, and small crack widths indicated a reliable joint design methodology was used.

Column Lateral Force versus Lateral Displacement. The complete force-displacement curve obtained for this specimen is shown in Figure 2.75. The lateral force presented is the actual lateral force considering the effects of system deformation during testing. Hysteretic response was stable up to a 6.0% drift ratio in terms of the stability of the hysteresis loops under repeated cycles. However, loss of lateral strength was observed in both the positive and negative directions following loading cycles to a 2.0% drift. This loss in lateral strength is attributable to the accumulation of damage within the grout bedding layer, which resulted in a continual decrease in the effective column diameter. According to the commonly accepted definition of failure as when the system lateral strength is 80% of the maximum, the concrete filled pipe specimen failed at a 5.0% drift ratio.

(a)

(b)

Figure 2.73. Specimen response at 2% drift (a) column base and (b) joint—HYB2.

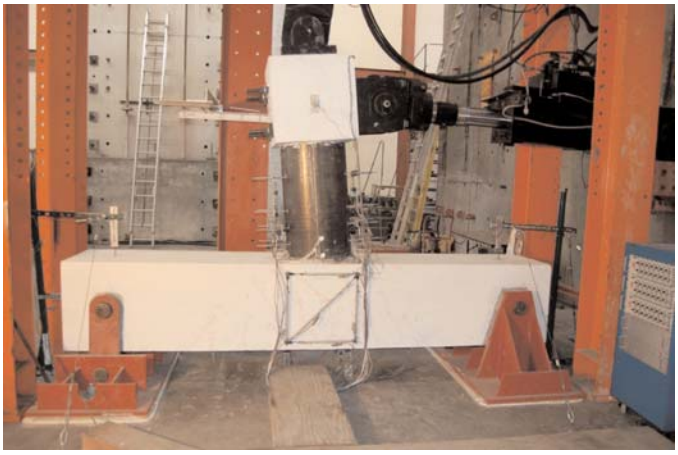

Figure 2.74. Specimen response at 6% drift—HYB2.

The nominal capacity calculated using the simplified analysis technique and the complete force-displacement prediction are also provided. Figure 2.75 indicates that the nominal capacity predicted using the simplified procedure provides a reasonable and slightly conservative estimate of the nominal lateral capacity of the specimen. Additionally, the complete force-displacement prediction matches very well with the recorded response up to the 2.0% drift level. Following the cycles to 2.0% drift, the degradation in the bedding layer was not captured by the prediction; thus, the expected lateral resistance continued to grow.

The force-displacement envelopes for all three hybrid specimens along with the CIP specimen, are shown in Figure 2.68. Comparison of the conventional (HYB1) and concrete filled pipe (HYB2) envelopes shows the stability of the lateral resistance for the conventional specimen whereas a continual reduction in strength is observed for the concrete filled pipe specimen.

Column Displacement Decomposition. Figure 2.76 provides a graphical breakdown of the key components of the lateral deformation captured with instrumentation during testing. This plot shows that with increasing lateral deformation, the relative contribution of end rotations increases and the relative contributions of column flexure and beam rotation decrease. This trend is expected as the system facilitates larger deformations through concentrated end rotations. The reduction in total displacement modes recorded at larger drift ratios indicates the presence of additional modes of response occurring at large drift ratios. The difference between the sum of the relative contributions and 100% is due to additional system deformations not explicitly isolated with instrumentation during testing. It is noted that an appreciable amount of deformation was not captured during the lower level loading cycles.

Joint Response. Observed bent cap joint damage following testing of the concrete filled pipe hybrid specimen is shown in Figure 2.70b. Figure 2.70b indicates that only minor damage occurred within the joint during the entirety of the testing, similar to what was observed in the conventional specimen. The level of observed damage is also of a similar magnitude even though the lateral demands, and therefore joint demands, were greater for this specimen. Diagonal cracking patterns indicate that joint shear cracking occurred, but the joint reinforcement design was adequate to resist extensive crack growth and subsequent joint damage.

Residual Drift. Review of Figure 2.72 shows the ratio of residual drift to maximum drift during that cycle for this specimen. The observed residual drift for this specimen is greater than that recorded for the conventional hybrid specimen,

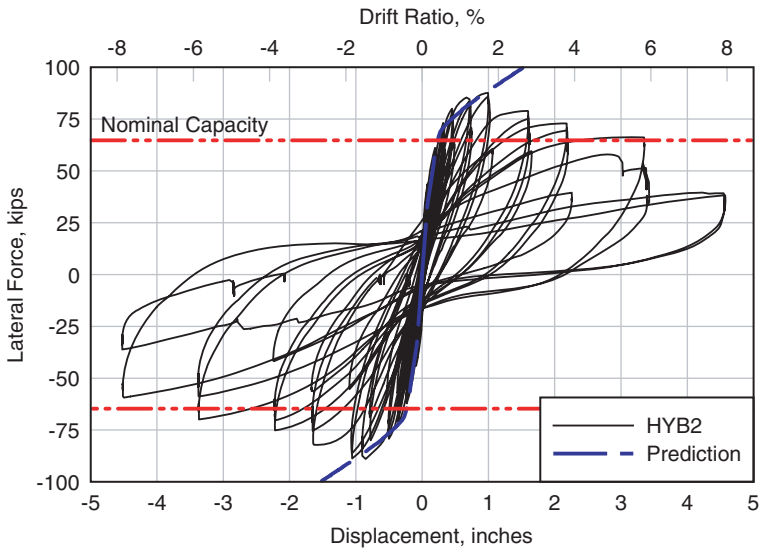

Figure 2.75. Lateral force versus lateral displacement—HYB2.

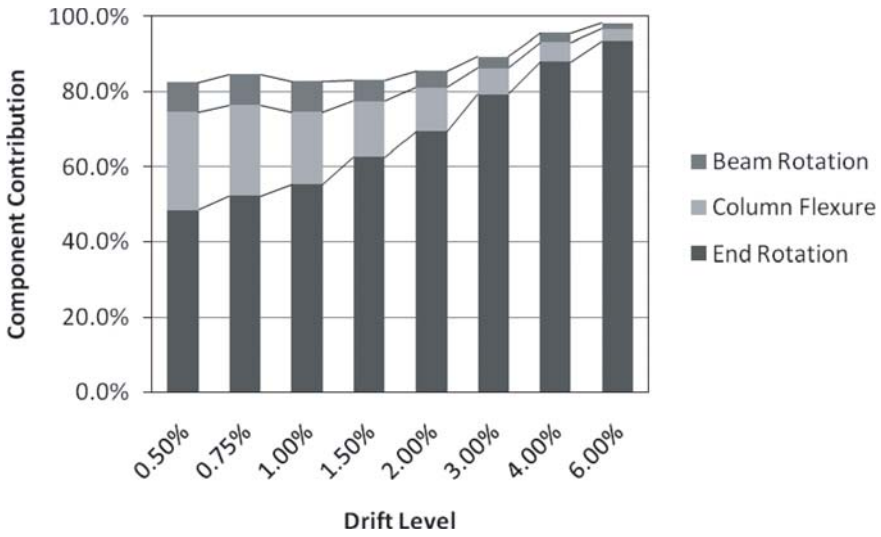

Figure 2.76. Lateral displacement decomposition—HYB2.

resulting from the increased damage in the bedding layer during this specimen's testing. Similar to the conventional hybrid specimen, only slightly greater residual drifts were recorded during the second cycle to a given drift. Even though the residual drifts were greater than those of the conventional hybrid specimen, the recorded residual drift was significantly less than the residual drift of the CIP specimen, indicating an overall improvement in the post-earthquake performance of the system.

Dual Steel Shell Hybrid Specimen

Similar to concrete filled pipe hybrid specimen, the primary lateral response of the dual steel shell hybrid specimen was dominated by the localized end rotations at the bedding layer, as shown in Figure 2.77 and Figure 2.78. Up to the 2.0% drift level, the overall response of the system was as anticipated. However, similar to the concrete filled pipe hybrid specimen, following the drift cycles to 2.0%, noticeable degradation of the grout bedding layer was observed, with deterioration continuing with increasing lateral drifts. The degradation in the bedding layer resulted in a continual loss of lateral strength due to a reduction in the effective column dimension. No damage was observed in the column outside of the bedding layer. Fracture of the reinforcement was noted on 6.0% drift ratio cycles with similar observed buckling leading to fracture. The bent cap responded as anticipated even with the increase in lateral demand recorded, similar to the conventional hybrid speci-

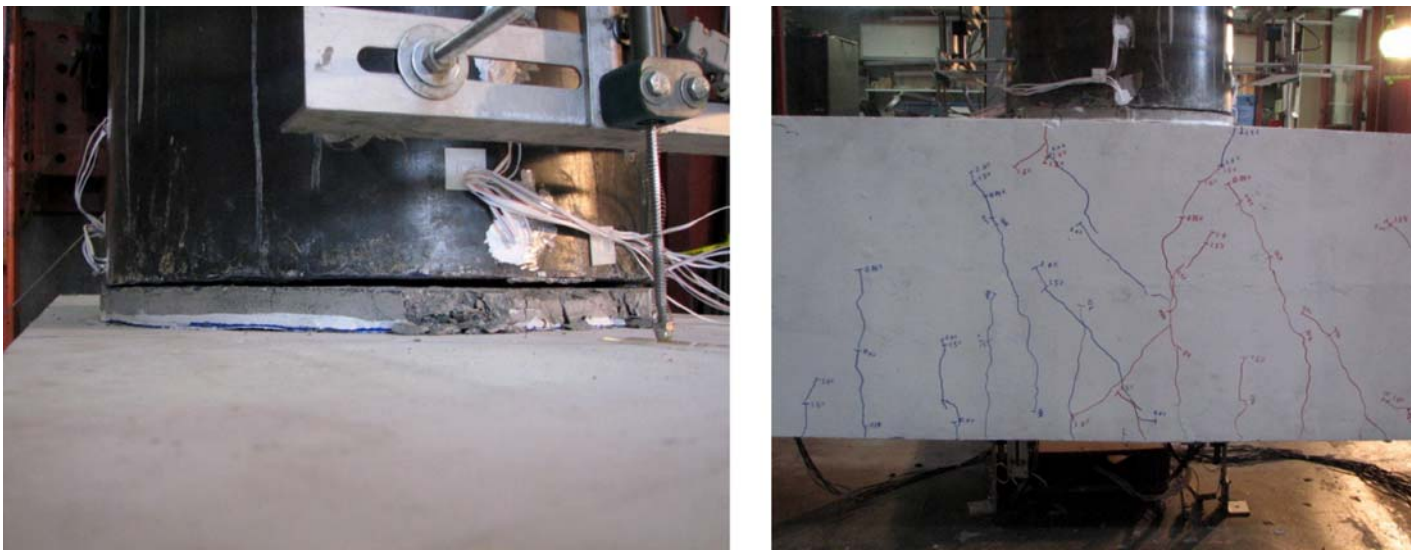

(a) **(b)**

Figure 2.77. Specimen response at 2% drift (a) column base and (b) joint—HYB3.

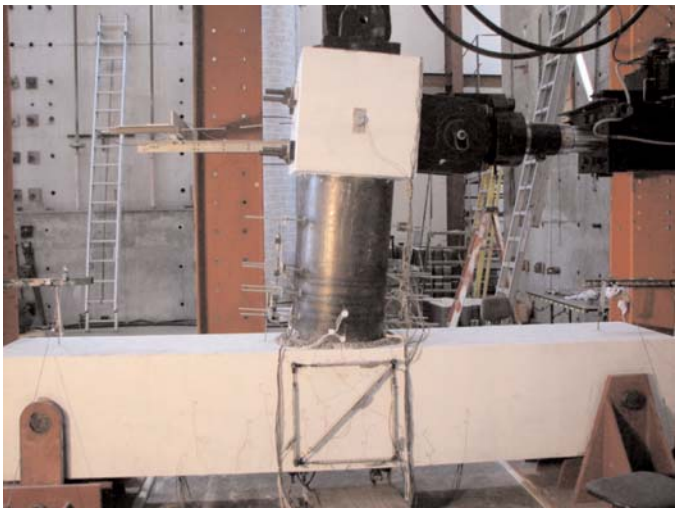

Figure 2.78. Specimen response at 6% drift—HYB3.

Figure 2.79. Bedding layer grout deterioration at end of test—HYB3.

men. The overall performance of the bent cap joint indicated only minor flexural cracking with small crack widths indicating that a reliable joint design methodology was used.

The overall condition of the bedding layer following testing is shown in Figure 2.79. The post-test consistency of much of the bedding layer grout was a very fine material indicating significant crushing and degradation of the grout matrix. The specimen was also observed to have decreased in overall height following seismic testing due to the reduction in bedding layer thickness associated with a reduction in the bearing area of the grout.

Column Lateral Force versus Lateral Displacement. The complete force-displacement curve obtained for this specimen is shown in Figure 2.80. The lateral force presented is the actual lateral force considering the effects of system deformation during testing. Hysteretic response was stable up to a 4.0% drift ratio in terms of stability of the hysteresis loops under repeated cycles. However, loss of lateral strength was observed in both the positive and negative directions following loading cycles to 2.0% drift. This loss in lateral strength is attributable to the accumulation of damage within the grout bedding layer, which resulted in a continual decrease in the effective column diameter. Considering the commonly accepted practice that failure is defined when the system lateral strength is 80% of the maximum, the dual steel shell hybrid specimen is said to have failed at 5.0% drift ratio.

The nominal capacity calculated using the simplified analysis technique and the complete force-displacement prediction is also provided. Review of Figure 2.80 indicates that the nominal capacity predicted using the simplified procedure provides a reasonable and slightly conservative estimate of

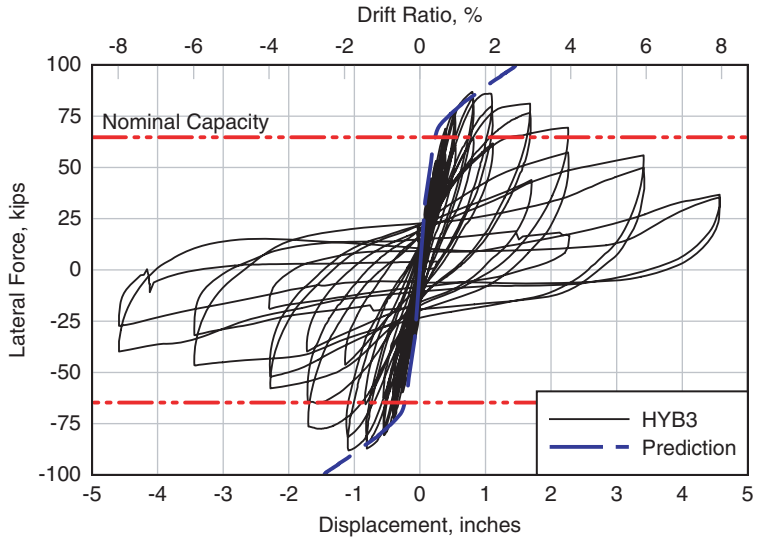

Figure 2.80. Lateral force versus lateral displacement—HYB3.

the nominal lateral capacity of the specimen. Additionally, the complete force-displacement prediction matches very well with the recorded response up to the 2.0% drift level. Following the cycles to 2.0% drift, the degradation in the bedding layer was not captured by the prediction, thus the expected lateral resistance continued to grow.

The force-displacement envelopes for all three hybrid specimens along with the CIP specimen are shown in Figure 2.68. Comparison of the conventional and dual shell envelopes shows the stability of the lateral resistance for the conventional specimen. A continual reduction in strength is observed for both the dual shell specimen and the concrete filled pipe specimen.

Column Displacement Decomposition. Figure 2.81 provides a graphical breakdown of the key components of lateral deformation captured with instrumentation during testing. From this plot, it can be seen that with increasing lateral deformation, the relative contribution of end rotations increases as the relative contribution of column flexure and beam rotation decreases. This trend is expected because the system facilitates larger deformations through concentrated end rotations. The reduction in total displacement modes recorded at larger drift ratios indicates the presence of additional modes of response occurring at large drift ratios. The difference between the sum of the relative contributions and 100% is due to additional system deformations not explicitly isolated with instrumentation during testing. It is noted that an increased amount of error accumulated during the testing, which resulted in the greatest amount of error at the end of testing.

Bedding Layer Response. As was mentioned in the general summary of the specimen response, the overall dimension of the bedding layer reduced during testing. This bedding layer deformation was captured using the lower curvature cages shown in Figure 2.82. The growth of the bedding layer compared with the lateral deformation followed a linear relationship of centroid joint growth during lateral loading and zero displacement upon return to zero drift up to the 3% drift cycles. Following this point, a noticeable reduction in stiffness of the column growth versus drift was observed. In addition, following this drift level, a continual reduction in the overall dimension was observed as the column passed through the zero drift point. This loss in bedding layer dimension also resulted in a loss of effective post-tensioning force due to a reduction in the length of tendon. This loss in effective tendon force also contributed to the continual reduction in lateral capacity of the specimen.

Joint Response. Observed bent cap joint damage following the testing is shown in Figure 2.70c. Review of this figure indicates that only minor damage occurred within the joint during the entirety of the testing, similar to what was observed in the other hybrid specimens. The level of observed damage is of a similar magnitude as the conventional hybrid specimen even though the lateral demands, and therefore joint demands, were greater for this specimen. Diagonal cracking patterns are observed, indicating that joint shear cracking occurred but that the joint reinforcement design was adequate to resist extensive crack growth and subsequent joint damage.

Residual Drift. Review of Figure 2.72 shows the ratio of residual drift to maximum drift during that cycle for this specimen. The observed residual drift for the dual steel shell hybrid specimen is similar to that observed for the concrete filled pipe hybrid specimen, which was greater than that recorded for the conventional hybrid specimen. This increase compared to the

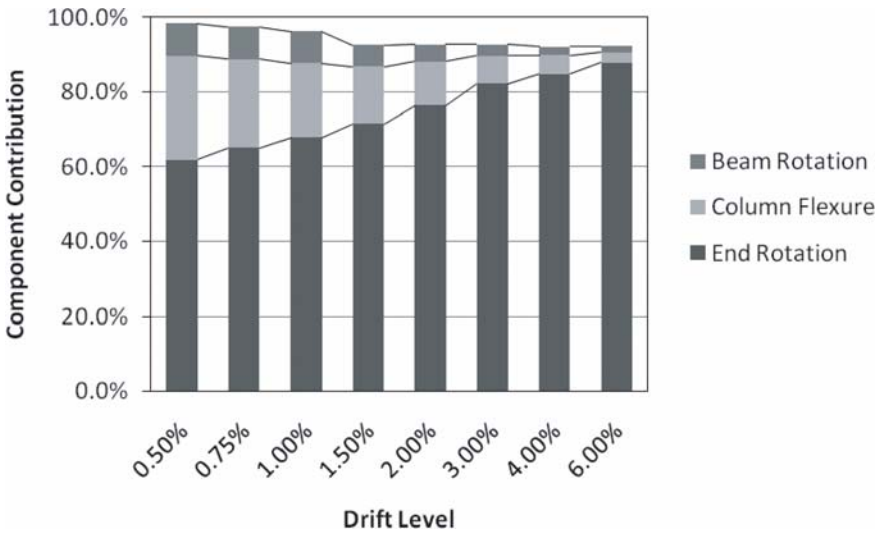

Figure 2.81. Lateral displacement decomposition—HYB3.

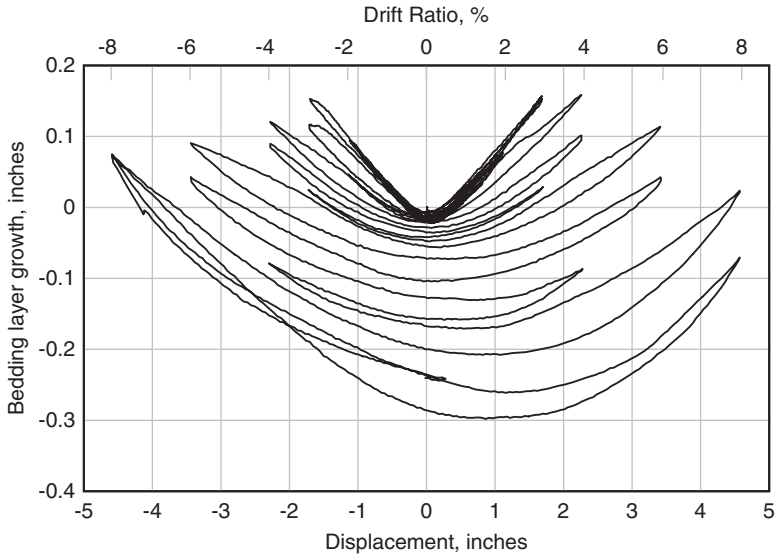

Figure 2.82. Bedding layer centerline axial deformation—HYB3.

conventional hybrid specimen is attributable to the increased damage in the bedding layer during the dual steel shell hybrid specimen's testing. Similar to the conventional hybrid specimen, only slightly greater residual drifts were recorded during the second cycle to a given drift. Even though the residual drifts are greater than those of the conventional hybrid specimen, in comparison to the CIP specimen, the recorded residual drift is significantly less, indicating an overall improvement in the post-earthquake performance of the system.

2.3.3 Integral Connection

The integral experimental specimen (INT) was subjected to a combination of elastic loading cycles and simulated seismic loadings. These loadings were developed to apply flexural demands nearing the anticipated point of nonlinearity in the negative flexural response. At this level, distributed cracking with crack widths less than 0.005 inches was evident. The overall response was characterized as essentially elastic, with no noticeable accumulation of seismic damage.

Seismic loading cycles subjected the girder to positive and negative flexural demands. Photographic records of certain loading cycles are shown in Figures 2.83 through 2.86. In the negative loading cycles, flexural response was representative of traditional CIP superstructure response. A defined compression fan was observed at the girder web at the end with the stabilization of cracking at 45 deg, a distance approximately equal to the superstructure depth. Distributed flexural cracking was observed within the deck with a larger crack width observed at the girder to reaction block joint. During increasing levels of seismic loading, the crack in the deck at the joint separated into two cracks a couple of inches apart. The lack of continuous reinforcement extending from the girder into the reaction block resulted in the observed concentrated opening at the joint during negative flexure; however, the presence of the deck flexural reinforcement served to reduce the concentration of cracking within the deck.

During positive loading cycles, flexural cracking was concentrated at the girder to reaction block joint. Essentially elastic response was observed within the section up to the point of joint opening. As the joint began to open, the concentrated rotations about the end resulted in a reduction in the positive flexural stiffness; however, the increase in flexural resistance continued. During reversed cycling, the fiber-reinforced closure joint performed well, with no observed reduction in

Figure 2.83. Girder end block region at −0.29% joint rotation.

Figure 2.84. Girder bottom flange joint opening at +0.19% joint rotation.

Figure 2.85. Girder to deck interface crack at −0.79% joint rotation.

joint integrity. Furthermore, at large rotation cycles, initial spalling of concrete in the bottom flange was observed with no observed damage to the joint, an indication of the exceptional joint performance.

During loading cycles past about a 0.6% joint rotation, a horizontal crack was observed between the top flange of the girder and the deck, as shown in Figure 2.85. Subsequent loading cycles caused a continued increase in the dimension of this crack, ultimately leading to a reduction in shear stiffness across the joint. This reduction in stiffness resulted in the slip between the girder and reaction block at large rotations, as shown in Figure 2.86b. The shear slip was caused by inadequately developed shear reinforcement within the girder end when subjected to flexural joint opening. Although a reduction of stiffness, and therefore an increase in shear slip, was observed, the ability to resist the applied seismic shear was not reduced.

Moment versus Rotation Response

The complete moment-rotation hysteretic response is shown in Figure 2.87. This plot indicates that there is appreciable energy dissipation capacity in the negative flexural direction with significantly less in the positive direction. This response characteristic is expected because the negative flexural direction has a significantly greater amount of mild reinforcement present, which is expected to yield and dissipate seismic energy under increasing load cycles. Under increasing

(a) (b)

Figure 2.86. (a) Bottom of closure joint and (b) shear slip at +1.03% joint rotation.

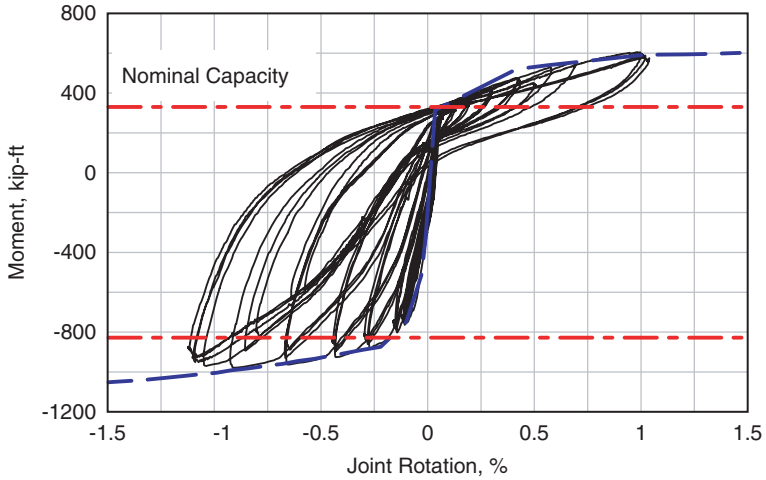

Figure 2.87. Moment versus rotation response.

levels of rotation demand at the joint, a noticeable reduction in the negative flexural stiffness is observed. This is caused by the yielding of mild reinforcement in the concrete deck, which decreases the effective stiffness of the reinforcement. In the positive flexural direction, the reduction in post-yield stiffness under increasing cycles is not as significant as in the negative direction.

The moment-rotation predicted envelope is also shown in Figure 2.87. The predicted response shows good agreement with the recorded results assuming an effective plastic hinge length equal to one-half times the superstructure depth including deck. Although the envelope captures the inelastic response with accuracy, the ultimate rotation capacity is over-predicted. The observed failure of the system occurred at approximately 1.3% drift in both the positive and negative directions. However, the predicted failures in the positive and negative directions were at joint rotations equal to 1.46% and −1.69%, respectively. The error in ultimate rotation is approximately 12% in the positive direction and 30% in the negative direction. Both the prediction and observed failure were controlled by fracture of the post-tensioning tendons. The failure strain in the post-tensioning tendon was equal to 0.03 in/in, per the 2009 LRFD SGS (*1*). The over-estimation of the ultimate rotation is caused by the observed kinking action in the tendon due to shear slip under large rotations. The recommended modification to the shear reinforcement detailing at the girder end is expected to alleviate much of this issue and thus result in an increase in the ultimate rotation capacity of the connection. Even with the reduction in ultimate rotation capacity due to the kinking action, the ultimate rotation capacity results in a system that can safely undergo relative settlements between adjacent bent caps in excess of 1 ft for a structure 100 ft long. This level of geometric demand is greater than would be expected in a properly designed bridge structure.

The simplified nominal section capacity is also shown on the moment-rotation plots. This capacity prediction provides a relatively accurate prediction of the nominal capacity in both positive and negative directions. The negative flexural capacity was predicted using standard design equations in the fifth edition of the AASHTO LRFD Bridge Design Specifications. This calculated capacity shows excellent agreement with the capacity determined using a strain compatibility method. For the positive flexural direction, capacity was calculated using a moment-curvature program that considers strain compatibility across the section. The decision to use a strain compatibility approach is due to the presence of unstressed post-tensioning in the bottom of the girder. In addition, it was observed that the moment-rotation prediction is highly sensitive to the tensile strength of the concrete, which is not accounted for in traditional design equations. While the use of simplified capacity equations for positive flexural capacity will be conservative, it is recommended to also perform a capacity calculation using strain compatibility to determine a better estimate of the connection capacity.

The recorded moment-rotation response at the joint is shown in Figure 2.88 for the 100 cycles of elastic loading. This response indicates that there is no noticeable degradation in stiffness or strength within this loading range. These loading cycles confirm the elastic response of the joint region when subjected to loading within the service load range. Figure 2.88 also overlays the elastic loading cyclic response over the lower level seismic response to provide a visual comparison of the relative elastic demand compared with the section capacity. The joint rotation in these plots is based on a zero rotation at the beginning of elastic loading and does not include the original rotation imposed during the application of simulated dead loading. The moment-rotation predication is also shown in Figure 2.88. The predicted response indicates the system was

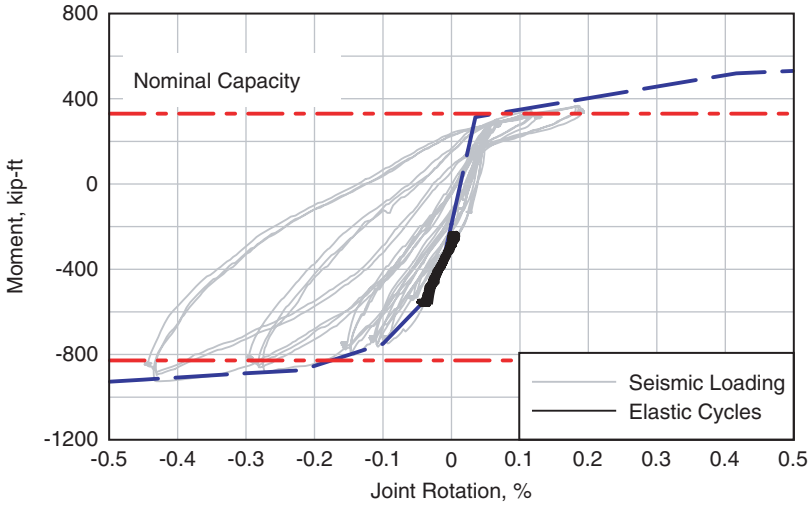

Figure 2.88. Moment versus rotation response at low level seismic and elastic loading.

loaded in the negative direction just prior to a predicted reduction in the stiffness of the system.

Girder Shear Slip

Figure 2.89 shows the recorded girder shear slip history during all loading stages. Results from this loading indicate that the maximum relative slip between the girder and reaction block is less than four-hundredths of an inch for the entirety of the elastic loading cycles. Interestingly, these results indicate that during the elastic loading cycles, the girder also slipped upwards during many cycles. This recorded response does not match the expected response as downward shear loading is applied to the system during all stages. The relatively minor differential movement between the girder and reaction block is not considered a significant response characteristic and is not expected to cause adverse impacts in structural response or functionality of a bridge structure.

All loading cycles below approximately –0.6% joint rotation have less than five-hundredths of an inch slip. As applied joint rotations increased, the recorded drifts continued to increase. Review of the recorded results indicate that during the larger joint rotation cycles, the positive loading cycles have less slip than the negative cycles. This trend is expected due to the decrease in applied shear loading during the positive cycles. Observations made during testing indicate a significant portion of the observed shear slip is due to the separation between the girder and the deck. This separation is caused by

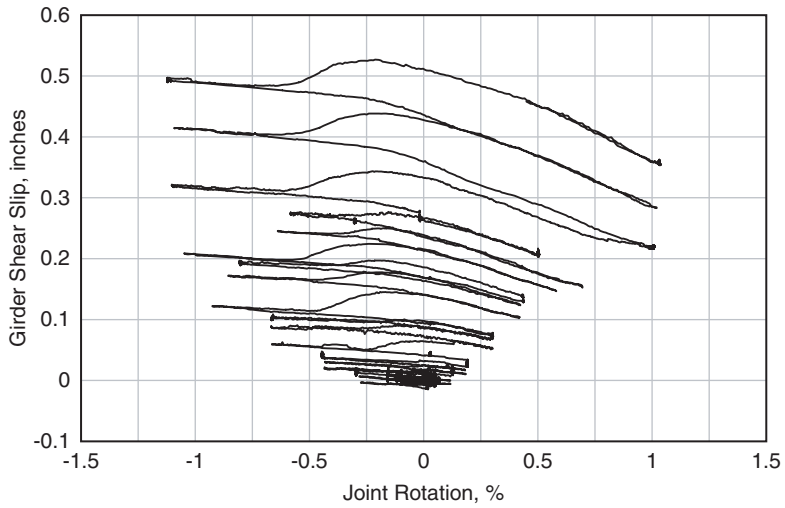

Figure 2.89. Recorded girder shear slip during seismic loading.

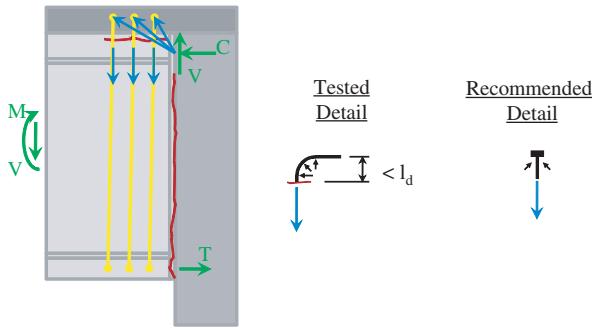

Figure 2.90. Girder shear slip mechanism.

the inadequately anchored shear reinforcement in the girder, which cannot develop the required shear within the deck. The use of headed reinforcing bars is expected to greatly reduce the observed shear slip by fully anchoring the shear reinforcement within the reinforced concrete deck.

As shown in Figure 2.90, the observed horizontal cracking between the deck and girder provided a length of embedded shear reinforcement that was less than the required development length. Therefore, although the shear strength of the system was maintained, there was continued slip of the bar during repeated cycles of testing. To mitigate this issue, the use of well-anchored shear reinforcement in the deck is recommended.

2.4 Analytical Results

2.4.1 Nonintegral Hybrid Connections

A series of analyses was conducted on the hybrid specimens in order to assess the adequacy of these systems for implementation in seismic regions. The first set of analyses relates to the adequacy of the presented simplified and complete prediction methodologies that are discussed in more detail in Tobolski 2010 (*5*). The second set of analyses relates to the investigation of the potential inelastic displacement demands for hybrid systems.

Analysis Prediction Methodologies

The design and implementation of hybrid systems relies heavily on the ability to predict the response of these systems. The lateral force-displacement response of the hybrid members is provided in Figure 2.67, Figure 2.75 and Figure 2.80. Each of these figures also includes the lateral force-displacement envelope prediction and the predicted nominal yield demand using the simplified procedure. For the conventional hybrid specimen, both the complete and simple prediction methods provide very good agreement with the recorded response from experimental testing. The lateral displacement capacity for this specimen was underpredicted due to the conservative estimate of experienced maximum concrete strain. This agreement indicates that the prediction methods shown in the attachments to this report are adequate for the implementation of the conventional hybrid detail. For the concrete filled pipe and dual shell specimens, the prediction methods used provide good agreement with the observed response up to a lateral drift ratio of 2.0%. Above this level of lateral demand, the observed response had continual reduction in lateral capacity due to grout bedding layer degradation. These details still provided acceptable lateral response up to a 5% drift ratio when the lateral capacity approached 80% of the maximum recorded capacity. Within the realm of design demands, the prediction methodology is reasonable and conservative. Future work is required to verify the benefits of modifications to the grout bedding layer for improving performance of the second and third hybrid specimens.

Nonlinear Time History Analyses

In presenting a new structural system for use in seismic regions, the potential implications of realized displacement demands during strong ground shaking must be investigated. A series of nonlinear time history analyses were conducted on a calibrated model to determine the level of displacement amplification in inelastic systems as compared to similar elastic systems. The results from the conventional hybrid specimen test were used to calibrate a lumped plasticity model for dynamic analysis. A comparison between the recorded experimental results and the calibrated model is shown in Figure 2.91. The calibrated model was developed in the analysis package RUAUMOKO (*32*) by combining a modified Takeda model and a bilinear elastic model. The input parameters were based on the response predictions, including the relative contribution of the post-tensioning and conventional reinforcement, and then finetuned based on quasi-static simulations in the analysis model.

The nonlinear time history analyses were performed for records developed for Site Class B, C, and D. A total of 30 ground motions recorded from California earthquakes were modified using the wavelet modification program WAVGEN (*33*). Each record was modified to be consistent with a specified design spectrum developed in accordance with the 2009 LRFD SGS (*1*). The records were manipulated and developed for each of the site classes, resulting in a total of 90 spectrum compatible records. The resulting response spectra for each site class, in addition to the actual modified response spectra, are shown in Figure 2.92. Review of Figure 2.92 indicates that the achieved mean response spectrum for each site class matches well with the target spectrum with variability between actual time history records.

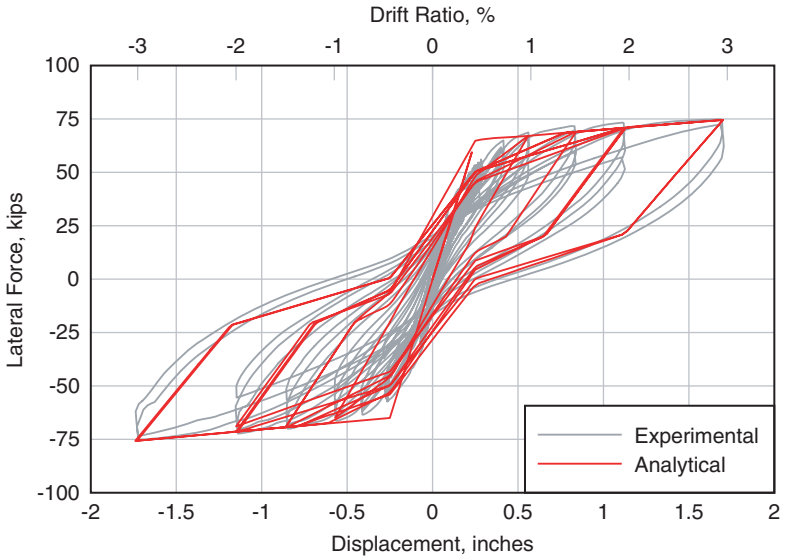

Figure 2.91. Comparison of analytical and experimental hysteresis (5).

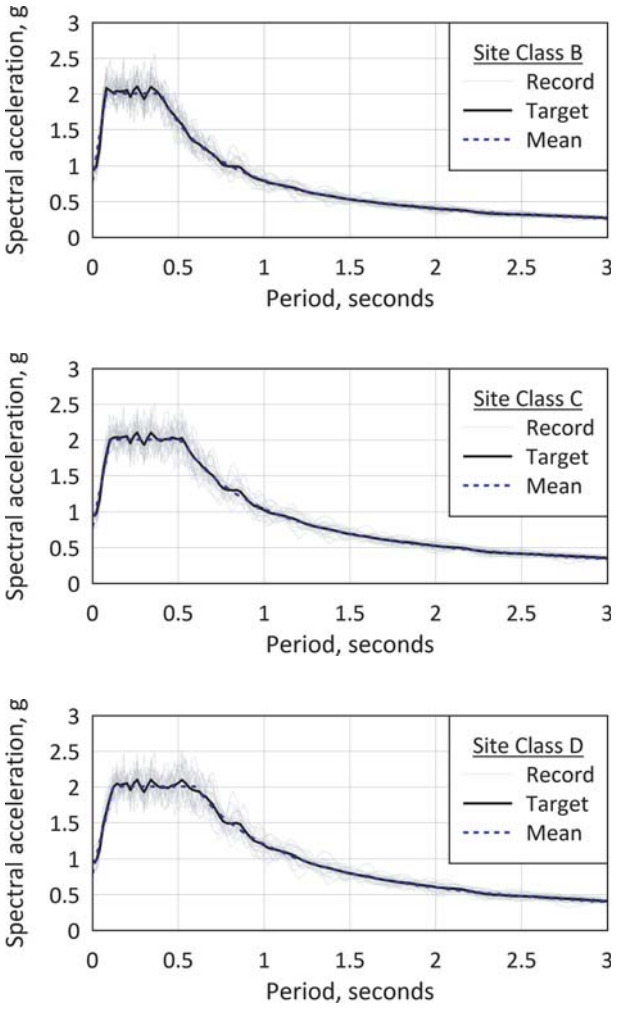

Figure 2.92. Acceleration response spectra (5).

Nonlinear time history analyses were conducted using the calibrated lumped plasticity model for periods ranging from 0.1 sec to 3.0 sec at 0.1 sec intervals. Specified viscous damping was equal to 5% using tangent stiffness damping. The analyses were performed for inelastic force reduction factors ranging from 2 to 6 for single degree-of-freedom systems. The initial runs were performed with elastic response in order to determine the expected yield force in the system. Considering the multiple site classes, earthquakes, and force reduction factors, a total of 13,500 analyses were performed.

The results of the analysis for Site Class D are presented in Figure 2.93, with individual "x" marks representing a single inelastic displacement modification factor from a specific earthquake. The line labeled "HYB Mean" represents the mean response parameters over a range of periods. Additionally, a plot titled "EPT Mean" is presented that represents the results from a similar series of analyses conducted on elastic-plastic single degree-of-freedom oscillators. The hatched region on the plots represents the region in which the experienced displacement demand results in ductility values in excess of the maximum code limit of 6. Results from these analyses indicate that the hybrid systems investigated have displacement demands similar to those of more conventional systems. Thus, these systems are not expected to experience displacement demands significantly greater than those experienced by CIP or emulative systems, and provisions published in the code for these systems can be used for hybrid systems with a similar level of safety. For all systems, the overall trend observed is that the mean inelastic displacement factor approaches unity as the period approaches infinity. This trend agrees with the commonly accepted equal displacement principle (*34*).

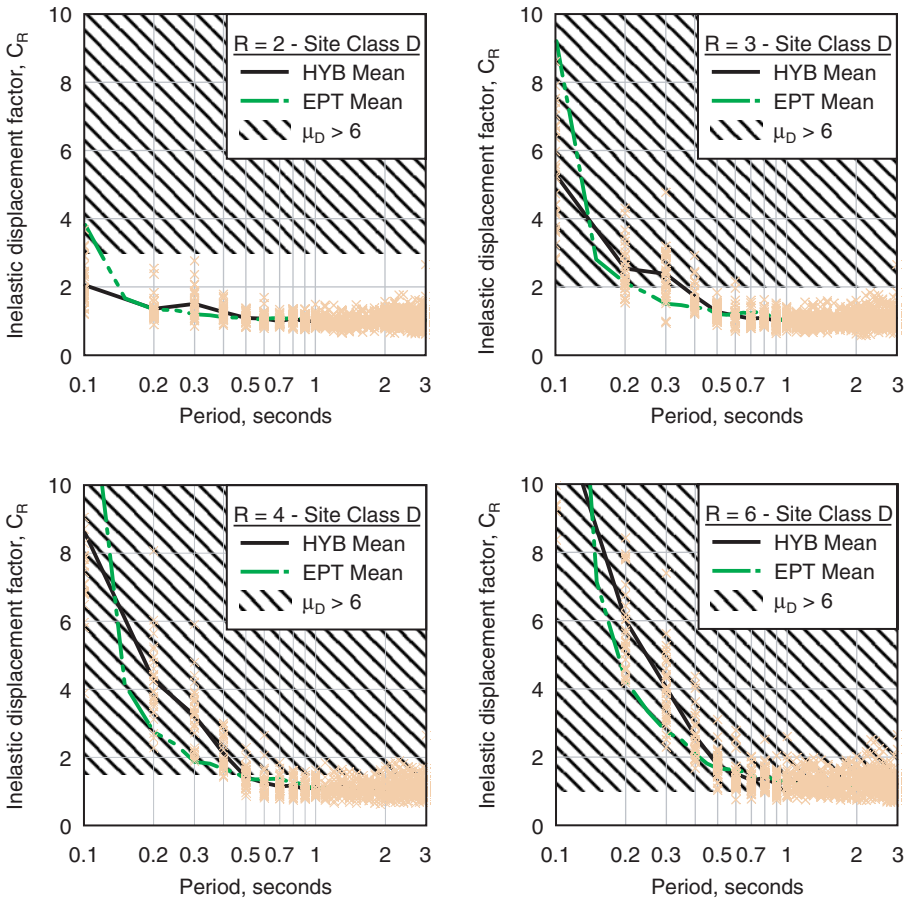

Figure 2.93. Hybrid system inelastic displacement modification factor (5).

CHAPTER 3

Interpretation, Appraisal, and Applications

3.1 Overview

This chapter provides interpretation, evaluation, and applications of the findings of Chapter 2 in developing research deliverables for the precast bent cap systems investigated. In particular, this chapter presents design specifications, design examples, and design flow charts developed using specimen test results and related references. Design methodologies for emulative connections generally follow existing CIP methodologies, but changes are incorporated into new or revised design specifications. Presented construction specifications were developed using specifications previously developed together with results from test specimen fabrication and assembly (*8, 21, 22, 23, 26*). All research deliverables are also presented as attachments to this report, grouped in the following categories: proposed design specifications (new and revised), design flow charts, design examples, construction specifications, and example connection details. In addition, an implementation plan is provided. The attachments provide a detailed list of these deliverables (attachments available at www.trb.org/Main/Blurbs/164089.aspx).

Design specifications for the SDCs—SDCs C and D, SDC B, and SDC A—are given in appropriate format for incorporation into a future edition of the AASHTO Guide Specifications for LRFD Seismic Bridge Design (LRFD SGS) (*1*). A major proposed change is to revise Article 8.13, "Joint Design for SDCs C and D" of the 2009 LRFD SGS to include precast bent cap connections (grouted duct and cap pocket). However, to address all seismic design categories, two new articles are also required. Therefore, current Article 8.13, "Joint Design for SDCs C and D" is renumbered as Article 8.15, "Joint Design for SDCs C and D." This allows two new articles to be added: Article 8.13, "Joint Design for SDC A" and Article 8.14, "Joint Design for SDC B."

Design flow charts and design examples are presented to illustrate the proper use of design specifications for both grouted duct and cap pocket connections at all SDC levels (SDCs A, B, C, and D). Construction specifications are provided as a new proposed article—Article 8.13.8, "Special Requirements for Precast Bent Cap Connections"—to be added to the AASHTO *LRFD Bridge Construction Specifications* (LRFD BCS) (*35*).

3.2 Development of Design Specifications

This section presents the basis for the provisions proposed for incorporation into the LRFD 2009 SGS (*1*). For simplicity, the following sections generally use the same outline as that found in the 2009 LRFD SGS. Proposed specifications are given below. References to articles within this section refer to the LRFD SGS (2009 edition or proposed specifications).

Proposed design specifications have been prepared in the format and language of the 2009 LRFD SGS with detailed commentary (*1*). In addition, detailed drawings are incorporated into the design specifications, including labeling of precast bent cap features and joint shear reinforcement. Many sections of this chapter are directly incorporated into the proposed design specifications, but not all sections of the specifications are shown herein. It is recommended that the accompanying attachments be reviewed together with this section.

Chapter 3 refers extensively to 2009 LRFD SGS (*1*) provisions, which adopt the AASHTO convention of using units of ksi for f'_c. This practice results in different coefficients than those presented formerly using units of psi. For example, terms such as $3.5\sqrt{f'_c}$ psi (likely joint cracking) appear as $0.11\sqrt{f'_c}$ ksi for the same provision (likely joint cracking). This chapter adds clarifying units as needed.

3.2.1 Overview

Based on specimen test results and analysis, the design specifications presented in the following sections differ in some

respects from the 2009 LRFD SGS provisions for nonintegral CIP bent caps (*1*). Precast bent cap connections conservatively require that the joint principal tensile stress be calculated to determine the additional joint shear reinforcement requirement not only for SDCs C and D (as required for CIP design), but also for SDC B. Where the joint principal tensile stress, p_t, indicates likely joint cracking ($0.11\sqrt{f_c'}$ ksi or larger), grouted duct design specifications for joint shear reinforcement closely match CIP specifications. Cap pocket specifications, however, account for use of a single corrugated pipe that replaces transverse joint reinforcement, require a supplementary hoop at each end of the pipe and a smaller area of vertical joint stirrups, and do not specify horizontal J-bars. Where the joint principal tensile stress indicates joint cracking is not expected (less than $0.11\sqrt{f_c'}$), precast bent cap connections in SDCs B, C, and D still require minimum transverse reinforcement and vertical stirrups within the joint. All precast bent cap connections require bedding layer reinforcement, and specifications ensure proper design and placement of the column top hoop. SDC A joints also prescribe minimum transverse reinforcement and vertical joint stirrups within the joint.

For hybrid bent cap connections, the experimental results indicated that many of the existing joint detailing provisions are reasonable for implementation. Therefore, the underlying joint transfer mechanism for CIP and emulative bent caps is employed for hybrid bent caps. New provisions were added to the LRFD SGS for the design of hybrid systems to ensure that the response characteristics of a hybrid system are achieved.

In the 2009 LRFD SGS, there are some disparities between the joint design provisions for nonintegral systems and for transverse design of integral systems (*1*). The general mechanism for transverse response of a multicolumn nonintegral or integral structure is essentially the same. Therefore, recommended modifications are presented for integral systems to develop a consistent design specification. Furthermore, a variety of design and detailing provisions is recommended for integral precast systems in order to ensure that reliable and safe seismic response is achieved.

3.2.2 Displacement Magnification for Short Period Structures

It is essential to consider the impacts on expected seismic demands when utilizing a system that has a significantly different mode of seismic response. The nonintegral emulative and integral details have been shown to perform in a similar manner to CIP structures. Therefore, these systems can be implemented using the same lateral seismic demand procedures that are currently employed in the LRFD SGS. However, the hybrid details investigated are aimed at providing a different mode of seismic response that has inherently less energy dissipation capacity when considering the hysteretic response. The series of nonlinear time history analyses conducted on hybrid systems described in Chapter 2 indicate that the experienced seismic demands for hybrid systems designed in accordance with the provisions described herein are of similar magnitude to a CIP system. Therefore, the current provisions as specified in Article 4.3.3 can be implemented for hybrid systems.

3.2.3 Vertical Ground Motion Design Requirements

The jointed nature of discontinuous integral precast superstructures with vertical joints at the bent cap face requires special attention when considering potential flexural and shear demands. The basic design philosophy for lateral loading is to use capacity design procedures to ensure the elastic response of the superstructure. However, vertical seismic loading cannot be handled with the same capacity design procedures because there is not a well-defined mechanism for inelastic response. The effects of vertical excitation can impose significant flexural and shear demands on the superstructure at the interface between the bent cap and girder whether it is a precast or CIP system. Therefore, seismic demands generated from vertical motions must be considered in seismic design. Additionally, seismically induced foundation movements such as relative settlement, lateral spreading, and liquefaction can induce substantial demands on the superstructure. This topic is covered in more detail in the discussion of superstructure design provisions. For precast systems, the potential implications of vertical excitation are greater than comparable CIP systems due to possible concentrated joint rotations and the reliance on shear friction mechanisms to resist vertical shear demands across the joint. It is recommended that more refined vertical seismic demand provisions be developed for all bridge systems; however, at a minimum, the following provision is recommended for inclusion in Article 4.7.2 of the LRFD SGS for precast systems:

> For integral precast bridge superstructures with primary members that are discontinuous at the face of the bent cap (i.e., precast segmental, integral spliced girder systems, etc.), vertical seismic demand shall be explicitly considered in superstructure design for both moment and shear using equivalent static, response spectrum, or time history analysis. Demands from vertical ground motion shall be combined with horizontal seismic demands based on plastic hinging forces developed in accordance with Article 4.11.2.
>
> Seismic demands shall be combined considering 100% of the demand in the vertical direction added with 30% of the seismic demand resulting from flexural hinging in one of the horizontal perpendicular directions (longitudinal) and 30% of the seismic demand resulting from

flexural hinging in the second perpendicular horizontal direction (transverse).

A major obstacle that must be overcome is the development of improved provisions for the development of vertical seismic loadings. Current provisions in the 2009 LRFD SGS admit that there are shortcomings in the design requirements for vertical excitation that must be resolved for all bridge systems (*1*).

3.2.4 Analytical Plastic Hinge Length

For integral bridge systems, it is desirable to have an understanding of the expected rotation capacity of the superstructure when considering demands associated with vertical loading or potential seismically induced relative settlement. Similar to column systems, the use of moment-curvature analysis and an analytical plastic hinge length can provide an easy-to-implement method for the estimation of the inelastic response of a superstructure joint and its ultimate rotation capacity. Moment-curvature analysis for capacity protected superstructure elements is already required for SDC C and D structures per the 2009 LRFD SGS Article 8.10 (*1*). The only obstacle in the determination of the inelastic flexural response is a reasonable estimate of the analytical plastic hinge length. For elements that are flexurally dominated, the analytical plastic hinge length can be reasonably approximated as one-half of the element depth in the direction of loading. Therefore, the following is a recommended addition to the 2009 LRFD SGS as Article 4.11.6.2:

$$L_{ps} = 0.5D_s \qquad \text{Proposed LRFD SGS Eq. 4.11.6.2-1}$$

where:

L_{ps} = analytical plastic hinge length for integral concrete superstructures (in)
D_s = total depth of superstructure (in)

3.2.5 Reinforcing Steel Modeling

Localized joint rotations associated with hybrid systems can cause increased straining in reinforcing bars due to geometric compatibility. As the joint opens, the rotation must be accommodated in the reinforcing bar with the bar being fixed at both ends. These additional strain demands caused by geometric loading can be accounted for by a conservative reduction in the ultimate tensile strain considered. The following recommended addition to Article 8.4.2 of the 2009 LRFD SGS accounts for this geometric loading in combination with the traditional reduced ultimate tensile strain (*1*):

> For hybrid connections, the reduced ultimate tensile strain, ϵ_{su}^{R}, shall equal one-half the ultimate tensile strain, ϵ_{su}.

3.2.6 Plastic Moment Capacity for SDC B, C, and D

The current provisions for the determination of plastic moment capacities of ductile concrete members are sufficient for CIP and precast emulative systems. However, the intentional debonding of post-tensioning and reinforcement within a hybrid system creates complications in the application of the existing provisions. With discrete joint rotations and distributed straining of steel elements, moment-curvature analysis cannot be directly implemented for hybrid concrete members. Therefore, additional provisions are required.

Debonded elements and associated distributed straining can be accounted for using moment-rotation analyses. The premise of moment-rotation analysis is similar to that of moment-curvature analysis where strain compatibility is used to perform sectional analysis of the member. In a moment-curvature analysis, the strain distribution is considered linear and identical for both steel and concrete elements at the same location. Moment-rotation analysis makes a similar plain section assumption, but allows for varying strain at a given section by considering a fixed length over which an element accumulates strain. To account for the analysis procedure required for hybrid members, a new Article 8.5.2 is recommended for addition to the 2009 LRFD SGS (*1*):

> For hybrid concrete members, the plastic moment capacity shall be calculated using a moment-rotation (M-θ) analysis based on the expected material properties. The moment-rotation analysis shall include the axial forces due to dead load together with the axial forces due to overturning as given in Article 4.11.4.
>
> The M-θ curve can be idealized with an elastic perfectly plastic response to estimate the plastic moment capacity of a member's cross section. The elastic portion of the idealized curve passes through the point marking the first reinforcing bar yield. The idealized plastic moment capacity is obtained by equating the areas between the actual and the idealized M-θ curves beyond the first reinforcing bar yield point similar to as shown in Figure 1.

In the execution of a moment-rotation analysis, the following are the recommended strain lengths for specific elements in the section. The concrete compressive strain length can be approximated as the neutral axis depth. In performing any strain-compatibility sectional analysis, the neutral axis depth is calculated to determine the cross-sectional deformation distribution. This depth can be used to define the region over which the concrete strain is approximately constant. The reinforcement strain length can be approximated as the length over which the reinforcement is intentionally debonded. The post-tensioning strain length can be approximated as the dis-

tance between anchorages as the tendons are debonded for their full length.

3.2.7 Hybrid Performance Requirements

To ensure that hybrid systems exhibit the desired lateral response characteristics of self-centering behavior and limited damage, a variety of provisions are recommended for inclusion in the LRFD SGS. These provisions are intended to limit various design parameters within specific target ranges to produce the intended mode of lateral response.

The aim of the first set of provisions is to ensure that the contribution of reinforcement is such that the system will be capable of a reduction in the residual deformations as compared to traditional bridge systems. A series of limits is recommended for inclusion in Article 8.8.1 of the LRFD SGS as outlined below. The first of the three equations ensures that the effective axial load acting on the column following a seismic event is large enough to force the column reinforcement back to a zero strain state, thereby aiding in the self-centering response. The second equation limits the contribution of the reinforcement on the overall flexural capacity in order to limit the potential residual deformations associated with traditional bridge construction. Increases over this limit will produce lateral response that is similar to traditional CIP bridges with more noticeable damage and residual deformation. The third equation is a limit on the neutral axis depth that is intended to limit the magnitude of strain in the concrete compression toe due to joint opening.

> The maximum longitudinal reinforcement for hybrid compression members shall be proportioned to satisfy Equations 2 through 4:

$$\frac{0.9P_D + P_{pse}}{T_s} > 1.0 \qquad \text{Proposed LRFD SGS Eq. 8.8.1-2}$$

where:

P_D = dead load axial load action on column (kip)
P_{pse} = effective force in post-tensioning tendon at end of service life (kip)
T_s = resultant column reinforcement tension force associated with ultimate moment capacity (kip)

$$\frac{M_s}{M_y} \le 0.33 \qquad \text{Proposed LRFD SGS Eq. 8.8.1-3}$$

where:

M_s = flexural moment capacity provided by longitudinal reinforcement at reference yield moment (kip-ft)
M_y = reference yield moment (kip-ft)

$$\frac{c}{D_c} \le 0.25 \qquad \text{Proposed LRFD SGS Eq. 8.8.1-4}$$

where:

c = distance from extreme compression fiber to the neutral axis at the reference yield point (in)
D_c = column diameter or smallest dimension in the direction of loading (in)

The next recommended modification is to Article 8.8.2 of the LRFD SGS. This provision specifies a minimum flexural contribution of mild reinforcement for hybrid systems to ensure that stable and predictable lateral response is achieved. The traditional minimum reinforcement requirements are not applicable to hybrid systems and therefore a new provision is added. For hybrid systems, the minimum amount of reinforcement ensures that the response predictions for reference yield are reasonable and the overall seismic demands as modified by Article 4.3.3 are valid. The recommended addition to Article 8.8.2 is the following:

> The minimum area of longitudinal reinforcement for hybrid compression members shall satisfy:

$$\frac{M_s}{M_y} \ge 0.25 \qquad \text{Proposed LRFD SGS Eq. 8.8.2-5}$$

where:

M_s = flexural moment capacity provided by longitudinal reinforcement at reference yield moment (kip-ft)
M_y = reference yield moment (kip-ft)

To prevent the premature fracture of column reinforcement in hybrid systems, the reinforcement must be intentionally debonded to accommodate the localized joint opening at the ultimate displacement capacity. A provision is recommended for inclusion in the LRFD SGS as Article 8.8.14 to explicitly enforce this requirement:

> Longitudinal reinforcement in hybrid columns shall be intentionally debonded from the surrounding concrete at hybrid column end connections. The minimum debonded length shall be such to ensure that the strain in the longitudinal reinforcement does not exceed the reduced ultimate tensile strain specified in Article 8.4.2 at the column ultimate rotation capacity.

As was previously discussed, the current provisions for short period displacement amplification are acceptable for use with hybrid systems within the bounds of the provisions presented in the LRFD SGS and herein. However, the influence of joint opening at the reference yield point must also be accounted for in the mathematical modeling of hybrid concrete members to ensure that the added flexibility is considered. The moment-rotation analysis performed in accordance with the recommended Article 8.5 modifications provides a means to approximate the added flexibility for equivalent

elastic analysis. To account for the added flexibility, the effective moment of inertia can be modified based on the effective section properties calculated using moment-rotation analysis. The recommended Article 5.6.6 of the LRFD SGS provides this requirement:

> The effective moment of inertia for calculation of elastic flexural deformations for hybrid bridge columns can be taken equal to the gross moment of inertia. For mathematical modeling, the increase in flexibility at reference yield due to joint opening shall be considered. The influence of joint rotation shall be determined in accordance with the provisions of Article 8.5 using moment-rotation analysis. For equivalent elastic analysis, I_{eff} shall be decreased to account for the additional flexibility due to joint rotation.

3.2.8 Superstructure Capacity for Longitudinal Direction, SDCs C and D

Superstructure Demand

As discussed in relation to the recommended modifications to the 2009 LRFD SGS, vertical seismic demands can play a significant role in the performance of integral precast bridge systems (*1*). Therefore, additional recommendations were specified for the development and consideration of vertical ground motions in the design of integral precast bridges. For longitudinal response, seismic actions are distributed into the superstructure based on an effective width calculated in accordance with Article 8.10. However, for vertical demands, the seismic loading can be distributed across the entire width of the bridge. To account for this, the recommended addition to Article 8.10 is the following:

> Vertical seismic demands determined in accordance with Article 4.7.2 shall be distributed to the entire width of the superstructure. The demands associated with the column overstrength moment, M_{po}, shall be considered concurrently with vertical seismic demands as specified in Article 4.7.2.

Minimum Superstructure Rotation Capacity

The use of capacity design procedures cannot ensure that a superstructure system does not experience loads in excess of the superstructure capacity when considering actual vertical seismic motions and seismically induced foundation movements. The potential for seismically induced relative settlements may induce substantial geometrically driven demands on a bridge superstructure system. These mechanisms can result in loadings in the superstructure that may cause inelastic superstructure action. To ensure that the superstructure can accommodate a limited amount of inelastic rotation demand, the superstructure to bent cap connection should be capable of experiencing a defined level of rotation demand. The intent of the following recommended Article 8.10.3 is to ensure that the superstructure can resist a limited amount of inelastic action:

> The superstructure to bent-cap connection shall have plastic rotation capacity equal to or greater than 0.01 radians. The plastic rotation capacity shall be calculated using the moment-curvature analysis required per Article 8.9 and the analytical plastic hinge length for superstructures as defined in Article 4.11.6.

Torsional Design for Open Soffit Superstructures

CIP integral bridge systems traditionally have a top deck slab and bottom soffit slab that provide reliable distribution of column overstrength demands into the superstructure. However, precast systems without a soffit slab cannot transfer the seismic demands through the same mechanism. The column flexural overstrength demands must be transferred into the superstructure by way of torsional response of the bent cap. Commonly used torsional mechanisms cannot develop over the short distance between the face of the column and girder. Instead, a modified torsional response must be considered. The following new Article 8.10.4 requires the explicit consideration of a torsional transfer mechanism for open soffit systems:

> The transfer of column overstrength moment, M_{po}, and associated shear and axial load via torsional mechanisms must be explicitly considered in the superstructure design for open soffit structures.

Shear Design for Integral Precast Superstructures

The potential for inelastic superstructure response due to vertical motion and seismically induced settlement was mentioned in the discussion of the minimum superstructure rotation capacity. The bottom flanges of precast girders in the superstructure should be detailed to accommodate the potential inelastic actions without degradation of the compression zone. Therefore, the use of closed hoops is recommended as a means to enhance the integrity of the girder flanges in the event of inelastic loading. The recommended addition to the 2009 LRFD SGS (*1*) is the following:

> The bottom flange of integral precast girders shall be reinforced with closed hoops within the region from the face of the bent cap equal to a distance equal to the superstructure depth. These hoops shall be spaced with the girder shear reinforcement, with spacing not to exceed 8 in. The hoops shall be the same size as the girder shear reinforcement, with a minimum bar size of No. 4.

Experimental results highlighted in Chapter 2 and described in detail in the attachments, indicate the importance of a well-developed shear transfer mechanism at the girder to bent cap connection. The potential for concentrated joint opening during seismic loading will result in a significant decrease in the effective shear depth across the joint that must be considered in design. The shear reinforcement can be distributed in the superstructure based on an assumed strut mechanism with a 30-deg maximum compression strut angle. Most importantly, the shear reinforcement must be extended as close to the top of the deck as possible while still satisfying concrete cover requirements. The recommended shear detailing uses headed reinforcement to ensure the sufficient anchorage of the reinforcement within the short distance allocated. The following is a recommended addition to the 2009 LRFD SGS (*1*) as Article 8.10.5:

> For integral precast superstructures with girders discontinuous at the face of the bent cap, headed shear reinforcement shall be placed within a distance from the face of the bent cap equal to 1.75 times the neutral axis depth at nominal capacity as determined in accordance with Article 8.9. The headed shear reinforcement within this distance shall be capable of resisting the factored shear demand including effects of vertical seismic loading in accordance with Article 4.7.2. The shear demand shall be calculated considering the direction of loading and shears generated during positive flexural loading of the superstructure. This reinforcement shall extend as close to the top of the deck as possible while maintaining required concrete cover dimensions.

3.2.9 Joint Definition

Specimen test results and related research provide a sufficient basis for safe, constructible, durable, and economical design of nonintegral emulative precast bent cap systems using grouted duct or cap pocket connections and hybrid connections in all SDC levels. However, as shown in Chapter 2, testing was limited to interior joints of multicolumn bent caps. Therefore, proposed provisions for all SDCs follow the precedent for CIP joints found in Article 8.13.4.1 of the 2009 LRFD SGS (*1*) in limiting specifications to interior joints of multicolumn bent caps:

> Interior joints of multicolumn bents shall be considered "T" joints for joint shear analysis. Exterior joints shall be considered knee joints and require special analysis and detailing that are not addressed herein, unless special analysis determines that "T" joint analysis is appropriate for an exterior joint based on the actual bent configuration.

Specifications for knee joints in CIP and precast bent cap systems should be developed.

3.2.10 Joint Performance

SDCs C and D

The joint performance for SDCs C and D is stated as follows:

> Moment-resisting connections shall be designed to transmit the maximum forces produced when the column has reached its overstrength capacity, M_{po}.

This matches the existing provision for SDCs C and D in the 2009 LRFD SGS (*1*).

SDC B

The joint performance for SDC B is stated as follows:

> Moment-resisting connections shall be designed to transmit the unreduced elastic seismic forces in columns where the column moment does not reach the plastic moment, M_p, and shall be designed to transmit the column forces associated with the column overstrength capacity, M_{po}, where the plastic moment, M_p, is reached.

Based on Article 8.3.2 of the 2009 LRFD SGS, this provision requires that connections be designed to transmit the lesser of the forces produced by M_{po} or the unreduced elastic seismic forces (*1*). However, when the elastic seismic moment reaches the plastic moment, M_p, significant plastic hinging may develop. Therefore, it is conservatively required in such cases that connections be designed to transmit the forces produced by M_{po}. For SDC B, the column section may be designed and governed by load cases other than seismic.

This proposed article is an application of Articles 8.3.2 and C8.3.2 of the 2009 LRFD SGS, which recognize that SDC B bridges may be subjected to seismic forces that can cause yielding of the columns and limited plastic hinging, as they are designed and detailed to achieve a displacement ductility, μ_D, of at least 2.0 (*1*). According to Article C4.8.1, SDC B columns are targeted for a drift capacity corresponding to concrete spalling. Article 4.8.1 provides an approximate equation for local displacement capacity, providing an approach that limits the required seismic analysis (i.e., expands the extent of a "No Analysis" zone). Thus, based on Article 4.11.1, joint shear checks and full capacity design using plastic overstrength forces are not required. This more liberal practice, as stated in Article C4.11.1, may be adopted for CIP joints. However, owners may also choose to implement the more conservative capacity-protection requirements given in Article 8.9.

Full and limited ductility specimen tests indicated initial concrete spalling of the column at drift ratios ranging from 0.9% to 1.8% (μ1.5 to μ3). Specimens used a moderate amount of column longitudinal reinforcement—1.58%. For this case, joint shear cracks developed at loads less than effective yield

($\mu 1$) for all specimens at principal tensile stresses that ranged from $2.95\sqrt{f_c'}$ psi to $4.3\sqrt{f_c'}$ psi, close to the $3.5\sqrt{f_c'}$ psi assumed by the 2009 LRFD SGS (*1*). At $\mu 2$, all specimens had significantly exceeded $3.5\sqrt{f_c'}$ and reached forces that were 88% to 100% of the maximum overall force induced in the joint during testing. Furthermore, the CPLD specimen, designed according to SDC B detailing requirements (i.e., no joint reinforcement other than the steel pipe), exhibited extensive joint shear cracking. As reported in Matsumoto 2009 (*26*), the absence of joint stirrups—in accordance with SDC B design—was the main cause of the development and growth of joint shear cracks. This indicates that SDC B joint design for precast connections should be based on a check of principal tensile stresses and that all SDC B joints should include at least minimum joint shear reinforcement, defined as transverse reinforcement and joint stirrups.

The proposed LRFD SGS adopts the more conservative provisions that principal tensile stresses be checked for SDC B and that joint design depend on this check. These provisions help ensure that the precast bent cap connections accommodate forces in an essentially elastic manner and do not become a weak link in the earthquake resisting system (Articles 4.11.1 and C4.11.1, 2009 LRFD SGS) (*1*).

SDC A

The joint performance for SDC A is stated as the following:

> Moment-resisting connections shall be designed to transmit the unreduced elastic seismic forces in columns.

According to the 2009 LRFD SGS, bridges designed for SDC A are expected to be subjected to only minor seismic displacements and forces; therefore, a force-based approach is specified to determine unreduced elastic seismic forces, in lieu of a more rigorous displacement-based analysis (Articles 4.1 and 4.2, 2009 LRFD SGS) (*1*).

However, some SDC A bridges may be exposed to seismic forces that may induce limited inelasticity, particularly in the columns. For this reason, Article 8.2 states that when S_{D1} is greater than or equal to 0.10 but less than 0.15, minimum column shear reinforcement shall be provided in accordance with Article 8.6.5 for SDC B, subject to Article 8.8.9 for the length over which this reinforcement is to extend. Although Article 8.8.9 does not specify placement of transverse column reinforcement into the joint, Articles 5.10.11.4.1e and 5.10.11.4.3 of AASHTO *LRFD Bridge Design Specifications (4th edition) with 2008 and 2009 Interims,* referenced by the alternative provisions in Articles 8.2 and 8.8.9, specify placement of transverse reinforcement into the joint for a distance not less than one-half the maximum column dimension or 15.0 in from the face of the column connection into the adjoining member (*29*).

According to these alternative provisions, when S_{D1} is greater than or equal to 0.10 but less than 0.15, minimum transverse reinforcement is required for CIP joints. When S_{D1} is less than 0.10, transverse shear reinforcement is not required. For all values of S_{D1} in SDC A, the designer may choose to conservatively provide joint reinforcement as specified for SDC B, although SDC A is typically considered a "No Analysis" region for which seismic analysis is not required (2009 LRFD SGS, Article C4.6) (*1*).

Precast bent cap connections for SDCs B, C, and D are designed and detailed to provide sufficient reinforcement for force transfer through the joint and bent cap. The precast bent cap design provisions for SDC A, including minimum provisions, are more liberal than those for precast bent caps for SDC B and may be considered "No Analysis" requirements for SDC A precast bent cap systems. They are deemed appropriate for all values of S_{D1} in SDC A.

When S_{D1} is less than 0.10, alternative precast bent cap connections developed for nonseismic regions may be used. Figure 3.1 and Figure 3.2 show several nonintegral precast bent cap details developed by Matsumoto et al. (*8*) for grouted duct, grout pocket, and bolted connections (*7*). Other references such as Brenes et al. (*36*) provide additional recommendations for detailing nonintegral precast bent cap connections using grouted ducts. It is recommended that minimum vertical stirrups within the joint be used, as required for SDC A details. In addition, column longitudinal reinforcement should be extended into the connection as close as practically possible to the opposite face of the bent cap.

3.2.11 Joint Proportioning

Two provisions should be satisfied in proportioning bent cap joints: (1) provide cross-sectional dimensions to satisfy limits on principal tensile and compression stresses and (2) provide sufficient anchorage length to develop column longitudinal reinforcement in the bent cap joint under seismic demand.

Principal Stress Requirements

SDCs C and D. Principal tensile and compression should be checked for SDCs C and D as required by Article 8.13.2 of the 2009 LRFD SGS for CIP connections (*1*).

SDC B. As mentioned previously, to ensure that SDC B structures using precast bent caps are designed and detailed to achieve a displacement ductility, μ_D, of at least 2.0 (Article C8.3.2, 2009 LRFD SGS) (*1*), the proposed provisions conservatively require that SDC B joints be proportioned based on a check of principal stress levels. The provisions of Article

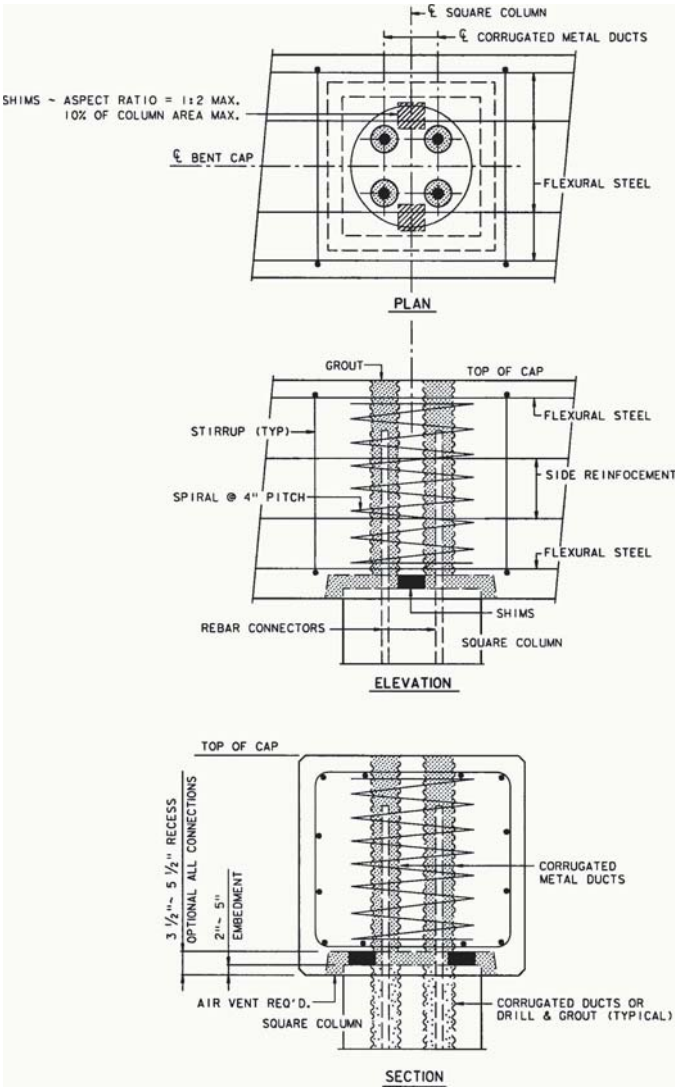

(a) Grouted Duct

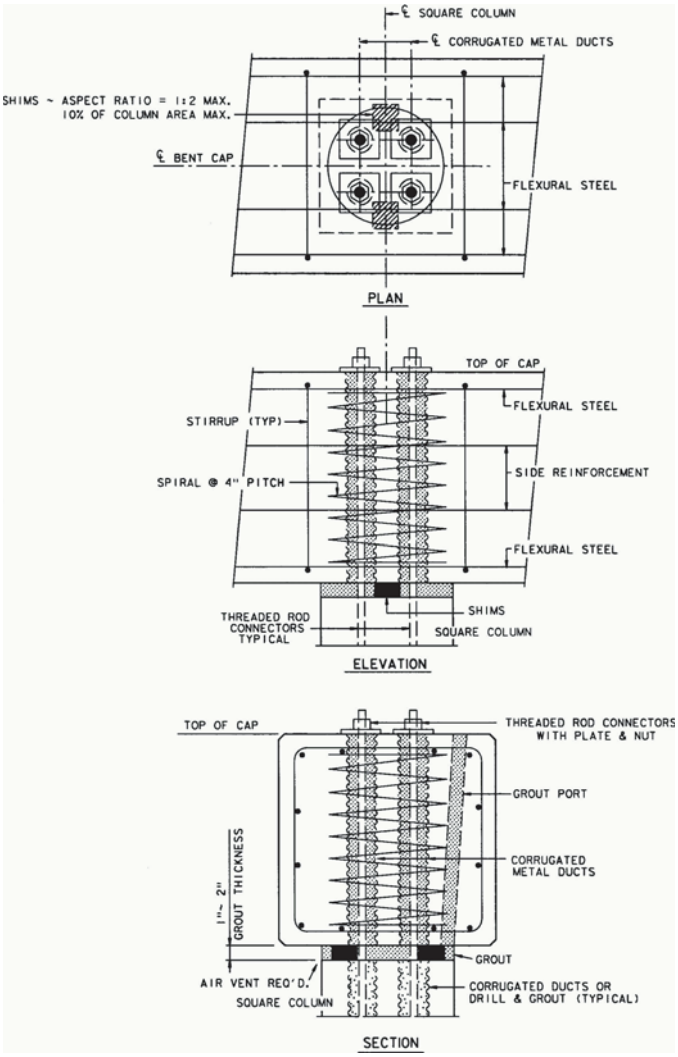

(b) Bolted

Figure 3.1. Alternative precast bent cap connections for SDC A (S_{D1} < 0.10) (7).

8.13.2 of the 2009 LRFD SGS are thus used for joint proportioning, except that the design moment used in determination of principal stresses should be the lesser of M_{po} or the unreduced elastic seismic column moment.

SDC A. Check of principal stresses is not required for SDC A.

Minimum Anchorage Length

Column longitudinal bars should be extended into joints a sufficient depth to ensure that the bars can achieve approximately 1.4 times the expected yield strength of the reinforcement, i.e., a level associated with extensive plastic hinging and strain hardening up to the expected tensile strength. For SDCs C and D, Article 8.8.4 of the 2009 LRFD SGS requires that column longitudinal reinforcement be extended into cap beams as close as practically possible to the opposite face of the cap beam and that for seismic loads, the anchorage length into the cap beam satisfy the following (*1*):

$$l_{ac} \geq \frac{0.79 d_{bl} f_{ye}}{\sqrt{f'_c}} \qquad \text{2009 LRFD SGS Eq. 8.8.4-1}$$

where:

l_{ac} = anchored length of longitudinal column reinforcing bars into cap beam (in)
d_{bl} = diameter of longitudinal column reinforcement (in)
f_{ye} = expected yield stress of longitudinal column reinforcement (ksi)
f'_c = nominal compressive strength of bent cap concrete (ksi)

Prior research by Matsumoto et al. (*7, 8*) and Mislinski (*9*) on anchorage of reinforcing bars in grouted ducts—confirmed

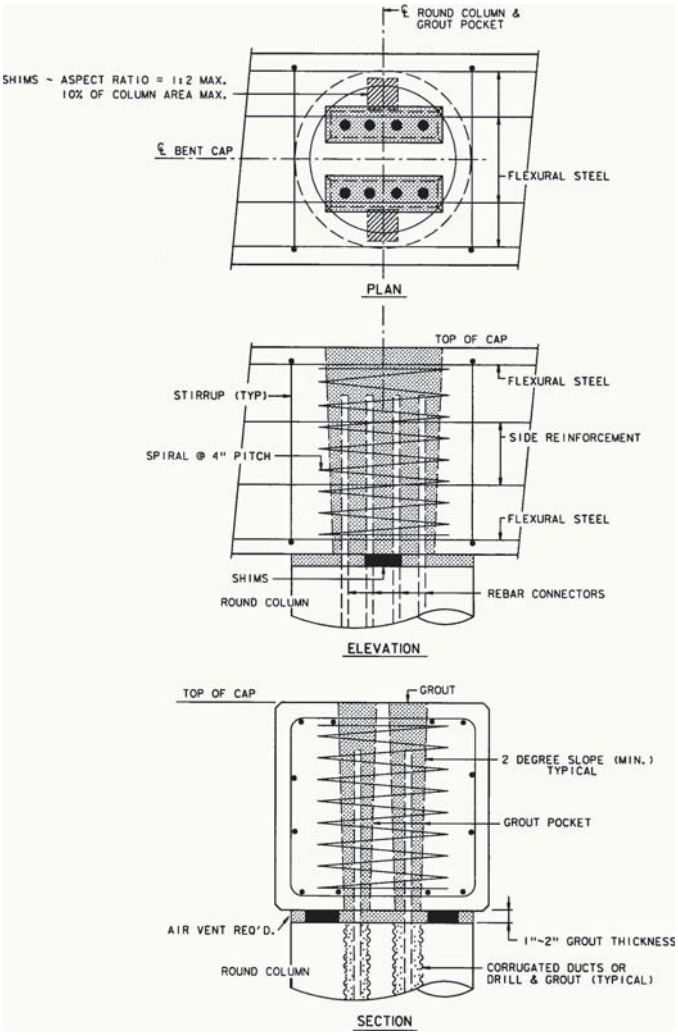

(a) Grouted Pocket (Double Line)

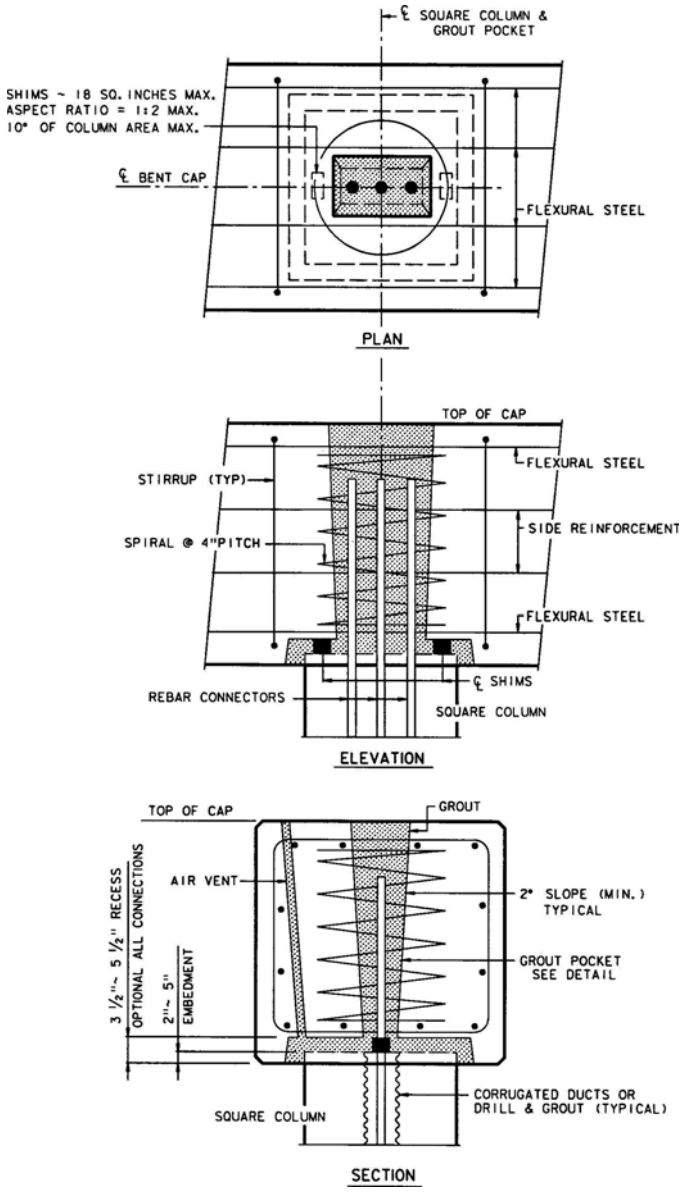

(b) Grouted Pocket (Single Line)

Figure 3.2. Alternative precast bent cap connections for SDC A (S_{D1} < 0.10) (7).

by the NCHRP Project 12-74 grouted duct specimen (*22*)—indicates that the following equation can be conservatively used for seismic applications:

$$l_{ac} \geq \frac{2 d_{bl} f_{ye}}{\sqrt{f'_{cg}}} \qquad \text{Proposed LRFD SGS Eq. 8.15.2.2.2-1}$$

where:

l_{ac} = anchored length of longitudinal column reinforcing bar into grouted duct (in)
d_{bl} = diameter of longitudinal column reinforcement (in)
f_{ye} = expected yield stress of longitudinal column reinforcement (ksi)
f_{cg} = nominal compressive strength of grout (cube strength) (ksi)

The maximum grout compressive strength used in Eq. 8.15.2.2.2-1 should be limited to 7,000 psi, even where the specified grout compressive strength (based on 2-in cubes) exceeds 7,000 psi. In addition, this equation applies #11 column reinforcing bars or smaller ones.

Anchorage of reinforcing bars in cap pocket connections can be based on prior precast bent cap research on grout pocket connections using trapezoidal prism-shaped pockets without a stay-in-place form (*7, 8*). Anchorage equations were modified by removing a 0.75 factor that accounted for extensive splitting cracks at reentrant corners of grout pockets. Such cracking did not develop for the cylindrical-shaped cap pocket connections for CPFD and CPLD that used steel pipes as stay-in-place forms. The following equation—confirmed by CPFD

and CPLD results—can be used for cap pocket connections (*7, 8, 23, 26*):

$$l_{ac} \geq \frac{2.3 d_{bl} f_{ye}}{\sqrt{f'_c}} \qquad \text{Proposed LRFD SGS Eq. 8.15.2.2.2-2}$$

where:

l_{ac} = anchored length of longitudinal column reinforcing bars into cap pocket (in)
d_{bl} = diameter of longitudinal column reinforcement (in)
f_{ye} = expected yield stress of longitudinal column reinforcement (ksi)
f'_c = nominal compressive strength of cap pocket concrete fill (ksi)

The anchored length includes the length of bar within the steel pipe and within the portion of the bent cap between the bottom of the steel pipe and the bent cap soffit.

Maximum compressive strength for the concrete fill used in Eq. 8.15.2.2.2-2 should be limited to 7,000 psi, even where the specified concrete fill compressive strength exceeds 7,000 psi. In addition, this equation applies to #11 column reinforcing bars or smaller ones.

As for CIP connections, the proposed specifications for grouted duct and cap pocket connections require that column longitudinal reinforcement be extended into precast bent caps as close as practically possible to the opposite face of the bent cap.

Only minor slip of column longitudinal bars was observed in the full ductility test specimens (CIP, GD, and CPFD). For example, for the CPFD specimen, bar slip contributed less than 7% to fixed end rotation, and bar slip was comparable to that of the CIP specimen (*21, 23*). However, significant bar slip was observed in the CPLD specimen, as summarized in Chapter 2 and detailed in Matsumoto 2009 (*26*). The level of bar slip observed is attributed to significant shear cracking in the joint that developed due to the lack of joint reinforcement, especially vertical stirrups. The proposed LRFD SGS requires at least minimum joint reinforcement (both transverse confinement and vertical stirrups) for all SDC levels.

In addition, the embedment depth of the CPLD column bars into the cap pocket was 26% less than that required by Eq. 8.15.2.2.2-2, due to the relatively low compressive strength of the concrete fill. Article 8.13.8.3 of the proposed *LRFD Bridge Construction Specifications* (*4*) requires a minimum 500-psi margin between the compressive strength of the bent cap and precast connection concrete fill (or grout). This margin accounts for the likelihood that the actual bent cap compressive strength will exceed its specified strength and the possibility of a low compressive strength of the grout or concrete fill. This provision is intended to ensure that the connection does not become a weak link in the system and helps limit bar slip.

Comparison of Anchorage Length Equations. Figure 3.3 compares seismic anchorage (or development) length requirements for anchoring column longitudinal reinforcement into bent cap joints, based on the equations given in Table 3.1. For simplicity, anchorage length, l_{ac}, is used herein for both anchorage and development lengths (l_{ac} and l_d) applied to anchorage of column bars in a joint. Provisions in the 2009

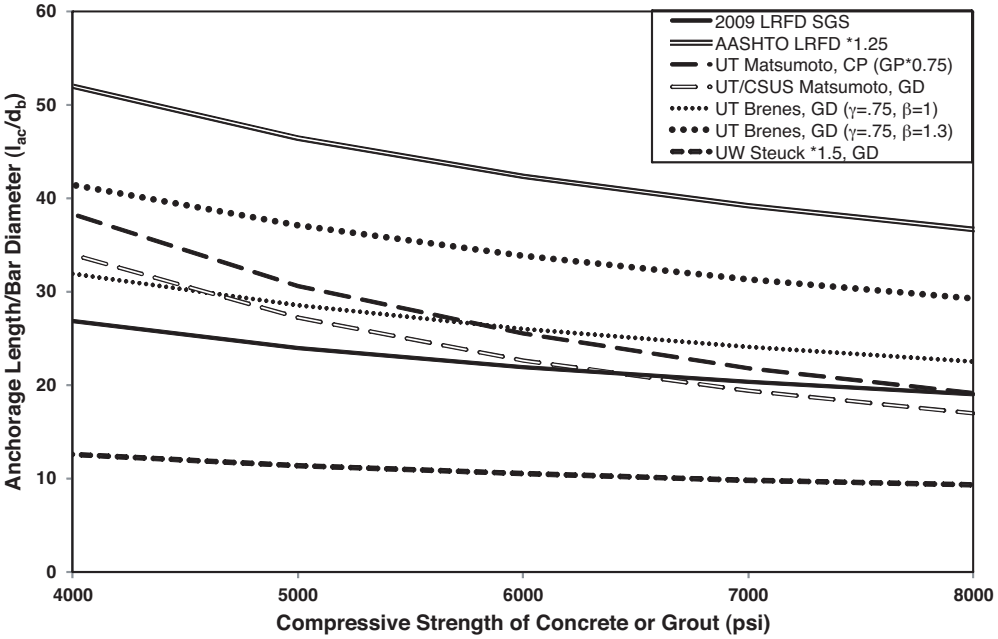

Figure 3.3. Anchorage length versus compressive strength—comparison of equations.

Table 3.1. Comparison of anchorage length equations.

Reference	Anchorage Length, l_{ac}	l_{ac}/d_b or , (#11; f_c' or f_{cg}', 6000 psi)	$\frac{l_{ac}/d_b}{l_{ac}/d_b, \text{2009 LRFD SGS}}$
2009 AASHTO LRFD SGS [15]	$\frac{0.79 d_{bl} f_{ye}}{\sqrt{f_c'}}$	30.9	1.00
AASHTO LRFD BDS[1] [27]	$\frac{(1.25)^2 A_b f_y}{\sqrt{f_c'}}$	59.8	1.94
UT Matsumoto, Cap Pocket[2] [3, 4]	$\frac{2.3 d_b f_{ye}}{f_c'}$	36.0	1.17
UT/CSUS Matsumoto, Grouted Duct [3, 4]	$\frac{2 d_b f_{ye}}{f_{cg}'}$	32.0	1.04
UT Brenes, Grouted Duct[3] [34]	$\frac{\beta f_{s,cr} d_b}{45\gamma\sqrt{f_c'}}$	36.7 ($\beta = 1.0$)	1.19 ($\beta = 1.0$)
		47.7 ($\beta = 1.3$)	1.54 ($\beta = 1.3$)
UW Steuck, Grouted Duct[4] [35]	$1.5\left(\frac{f_y d_b}{130\sqrt{f_g'}} + \frac{d_{duct} - d_b}{2}\right)$	14.9	0.48

[1]Includes 1.25 seismic factor
[2]Embedment includes 0.75 factor
[3] $f_{s,cr}$ taken as $f_{ye.}$; $\gamma = 0.75$; $\beta = 1.0$ for galvanized steel; $\beta = 1.3$ for plastic duct
[4]Includes 1.5 seismic factor; $\frac{d_{duct}-d_b}{2}$ taken as 1.5 in.

LRFD SGS (Article 8.8.4) and LRFD BDS (Article 5.10.11.4.3) apply to CIP connections (*29, 1*). The grouted duct and cap pocket column bar anchorage equations (Eq. 8.15.2.2.2-1 and Eq. 8.15.2.2.2-2) are recommended for use in precast bent cap connections. Additional equations for grouted duct connections based on recent research are also provided (*28, 37*).

Table 3.1 also compares the ratio of anchorage length to bar diameter (l_{ac}/d_b) for #11 rebar and compressive strength of 6,000 psi (grout or concrete) as an example. In addition, the l_{ac}/d_b ratio for each equation is compared to that of the 2009 LRFD SGS (Eq. 8.8.4-1), which is taken as a reference (*1*). Figure 3.3 and Table 3.1 indicate that the LRFD BDS equation is extremely conservative, requiring nearly twice the anchorage length required by the 2009 LRFD SGS. The proposed grouted duct and cap pocket (CP) equations are slightly more conservative (4% and 17%, respectively) than the 2009 LRFD SGS equation for the example, although Figure 3.3 shows the change in anchorage length with compressive strength. The proposed grouted duct equation is based on both tension cyclic and monotonic tension tests and includes a factor of safety of at least 2.0. In addition, this equation can be conservatively used for epoxy-coated bars. The use of f_{cg}' rather than $\sqrt{f_{cg}'}$ in the denominator is explained in Matsumoto et al. (*7*).

Brenes et al. (*36*) extended the grouted duct research of Matsumoto et al. (*8*), examining group effects (γ factor) and plastic ducts (β factor), among other variables. Values of γ range from 0.45 to 0.9 for typical configurations of bars in a grouted duct connection. The case of γ = 0.75 and β = 1.0 shown in Figure 3.3 represents bar anchorage that accounts for group effects based on a moderate number of grouted column bars simultaneously subjected to tension under the design load combinations (γ = 0.75) as well as galvanized steel duct material (β = 1.0). The equation in Brenes et al. for grouted ducts is slightly more conservative than that of Matsumoto et al. for the assumed values of γ and β. Significantly, Brenes et al. found that the required anchorage length increased by 30% when polyethylene or polypropylene (plastic) ducts are used instead of steel. Tension cyclic tests were not conducted. The University of Washington equation, which is multiplied by the recommended 1.5 seismic factor (*37*), results in an exceptionally short development length and is not recommended for use in precast bent cap design.

SDCs B, C, and D. Based on the foregoing development, Eq. 8.15.2.2.2-1 and Eq. 8.15.2.2.2-2 are proposed for anchorage of column bars in grouted duct and cap pocket connections, respectively.

SDC A. SDC A incorporates the same requirements as those for SDCs B, C, and D except that the nominal yield stress of the column longitudinal reinforcement may be used in lieu of the expected yield stress. This allows for a slightly reduced safety margin due to the significantly lower seismic demand and limited inelasticity in the columns.

3.2.12 Minimum Joint Shear Reinforcement

SDCs C and D. Minimum joint shear reinforcement refers to transverse reinforcement within the joint region in the form of column reinforcement, spirals, hoops, intersecting spirals or hoops, or column transverse or exterior transverse reinforcement continued into the bent cap. For precast connections, minimum transverse joint reinforcement is required to help ensure that the connection does not become a weak link in a precast bent cap system. Transverse reinforcement for a grouted duct connection is the same as that for a CIP connection. However, for a cap pocket connection, the steel pipe serves as the transverse reinforcement.

For SDCs C and D, the minimum joint shear reinforcement for precast and hybrid connections is determined using essentially the same basis as that used for CIP connections. If the nominal principal tensile stress in the joint, p_t, is less than $0.11\sqrt{f_c'}$, then the transverse reinforcement in the joint, ρ_s, must satisfy the following equation and no additional reinforcement within the joint is required:

$$\rho_s \geq \frac{0.11\sqrt{f_c'}}{f_{yh}} \qquad \text{2009 LRFD SGS Eq. 8.13.3-1}$$

where:

f_{yh} = nominal yield stress of transverse reinforcing (ksi)
f_c' = nominal compressive strength of concrete (ksi)
ρ_s = volumetric reinforcement ratio of transverse reinforcing provided within the cap

Where the principal tensile stress in the joint, p_t, is greater than or equal to $0.11\sqrt{f_c'}$, then transverse reinforcement in the joint, ρ_s, must satisfy both Eq. 8.13.3-1 and the following equation:

$$\rho_s \geq 0.40\frac{A_{st}}{l_{ac}^2} \qquad \text{2009 LRFD SGS Eq. 8.13.3-2}$$

where:

A_{st} = total area of column longitudinal reinforcement anchored in the joint (in^2)
l_{ac} = length of column longitudinal reinforcement embedded into the bent cap (in)

For this case, additional joint reinforcement is also required.

The 2009 LRFD SGS requires only Eq. 8.13.3-1 to be satisfied (*1*). However, the proposed specifications require that the larger of Eq. 8.13.3-1 and Eq. 8.13.3-2 be used because the transverse reinforcement requirement of Eq. 8.13.3-2 can become less than that of Eq. 8.13.3-1 in some cases, as shown in this research.

SDC B. The proposed provisions for precast connections in SDC B require the same check of principal tensile stress to determine transverse reinforcement in the joint as is required for SDCs C and D.

However, the 2009 LRFD SGS does not include provisions for minimum transverse reinforcement for CIP structures in SDC B (*1*). The SDC B design requirement for CIP would then default to Article 5.10.11.3 of the 2009 LRFD BDS for Seismic Zone 2, which refers the designer to Article 5.10.11.4.3 (Seismic Zones 3 and 4). Article 5.10.11.4.3 requires the following:

> Column transverse reinforcement, as specified in Article 5.10.11.4.1d, shall be continued for a distance not less than one-half the maximum column dimension or 15.0 in from the face of the column connection into the adjoining member.

It is judged that this reinforcement is not adequate for CIP limited ductility connections. It is therefore recommended that minimum joint transverse reinforcement requirements also be established for CIP bridges in SDC B. For limited or simplified seismic analysis (i.e., a "No Analysis"-type approach), minimum reinforcement satisfying Eq. 8.13.3-1 of the 2009 LRFD SGS is recommended (*1*).

SDC A. For SDC A, principal stresses are not checked, but minimum joint shear reinforcement is proposed for precast connections. This is simple, yet conservative and should be considered good detailing practice. Such reinforcement is not required for CIP joints per the 2009 LRFD SGS, but is recommended (*1*).

Grouted Duct Connections

SDCs B, C, and D. Grouted duct connections use the same basis as CIP connections in SDCs C and D, with the additional requirement that spacing of transverse reinforcement not exceed $0.3D_s$ nor 12 in. This is intended to provide a reasonable number of hoops within the joint when the minimum requirement governs.

SDC A. Joint transverse reinforcement provisions conservatively match minimum requirements for SDC B.

Cap Pocket Connections

SDCs B, C, and D—Basic Equation for Pipe Thickness. For cap pocket connections, the thickness of the corrugated

steel pipe, t_{pipe}, is based on providing shear resistance to the joint that is approximately the same as that provided by the hoops required for CIP joints:

> Cap pocket connections shall use a helical, lock-seam, corrugated steel pipe conforming to ASTM A760 to form the bent cap pocket. A minimum thickness of corrugated steel pipe shall be used to satisfy the transverse reinforcement ratio requirements specified in Article 8.15.3.1. The thickness of the steel pipe, t_{pipe}, shall not be taken less than that determined by Eq. 1:

$$t_{pipe} \geq \max \begin{cases} \dfrac{F_H}{H_p f_{yp} \cos\theta} \\ 0.060 \text{ in.} \end{cases}$$

Proposed LRFD SGS Eq. 8.15.3.2.2-1

In which:

$$F_H \geq n_h A_{sp} f_{yh}$$

Proposed LRFD SGS Eq. 8.15.3.2.2-2

where:

F_H = nominal confining hoop force in the joint (kips)
H_p = height of steel pipe (in)
f_{yp} = nominal yield stress of steel pipe (ksi)
θ = angle between horizontal axis of bent cap and pipe helical corrugation or lock seam (deg)
n_h = number of transverse hoops in equivalent CIP joint
A_{sp} = area of one hoop reinforcing bar (in^2)
f_{yh} = nominal yield stress of transverse reinforcement (ksi)

The derivation of this equation is provided in the CPT Attachment. As shown in the design examples provided in the attachments, the spacing of transverse joint hoops can be directly related to the number of hoops, n_h, by the volumetric reinforcement ratio for transverse joint hoops, ρ_s, using Eq. 8.6.2-7 of the 2009 LRFD SGS (*1*).

The maximum spacing requirements of $0.3D_s$ and 12 in do not apply to the determination of n_h.

The minimum thickness of the steel pipe, t_{pipe}, of 0.060 in corresponds to 16-gage steel pipe, which was used for the 18-in nominal diameter pipe in the cap pocket specimens (with a 20-in diameter column). As shown in Table 3.2, this is the thinnest gage typically available off the shelf for corrugated steel pipe. Other pipe thicknesses (nominal and tolerance range) are shown in Table 3.2, with specified and minimum values for coated steel sheet per ASTM A929 (*25*). Thicker pipes (gages 8, 7, and 5) are usually available through special order. Material costs increase roughly according to the weight shown in the last column of Table 3.2.

SDCs B, C, and D—Alternative Equation for Pipe Thickness. The following simplified equations, Eq. C8.15.3.2.2-1 and Eq. C8.15.3.2.2-2, may be used to conservatively determine pipe thickness, t_{pipe}, in lieu of calculating the number of hoops in an equivalent CIP joint, n_h, as the basis for determining pipe thickness. This avoids iteration in design calculations, but may result in thicker gage pipe used in design.

Where the principal tensile stress in the joint, p_t, specified in Article 8.15.2.1, is less than $0.11\sqrt{f_c'}$, the thickness of the steel pipe, t_{pipe}, may be determined from the following:

$$t_{pipe} \geq 0.04 \frac{\sqrt{f_c'} D_{cp}'}{f_{yp} \cos\theta}$$

Proposed LRFD SGS Eq. C8.15.3.2.2-1

where:

f_c' = nominal compressive strength of the bent cap concrete (ksi)
D_{cp}' = average diameter of confined cap pocket fill between corrugated pipe walls (in)
f_{yp} = nominal yield stress of steel pipe (ksi)
θ = angle between horizontal axis of bent cap and pipe helical corrugation or lock seam (deg)

Table 3.2. Steel corrugated pipe thicknesses.

Gage Number	Thickness (in)				Pounds per Square Foot
	Nominal	Tolerance Range	Specified†	Minimum†	
16	0.0598	0.0648 to 0.0548	0.064	0.057	2.439
14	0.0747	0.0797 to 0.0697	0.079	0.072	3.047
12	0.1046	0.1106 to 0.0986	0.109	0.101	4.267
10	0.1345	0.1405 to 0.1285	0.138	0.129	5.486
8*	0.1644	0.1742 to 0.1564	0.168	0.159	6.875
7*	0.1838	0.1883 to 0.1703	No value	No value	7.500
5*	0.2092	0.2162 to 0.2022	No value	No value	8.750

*Nonstandard size available by special order
†Values refer to coated steel sheet thicknesses per ASTM A929 (*25*)

Where the principal tensile stress in the joint, p_t, is greater than or equal to $0.11\sqrt{f_c'}$, the thickness of the steel pipe, t_{pipe}, may be determined from the larger of Eq. C8.15.3.2.2-1 and the following equation:

$$t_{pipe} \geq 0.14 \frac{A_{st} D_{cp}' f_{yh}}{l_{ac}^2 f_{yp} \cos\theta}$$

Proposed LRFD SGS Eq. C8.15.3.2.2-2

where:

A_{st} = total area of column longitudinal reinforcement anchored in the joint (in²)
D_{cp}' = average diameter of confined cap pocket fill between corrugated pipe walls (in)
f_{yh} = nominal yield stress of transverse reinforcing (ksi)
l_{ac} = anchored length of longitudinal column reinforcing bars into precast bent cap (in)
f_{yp} = nominal yield stress of steel pipe (ksi)
θ = angle between horizontal axis of bent cap and pipe helical corrugation or lock seam (deg)

The derivations of these equations are provided in an attachment together with a comparison of the influence of different variables in these equations. For example, Figure 3.4 compares the pipe thicknesses required by Eq. 8.15.3.2.2-1, Eq. C8.15.3.2.2-1, and Eq. C8.15.3.2.2-2. For comparison, column diameters range from 24 in to 60 in; equivalent hoop sizes vary according to the column diameter; the column is assumed to have a longitudinal steel ratio, A_{st}/A_{col}, of 0.015; and the bent cap compressive strength is assumed to be 6,000 psi. Figure 3.4 reveals that (1) using the general (refined) equation results in the thinnest required pipe; (2) using the approximate equations (larger of the two equations, where principal tensile stress is greater than or equal to $0.11\sqrt{f_c'}$) usually results in a pipe thickness one gage size larger than that required by the general equation, using the gage sizes given in Table 3.2; (3) a reasonable pipe thickness results in all cases; and (4) Eq. C8.15.3.2.2-1 governs over Eq. C8.15.3.2.2-2 for all but the largest column diameter (60 in).

Figure 3.5 compares the pipe thicknesses for column longitudinal steel ratios, A_{st}/A_{col} of 0.010, 0.015, and 0.020. This figure shows the expected significant impact of A_{st}/A_{col} on required pipe thickness. It also shows that Eq. C8.15.3.2.2-2 results in thick gage pipes for larger columns, indicating that the designer may prefer to use the general equation in such conditions to minimize the required pipe thickness.

The CPT Attachment provides additional plots that show the effect of f_c' on pipe thickness for 4,000 psi, 6,000 psi, and 8,000 psi bent cap concrete. The required pipe thickness increases approximately 10% to 30% with f_c' based on Eqs. C8.15.3.2.2-1 and C8.15.3.2.2-2. For example, for a 36-in diameter column with #6 hoops (A_{st}/A_{col} = 0.015), the pipe thickness increases 18% as f_c' increases from 4,000 psi to 8,000 psi. Eq. C8.15.3.2.2-1 results in a larger increase of 41% (proportional to $\sqrt{f_c'}$). Eq. C8.15.3.2.2-2 is not dependent on f_c'.

SDC A. Cap pocket pipe thickness for SDC A is based on the minimum provision for transverse reinforcement, as given in Eq. 8.15.3.2.2-1. Eq. C8.13.3.2.2-1 may be alternatively used.

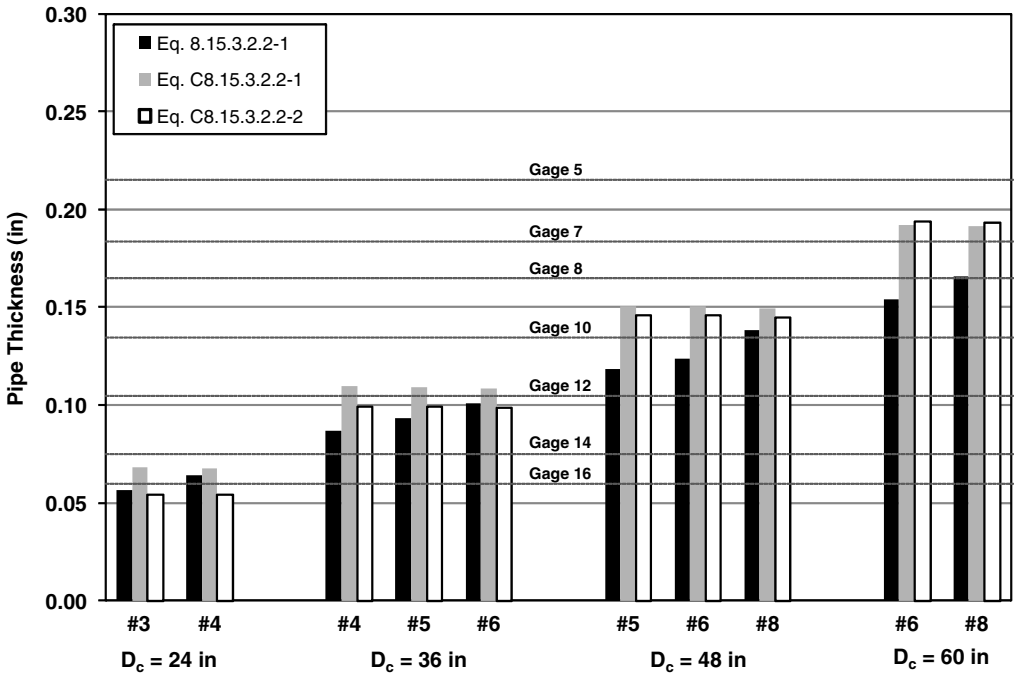

Figure 3.4. Pipe thickness versus column diameter (D_c) and equivalent hoop size (A_{st}/A_{col} = 0.015, f_c' = 6,000 psi for bent cap).

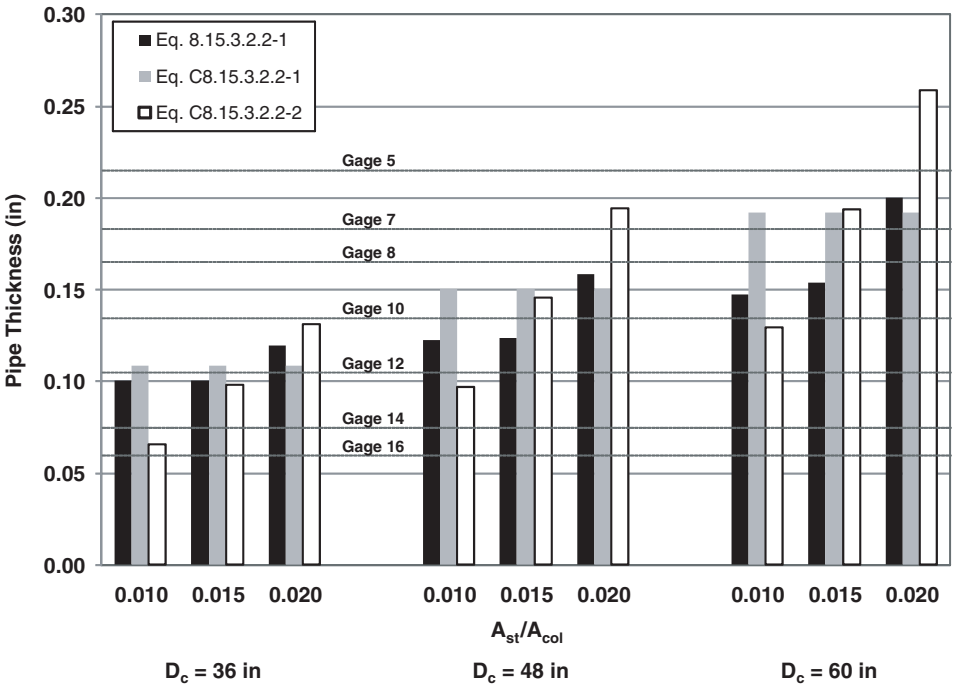

Figure 3.5. Pipe thickness versus column diameter (D_c) and column flexural reinforcement ratio (#6 hoop, f'_c = 6,000 psi for bent cap).

3.2.13 Integral Bent Cap Joint Shear Design

Per 2009 LRFD SGS, joint shear design is required for SDCs C and D, but not SDC B (*1*). Where the principal tensile stress, p_t, is greater than or equal to $0.11\sqrt{f'_c}$, additional joint shear reinforcement is required. The 2009 LRFD SGS requires placement of joint shear reinforcement based on assumed force transfer mechanisms in the longitudinal and transverse directions. Based on a review of the testing presented in Chapter 2 and other previous research on precast integral bridge systems, the assumed force transfer mechanism for longitudinal loading is adequate for the system considered.

However, the requirements presented in the 2009 LRFD SGS for transverse response vary from the requirements for nonintegral transverse response (*1*). The mechanism for transverse response is the same whether an integral or nonintegral connection is used. Therefore, there are recommended modifications to the integral design provisions to account for these differences.

Vertical Stirrups

Requirements specified in the 2009 LRFD SGS for vertical stirrups in integral bridge systems are based on longitudinal and transverse loadings. Per Figure 8.13.4.2.1-1 of the 2009 LRFD SGS, for single column bent caps only vertical stirrups are required along both faces of the bent cap extending one-half the column dimension on both sides of the column (*1*). This requirement is based on an assumed longitudinal force transfer mechanism and is appropriate for use in both CIP and precast integral bridge connections. In accordance with Figure 8.13.4.2.1-1, for multicolumn bent caps additional reinforcement is required on both sides of the column based on an assumed transverse force transfer mechanism. These requirements vary from those presented for nonintegral bent caps and must be updated for consistency.

The recommended modifications to this provision eliminate the second portion of Figure 8.13.4.2.1-1 for multicolumn bent caps. Instead, this article should reference the recommended provisions of LRFD SGS Article 8.15.5 for vertical stirrups inside and outside of the joint. The transverse provisions for nonintegral bent caps are described in more detail in subsequent sections of this report.

Horizontal Stirrups

The 2009 LRFD SGS requires the placement of horizontal stirrups around the vertical stirrups within the bent cap (*1*). These provisions are adequate for integral systems in the longitudinal direction but must also be updated to be in agreement with the nonintegral transverse requirements. The provisions of Article 8.13.4.2.2 of the 2009 LRFD SGS provide a minimum quantity of horizontal stirrups required in addition to spacing requirements. The provisions for nonintegral bent caps specify only spacing and size requirements. The recommended modification for integral bent caps is the addition of a provision to

ensure that the horizontal stirrups for multicolumn bent caps also satisfy the nonintegral provisions.

Additional Longitudinal Cap Beam Reinforcement

Provisions for nonintegral bent caps per the 2009 LRFD SGS require the placement of additional longitudinal reinforcement within the cap beam (*1*). There is currently no requirement for the placement of this reinforcement for multicolumn integral bent caps. Therefore, it is recommended that a provision for integral bent caps that requires the placement of additional longitudinal cap beam reinforcement for multicolumn bent caps be added. The adequacy of this requirement for transverse response of nonintegral bent caps is discussed in more detail in a subsequent section.

3.2.14 Nonintegral Bent Cap Joint Shear Design

Per the 2009 LRFD SGS, joint shear design is required for SDCs C and D, but not SDC B (*1*). For SDCs C and D, where the principal tensile stress, p_t, is less than $0.11\sqrt{f_c'}$, minimum joint shear (transverse) reinforcement is required. Where p_t is greater than or equal to $0.11\sqrt{f_c'}$, the additional joint shear reinforcement (A_s^{jvi}, A_s^{jvo}, A_s^{jl}, and horizontal J-bars) is required.

The proposed joint shear design approach for nonintegral precast bent caps and integral bent caps in the transverse direction follows the same approach, but conservatively requires the principal tensile stress check for SDC B as well as SDCs C and D. In addition, the additional joint shear reinforcement differs in certain regards from CIP requirements. Although vertical joint stirrups, horizontal J-bars, and additional longitudinal bent cap reinforcement are addressed, other provisions, such as bedding layer reinforcement and supplementary hoops, are included. In addition, minimum joint shear reinforcement—both transverse joint reinforcement and vertical joint stirrups inside the joint—is conservatively required for all SDC levels.

The proposed joint shear reinforcement provisions are based on precast bent cap specimen response reported in the work of Matsumoto (*21, 22, 23, 26*) as well as additional analysis presented herein. Table 3.3 compares the joint reinforcement used in the full ductility specimen design to that required by the 2006 LRFD RSGS, which was the original design basis of specimens, and the 2009 LRFD SGS, the current AASHTO seismic guide specifications (*2, 1*). The proposed LRFD SGS for precast bent caps for SDCs C and D is also listed and compared to the test specimens (Proposed Specification/Test Specimen) and to the 2009 LRFD SGS (Proposed Specification/2009 LRFD SGS).

Table 3.3. Comparison of joint reinforcement for various seismic guide specifications—SDCs C and D.

Reinforcement Type	Term	Specimen Quantity	2006 LRFD RSGS	2009 LRFD SGS	Proposed Guide Specification		Proposed Specification / Test Specimen		Proposed Specification / 2009 LRFD SGS	
Transverse Hoop	ρ_s	-[A]	$\rho_s \geq 0.40\left(\frac{A_{st}}{l_{ac}^2}\right)$	$\rho_s \geq 0.40\left(\frac{A_{st}}{l_{ac}^2}\right)$	$\rho_s \geq$ max of $\left(0.40\left(\frac{A_{st}}{l_{ac}^2}\right), \frac{0.11\sqrt{f_c'}}{f_{yh}}\right)$		-[A, B]		1.00[B]	
Vertical Joint	$\frac{A_s^{jvo}}{A_{st}}$	0.27	0.20[C]	0.175	0.175		0.65[D]		1.00	
	$\frac{A_s^{jvi}}{A_{st}}$	0.089[E]	-	0.135	GD: 0.135	CPFD: 0.12	GD: 1.52	CPFD: 1.35	GD: 1.00	CPFD: 0.89
Additional Bent Cap Longitudinal	$\frac{A_s^{jl}}{A_{st}}$	0.0	0.0	0.245	0.245		-[F]		1.00	
Horizontal J-bar	$\frac{A_s^{jh}}{A_{st}}$	0.13[G]	0.10[G]	Every other intersection in joint	Every other intersection in joint		-[G]		GD: 1.00	CPFD: -[H]
Bedding Layer Hoop	-	-	-	-	Reinforcement per specification		-[I]		-[I]	

Notes:
[A] GD test specimen used hoops close to minimum per 2006 LRFD RSGS, and CPFD used a steel corrugated pipe thickness based on 2006 LRFD RSGS.
[B] Typically this will be 1.0, except that the proposed specification requires the larger of 2009 LRFD SGS Eq. 8.13.3-1 and Eq. 8.13.3-2 be used.
[C] Placed transversely within D_c from either side of column center line per 2006 LRFD RSGS. Placement was adjacent to joint.
[D] Difference was due to change in design requirements and rounding of bar sizes in specimen.
[E] Specimen used construction stirrups; 2006 LRFD RSGS did not require A_s^{jvi}.
[F] Not used because 2006 LRFD RSGS did not require A_s^{jl}.
[G] Proposed Guide Specification and 2009 LRFD SGS require A_s^{jh} in joint for GD; GD specimen used A_s^{jh} adjacent to joint per 2006 LRFD RSGS.
[H] Horizontal J-bars are not used for cap pocket connections.
[I] Specimen did not use hoop in scaled 1- in bedding layer. Bedding layer hoop applies only to precast connections.

From Table 3.3, it is evident that the joint design requirements became considerably more conservative from the 2006 LRFD RSGS to 2009 LRFD SGS and that the differences between the test specimens and the 2009 LRFD SGS reflect this (*2, 1*). As a whole, the proposed joint reinforcement is conservative compared to that used in the test specimens. In addition, there is considerable consistency (i.e., a ratio of 1.00 for Proposed Specification/2009 LRFD SGS) between the proposed specifications and 2009 LRFD SGS for SDCs C and D where principal tensile stress, p_t, is greater than or equal to $0.11\sqrt{f'_c}$. However, there are still considerable differences in design specifications between nonintegral CIP and precast bent caps, as shown in the following sections.

Limits on Bent Cap Depth

Nonintegral precast bent caps are subject to the same bent cap depth limitations and the alternative design basis required by Article 8.13.5 of the 2009 LRFD SGS (for CIP bent caps) (*1*). The proposed provision is the following:

> Cast-in-place, emulative precast and hybrid bent cap beams satisfying Eq. 1 shall be reinforced in accordance with the requirements of Articles 8.15.5.1 and 8.15.5.2. Bent cap beams not satisfying Eq. 1 shall be designed on the basis of the strut and tie provisions of the AASHTO LRFD Bridge Design Specifications and as approved by the Owner.
>
> $D_c \le d \le 1.25D_c$ Proposed LRFD SGS Eq. 8.15.5-1
>
> where:
>
> D_c = column diameter (in)
> d = total depth of the bent cap beam (in)

Vertical Stirrups Inside and Outside the Joint

SDCs C and D—Principal Tensile Stress, p_t, $0.11\sqrt{f'_c}$ or Larger. The 2006 LRFD RSGS used for the design of the prototype bridge and full ductility test specimens did not distinguish between integral and nonintegral bent cap systems, nor between the design of vertical stirrups inside the joint region and outside (i.e., adjacent to) the joint region (*2*). Based on the work of Sritharan (*38*), the 2009 LRFD SGS (*1*) for nonintegral bent caps increased the required total area of vertical joint stirrups (inside and outside the joint) approximately 21% over the 2006 LRFD RSGS requirement. In addition, Articles 8.13.5.1.1 and 8.13.5.1.2 of the 2009 LRFD SGS require placement of $0.175A_{st}$ outside the joint (adjacent to each side of the column) as well as $0.135A_{st}$ inside the joint. These are major changes in joint stirrup requirements over the 2006 LRFD RSGS provisions. These provisions should also be required for the design of integral bent cap systems in the transverse direction as the response mechanism is the same.

The full ductility specimens used the more liberal (and constructible) placement of joint stirrups outside the joint as the more severe condition for investigating joint response, permissible by the 2006 LRFD RSGS (*2*). Rounding stirrup bar diameters to practical sizes for the test specimens resulted in a larger area of vertical stirrups outside the joint region than required. However, two 2-leg construction stirrups with a total area of $0.089A_{st}$ were included within the joint region, as mentioned in Matsumoto (*21*). As shown in Table 3.3, this resulted in an area 66% of that required by the 2009 LRFD SGS ($0.135A_{st}$) (*1*).

As shown in the strain profiles of Figure 2.48 (CIP), Figure 2.54 (GD), and Figure 2.59 (CPFD), vertical joint stirrups were highly effective for the CIP and GD specimens for which maximum joint crack widths were 0.025 in and 0.040 in, respectively. This confirms the importance of such stirrups in achieving emulative response. Smaller joint stirrup strains were evident for the CPFD specimen, which exhibited much smaller crack widths and a crack pattern that differed from the CIP and GD specimens. In contrast, the CPLD specimen exhibited severe joint cracking, which is attributed to the absence of joint reinforcement, especially joint stirrups. Figure 2.46 and Figure 2.64 portray the significant effect of the CPLD joint shear cracking on joint shear stiffness and system displacement, even though the specimen achieved an exceptionally large drift of 5.0% in the presence of cracks up to 0.080 in wide. Outside the joint, the GD and CPLD stirrup strains were the largest, 68% of yield and 61% of yield, respectively.

Based on a comparison of GD and CIP results and the overall GD emulative response, the proposed specification requires full ductility grouted duct connections to use the same joint stirrups inside the joint as required by the 2009 LRFD SGS (*1*).

Based on a comparison of the CPFD and CIP response, it is deemed reasonably conservative to require $0.12A_{st}$—12% less than the CIP requirement ($0.135A_{st}$) but 35% more than that used in the CPFD specimen ($0.089A_{st}$), which exhibited minimal joint distress and exceptional joint performance:

> Vertical stirrups inside the joint with a total area, A_s^{jvi}, spaced evenly over a length, D_c, through the joint shall satisfy:
>
> $A_s^{jvi} \ge 0.12\, A_{st}$ Proposed LRFD SGS Eq. 8.15.5.2.3a-1
>
> Vertical stirrups inside the joint shall consist of double leg stirrups or ties of a bar size no smaller than that of the bent cap transverse reinforcement. A minimum of two stirrups or equivalent ties shall be used.

Due to the presence of the pipe, overlapping double-leg vertical stirrups are not practical.

Figure 3.6 shows the minimum number of two-leg vertical joint stirrups required for values of A_s^{jvi}/A_{st} ranging from 0.08

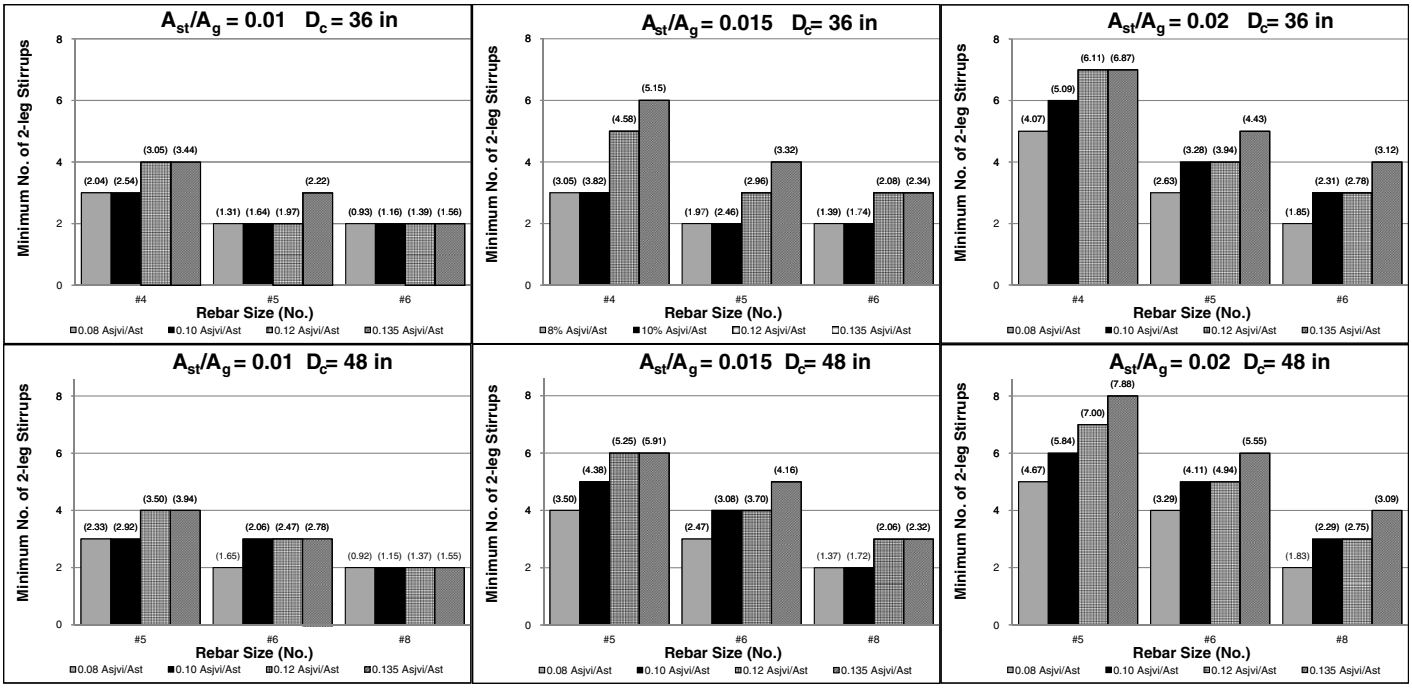

Figure 3.6. Minimum number of 2-leg stirrups inside the joint—36-in and 48-in diameter columns.

to 0.135, based on several stirrup sizes. Results are shown for 36-in and 48-in diameter columns and for column longitudinal reinforcement ratios, A_{st}/A_g, of 0.01, 0.015, and 0.02. The height of the bar indicates the number of required stirrups, subject to the proposed specification minimum of two stirrups. Additionally, the number in parentheses at the top of the bar indicates the calculated stirrup requirement (i.e., without rounding or the 2-stirrup minimum). Figure 3.6 shows that both the $0.135A_{st}$ requirement for grouted ducts and the $0.12A_{st}$ requirement for cap pocket connections produce a number of stirrups that can be reasonably satisfied in design and construction.

Although the design requirement can become significant for larger percentages of column longitudinal reinforcement (A_{st}), potential congestion can be alleviated by the use of larger stirrup bar sizes. Grouted duct connections require a larger area of vertical stirrups than cap pocket connections, and as shown in Figure 3.6, this sometimes results in a larger number of stirrups; however, the area requirement can be satisfied by using overlapping two-leg stirrups. Cap pocket connections accommodate only two-leg stirrups; therefore, it is important that the designer carefully consider using larger stirrup sizes and possibly bundling stirrups, especially when a larger column reinforcement ratio is used. In addition, care should be taken in design to ensure that the number and placement of stirrups over the top opening of the pocket does not unduly interfere with concrete placement in the pocket during the assembly operation. For both connection types, stirrups should be placed symmetrically. Three sets of stirrups can be placed symmetrically when column bars are rotated a half turn (to avoid conflict); however, conflict between bent cap longitudinal bars and column bars and/or corrugated ducts should also be avoided.

Based on a comparison of CIP results with GD and CPFD response and the overall GD and CPFD emulative response, the proposed specification requires grouted duct and cap pocket full ductility connections to use the same joint-related vertical stirrup area outside the joint (A_s^{jvo}) as required by the 2009 LRFD SGS (*1*).

SDCs C and D—Principal Tensile Stress, p_t, Less than $0.11\sqrt{f_c'}$. Per the 2009 LRFD SGS, where the principal tensile stress, p_t, for a CIP connection is less than $0.11\sqrt{f_c'}$, only minimum joint transverse (hoop) reinforcement is required; vertical joint stirrups are not required (*1*). As mentioned previously, additional joint shear reinforcement for precast bent caps should be based on principal tensile stress exceeding $0.11\sqrt{f_c'}$ (i.e., likely joint shear cracking). However, given the inherent variability in actual bridge fabrication, assembly, and seismic response and the potentially severe impact of joint shear cracking on intended emulative response, the proposed specifications conservatively require a minimal area of vertical joint stirrups in grouted duct and cap pocket connections in SDCs C and D, even where the principal tensile stress, p_t, is less than $0.11\sqrt{f_c'}$. This provision is expected to be more commonly associated with SDC B and

is therefore addressed in the next section (SDC B). Vertical stirrups outside the joint are not required.

SDC B. Where the principal tensile stress, p_t, for an SDC B bridge using a precast bent cap connection is $0.11\sqrt{f_c'}$ or larger, the joint shear design provisions for SDCs C and D are conservatively required. Where the principal tensile stress is less than $0.11\sqrt{f_c'}$, the following minimum provision for vertical stirrups in the joint must be satisfied for grouted duct connections:

> Vertical stirrups with a total area, A_s^{jvi}, spaced evenly over a length, D_c, through the joint shall satisfy:
>
> $A_s^{jvi} \geq 0.10\, A_{st}$ Proposed LRFD SGS Eq. 8.14.5.2.2a-1
>
> Vertical stirrups inside the joint shall consist of double leg stirrups or ties of a bar size no smaller than that of the bent cap transverse reinforcement. A minimum of two stirrups or equivalent ties shall be used.

This limited provision, which still results in a highly constructible joint region, provides reinforcement to restrict joint shear effects in the event of joint shear cracking. As shown in Figure 3.6, joints will typically require only two to three 2-leg stirrups. Vertical stirrups outside the joint are not required.

The A_s^{jvi} requirement for cap pocket connections is identical to that for the grouted duct connections.

SDC A. For SDC A, the principal tensile stress, p_t, is not calculated. However, the following minimum provision for vertical stirrups in the joint conservatively applies for grouted duct connections:

> Vertical stirrups with a total area, A_s^{jvi}, spaced evenly over a length, D_c, through the joint shall satisfy:
>
> $A_s^{jvi} \geq 0.08\, A_{st}$ Proposed LRFD SGS Eq. 8.13.4.2.2a-1
>
> Vertical stirrups inside the joint shall consist of double leg stirrups or ties of a bar size no smaller than that of the bent cap transverse reinforcement. A minimum of two stirrups or equivalent ties shall be used.

As shown in Figure 3.6, the minimum 2-stirrup requirement is expected to govern.

The provision for cap pocket connections is identical to that for the grouted duct connections.

Additional Longitudinal Cap Beam Reinforcement

SDCs C and D. The 2006 LRFD RSGS (*2*) used in the design of the prototype bridge and emulative test specimens did not include the significant additional longitudinal bent cap reinforcement, which is prescribed in the 2009 LRFD SGS (*1*) for nonintegral bent caps as follows:

> Longitudinal reinforcement, A_s^{jl}, in both the top and bottom faces of the cap beam shall be provided in addition to that required to resist other loads. The additional area of the longitudinal steel shall satisfy:
>
> $A_s^{jl} \geq 0.245 A_{st}$ Proposed LRFD SGS Eq. 8.13.5.1.3-1

Maximum bent cap longitudinal bar strains for the specimens were limited to 46% of yield for CIP and 53% of yield for GD, but exceeded yield for CPFD and CPLD. The area of the CPLD bent cap longitudinal reinforcement was reduced 30% from the CPFD, which contributed to the extent of yielding, as discussed in Matsumoto (*26*).

Based on specimen response, the proposed specifications do not modify the 2009 LRFD SGS (*1*). Therefore, this additional reinforcement is required where the principal tensile stress, p_t, for a precast bent cap connection is $0.11\sqrt{f_c'}$ or larger.

As shown in the example connection details for cap pocket connections for SDCs B, C, and D provided in the attachments, inverted U-bars or hairpins may be placed within the pocket to help restrain potential splitting cracks and buckling of top bent cap flexural bars within the joint. This additional conservative measure is optional but recommended where the principal tensile stress, p_t, is $0.11\sqrt{f_c'}$ or larger. It is not required for grouted duct connections where overlapping vertical stirrups within the joint can serve the same purpose.

SDC B. As for other additional joint shear reinforcement, the additional longitudinal bent cap reinforcement stipulated in the previous section for SDCs C and D is conservatively required for SDC B where the principal tensile stress, p_t, for a precast bent cap connection is $0.11\sqrt{f_c'}$ or larger.

SDC A. For SDC A, additional longitudinal cap beam reinforcement is not required.

Horizontal J-Bars

SDCs C and D. In accordance with the 2006 LRFD RSGS (*2*), horizontal J-bars with an area, A_s^{jk}, of at least $0.10A_{st}$ was used in the CIP and GD specimens together with A_s^{jv} reinforcement adjacent to the joint (within $D_c/2$ of column face). The 2009 LRFD SGS for nonintegral bent caps modified this requirement as follows (*1*):

> Horizontal J-bars hooked around the longitudinal reinforcement on each face of the cap beam shall be provided as shown in Figure 8.15.5.1.1-1. At a minimum, horizontal J-bars shall be located at every other vertical-to-longitudinal bar intersection within the joint.

The J-dowel reinforcement bar shall be at least a #4 size bar.

This provision is included in the proposed LRFD SGS for grouted duct connections, when the principal tensile stress, p_t, for a precast bent cap connection is $0.11\sqrt{f_c'}$ or larger. However, based on specimen response, cap pocket connections were shown not to require horizontal J-bars.

SDC B. Where the principal tensile stress, p_t, for a precast bent cap connection is $0.11\sqrt{f_c'}$ or larger, J-bars stipulated for SDCs C and D are similarly required for grouted duct connections in SDC B.

SDC A. For SDC A, horizontal J-bars are not required.

Supplementary Hoops for Cap Pocket Connections

SDCs C and D. The CPFD specimen response demonstrated the effectiveness of a supplementary hoop placed at each end of the steel pipe to limit dilation and potential unraveling. This reinforcement, which matched the column hoop bar size, reached up to 52% of yield during the test, indicating its contribution to joint performance. Therefore, where the principal tensile stress, p_t, is $0.11\sqrt{f_c'}$ or larger, cap pocket connections in SDCs C and D require the use of supplementary hoops:

A supplementary hoop shall be placed one inch from each end of the corrugated pipe. The bar size of the hoop shall match the size of the bedding layer reinforcement required by Article 8.15.5.2.1.

The hoop area meeting the requirement of the bedding layer reinforcement (and column hoop) is considered sufficient. Where the principal tensile stress, p_t, is less than $0.11\sqrt{f_c'}$, hoops are not required but may be conservatively included.

SDC B. As for the additional joint shear reinforcement, supplementary hoops stipulated in the previous section for SDCs C and D are conservatively required for SDC B where the principal tensile stress, p_t, for a precast bent cap connection is $0.11\sqrt{f_c'}$ or larger. Where the principal tensile stress, p_t, is less than $0.11\sqrt{f_c'}$, supplementary hoops may be optionally included as a simple, inexpensive, and conservative measure.

SDC A. For SDC A, supplementary hoops are not required.

Reinforcement at the Bedding Layer and Top of Column

Bedding Layer Reinforcement. A bedding layer between the bent cap soffit and the top of column is used to accommodate fabrication and placement tolerances. Transverse reinforcement around the column bars within the bedding layer provides confinement and reduces the unsupported length of column bars, thereby reducing the potential for buckling during plastic hinging of the column. Accurate placement of reinforcement is, therefore, essential to achieving the expected system ductility capacity. Reinforcement should normally be placed evenly through the depth of the bedding layer. However, in some cases, an uneven bedding layer (e.g., a sloping bent cap on top of a large diameter column) or a bedding layer of an unusual shape may be encountered, requiring placement of bedding layer reinforcement that is not uniformly distributed, to minimize the unsupported length of column bars. In all cases, plan sheets should show the intended placement of the bedding layer reinforcement. The associated requirement for shop drawings is addressed in proposed Article 8.13.8.4.4 of the AASHTO *LRFD Bridge Construction Specifications* (LRFD BCS) (*35*). Adequate flowability of the concrete fill or grout should not be prevented by the size and placement of the bedding layer reinforcement. Matsumoto et al. (*8*) present an alternative approach to accommodating tolerances and enhancing durability by embedding the column or pile into the bent cap.

The proposed design specification is as follows:

Bedding layers between columns and precast bent caps shall be reinforced with transverse reinforcement, as shown in Figure 8.15.5.2.2-1 and Figure 8.15.5.2.3-1. Bedding layer reinforcement shall match the size and type of transverse reinforcement required for the column plastic hinging region and shall be placed evenly through the depth of the bedding layer.

Grout bedding layer heights shall not exceed 3 in.

For seismic loading scenarios, the bedding layer thickness is limited to 3 in when constructed of a cementitious grout material. Grout properties do not show the same improvement with lateral confinement that concrete materials show. Increasingly large grout bedding layer thicknesses can result in the development of poor lateral response due to the degradation of the bedding layer. Therefore, the use of grout materials is limited to joints 3 in or less in dimension.

Lateral Reinforcement Requirement for Columns Connecting to a Precast Bent Cap. Uniform spacing between hoops at the top of the column and the bedding layer is critical to ensuring that system ductility is not compromised. Hoop spacing is addressed in Article 8.8.14 of the proposed LRFD SGS and Article 8.13.8.4.4 of the proposed LRFD BCS. A smaller cover than that used for typical column applications is permitted for the top hoop because the placement of the bedding layer concrete or grout will provide additional cover after the precast bent cap is set. Plan sheets and shop drawings are required to show the intended placement of the first hoop at the top of the column.

Figure 3.7. View of column bar buckling at interface between the bent cap and column–CPFD (after removal of concrete post-test).

GD and CPFD specimen tests confirmed the importance of accurate placement of the column top hoop and the unsupported column bar length (*22, 23*). Figure 3.7 shows column bar buckling at the interface between the cap and column for the CPFD specimen (post-test). The unsupported column bar length was considerably larger than the regular column hoop spacing. Although this did not affect the maximum force induced in the joint and the specimen achieved over 4% drift, system ductility was limited by buckling of column longitudinal reinforcement.

The proposed specification addresses this issue as follows:

> The spacing between the first hoop at the top of the column and the bedding layer hoop shall not exceed the spacing used for hoops in the plastic hinge region. The concrete cover above the first hoop at the top of the column shall be permitted to be less than that specified in Article 5.12.3 of the AASHTO LRFD Bridge Design Specifications. Transverse reinforcement used for piles shall be similarly detailed.

3.3 Proposed Changes to AASHTO *Guide Specifications for LRFD Seismic Bridge Design* and AASHTO *LRFD Bridge Design Specifications*

Based on the test results and development of design specifications, proposed design specifications have been prepared and are provided as attachments to this report (available online at www.trb.org/Main/Blurbs/164089.aspx). Proposed additions or revisions to the AASHTO *Guide Specifications for LRFD Seismic Bridge Design, 1st Edition* (*1*), are as follows:

- Attachment DS1: Revised Article 2.1 Definitions
  - Revision of current article to include definitions of emulative and hybrid systems
- Attachment DS2: Revised Article 4.3.3 Displacement Magnification for Short Period Structures
  - Revised Article to account for hybrid systems
- Attachment DS3: Revised Article 4.7.2 Vertical Ground Motion, Design Requirements for SDC D
  - Expanded Article to include explicit requirements for consideration of vertical excitation with integral precast bent caps discontinuous at bent
- Attachment DS4: Revised Article 4.11.6 Analytical Plastic Hinge Length
  - Revised Article to account for integral concrete superstructures
- Attachment DS5: Proposed Article 5.6.6 I_{eff} for Hybrid Systems
  - New Article for hybrid systems
- Attachment DS6: Revised Article 8.4.2 Reinforcing Steel Modeling
  - Revised Article for hybrid systems
- Attachment DS7: Proposed Article 8.8.14 Lateral Reinforcement Requirement for Columns Connecting to a Precast Bent Cap
  - New Article to ensure spacing between the hoop at top of column and the bedding layer hoop does not compromise system ductility
- Attachment DS8: Revised Article 8.5 Plastic Moment Capacity for SDC B, C, and D
  - Revised Article for hybrid systems
- Attachment DS9: Revised Article 8.8.1 Maximum Longitudinal Reinforcement
  - Revised Article for hybrid systems
- Attachment DS10: Revised Article 8.8.2 Minimum Longitudinal Reinforcement
  - Revised Article for hybrid systems
- Attachment DS11: Proposed Article 8.8.14 Minimum Debonded Length of Longitudinal Reinforcement for Hybrid Columns
  - New Article for hybrid systems
- Attachment DS12: Revised Article 8.10 Superstructure Capacity Design for Longitudinal Direction for SDC C and D
  - Revised Article for integral precast systems
- Attachment DS13: Proposed Article 8.13 Joint Design for SDC A
  - New Article for SDC A precast bent cap connection design
- Attachment DS14: Proposed Article 8.14—Joint Design for SDC B
  - New Article for SDC B precast bent cap connection design
- Attachment DS15: Revised Article 8.15—Joint Design for SDCs C and D

  - Revision of current Article 8.13 for SDCs C and D to Article 8.15 for precast bent cap connection design

Other proposed articles for the AASHTO *LRFD Bridge Design Specifications (4th Edition)* are as follows (*29*):

- Attachment DS16: Revised Article 5.10.11.4.3—Column Connections
  - Revised Article to ensure AASHTO LRFD SGS is used for emulative precast bent cap to column connection design.
- Attachment DS17: Proposed Article 5.11.1.2.4—Moment Resisting Joints
  - Revised Article to ensure AASHTO LRFD SGS is used for emulative precast bent cap to column connection design.

3.4 Design Flow Charts and Design Examples

Design flow charts and design examples have been developed for the systems and connections investigated under this project. The design flow charts and design examples illustrate the design process, including proper application of the design specifications, for all SDC levels using precast bent cap to column connections with practical reinforcement and detailing.

Two design flow charts are provided, one for SDC A and another for SDCs B, C, and D. Consolidation of SDCs B, C, and D into one flow chart highlights the fact that the amount and type of joint shear reinforcement are based on the determination of the principal tensile stress and that, even for SDC B, the likelihood of joint shear cracking should be determined. Finally, as required, the effects should be mitigated through the use of joint shear reinforcement.

Design examples are provided for SDC A, SDC B, and SDCs C and D. The examples include extensive commentary and figures and list applicable references to the LRFD SGS and LRFD BCS. The design examples for SDCs C and D illustrate the case in which additional joint shear reinforcement is required (i.e., principal tensile stress, p_t, $0.11\sqrt{f_c'}$ or larger). The SDC B and SDC A examples illustrate the case in which minimum joint reinforcement governs. Special consideration is given to clarity, completeness, and accuracy.

Design flow charts and design examples are provided as attachments to this report (available online at www.trb.org/Main/Blurbs/164089.aspx), as follows:

- Attachment DE1: SDC A Design Flow Chart
  - Flow chart for design of precast bent cap connections in SDC A
- Attachment DE2: SDC A Design Example—Grouted Duct Connection
  - Design example for grouted duct connection in SDC A (minimum joint reinforcement)
- Attachment DE3: SDC A Design Example—Cap Pocket Connection
  - Design example for cap pocket connection in SDC A (minimum joint reinforcement)
- Attachment DE4: SDCs B, C, and D Design Flow Chart
  - Flow chart for design of precast bent cap connections in SDCs B, C, and D
- Attachment DE5: SDC B Design Example—Grouted Duct Connection
  - Design example for grouted duct connection in SDC B (minimum joint reinforcement)
- Attachment DE6: SDC B Design Example—Cap Pocket Connection
  - Design example for cap pocket connection in SDC B (minimum joint reinforcement)
- Attachment DE7: SDCs C and D Design Example—Grouted Duct Connection
  - Design example for grouted duct connection in SDCs C and D (additional joint reinforcement)
- Attachment DE8: SDCs C and D Design Example—Cap Pocket Connection
  - Design example for cap pocket connection in SDCs C and D (additional joint reinforcement)
- Attachment DE9: SDCs C and D Design Example—Hybrid Connection
  - Design example for hybrid connection in SDCs C and D
- Attachment DE10: SDCs C and D Design Example—Integral Connection
  - Design example for integral connection in SDCs C and D

3.5 Development of Construction Specifications

This section provides the basis for proposed Article 8.13.8—Special Requirements for Precast Bent Cap Connections to be added to AASHTO *LRFD Bridge Construction Specifications, 2nd Edition, 2004 with 2006, 2007, 2008, and 2009 Interims* (LRFD BCS) (*35*) to address nonintegral precast bent cap systems using grouted duct and cap pocket connections.

Proposed construction specifications are based on specifications developed by Matsumoto et al. (*8*) together with results from the experimental test results. Major sections of the construction specification address the following:

- Materials
  - portland cement concrete for the precast bent cap and cap pocket fill
  - hydraulic cement (non-shrink) grout

  - corrugated metal duct
  - lock-seam, helical corrugated steel pipe
  - connection hardware
- Contractor submittal including a precast bent cap placement plan
- Construction methods including grouting of grouted duct connections and concreting of cap pocket connections (trial batch, placement, material testing)

In addition, a grout specification for the grouted duct connection from Matsumoto et al. (*8*) is presented.

Most of this section is incorporated within the proposed specification as code and commentary. Proposed specifications are set off from the main text. The following sections use the same outline as that used in the proposed specifications. References to articles within this section refer primarily to existing or proposed Articles of the LRFD BCS.

3.5.1 General

This article addresses construction of precast bent cap connections:

> This article describes special requirements for integral and nonintegral emulative and hybrid precast bent cap connections using the grouted ducts or cap pockets.

These special requirements are intended to ensure precast bent cap connections studied are constructible and also provide the expected seismic performance, durability, and economy.

The grouted duct connection uses corrugated ducts embedded in the precast bent cap to anchor individual column longitudinal bars. The ducts and bedding layer between the cap and column or pile are grouted with high-strength, non-shrink cementitious grout to complete the precast connection. Ducts are sized to provide adequate tolerance for bent cap fabrication and placement and should be accounted for in sizing the bent cap to minimize potential congestion.

The cap pocket connection uses a single, helical, corrugated steel pipe embedded in the precast bent cap to form the cap pocket, which anchors the column longitudinal bars. This pipe, placed between top and bottom bent cap longitudinal reinforcement, serves as both a stay-in-place form and as joint transverse reinforcement. Special forming is required above and below the pipe to form the cap pocket void through the full depth of the bent cap. A flowable CIP concrete is used to fill the void and complete the precast connection. The pipe diameter is sized to provide adequate field tolerance for placement of the precast bent cap over column longitudinal bars, and the pipe thickness is sized to satisfy transverse joint reinforcement requirements.

Hybrid connections use grouted duct connections to anchor column longitudinal reinforcement. Unbonded post-tensioning is also used in the section to resist lateral demands.

The integral connections must provide a stable flexural connection between the superstructure and substructure. These connections can include systems with discontinuous girders at the bent cap made continuous through longitudinal post-tensioning.

In Article 8.13.8, the term "column bars" refers to column bars, column dowels, and pile dowels.

3.5.2 Materials

Materials used for precast bent cap connections include Portland cement concrete for the precast bent cap, connection hardware, and materials specific to each connection type. Grouted duct connection materials include hydraulic cement grout (non-shrink) and corrugated metal ducts. Cap pocket connection materials include Portland cement concrete for the cap pocket fill and the steel (corrugated) pipe. Hybrid connections use grouted duct connections in combination with post-tensioning.

The proposed specification states the following:

> The materials and manufacturing processes used for precast concrete bent caps shall conform to the requirements of Article 8.13.3 except as those requirements are modified or supplemented by the provisions that follow.

Portland Cement Concrete for Precast Bent Cap

Bent cap concrete is required to satisfy provisions for normal-weight Portland cement concrete and provide a strength margin between the cap and the connection. The specified compressive strength of the connection grout or concrete fill is required to exceed the expected bent cap concrete compressive strength by at least 500 psi to help ensure that the connection does not become a weak link in the system:

> Portland cement concrete for the precast bent cap shall conform to the provisions of Article 8.2.2 for normal-weight concrete. The concrete mix design for the precast bent cap shall conform to the requirements of Articles 8.13.8.3.2a and 8.13.8.3.3a to achieve the required 500 psi strength margin between the bent cap compressive strength and the specified compressive strength of the connection grout or cap pocket concrete fill.

Lightweight concrete can provide significant advantages for a precast bent cap system. However, its use should be based on relevant research including research on its effect on the seismic performance of the connection.

Use of lightweight concrete shall be based on applicable research of connection performance, including seismic effects, and approval by the Engineer.

Grouted Duct Connection

Hydraulic Cement Grout (Non-Shrink). Grout for the grouted duct connection is carefully specified:

Grout used in grouted duct connections shall consist of prepackaged, cementitious, non-shrink grout in accordance with ASTM C1107 and the additional performance requirements listed in Table 8.13.8-1, including the following properties: mechanical, compatibility, constructability, and durability. Table 8.13.8-1 requirements shall govern over ASTM C1107 requirements.

Grout shall contain no aluminum powder or gas-generating system that produces hydrogen, carbon dioxide, or oxygen. Grout using metallic formulations shall not be permitted. Grout shall be free of chlorides. No additives or admixtures, including retarders, shall be added to prepackaged grout. Extension of grout shall only be permitted when recommended by the manufacturer and approved by the Engineer.

At a minimum, grout compressive strength and flowability shall be established during trial batches per Article 8.13.8.5.4a. Laboratory testing shall be permitted to establish other properties listed in Table 8.13.8-1.

Grouted joints shall not exceed 3 in. in thickness for structures located in Seismic Design Categories B, C, and D.

Proposed LRFD BCS Table 8.13.8-1 is shown as Table 3.4 of this report. This table includes provisions intended to ensure that the grout used in the connection develops mechanical, compatibility, constructability, and durability properties that help ensure that the grout is placed efficiently, achieves performance for rapid construction, and does not become a weak link in the system under the various limit states. For example, Table 3.4 requires the 28-day grout compressive strength to have a minimum 500-psi margin over the 28-day expected bent cap concrete compressive strength. This margin accounts for the likelihood that the actual concrete strength will exceed its specified strength as well as the possibility of a low grout strength. The 1.25 factor applied to f'_{ce_cap} in Table 3.4 accounts for the higher 2-in grout cube compressive strength compared to standard concrete cylinder compressive strength.

Grout should be selected with a compressive strength based on water required for fluid consistency using the ASTM C939 Flow Cone Test. Grouts mixed to a flowable or plastic consistency in accordance with ASTM C230 achieve a higher compressive strength but possess inadequate fluidity for filling voids in a precast bent cap system and therefore should be avoided.

Prepackaged grouts are proprietary mixes, and thus no additives should be used in the grout. Additives may adversely affect grout properties and void manufacturer warranties.

Modification of prepackaged grout, including extension with small-size aggregate, is discouraged because of the additional uncertainty introduced in achieving the required

Table 3.4. Grout specification for grouted duct connection (*8*).

Property	Value	
Mechanical	Age	Compressive strength (psi)
Compressive strength (ASTM C109, 2" cubes)	1 day 3 days 7 days 28 days	2,500 4,000 5,000 Maximum [6000, 1.25 (f'_{ce_cap}) + 500]
Compatibility		
Expansion requirements (ASTM C827 & ASTM C1090)	Grade B or C—expansion per ASTM C1107	
Modulus of elasticity (ASTM C 469)	$2.8\text{-}5.0\times10^{6}$ psi	
Coefficient of thermal expansion (ASTM C 531)	$3.0\text{-}10.0\times10^{-6}$/deg F	
Constructability		
Flowability (ASTM C939 Flow Cone)	Fluid consistency efflux time: 20–30 sec	
Set Time (ASTM C191)		
Initial	2.5–5.0 hrs	
Final	4.0–8.0 hrs	
Durability		
Freeze Thaw (ASTM C666)	300 cycles, relative durability factor 90%	
Sulfate Resistance (ASTM C1012)	Expansion at 26 weeks < 0.1%	

properties and the potential risk in resolving liability if the quality of grouted connections is believed to be deficient. For example, ASTM C33 No. 8 Hard Pea Gravel or Hard Aggregate Chips may contain excessive fines that adversely affect the flow of the prepackaged grout.

Clear spacing between the reinforcing and the formed surfaces should be at least three times the top size of the aggregate to ensure adequate flow of grout to fill all voids.

Corrugated Metal Duct. Corrugated metal ducts used to anchor column bars within the bent cap are specified as follows:

> The use of ducts in a grouted duct connection shall conform to the requirements of Article 10.8.1 except as those requirements are modified or supplemented by the provisions that follow.
>
> Ducts used to provide holes in the precast bent cap concrete shall be formed with semi-rigid steel ducts that are cast into the concrete. Ducts shall be galvanized ferrous metal per ASTM A653 and shall be fabricated with either welded or interlocked seams. Ducts shall be corrugated with a minimum wall thickness of 26 gage for ducts less than or equal to 4-in diameter and 24 gage for ducts greater than 4-in diameter. Rib height of the corrugation shall be at least 0.12 in.
>
> Plastic ducts shall only be used based on applicable research and when approved by the Engineer.
>
> Duct diameter shall be based on fabrication and placement tolerances established for the job.
>
> Placement and anchorage of ducts shall conform to the requirements of Article 10.4.1.1.

Corrugated galvanized steel ducts for grouted duct connections have been successfully used in seismic and nonseismic research as well as in practice. Steel ducts provide excellent mechanical interlock with the bent cap concrete and connection grout as well as confinement for the grouted column bar. When steel ducts with the minimum specified duct thickness and corrugation rib height are used together with grouts satisfying Table 8.13.8-1, excellent bond develops and column bars can be safely anchored in a grouted duct within the relatively short anchorage length given in Article 8.15.2.2.2 of the 2009 LRFD SGS (*1*).

Use of plastic ducts can have a significant impact on the behavior, failure mode, and strength of grouted duct connections and should not be used without investigation and approval of the Engineer. Brenes et al. (*36*) provide guidelines for use of high-density polyethylene and polypropylene ducts in grouted duct connections, including minimum duct wall thickness, corrugation rib height, and maximum spacing between ribs. An increase in development length of approximately 30% was recommended for plastic ducts tested under monotonic tension. However, tension cyclic tests were not conducted.

Cap Pocket Connection

Portland Cement Concrete for Cap Pocket Fill. Portland cement concrete for the cap pocket fill has additional requirements beyond that of typical normal-weight concrete:

> Portland cement concrete for the cap pocket fill shall follow the provisions of Article 8.2.2 for normal-weight concrete and Article 8.3 for associated materials. The mix design for the concrete fill shall be based on achieving a concrete compressive strength at least 500 psi greater than the expected concrete strength of the precast bent cap.
>
> Lightweight concrete shall not be used.
>
> Concrete shall satisfy Article 8.13.8.5.5a to ensure pocket and bedding layer are completely filled and without voids.

The probable concrete strength for the cap pocket fill is required to provide a minimum 500-psi margin over the expected bent cap concrete compressive strength to ensure that the cap fill concrete is not the weak link in the connection. This margin accounts for the likelihood that the actual bent cap compressive strength will exceed its specified strength as well as the possibility of a low compressive strength of the fill.

Use of lightweight concrete is not permitted in the cap pocket because it may pose an unnecessary risk in the seismic performance of the connection.

Concrete should be sufficiently flowable to fill the pocket and bedding layer and to flow out of air vents at the top of the bedding layer. In addition, clear spacing between the reinforcing and the formed surfaces should be at least three times the top size of the aggregate to ensure adequate flow of concrete to fill all voids, including the bedding layer.

Steel Pipe. The steel pipe, which serves a critical dual purpose in fabrication and seismic reinforcement, is specified as follows:

> The steel pipe used to form the void in the precast bent cap concrete shall be a lock seam, helical corrugated pipe cast into the concrete. The steel pipe shall satisfy the requirements of ASTM A760, Standard Specification for Corrugated Steel Pipe, Metallic-Coated for Sewers and Drains, and the lock seam shall satisfy the requirements of AASHTO T 249, Standard Method of Test for Helical Lock Seam Corrugated Pipe. The pipe shall satisfy the thickness required by Article 8.15.3.2.2 of the AASHTO Guide Specifications for LRFD Seismic Bridge Design. Where required, coupon testing to determine material properties shall be conducted in accordance with ASTM A370.
>
> Plastic pipe shall not be used.
>
> The pipe diameter shall be based on fabrication and placement tolerances established for the job.
>
> Placement and anchorage of steel pipe shall conform to the requirements of Article 10.4.1.1.

Lock seam, helical corrugated steel pipe has been successfully used in seismic research as well as in practice for precast cap pocket connections. These pipes provide excellent mechanical interlock with the bent cap concrete and connection concrete fill and also serve as joint reinforcement. When the steel pipe is designed in accordance with Article 8.15.3.2.2 of the *AASHTO Guide Specifications for LRFD Seismic Bridge Design* and is used together with concrete satisfying Article 8.13.8.3.3a, excellent bond is expected to develop and column bars are expected to be anchored in the pipe within the relatively short anchorage length given in Article 8.15.2.2.2 of the *AASHTO Guide Specifications for LRFD Seismic Bridge Design* (*1*).

Plastic pipe should not be used because it cannot serve as seismic reinforcement.

Connection Hardware. Connection hardware is specified as follows:

> All connection hardware such as friction collars, shims, falsework, or other support systems shall be in accordance with the requirements shown in the plans.

Friction collars and shims may be used to support the cap during placement. When shims are used, compressible shims such as those made of plastic are preferred over steel shims to help ensure that load eventually transfers to the hardened bedding layer grout. Plastic shims should be made of engineered multipolymer, high-strength plastic with a modulus of elasticity slightly less than the hardened grout at the time of load transfer. Steel shims have a stiffness at least five times that of the bedding grout and therefore can act as hard points between the column and bent cap. Calculations should be made to determine the potential effect of shims in the compression zone of the bedding layer. Where steel shims are used, additional cover should be provided for corrosion protection.

Specific measures to prevent movement of shims during cap placement should be detailed in the plan sheets. To facilitate complete grouting of the bedding layer, the total shim plan area should be limited and shims should be placed away from the exposed surface of the bedding layer unless shim removal is planned.

Hybrid Precast Concrete Connections

Hybrid connections constructed with precast components use a combination of column longitudinal reinforcement and unbonded post-tensioning. The connection of column longitudinal reinforcement is traditionally made using a grouted duct connection. The construction specifications for grouted duct connections shall therefore be implemented for these connections. However, experimental testing described in Chapter 2 indicated a need to place fibers within the bedding layer for hybrid precast connections. Therefore, the following article is recommended for hydraulic cement grout in hybrid precast connections:

> Grout used in grouted duct connections in conjunction with hybrid precast connections shall meet the requirements of Article 8.13.8.3.2a. Polypropylene fibers shall be added to the grout matrix during mixing at a 3 lb/cu yd fraction. Fibers shall meet the requirements of ASTM C1116.

Integral Precast Connections with Vertical Joints

The integrity of vertical closure joints in integral precast connections is essential to satisfactory flexural response. To promote joint integrity, a high-quality, non-shrink grout containing fiber reinforcement is necessary. The following article is therefore recommended:

> Grout used in grouted duct connections shall consist of prepackaged, cementitious, non-shrink grout in accordance with ASTM C1107 and the additional performance requirements listed in Table 8.13.8-1, including the following properties: mechanical, compatibility, constructability, and durability. Table 8.13.8-1 requirements shall govern over ASTM C1107 requirements.
>
> Grout shall contain no aluminum powder or gas-generating system that produces hydrogen, carbon dioxide, or oxygen. Grout using metallic formulations shall not be permitted. Grout shall be free of chlorides. No additives or admixtures, including retarders, shall be added to prepackaged grout. Extension of grout shall only be permitted when recommended by the manufacturer and approved by the Engineer.
>
> At a minimum, grout compressive strength and flowability shall be established during trial batches per Article 8.13.8.5.4a. Laboratory testing shall be permitted to establish other properties listed in Table 8.13.8-1.
>
> Polypropylene fibers shall be added to the grout matrix during mixing at a 3 lb/cu yd fraction. Fibers shall meet the requirements of ASTM C1116.
>
> Grouted joints shall not exceed 3 in for structures located in Seismic Design Categories B, C, and D.

3.5.3 Contractor Submittal

As explained in Matsumoto et al. (*8*), the contractor should provide a detailed submittal to ensure successful construction of the precast bent cap connection:

> In advance of the start of precast bent cap placement operations in the field, to allow the Engineer not less than a 30-calendar-day review period, the Contractor shall submit the following documents: (1) Precast Bent Cap Placement Plan per Article 8.13.8.4.2, (2) Design Calculations for Construction Procedures per Article 8.13.8.4.3, and (3) Shop Drawings per Article 8.13.8.4.4.

Bent caps shall not be set until the Engineer has approved all required submittals. Any subsequent deviation from the approved materials and/or details shall not be permitted unless details are submitted by the Contractor and approved by the Engineer in advance of use. Two sets of the Precast Bent Cap Placement Plan, calculations, and required drawings shall be submitted and resubmitted if and as necessary until approved by the Engineer. The specified number of distribution copies shall be furnished after approval.

Precast Bent Cap Placement Plan

The Precast Bent Cap Placement Plan is specified as follows:

The Precast Bent Cap Placement Plan, at a minimum, shall contain the following items:

(a) Step-by-step description of bent cap placement for each bent, including placement of the bent cap on the columns or piles and the proposed method for forming the bedding layer, placing grout in ducts or concrete in cap pockets, and ensuring that grout or concrete is properly consolidated in the connection and bedding layer.

(b) Method and description of hardware used to hold bent cap in position prior to connection grouting or concreting. Hardware shall be permitted to consist of friction collars, plastic or steel shims, shoring, or other support systems. A hardware submittal shall consist of product information, material descriptions, and drawings for friction collars and shims and shop drawings for shoring if used.

(c) For grouted duct connections, manufacturer's product information for at least two candidate grouts, including a description of the performance characteristics as specified in Table 8.13.8-1, mixing requirements, working time, curing requirements, and other information related to grouting of precast connections utilizing ducts. For cap pocket connections, concrete fill mix design, description of the method to achieve concrete consistency for filling the pocket and bedding layer, curing requirements, and other information related to concreting precast connections using a steel pipe should be provided.

(d) Hardware and equipment associated with grouting grouted duct connections or concreting cap pocket connections.

(e) A mitigation plan to repair any voids observed within the bedding layer, coordinated and approved by the Engineer.

(f) Other required submittals shown on the plans or requested by the Engineer relating to successful installation of precast bent caps and associated hardware.

Design Calculations for Construction Procedures

Design calculations related to construction procedures are specified as follows:

Design calculations shall be submitted for friction collars, shims, falsework, erection devices, formwork, or other temporary construction that will be subject to calculated stresses.

Design of the friction collars, shims, and falsework or erection devices for all bent cap concrete, duct grout, or cap pocket concrete shall be completed under the direction of and sealed by a registered Professional Engineer.

Post-tensioned precast bent caps shall also follow the provisions of Article 8.16.3.2.

Shop Drawings

Detailed shop drawings are specified as follows:

The Contractor shall submit detailed shop drawings for approval in accordance with the contract documents. The shop drawings shall follow the provisions of Article 8.16.3.3, with the following additions:

(a) Shop drawings shall completely describe the proposed construction sequence and shall show enough detail to enable construction of the bent cap without the use of the plan sheets.

(b) Size and type of ducts or pipes for all bent cap connections shall be clearly detailed. Duct or pipe supports, tremie tubes, air vents, and drains shall be shown, including size, type, and locations.

(c) Bedding layer reinforcement, as well as its location within the bedding layer and its location relative to the first hoop at the top of the column or pile, shall be shown.

(d) Spacing between the first hoop at the top of the column or pile and the bedding layer hoop shall be shown. This spacing shall not exceed the spacing used for hoops in the plastic hinge region. The concrete cover above the first hoop at the top of the column shall be permitted to be less than that specified in Article 5.12.3 of the *AASHTO LRFD Bridge Design Specifications.*

(e) A table showing elevations and geometry to be used in positioning the bedding layer collar for bent cap placement shall be provided.

(f) For the grouted duct connection, details of grouting equipment, grout mix design, and method of mixing, placing, and curing grout shall be provided.

(g) For the cap pocket connection, details of concrete fill mix design and method of mixing, placing, and curing concrete fill shall be provided.

(h) Other required submittals shown on the plans or requested by the Engineer relating to successful installation of precast bent caps and associated hardware shall be provided.

As discussed in Chapter 2, uniform spacing between hoops at the top of the column and the bedding layer is critical to ensuring that system ductility is not compromised. A smaller cover than that used for typical column applications is permitted for the top hoop because the bedding layer provides additional cover after placement of the precast bent cap. Plan sheets

should show the intended placement of the first hoop at the top of the column. This requirement for design is addressed in the proposed Article 8.8.14 of the *AASHTO Guide Specifications for LRFD Seismic Bridge Design.*

3.5.4 Construction Methods

General

Construction of precast bent cap systems must account for tolerances:

> All tolerances shall be established on a project-specific basis. Combined tolerances shall include, but are not limited to, fabrication of the bent cap and columns or piles and placement of the bent cap over the columns or piles, including location of column bars or other dowels within the corrugated metal ducts or steel pipe.
>
> All form release agents and curing membranes shall be completely removed from areas of the cap that will be in contact with bearing seat and connection grout.

Combined fabrication and placement tolerances should be established for each project. The following issues should be considered: differences in tolerances for longitudinal and transverse directions; accuracy of column bars or dowels within corrugated ducts or steel pipes; size, type, location and orientation of ducts or pipe to account for cap slope; plumbness of column bars or dowels; and provisions for out-of-tolerance substructure elements.

Handling and placement are specified as follows:

> Handling of precast bent caps shall satisfy the provisions of Article 8.16.7.4.
>
> The Contractor is solely responsible for ensuring the stability of the bent cap prior to and during grouting or concreting operations.
>
> All grades, dimensions, and elevations shall be determined and verified before the bent cap is placed. The contractor shall verify proper alignment between the columns or piles, including column bars, dowels, corrugated metal ducts, steel pipes, and other connection hardware cast into the bent cap.
>
> All loose material, dirt, and foreign matter shall be removed from the tops of columns or piles before the cap is set.

Grouting of Grouted Duct Connection

Grouting is a crucial operation for use of a precast bent cap system using the grouted duct connection. Because it involves procedures, operations, and equipment that may not be familiar to the Contractor, specifications provide sufficient detail to ensure that connections are properly made in the field. Specifications address general grouting issues, trial batches, grout placement, and grout testing. Matsumoto et al. (*8*) provide further background and details on these provisions.

General Issues. General issues are specified as follows:

> The preparation and use of grout for precast bent cap connections shall conform to the requirements of Article 10.9 except as those requirements are modified or supplemented by the provisions that follow.
>
> Prepackaged, cementitious, non-shrink grout shall be used in strict accordance with manufacturer's recommendations.
>
> Per Article 8.13.8.3.2a, additives or admixtures, including retarders, shall not be added to grout. However, it shall be permitted to adjust the temperature of mixing water or substitute ice for water to extend the working time and pot life.
>
> Addition of water to previously mixed grout or remixing of grout shall not be permitted. Water exceeding manufacturer's recommendations shall not be added to the grout to increase flowability.

Trial Batch. The trial batch is a key step in achieving the required installation and performance of a grouted duct connection. The purposes of a trial batch are to do the following:

- Determine the required amount of water to be added to a particular grout brand to achieve acceptable flowability per Table 3.4 and pot life under the temperature and humidity conditions expected in the field;
- Determine the grout cube strength corresponding to the flow achieved;
- Examine grout for undesirable properties such as segregation;
- Establish the adequacy of proposed grouting equipment such as the mixer, pump, tremie tubes, and vent tubes;
- Provide jobsite personnel experience in mixing and handling grout prior to actual connection grouting; and
- Help the contractor to make a judicious decision regarding grout brand and its use.

The trial batch is specified as follows:

> At least 2 weeks prior to grouting of connections, a trial batch of grout shall be prepared to demonstrate grout properties per Article 8.13.8.3.2a and adequacy of equipment and to familiarize job site personnel with grouting procedures.
>
> A batch of grout shall be the amount of grout sufficient to complete an entire connection or number of connections and is limited to the amount of grout that can be placed within the pot life determined in the trial batch. For continuous placement using a grout pump, a batch shall be defined as one connection or one bent cap. Partial batches will not be allowed and shall be discarded.
>
> The Contractor shall establish grout flowability by measuring efflux (flow) time of the grout with a standard

flow cone according to the Corps of Engineers Flow Cone Method, CRD-C 611 and ASTM C939. The flow time shall be determined twice: (1) immediately after mixing and (2) at the expected working time corresponding to the pot life of the grout. The ambient temperature and mixing water temperature at the time of trial batch mixing shall be within +/– 5 deg F of that expected at the time of grout placement. The Contractor shall establish that the grout flow time satisfies the limits prescribed in Table 8.13.8-1.

Observation of segregation, clumps of grout, or other anomalies in the final trial batch shall be cause for rejection of the proposed brand of grout. Samples used for testing shall be taken from the middle of the batch.

One set of six (6) grout cubes shall be prepared as specified in Article 8.13.8.5.4c to verify the compressive strengths shown in Table 8.13.8-1.

The Contractor shall validate the proposed grout placement technique by using the trial batch grout and grout equipment in a sample grouting operation similar to the proposed connection grouting. Pumping shall be validated in the trial batch in cases where it is proposed for field placement. Adequacy of the mixer, pump, tremie tubes, vent tubes, and other grouting equipment shall be established. The contractor shall demonstrate that the equipment is adequate for mixing the grout and grouting the connection within the pot life of the batch and does not introduce air into the grout or connection. A wire mesh shall be used to filter out potential clumps when transferring grout between the mixer and containers.

Grout Placement. Grout placement is specified as follows:

All equipment necessary to properly perform grouting operations shall be present before actual grouting operations begin. All grouting operations shall be performed in the presence of the Engineer in accordance with the Precast Bent Cap Placement Plan. Grouting operations shall be performed under the same weather limitations as cast-in-place concrete and as required by the grout manufacturer. Grout pumping shall be required for connections that cannot be completed by other methods within the pot life established for the grout during the trial batch.

All additional materials required to ensure proper connection of bent cap to column, such as but not limited to bedding layer hoops, shall be properly placed according to shop drawings.

All surfaces to be in contact with the grout shall be cleaned of all loose or foreign material that would in any way prevent bond prior to setting bedding layer forms.

Bedding layer forms shall be drawn tight against the existing concrete to avoid leakage or offsets at the joint. All previously hardened concrete surfaces that will be in contact with the grout shall be pre-wetted to a surface-saturated moist condition when the grout is placed. Drain ports or holes shall be provided to allow residual water from pre-wetting to drain prior to grouting. Forms for the closure pour between the cap and column shall be adequately vented to allow air to escape during grouting. Vent tubes shall have a minimum ½-in. inner diameter and shall be flush with the top of the bedding layer. Vents shall not be plugged until a steady stream of grout flows out.

Grout shall be deposited such that all voids in the bedding layer and bent cap are completely filled. Grout shall be consolidated at intervals during placement operations as needed. All connections shall be grouted in a manner that deposits the grout from the bedding layer or bottom of connection upward. When pumping is used, grout shall be placed through ports located at the bottom of the bedding layer. To prevent introducing air into the system, when continuous flow grouting is not possible, shutoff valves shall be required.

All exposed grout surfaces shall be cured in accordance with manufacturer's recommendations.

All grout surfaces shall be inspected post-grouting in coordination with the Engineer. Any voids shall be repaired as specified in the mitigation plan in Article 8.13.8.4.2.

Grout shall not be disturbed and connections shall not be loaded until final acceptance of the connection. Final acceptance of the connection shall be after the grout has reached a compressive strength in accordance with the "Final Strength" shown in the plans or as approved by the Engineer.

Grout Testing. Grout testing is specified as follows:

The compressive strength of the grout for "Beam Setting Strength" and "Final Strength" shall be determined using grout cubes prepared and tested in accordance with ASTM C109. The contractor shall prepare a minimum of six (6) cubes per batch. A Commercial Testing Laboratory approved by the Engineer shall test the specimens for "Beam Setting Strength" and "Final Strength." Grout failing to meet the minimum required compressive strength may be cause for rejection of the connection, grout removal, and re-grouting of the connection by means approved by the Engineer.

Protection of the grout cube specimens in the field is critical and should be performed as required by ASTM C942. Prior to testing, all cubes should be measured for mass determination. The typical break pattern is also to be noted. Curing and ambient temperatures are to be reported as well as flow determinations per ASTM C939.

Concreting of Cap Pocket Connection

Concreting of cap pocket connections addresses similar issues as grouting of the grouted duct connection: trial batch, concrete placement, and concrete testing.

The handling and placing of concrete for the cap pocket fill in precast bent cap connections shall conform to the requirements of Article 8.7 except as those

requirements are modified or supplemented by the provisions that follow.

Trial Batch. The trial batch is a key step in achieving the required installation and performance of a cap pocket connection. The purposes of a trial batch are to do the following:

- Determine the required amount of water and admixtures required to achieve acceptable flowability and pot life under the temperature and humidity conditions expected in the field;
- Determine the corresponding cylinder strength;
- Examine the concrete for undesirable properties;
- Establish the adequacy of proposed concreting equipment such as the mixer, pump, tremie tubes, vibrators, and vent tubes;
- Provide jobsite personnel experience in mixing, placing, and consolidating the concrete in the connection prior to actual connection concreting; and
- Help the contractor to make a judicious decision regarding concrete mix and associated operations.

The trial batch for cap pocket concrete is specified as follows:

> At least 2 weeks prior to concreting of connections, a trial batch of concrete shall be prepared to demonstrate concrete properties per Article 8.13.8.3.3a and adequacy of equipment and to familiarize jobsite personnel with concreting procedures.
>
> A batch of concrete shall be the amount of concrete sufficient to complete an entire connection or number of connections and is limited to the amount of concrete that can be placed within the pot life as determined in the trial batch. For continuous placement using a concrete pump, a batch shall be defined as one connection or one bent cap. Partial batches will not be allowed and shall be discarded.
>
> The Contractor shall establish concrete flowability using AASHTO T 119, Slump of Hydraulic Cement Concrete. The Contractor shall establish that the slump satisfies the requirements of Article 8.13.8.3.3a during all stages of placement of the concrete fill.
>
> Observation of segregation or other anomalies in the final trial batch shall be cause for rejection. Samples used for testing shall be taken from the middle of the batch.
>
> One set of six (6) cylinders shall be prepared and tested in accordance with Article 8.5.7 to verify the compressive strengths required by Article 8.13.8.3.3a.
>
> The Contractor shall validate the proposed concrete placement technique by using the trial batch concrete and concreting equipment in a sample concreting operation similar to the proposed connection concreting. Pumping shall be validated in the trial batch if it is to be used in the field placement. Adequacy of the mixer, pump, tremie tubes, vibrators, vent tubes, and other concreting equipment shall be established. The contractor shall demonstrate that the equipment is adequate for mixing, placing, and consolidating the concrete in the connection within the pot life of the batch and does not introduce air into the connection.

Concrete Placement. Concrete placement in the cap pocket is specified as follows:

> All equipment necessary to properly perform concreting operations shall be present before actual concreting operations begin. All concreting operations shall be performed in the presence of the Engineer in accordance with the Precast Bent Cap Placement Plan. Concreting operations shall be performed under the same weather limitations as cast-in-place concrete. Concrete pumping shall be required for connections that cannot be completed by other methods within the pot life established for the concrete during the trial batch.
>
> All additional materials required to ensure proper connection of bent cap to column, such as but not limited to bedding layer hoops, shall be properly placed according to shop drawings.
>
> All surfaces to be in contact with the cap pocket concrete shall be cleaned of all loose or foreign material that may in any way prevent bond prior to setting bedding layer forms.
>
> Bedding layer forms shall be drawn tight against the existing concrete to avoid leakage or offsets at the joint. All previously hardened concrete surfaces that will be in contact with the cap pocket concrete shall be pre-wetted to a surface-saturated moist condition when the concrete is placed. Drain ports or holes shall be provided to allow residual water from pre-wetting to drain prior to concreting. Forms for the closure pour between the cap and column shall be adequately vented to allow air to escape during concreting. Vent tubes shall be flush with the top of the bedding layer and have an inner diameter adequate for venting air and allowing concrete to flow out. Vents shall not be plugged until a steady stream of concrete flows out.
>
> Concrete shall be deposited such that all voids in the bedding layer and bent cap are completely filled. Concrete shall be deposited through the top opening of the cap pocket in a manner that deposits the concrete from the bedding layer or bottom of connection upward. Concrete in the pocket shall be vibrated in accordance with Article 8.7.3. All exposed cap pocket concrete surfaces shall be cured in accordance with Article 8.11.
>
> All concrete surfaces shall be inspected post-concreting in coordination with the Engineer. Any voids shall be repaired as specified in the mitigation plan in Article 8.13.8.4.2.
>
> Concrete shall not be disturbed and connections shall not be loaded until final acceptance of the connection. Final acceptance of the connection shall be after the cap pocket fill concrete has reached the

"Final Strength" shown in the plans or as approved by the Engineer.

Testing of Cap Pocket Fill Concrete. Testing of the cap pocket fill concrete is specified as follows:

The compressive strength of the concrete for "Beam Setting Strength" and "Final Strength" shall be determined using concrete cylinders prepared and tested in accordance with Article 8.5.7. The contractor shall prepare a minimum of six (6) cylinders per batch. A Commercial Testing Laboratory approved by the Engineer shall test the specimens for "Beam Setting Strength" and "Final Strength." Concrete failing to meet the minimum required compressive strength may be cause for rejection of the connection, concrete removal, and re-concreting of the connection by means approved by the Engineer.

Beam Placement

Placement of beams on the precast bent cap is specified as follows:

The top surface of any precast bent cap anchorage shall be finished and waterproofed as shown in the plans. Lifting loops shall be burned off 1 in below the surface of surrounding concrete and patched using material approved by the Engineer.

Beams shall not be set until the grout for grouted duct connections or concrete for cap pocket connections has reached a compressive strength equal to the "Beam Setting Strength" shown on the plans.

3.5.5 Measurement and Payment

Measurement and payment are specified as follows:

The measurement and payment processes used for precast concrete members shall conform to the requirements of Article 8.17.

3.6 Proposed Changes to AASHTO *LRFD Bridge Construction Specifications*

Based on the work of Matsumoto et al. (*8*) and the results presented in this report, the proposed Article 8.13.8—Special Requirements for Precast Bent Cap Connections for the AASHTO *LRFD Bridge Construction Specifications* (*35*) has been prepared. This construction specification is provided as an attachment to this report.

Major sections of the construction specification address the following:

- Materials
  - portland cement concrete for the precast bent cap and cap pocket fill;
  - hydraulic cement (non-shrink) grout;
  - corrugated metal duct;
  - lock seam, helical corrugated steel pipe;
  - connection hardware;
- Contractor submittal including a Precast Bent Cap Placement Plan; and
- Construction methods including grouting of grouted duct connections and concreting of cap pocket connections (trial batch, placement, and material testing).

In addition, a grout specification for the grouted duct connection from Matsumoto et al. (*8*) is presented.

The proposed addition to the AASHTO *LRFD Bridge Construction Specifications, 2nd Edition,* is as follows (*35*):

- Attachment CS1: Proposed Article 8.13.8—Special Requirements for Precast Bent Cap Connections (AASHTO LRFD Bridge Construction Specifications, 2nd Edition, 2004 with 2005–2009 Interims)
  - New Article that adds specifications for precast bent cap connections.

3.7 Example Connection Details

Based on test results and design and construction specifications, a set of example precast bent cap connection details have been prepared—three for the grouted duct connection (SDC A, SDC B, and SDCs B, C, and D), three for the cap pocket connection (SDC A, SDC B, and SDCs B, C, and D), one for hybrid connection, and one for integral connection. To address the possibility that additional joint shear reinforcement may be required for SDC B, two sets of details are shown for the emulative connections related to SDC B: (1) SDC B: principal tensile stress, p_t, less than $0.11\sqrt{f_c'}$ and (2) SDCs B, C, and D: principal tensile stress, p_t, greater than or equal to $0.11\sqrt{f_c'}$. Details similar to the SDC B example apply for SDCs C and D where additional joint reinforcement is not required.

The following drawings are provided as attachments to this report:

- Attachment ECD1: SDC A—Grouted Duct Connection
  - Example bent cap details for grouted duct connection in SDC A
- Attachment ECD2: SDC A—Cap Pocket Connection
  - Example bent cap details for cap pocket connection in SDC A

- Attachment ECD3: SDC B—Grouted Duct Connection
  - Example bent cap details for grouted duct connection in SDC B (minimum joint reinforcement used)
- Attachment ECD4: SDC B—Cap Pocket Connection
  - Example bent cap details for cap pocket connection in SDC B (minimum joint reinforcement used)
- Attachment ECD5: SDCs B, C, and D—Grouted Duct Connection
  - Example bent cap details for grouted duct connection in SDCs B, C, and D (additional joint reinforcement required)
- Attachment ECD6: SDCs B, C, and D—Cap Pocket Connection
  - Example bent cap details for cap pocket connection in SDCs B, C, and D (additional joint reinforcement required)
- Attachment ECD7: SDCs B, C, and D—Hybrid Connection
  - Example bent cap details for hybrid connection in SDCs B, C, and D
- Attachment ECD8: SDCs B, C, and D—Integral Connection
  - Example bent cap details for integral connection in SDCs B, C, and D

CHAPTER 4

Conclusions

This chapter summarizes all major observations and conclusions from the precast bent cap connection research conducted under NCHRP Project 12-74, including results from the seven bent cap to column connection tests, one girder to bent cap connection test, design specifications including design methodologies, design flow charts and design examples, construction specifications, example connection details, and implementation plan.

4.1 Test Specimens

Based on the observed specimen response and data analysis, the following conclusions can be drawn.

4.1.1 Cast-in-Place (CIP) Control Specimen

- Despite the less conservative design basis used from the *2006 Recommended LRFD Guidelines for the Seismic Design of Highway Bridges* (2006 LRFD RSGS) compared to the 2009 AASHTO *Guide Specifications for LRFD Seismic Bridge Design* (2009 LRFD SGS), including a smaller area of vertical stirrups within the joint and smaller area of bent cap longitudinal reinforcement, the CIP specimen satisfied the performance goal of the design—achieving an extensive drift without appreciable strength degradation and exhibiting extensive plastic hinging of the column, limited joint distress, and essentially elastic behavior of the bent cap (*2, 1*).
- The CIP specimen provided an appropriate benchmark (control) for comparison with the precast grouted duct and cap pocket specimens. In addition, test results can be reliably used as a supporting basis for developing design and construction specifications for seismic precast bent cap systems.

4.1.2 Grouted Duct (GD) Specimen

- Despite the less conservative design used from the 2006 LRFD RSGS compared to the 2009 LRFD SGS—including a smaller area of vertical stirrups within the joint and smaller area of bent cap longitudinal reinforcement—the Grouted Duct (GD) specimen satisfied the performance goal of the design, achieving an extensive drift without appreciable strength degradation and exhibiting extensive plastic hinging of the column, limited joint distress, and essentially elastic behavior of the bent cap (*2, 1*).
- Emulative performance is concluded for the GD specimen based on the close match between its overall behavior and that of the CIP control specimen, including lateral force-displacement response; plastic hinging; joint shear stiffness; level of joint distress; pattern of joint cracking; strain patterns of bent cap and joint reinforcement; integral behavior between the bedding layer, column, ducts, and bent cap; and minor bar slip.
- GD response indicates that design specifications for a full ductility grouted duct connection should address vertical joint stirrups inside and outside the joint, horizontal cross ties inside the joint, transverse joint shear reinforcement, and additional longitudinal bent cap reinforcement.
- Construction specifications should address fabrication and assembly processes as well as grout used for the connection.

4.1.3 Cap Pocket Full Ductility (CPFD) Specimen

- Despite the less conservative design basis used from the 2006 LRFD RSGS compared to the 2009 LRFD SGS—including a smaller area of vertical stirrups within the joint and smaller area of bent cap longitudinal reinforcement—the Cap Pocket Full Ductility (CPFD) specimen satisfied the performance goal of the design, achieving an extensive drift without appreciable strength degradation and exhibiting extensive plastic hinging of the column, limited joint distress, and essentially elastic behavior of the bent cap (*2, 1*).
- Emulative performance is concluded for the CPFD specimen based on the close match between its overall behavior

and that of the CIP control specimen, including lateral force-displacement response; plastic hinging; joint shear stiffness; strain patterns of bent cap longitudinal reinforcement; integral behavior between the bedding layer, column, pipe, and bent cap; and minor bar slip.
- CPFD response indicates that design specifications for a full ductility cap pocket connection should address vertical joint stirrups inside and outside the joint, pipe thickness based on providing the same circumferential hoop force in the joint as that required by transverse reinforcement provisions of Article 8.13.3 of the 2009 LRFD SGS, supplementary hoop at ends of the pipe, and additional longitudinal bent cap reinforcement (*1*).
- Construction specifications should address fabrication and assembly processes as well as concrete within the cap pocket.

4.1.4 Cap Pocket Limited Ductility (CPLD) Specimen

- Despite elimination of the joint reinforcement used in the full ductility specimens (vertical stirrups within the joint, joint-related stirrups and horizontal cross ties external to the joint, and hoops at the ends of the pipe) and reduction of bent cap flexural reinforcement and bent cap transverse reinforcement, the CPLD specimen satisfied the main performance goal of the Seismic Design Category (SDC) B design. The CPLD specimen exhibited ductile plastic hinging and reached an extensive drift of 5.1% (μ8 nominal), well beyond a displacement ductility of 2.0 (μ2), with only minor (12%) load degradation at maximum drift. This is attributed to the effectiveness of the corrugated steel pipe within the joint.
- Extensive joint shear cracking softened the CPLD joint, contributed significantly to column drift, and delayed (but did not prevent) flexural plastic hinging. This response is attributed to the absence of vertical joint stirrups, which permitted unrestrained development, growth, and widening of joint shear cracks. This response was in contrast to the full ductility CIP and CPFD specimens. However, it can be reasonably deduced that similar, or more severe, joint behavior would likely develop for a similarly detailed CIP limited ductility connection because an SDC B CIP joint would incorporate less extensive and less effective transverse reinforcement (based on the limited provisions of current AASHTO *LRFD Bridge Design Specifications*) than that provided by the steel pipe.
- Based on the foregoing conclusions, emulative behavior (relative to a limited ductility CIP connection) can be concluded for the CPLD specimen. Similarities in performance between the limited ductility and full ductility specimens including plastic hinging; lateral force-displacement response; equivalent viscous damping; and integral behavior between the bedding layer, column, pipe, and bent cap support this conclusion.
- Despite the extensive plastic hinging, the development of significant joint shear damage (but not failure) observed for the CPLD specimen does not match the expressed intent of Article 4.7.1 of the 2009 LRFD SGS for limited ductility structures, including the requirement that "Inelastic action is intended to be restricted to flexural plastic hinges in the column (*1*)."
- CPLD response indicates that design specifications for a limited ductility cap pocket connection should incorporate minimum reinforcement requirements to help produce emulative behavior characterized by flexural plastic hinging with limited effects of joint shear cracking: (1) minimum area of vertical joint stirrups and (2) pipe thickness based on providing the same circumferential hoop force in the joint as that required by minimum transverse reinforcement provisions of Article 8.13.3 of the 2009 LRFD SGS (*1*). In addition, where the principal tensile stress, p_t, is greater than or equal to $3.5\sqrt{f_c'}$ psi (or $0.11\sqrt{f_c'}$ ksi), additional joint reinforcement should be required.
- CPLD response also has important implications for CIP design. The following provisions are recommended for inclusion in the LRFD SGS for CIP structures in SDC B (limited ductility) to help produce emulative behavior characterized by flexural plastic hinging with limited effects of joint shear cracking: (1) minimum area of vertical joint stirrups and (2) minimum joint transverse reinforcement based on Article 8.13.3 of 2009 LRFD SGS (*1*). This reinforcement can be determined prescriptively, avoiding extensive seismic analysis, and can result in constructible details. Similar provisions can also be adopted for SDC A.

4.1.5 All Emulative Precast Specimens (GD, CPFD, CPLD)

Additional analysis is required to develop a new model that fully characterizes grouted duct and cap pocket joint behavior including joint forces, pipe effects, crack patterns, pipe effects, and differences in strain distributions between the specimens and the CIP control specimen.

4.1.6 Conventional Hybrid Specimen

- The design methodology used for the conventional hybrid specimen resulted in a system that satisfied performance objectives up to the design level drift. The ultimate lateral deformation capacity was in excess of a 6% drift ratio, with significant reductions in damage and residual offset as compared to CIP and emulative systems.
- Lateral force-displacement predictions based on the procedures presented by Tobolski (*5*) and in the attachments

match well with the recorded system response up to the predicted failure point. The predicted ultimate displacement capacity was conservative in comparison to the actual observed lateral capacity. Predictions indicated that the failure of the system would be attributable to the crushing of the confined concrete core whereas the observed failure mode was fracture of column reinforcement.
- Use of current joint force transfer models as presented in the 2009 LRFD SGS are reasonable and conservative for the design of joints in hybrid bridge column systems with the consideration of column post-tensioning forces (*1*).
- Larger-than-expected column post-tensioning forces were obtained due to a smaller-than-anticipated anchor set loss in the tendons. Based on observed damage and residual offsets, it is recommended that the ratio of the neutral axis depth to column diameter be limited to 0.25 to minimize the level of compressive straining in the column and enhance the self-centering capacity of the system.

4.1.7 Concrete Filled Pipe Hybrid Specimen

- The design methodology used for the concrete filled pipe hybrid specimen resulted in a system that satisfied performance objectives up to approximately the design level drift. The ultimate deformation capacity was approximately equal to a 6% drift ratio, with appreciable reduction in damage and residual displacements as compared to the CIP specimen.
- Lateral force-displacement predictions based on the procedures presented by Tobolski (*5*) and in the attachments match well with the recorded system response up to approximately a 2% drift ratio. After cycles at a 2% drift ratio, damage was observed in the grout bedding layer, ultimately leading to a continual reduction in the lateral capacity until ultimate fracture of a column reinforcing bar. The reduction in capacity is attributable to the progressive damage to the bedding layer, which resulted in a reduction in the effective column diameter at the base.
- Use of current joint force transfer models as presented in the 2009 LRFD SGS are reasonable and conservative for the design of joints in hybrid bridge column systems with the consideration of column post-tensioning forces (*1*).
- Results indicated that the use of fiber-reinforced grout in the bedding layer may enhance overall system performance by maintaining the integrity of the bedding layer and thereby maintaining the column compression toe.

4.1.8 Dual Steel Shell Hybrid Specimen

- The design methodology used for the dual steel shell hybrid specimen resulted in a system that satisfied performance objectives up to approximately the design level drift. The ultimate deformation capacity was approximately equal to a 6% drift ratio, with appreciable reduction in damage and residual displacements as compared to the CIP specimen.
- Lateral force-displacement predictions based on the procedures presented by Tobolski (*5*) and in the attachments match well with the recorded system response up to approximately a 2% drift ratio. After cycles at a 2% drift ratio, damage was observed in the grout bedding layer, ultimately leading to a continual reduction in the lateral capacity until ultimate fracture of a column reinforcing bar. The reduction in capacity is attributable to the progressive damage to the bedding layer, which resulted in a reduction in the effective column diameter at the base.
- Use of current joint force transfer models as presented in the 2009 LRFD SGS are reasonable and conservative for the design of joints in hybrid bridge column systems with the consideration of column post-tensioning forces (*1*).
- Results indicated that the use of fiber-reinforced grout in the bedding layer may enhance overall system performance by maintaining the integrity of the bedding layer and thereby maintaining the column compression toe.

4.1.9 All Hybrid Specimens

The use of fiber-reinforced grout in the bedding layer of hybrid specimens is expected to enhance overall performance by maintaining the integrity of the compression toe during cyclic loading. This is expected to minimize the observed reductions in lateral capacity during larger deformation cycles and enhance the self-centering performance of the systems.

4.1.10 Integral Specimen

- During cycling at essentially elastic service demands, the superstructure responded without any observed reduction in stiffness or slip between the girder and reaction block. Under essentially elastic seismic demands, there was similarly no observed reduction in stiffness or slip indicating that the system is capable of satisfying operational and service level demands in accordance with LRFD code provisions.
- The superstructure connection studied is capable of undergoing rotation demands in excess of 0.01 radians in a safe and reliable manner. Under both positive and negative flexural loading, the flexural capacity was maintained with significant energy dissipation under negative loading due to yielding of deck flexural reinforcement. Under positive flexural loading, deformations were concentrated at the joint with pronounced joint opening.
- At cycles to approximately 0.006 radians, a horizontal crack was observed between the deck and the top of the girder. This crack is attributable to the inadequate anchorage of the girder shear reinforcement provided by traditional 90-deg hooks. It is recommended that headed reinforcement or similarly well-anchored reinforcement is used to minimize

shear slip during flexural joint opening. Although shear slip was observed, the overall resistance of the system did not appear to be adversely affected.
- Predictions of the moment-rotation response based on traditional moment-curvature analysis and an assumed effective hinge length equal to one-half the superstructure depth yielded reasonable predictions for use in design.

4.2 Design Specifications

The conclusions that follow for design specifications of nonintegral emulative grouted duct and cap pocket connections are based on test specimen results and analysis of test results, related research, and existing specifications.

4.2.1 Design Methodology

The current design methodology for CIP joint shear design in the 2009 LRFD SGS for SDCs C and D can be reasonably and conservatively modified for design of integral and nonintegral, emulative, and hybrid precast bent cap grouted duct and cap pocket connections (*1*).

4.2.2 Principal Tensile Stress Calculation

For SDCs C and D, precast bent cap connections should require calculation of the principal tensile stress, p_t, in the joint to establish the need for additional joint shear reinforcement, as required for CIP joints by the 2009 LRFD SGS (*1*). However, to incorporate a reasonable safety margin, design of precast connections should adopt the more conservative provisions identified in the 2009 LRFD SGS (Articles 4.11.1 and C4.11.1) for SDC B (*1*). Therefore, calculation of the principal tensile stress, p_t, for SDC B joints is required to establish the need for additional joint shear reinforcement, as required for SDCs C and D. In addition, where additional joint shear reinforcement is not required (principal tensile stress, p_t, less than $0.11\sqrt{f_c'}$ ksi), minimum transverse joint shear reinforcement (hoops) and joint stirrups are conservatively required to help ensure that joints resist forces in an essentially elastic manner and do not become a weak link in the earthquake resisting system.

4.2.3 Minimum Transverse Joint Shear Reinforcement

- For SDCs B, C, and D, precast bent cap connections should require minimum joint shear reinforcing (transverse hoops), as required for CIP joints in SDCs C and D per the 2009 LRFD SGS (*1*). However, where the principal tensile stress, p_t, is greater than or equal to $0.11\sqrt{f_c'}$ ksi, the larger of the two transverse joint reinforcement equations, 2009 LRFD SGS Eq. 8.13.3-1 and Eq. 8.13.3-2, should be specified for use because the transverse reinforcement requirement of Eq. 8.13.3-2 can become less than that of Eq. 8.13.3-1 in some cases.
- Instead of hoops, cap pocket connections should use a thickness of corrugated steel pipe, t_{pipe}, based on the average joint confining hoop force provided by the transverse reinforcement required per the 2009 LRFD SGS (*1*). The proposed general equation for t_{pipe} results in a reasonable pipe thickness for design. The general equation for t_{pipe} may also be conservatively replaced by the simplified equations provided in the proposed commentary; however, use of the simplified equations can result in a significantly thicker pipe requirement in some cases.
- In SDCs B, C, and D, where the principal tensile stress, p_t, is less than $0.11\sqrt{f_c'}$, minimum transverse joint shear reinforcement should be required.
- For SDC A, minimum transverse joint shear reinforcement should be conservatively required, without calculation of the principal tensile stress.

4.2.4 Integral Bent Caps

The 2009 LRFD SGS has discrepancies between the required joint shear reinforcement for integral bent cap systems in the transverse direction and the required joint shear reinforcement for nonintegral bent caps (*1*). For consistency in design practice, it is recommended that the integral bent cap requirements be updated for consistency. Integral bent caps will require reinforcement along the face of the bent cap based on longitudinal flexural response; however, additional reinforcement based on the 2009 LRFD SGS nonintegral specifications should be required.

4.2.5 Additional Joint Reinforcement for Grouted Duct Connections

Based on the emulative response of the grouted duct specimen, design specifications for grouted duct connections should adopt the 2009 LRFD SGS provisions for additional joint shear reinforcement (A_s^{jvi}, A_s^{jvo}, A_s^{jl}, and horizontal J-bars) used in joint shear design (*1*).

4.2.6 Additional Bent Cap Longitudinal Reinforcement

The 2009 LRFD SGS requirement of an additional area of bent cap longitudinal reinforcement, A_s^{jl}, equal to $0.245A_{st}$, should be required for cap pocket connections but may be excessive for grouted duct (and CIP) connections (*1*). However, this requirement should be conservatively adopted for all precast connections until a potentially lower value is determined through further research.

4.2.7 Additional Vertical Joint Stirrups Outside the Joint

The 2009 LRFD SGS requirement of an additional area of vertical stirrups outside the joint, A_s^{jvo}, equal to $0.175A_{st}$, is conservative for precast bent cap connections and should be adopted (*1*). Future development of a new joint force transfer model may assist in determining whether this requirement is too conservative.

4.2.8 Additional Vertical Joint Stirrups Inside the Joint

The 2009 LRFD SGS requirement of an additional area of vertical stirrups inside the joint, A_s^{jvi}, equal to $0.135A_{st}$, is appropriate for grouted duct connections and should be adopted (*1*). A smaller A_s^{jvi} requirement equal to $0.12A_{st}$ is conservative for cap pocket connections and should be adopted.

4.2.9 Vertical Joint Stirrups Inside the Joint

For cases in which the additional joint shear reinforcement is not required for SDCs B, C, and D (principal tensile stress, p_t, less than $0.11\sqrt{f_c'}$), an area of vertical stirrups inside the joint, A_s^{jvi}, equal to $0.10A_{st}$, is conservative for grouted duct and cap pocket connections and should be adopted. In SDC A, a reduced area of vertical joint stirrups inside the joint, A_s^{jvi}, equal to $0.08A_{st}$, is conservative for grouted duct and cap pocket connections and should be adopted.

4.2.10 Horizontal J-bars Inside the Joint

Horizontal J-bars are not required for cap pocket connections to achieve emulative response. Use of horizontal J-bars is also not practical due to the presence of the pipe and therefore should not be adopted.

4.2.11 Supplementary Hoop for Cap Pocket Connections

Use of a supplementary hoop at each end of the steel corrugated pipe in a cap pocket connection helps limit dilation and potential unraveling and should be adopted.

4.2.12 Anchorage Length of Column Bars

The depth of a precast bent cap should accommodate column bar anchorage. The proposed equations for anchorage length of column bars in grouted duct and cap pocket connections are conservative for all SDCs, require anchorage lengths comparable to the lengths required for CIP connections, and should be adopted, subject to the stated limitations. However, the 2009 LRFD SGS (*1*) anchorage length equation, developed for CIP bent caps in SDCs C and D, and the AASHTO *LRFD Bridge Design Specifications* equation do not apply to precast bent cap connections. Use of plastic ducts in precast bent cap connections should be based on provisions developed in ASTM A929/A929M-01(2007) (*25*) and the owner's approval.

4.2.13 Provisions for Knee Joints

Following the precedent for CIP joints, the proposed design specifications and detailing for precast bent cap connections are limited to interior joints of multicolumn bent caps. Specifications for knee joints in precast bent cap systems should be developed together with CIP knee joint provisions.

4.2.14 Alternative Connection Design and Details for SDC A

For SDC A, when S_{D1} is less than 0.10, alternative precast bent cap connections and specifications may be used, as detailed in Matsumoto et al. (*7*) and ASTM A929/A929M-01(2007) (*25*). However, minimum vertical stirrups in the joint are recommended, as proposed for the seismic precast bent cap connections in SDC A, as well as extension of column longitudinal reinforcement as close as practically possible to the opposite face of the bent cap.

4.2.15 Reinforcement in Bedding Layer and at Column Top

An adequate area and precise placement of transverse reinforcement in the bedding layer and at the column top are required for precast bent cap connections to ensure that the required system ductility is achieved. Specifications should adopt these requirements.

4.2.16 Recommended Modifications to the 2009 LRFD SGS for CIP Joint Design

The following changes to the 2009 LRFD SGS (*1*) are recommended for joint shear design of CIP joints:

- Integral joint design in the transverse direction should be updated for consistency with the provisions for nonintegral systems in the transverse direction. The general mechanism of transverse response in a multicolumn bent cap for both integral and nonintegral bent caps is similar and therefore should adopt the same detailing provisions.
- In SDC B, joint shear (transverse) reinforcement and additional joint shear reinforcement should be based on calculation of principal tensile stress, p_t. This will help produce emulative behavior of limited ductility systems characterized by flexural plastic hinging with limited effects of joint shear cracking.

- Where the principal tensile stress, p_t, is greater than or equal to $0.11\sqrt{f_c'}$, the larger of the two transverse joint reinforcement equations, Eq. 8.13.3-1 and Eq. 8.13.3-2, should be specified for use because the transverse reinforcement requirement of Eq. 8.13.3-2 can become less than that of Eq. 8.13.3-1 in some cases.
- For SDCs B, C, and D, where the principal tensile stress, p_t, is less than $0.11\sqrt{f_c'}$, minimum joint reinforcement consisting of both transverse hoops (per Article 8.13.3 of the 2009 LRFD SGS) as well as an area of vertical stirrups inside the joint, A_s^{jvi}, equal to $0.10A_{st}$, should be used (*1*). Minimum joint reinforcement should also be considered for SDC A. However, requirements for transverse reinforcement in the joint per AASHTO *LRFD Bridge Design Specifications* (Article 5.10.11.3 and related Articles 5.10.11.4.3 and 5.10.11.4.1d) are inadequate and should not be used for SDC B or Seismic Zone 2.
- Specifications for knee joints should be developed.

4.3 Design Flow Charts and Design Examples

Based on application of the proposed specifications to various precast bent cap to column joint configurations, the following conclusions for design flow charts and design examples of nonintegral emulative grouted duct and cap pocket connections can be drawn:

- Design flow charts and design examples developed for all SDC levels demonstrate the practical application of the proposed specifications. These deliverables provide accessibility and are expected to encourage implementation of Accelerated Bridge Construction practices by removing potential hindrances in design. It is expected that designers familiar with current methods of AASHTO LRFD seismic design and joint detailing will be equally comfortable with the proposed specifications.
- Designers should consult the design flow charts before designing a precast bent cap to column connection. Flow charts provide a clear outline of the design path, thereby reducing the possibility of designer confusion or inadvertent omission of applicable specifications.
- Consolidation of SDCs B, C, and D into an integrated flow chart clearly shows the designer the main provisions that can control full and limited ductility design. For example, the flow chart illustrates that a similar design path is followed for SDCs B, C, and D where the principal tensile stress, p_t, is $0.11\sqrt{f_c'}$ or larger. This allows the designer to distinguish the various articles of the design specifications and understand the governing seismic provisions.
- The SDC C and D design examples for the grouted duct and cap pocket connections for which additional joint shear reinforcement is required (principal tensile stress, p_t, greater than or equal to $0.11\sqrt{f_c'}$) demonstrate that design specifications produce full ductility bent cap connections that are constructible and of similar congestion to a CIP design. The grouted duct connection design process is straightforward. The cap pocket connection design example is similarly straightforward and illustrates a noniterative design approach for satisfying the general equation for pipe thickness as well as the greater pipe thickness required when simplified equations from the commentary are used.
- The SDC B design examples for the grouted duct and cap pocket connections for which additional joint shear reinforcement is not required (principal tensile stress, p_t, less than $0.11\sqrt{f_c'}$) demonstrate two points. First, design specifications produce limited ductility bent cap connections that are constructible but more conservative than CIP designs, due to the requirement for minimum joint shear (transverse) reinforcement and minimum stirrups within the joint. The impact of these more conservative provisions on cost and constructability is expected to be negligible, while the potential impact on seismic performance is substantial. Second, the grouted duct and cap pocket connection design processes are straightforward.
- SDC A design examples for grouted duct and cap pocket connections demonstrate that design specifications produce precast bent cap designs that are more conservative than CIP designs, due to the requirement for minimum joint shear (transverse) reinforcement and minimum stirrups within the joint. However, the impact of these more conservative provisions on cost and constructability is considered negligible, while the potential impact on seismic performance is considered important.
- The design example for hybrid bent cap systems provides designers with a simple method to perform the lateral design of these systems, which exhibit different performance characteristics as compared to CIP systems. This design example presents methods for predicting the lateral response as well as associated detailing requirements for hybrid precast bent cap systems.
- The integral design example presented designers with a complete example of the design and detailing requirements for the implementation of the studied integral system in moderate and high seismic regions. Designers familiar with the design of integral bridge systems will be able to adopt the design of this system with relative ease once a widespread understanding of vertical seismic design requirements is obtained. There is an overall need in bridge design in high seismic regions to better understand the demands associated with vertical loading, as no

capacity design procedures can be used in this loading direction.

4.4 Construction Specifications

Based on specifications from Matsumoto et al. (*4*) and test specimen fabrication and assembly, the following conclusions for construction specifications of precast bent cap connections can be drawn:

- Construction specifications are expected to help ensure that precast bent cap connections using precast connections are constructible and also to provide the expected seismic performance, durability, and economy.
- Fabrication of precast bent caps using grouted ducts and cap pockets is feasible and relatively straightforward, facilitated by the use of readily available, stay-in-place corrugated ducts (grouted duct connection) or corrugated steel pipe (cap pocket connection).
- Grouting or concreting of a precast bent cap connection involves procedures, operations, and equipment that may not be familiar to the Contractor, and thus specifications include detailed provisions and commentary to ensure connections are made properly in the field.
- Semi-rigid corrugated metal (steel) ducts specified per ASTM A653 should be adopted, based on excellent anchorage between the column bar, grout, and surrounding concrete in grouted duct connections. Plastic ducts should only be used based on applicable research and when approved by the Engineer.
- Lock seam, helical corrugated steel pipe per ASTM A760, using a pipe thickness that provides equivalent CIP joint hoop reinforcement should be adopted for cap pocket connections. This pipe can effectively be used as a stay-in-place form and seismic joint reinforcement, and can also provide excellent confinement and mechanical interlock, allowing column bars to be anchored within lengths comparable to CIP connections. Plastic pipe should not be used.
- Special forming is required above and below the steel corrugated pipe to form the cap pocket void through the full depth of the precast bent cap.
- Fabrication and placement tolerances should be established on a job-specific basis and be considered in the establishment of duct and pipe diameters.
- Accurate positioning of ducts and column bars may be achieved using templates and/or supplementary reinforcement. Guide pipes may be used to facilitate cap setting.
- Friction collars and shims may be used to support the cap during placement. Compressible shims should be preferred over steel shims, where possible. Compressible shims such as engineered multipolymer high-strength plastic should have a modulus of elasticity slightly less than the hardened grout at the time of load transfer. Shim stacks should be stabilized and prevented from moving during cap setting.
- A minimum 500-psi strength margin between the expected compressive strength of the precast bent cap concrete and the specified compressive strength of the connection material (grout for grouted duct and concrete fill for cap pocket) should be adopted to help ensure that the connection does not become a weak link in the system.
- For seismic applications, the maximum thickness of a grouted bedding layer should be limited to 3 in to maintain the overall integrity. For hybrid bent caps, polypropylene fibers should be included in the grout matrix to maintain the overall integrity of the joint at a 3 lb/cu yd fraction.
- Grout used in vertical joints of integral bridge systems should contain a minimum 3 lb/cu yd fraction of polypropylene fibers to ensure that the essential joint integrity is maintained during loading.
- Although lightweight concrete can provide significant advantages for a precast bent cap system, its use should be based on relevant research, including its effect on the seismic performance of the connection.
- To ensure appropriate mechanical properties, compatibility, constructability, and durability, grout for the grouted duct connection should be specified as shown in proposed Table 8.13.8-1.
- Concrete should be sufficiently flowable to fill the pocket and bedding layer and to flow out of air vents at the top of the bedding layer.
- To accommodate fabrication and placement tolerances as well as grouting or concreting operations, a bedding layer with transverse reinforcement should be used between the column top and bent cap soffit. Clear spacing between the transverse reinforcement and the formed surfaces should be at least three times the top size of the aggregate, to ensure adequate flow of grout to fill all voids. In addition, bedding layers greater than 3 in should be reinforced based on provisions established by the owner.
- Uniform spacing between hoops at the top of the column and the bedding layer is critical to ensure that the system ductility is not compromised. Shop drawings should show the intended placement of the first hoop at the top of the column as well as the bedding layer reinforcement.
- Contractors should submit a Precast Bent Cap Placement Plan, including (1) a description of bent cap placement, (2) a description of the hardware and method used to hold the bent cap in position, (3) product information for candidate grouts or concrete mixes, (4) a description of hardware and equipment for grouting or concreting, and (5) the mitigation plan to repair any voids.
- Contractors should submit detailed shop drawings, including (1) the proposed construction sequence; (2) the size and type of ducts or pipes, supports, tremie tubes, air vents, and

drains; (3) bedding layer reinforcement and its location relative to the first hoop at the top of the column; (4) the elevations and geometry for positioning the bedding layer collar for bent cap placement; and (5) the details of grouting or concreting equipment and mix design and the method of mixing, placing, and curing.
- The trial batch is a key step in achieving the required installation and performance of connection material—grout for grouted duct and concrete fill for cap pocket—and should be specified to (1) determine the required amount of water to be added to achieve acceptable flowability and pot life under expected field conditions, (2) determine the associated compressive strength, (3) examine the material for undesirable properties, (4) establish the adequacy of proposed equipment, (5) provide jobsite personnel experience in mixing and handling the connection material prior to actual operations (grouting or concreting), and (6) help the contractor to make a judicious decision regarding selection of connection material (grout brand or concrete mix).
- Placement of the grout and concrete fill is a critical step in construction of precast bent cap connections and should be conducted as detailed in the proposed specifications.

4.5 Example Connection Details

Based on the development of example connection details for precast bent cap connections in SDCs A through D, the following conclusions can be drawn:

- Example precast bent cap connection details provide clear illustrations and sufficient detail and notes for a thorough understanding of key features of grouted duct and cap pocket connections.
- Precast bent cap connection details are expected to be constructible.
- Precast bent cap connections incorporate certain details not found in CIP connections that require attention:
  - Use of a reinforced bedding layer.
  - Accurate placement and spacing of the hoop at the top of the column and within the bedding layer.
  - Minimum joint shear (transverse) reinforcement for all SDC levels.
  - Vertical stirrups inside the joint for all SDC levels.
  - Cap pocket connections: stay-in-place, partial-depth steel pipe serving as joint shear (transverse) reinforcement; concrete fill in cap pocket void and bedding layer; 2-leg vertical stirrups without overlapping within the joint; supplementary hoop for full ductility; column bar anchorage nearly full depth; and optional U-bars for full ductility.
  - Grouted duct connections: stay-in-place, full-depth steel corrugated ducts; grout in grouted ducts and bedding layer; and column bar anchorage nearly full depth.

4.6 Implementation Plan

Based on the development of an Implementation Plan, the following conclusions can be drawn:

- The Implementation Plan provides an effective roadmap for implementing NCHRP Project 12-74 research products.
- All steps of the Implementation Plan should be closely followed through the appropriate channels to ensure that the NCHRP Project 12-74 research products are implemented in a timely and comprehensive manner.
- The extent of Research Team participation depends on future funding.

References

1. AASHTO. *Guide Specifications for LRFD Seismic Bridge Design (1st Edition).* Washington, DC: American Association of State Highway and Transportation Officials, 2009. (2009 LRFD SGS).
2. Imbsen, R. A. *Recommended LRFD Guidelines for the Seismic Design of Highway Bridges, 2006, Task 193.* Rancho Cordova, CA: TRC/Imbsen & Associates, Inc., 2006. (2006 LRFD RSGS).
3. AASHTO. *LRFD Bridge Design Specifications (5th Edition).* Washington, DC: American Association of State Highway and Transportation Officials, 2010.
4. ———. *LRFD Bridge Construction Specifications (3rd Edition).* Washington, DC: American Association of State Highway and Transportation Officials, 2010.
5. Tobolski, M. J. *Improving the Design and Performance of Concrete Bridges in Seismic Regions.* La Jolla, CA: University of California, San Diego, 2010. PhD Thesis.
6. Ralls, M. L., et al. Current U.S. Practice and Issues. *Proceedings of FHWA/AASHTO Second National Prefabricated Bridge Elements & Systems Workshop.* September 8–10, 2004.
7. Matsumoto, E. E., et al. Development of a Precast Concrete Bent-Cap System. *PCI Journal.* 2008, Vol. 53, 3, pp. 74–99.
8. Matsumoto, E. E., et al. *Development of a Precast Bent Cap System.* Austin, TX: Center for Transportation Research, The University of Texas at Austin, 2001, p. 372, Research Report 1748-2.
9. Mislinski, S. *Anchorage of Grouted Connectors for a Precast Bent Cap System in Seismic Regions (Part 2).* Sacramento, CA: California State University, Sacramento, 2003. p. 91, MS Thesis.
10. Tobolski, M. J., et al. *Development of Precast Bent Cap Concepts.* La Jolla, CA: University of California, San Diego, 2006. p. 176, SSRP Report No. 06/10.
11. Park, R. and Paulay, T. Strength and Ductility of Concrete Substructures of Bridges. *RRU Bulletin.* 1990, Vol. 84.
12. Asnaashari, A., Grafton, J. and Johnnie, M. Precast Concrete Design-Construction of San Mateo-Hayward Bridge Widening Project. *PCI Journal.* 2005, Vol. 50, 1, pp. 26–43.
13. Hines, E. M., Restrepo, J. I. and Seible, F. Force-Displacement Characterization of Well-Confined Bridge Piers. *ACI Structural Journal.* 2004, Vol. 101, 4, pp. 537–548.
14. Priestley, M. J. N. and Tao, J. R. T. Seismic Response of Precast Prestressed Concrete Frames with Partially Debonded Tendons. *PCI Journal.* 1993, Vol. 38, 1, pp. 58–69.
15. Matsumoto, E. E., et al. *Proposed Bridge Design Calculations and Drawings of the Prototype Bridge and Test Specimen.* s.l.: Submitted by J. I. Restrepo and E. E. Matsumoto to NCHRP, 2006. p. 232.
16. AASHTO. *LRFD Bridge Design Specifications (3rd Edition with 2006 Interims).* Washington, DC: American Association of State Highway and Transportation Officials, 2004. (2006 LRFD BDS).
17. Imbsen, R. A. Proposed AASHTO Guide Specifications for LRFD Seismic Bridge Design. [Online] March 22, 2007. (2007 LRFD PSGS). http://www.sciop.net/sites/bridges/docs/2007-03-09GuideSpec.pdf.
18. TRC/Imbsen Software Systems. *SEISAB User's Manual.* Ranco Cordova, CA: s.n., 2006.
19. Sayed-Mahan, M. *User's Manual for WFprep and WFrame, 2-D Push Analysis of Bridge Bents and Frames.* Sacramento, CA: California Department of Transportation, 1995.
20. ———. *User's Manual for XSection, Cross Section Analysis Program.* Sacramento, CA: California Department of Transportation, 1998.
21. Matsumoto, E. E. *Emulative Precast Bent Cap Connections for Seismic Regions: Component Tests-Cast-in-place Specimen (Unit 1).* Sacramento, CA: California State University, 2009. p. 99, ECS Report No. ECS-CSUS-2009-01.
22. ———. *Emulative Precast Bent Cap Connections for Seismic Regions: Component Test Report-Grouted Duct Specimen (Unit 2).* Sacramento, CA: California State University, Sacramento, 2009. p. 114.
23. ———. *Emulative Precast Bent Cap Connections for Seismic Regions: Component Tests-Cap Pocket Full Ductility Specimen (Unit 3).* Sacramento, CA: California State University, 2009. p. 126, ECS-CSUS-2009-03.
24. ASTM. *Standard Specification for Corrugated Steel Pipe, Metallic-Coated for Sewers and Drains, AASHTO Standard Specifications for Transportation Materials and Methods of Sampling and Testing.* Philadelphia, PA: American Society for Testing and Materials, 2009. ASTM Designation A760/A760-M-09.
25. ———. *Standard Specification for Steel Sheet, Metallic-Coated by the Hot-Dip Process for Corrugated Steel Pipe.* Philadelphia, PA: American Society for Testing and Materials, 2007. ASTM Designation A 929/A929M-01.
26. Matsumoto, E. E. *Emulative Precast Bent Cap Connections for Seismic Regions: Component Test Report-Cap Pocket Limited Ductility Specimen (Unit 4).* Sacramento, CA: California State University, Sacramento, 2009. p. 149.
27. ASTM. *Standard Test Method for Flow of Grout for Preplaced-Aggregate Concrete (Flow Cone Method).* Philadelphia, PA: American Society for Testing and Materials, 2006. ASTM Designation C 939-02.
28. Sritharan, S., Priestley, M. J. N. and Seible, F. *Seismic Response of Column/Cap Beam Tee Connections with Cap Beam Prestressing.* La

Jolla, CA: University of California, San Diego, 1996. p. 296, SSRP Report No. 96/09.
29. AASHTO. *LRFD Bridge Design Specifications (4th Edition with 2008 and 2009 Interims).* Washington, DC: American Association of State Highway and Transportation Officials, 2007.
30. Matsumoto, E. E. *Emulative Precast Bent Cap Connections for Seismic Regions: Grouted Duct and Cap Pocket Test Results, Design and Construction Specifications, Design Examples, and Connection Details.* Sacramento, CA: California State University, Sacramento, 2009. p. 749, ECS Report No. ECS-CSUS-2009-05.
31. Mander, J. B., Priestley, M. J. N and Park, R. Theoretical Stress-Strain Model for Confined Concrete. *ASCE Journal of Structural Engineering.* 1988, Vol. 114, 8, pp. 1804–1826.
32. Carr, A. J. *RUAUMOKO—Users Manual.* Christchurch, New Zealand: University of Canterbury, 2004.
33. Mukherjee, S. and Gupta, V. K. Wavelet-based Generation of Spectrum-Compatible Time Histories. *Soil Dynamics and Earthquake Engineering.* 2002, Vol. 22, pp. 799–804.
34. Newmark, N. M. A Method of Computation for Structural Dynamics. *ASCE Journal of the Engineering Mechanics Division.* 1959, Vol. 85, pp. 67–94.
35. AASHTO. *LRFD Bridge Construction Specifications (2nd Edition with 2006, 2007, 2008 and 2009 Interims).* Washington, DC: American Association of State Highway and Transportation Officials, 2004. (LRFD BCS).
36. Brenes, F. J., Wood, S. L. and Kreger, M. E. *Anchorage Requirements for Grouted Vertical-Duct Connectors in Precast Bent Cap Systems.* Austin, TX: Center for Transportation Research, The University of Texas at Austin, 2006. p. 252, FHWA/TxDOT Research Report No. FHWA/TX-06-0-4176-1.
37. Steuk, K. P., Eberhard, M. O. and Stanton, J. F. Anchorage of Large-Diameter Reinforcing Bars in Ducts. *ACI Structural Journal.* 2009, Vols. July–August, pp. 506–513.
38. Sritharan, S. Improved Seismic Design Procedure for Concrete Bridge Joints. *ASCE Journal of Structural Engineering.* 2005, Vol. 131, 9, pp. 1334–1344.

Unpublished Material

Attachments to the contractor's final report for NCHRP Project 12-74 are not published herein but are available online at www.trb.org/Main/Blurbs/164089.aspx. A list of attachments is provided below.

Design Specifications

- Attachment DS1: Revised Article 2.1 Definitions
  - Revision of current article to include definitions of emulative and hybrid systems
- Attachment DS2: Revised Article 4.3.3 Displacement Magnification for Short Period Structures
  - Revised Article to account for hybrid systems
- Attachment DS3: Revised Article 4.7.2 Vertical Ground Motion, Design Requirements for SDC D
  - Expanded Article to include explicit requirements for consideration of vertical excitation with integral precast bent caps discontinuous at bent
- Attachment DS4: Revised Article 4.11.6 Analytical Plastic Hinge Length
  - Revised Article to account for integral concrete superstructures
- Attachment DS5: Proposed Article 5.6.6 Ieff for Hybrid Systems
  - New Article for hybrid systems
- Attachment DS6: Revised Article 8.4.2 Reinforcing Steel Modeling
  - Revised Article for hybrid systems
- Attachment DS7: Proposed Article 8.8.14 Lateral Reinforcement Requirement for Columns Connecting to a Precast Bent Cap
  - New Article to ensure spacing between the hoop at top of column and the bedding layer hoop does not compromise system ductility
- Attachment DS8: Revised Article 8.5 Plastic Moment Capacity for SDC B, C, and D
  - Revised Article for hybrid systems
- Attachment DS9: Revised Article 8.8.1 Maximum Longitudinal Reinforcement
  - Revised Article for hybrid systems
- Attachment DS10: Revised Article 8.8.2 Minimum Longitudinal Reinforcement
  - Revised Article for hybrid systems
- Attachment DS11: Proposed Article 8.8.14 Minimum Debonded Length of Longitudinal Reinforcement for Hybrid Columns
  - New Article for hybrid systems
- Attachment DS12: Revised Article 8.10 Superstructure Capacity Design for Longitudinal Direction for SDC C and D
  - Revised Article for integral precast systems
- Attachment DS13: Proposed Article 8.13 Joint Design for SDC A
  - New Article for SDC A precast bent cap connection design
- Attachment DS14: Proposed Article 8.14—Joint Design for SDC B
  - New Article for SDC B precast bent cap connection design
- Attachment DS15: Revised Article 8.15—Joint Design for SDCs C and D
  - Revision of current Article 8.13 for SDCs C and D to Article 8.15 for precast bent cap connection design
- Attachment DS16: Revised Article 5.10.11.4.3—Column Connections
  - Revised Article to ensure AASHTO LRFD SGS is used for emulative precast bent cap-to-column connection design
- Attachment DS17: Proposed Article 5.11.1.2.4—Moment Resisting Joints
  - Revised Article to ensure AASHTO LRFD SGS is used for emulative precast bent cap-to-column connection design

Design Examples

- Attachment DE1: SDC A Design Flow Chart
  - Flow chart for design of precast bent cap connections in SDC A

- Attachment DE2: SDC A Design Example—Grouted Duct Connection
  - Design example for grouted duct connection in SDC A (minimum joint reinforcement)
- Attachment DE3: SDC A Design Example—Cap Pocket Connection
  - Design example for cap pocket connection in SDC A (minimum joint reinforcement)
- Attachment DE4: SDCs B, C, and D Design Flow Chart
  - Flow chart for design of precast bent cap connections in SDCs B, C, and D
- Attachment DE5: SDC B Design Example—Grouted Duct Connection
  - Design example for grouted duct connection in SDC B (minimum joint reinforcement)
- Attachment DE6: SDC B Design Example—Cap Pocket Connection
  - Design example for cap pocket connection in SDC B (minimum joint reinforcement)
- Attachment DE7: SDCs C and D Design Example—Grouted Duct Connection
  - Design example for grouted duct connection in SDCs C and D (additional joint reinforcement)
- Attachment DE8: SDCs C and D Design Example—Cap Pocket Connection
  - Design example for cap pocket connection in SDCs C and D (additional joint reinforcement)
- Attachment DE9: SDCs C and D Design Example—Hybrid Connection
  - Design example for hybrid connection in SDCs C and D
- Attachment DE10: SDCs C and D Design Example—Integral Connection
  - Design example for integral connection in SDCs C and D

Construction Specifications

- Attachment CS1: Proposed Article 8.13.8—Special Requirements for Precast Bent Cap Connections (AASHTO LRFD Bridge Construction Specifications, 2nd Edition, 2004 with 2005–2009 Interims)
  - New Article that adds specifications for precast bent cap connections

Example Connection Details

- Attachment ECD1: SDC A—Grouted Duct Connection
  - Example bent cap details for grouted duct connection in SDC A
- Attachment ECD2: SDC A—Cap Pocket Connection
  - Example bent cap details for cap pocket connection in SDC A
- Attachment ECD3: SDC B—Grouted Duct Connection
  - Example bent cap details for grouted duct connection in SDC B (minimum joint reinforcement used)
- Attachment ECD4: SDC B—Cap Pocket Connection
  - Example bent cap details for cap pocket connection in SDC B (minimum joint reinforcement used)
- Attachment ECD5: SDCs B, C and D—Grouted Duct Connection
  - Example bent cap details for grouted duct connection in SDCs B, C, and D (additional joint reinforcement required)
- Attachment ECD6: SDCs B, C and D—Cap Pocket Connection
  - Example bent cap details for cap pocket connection in SDCs B, C, and D (additional joint reinforcement required)
- Attachment ECD7: SDCs B, C and D—Hybrid Connection
  - Example bent cap details for hybrid connection in SDCs B, C, and D
- Attachment ECD8: SDCs B, C and D—Integral Connection
  - Example bent cap details for integral connection in SDCs B, C, and D

Specimen Drawings

- Attachment SD1: Nonintegral Prototype Drawings
  - Design drawings for nonintegral prototype structure
- Attachment SD2: Cast-in-place Specimen Drawings
  - Design drawings for cast-in-place specimen
- Attachment SD3: Grouted Duct Specimen Drawings
  - Design drawings for grouted duct specimen
- Attachment SD4: Cap Pocket Full Ductility Specimen Drawings
  - Design drawings for cap pocket full ductility specimen
- Attachment SD5: Cap Pocket Limited Ductility Specimen Drawings
  - Design drawings for cap pocket limited ductility specimen
- Attachment SD6: Conventional Hybrid Specimen Drawings
  - Design drawings for conventional hybrid specimen
- Attachment SD7: Concrete Filled Pipe Hybrid Specimen Drawings
  - Design drawings for concrete filled pipe hybrid specimen
- Attachment SD8: Dual Steel Shell Hybrid Specimen Drawings
  - Design drawings for dual steel shell hybrid specimen
- Attachment SD9: Integral Specimen Drawings
  - Design drawings for integral hybrid specimen

Test Reports

- Attachment TR1: Cast-in-place Specimen Test Report
  - Final report for experimental results from cast-in-place specimen

- Attachment TR2: Grouted Duct Specimen Test Report
  - Final report for experimental results from grouted duct specimen
- Attachment TR3: Cap Pocket Full Ductility Specimen Test Report
  - Final report for experimental results from cap pocket full ductility specimen
- Attachment TR4: Cap Pocket Limited Ductility Specimen Test Report
  - Final report for experimental results from cap pocket limited ductility specimen
- Attachment TR5: Hybrid Specimens Test Report
  - Final report for experimental results from hybrid specimens
- Attachment TR6: Integral Specimen Test Report
  - Final report for experimental results from integral specimen

Corrugated Pipe Thickness

- Attachment CPT1: Cap Pocket Corrugated Pipe Thickness Derivation
  - Derivation of required pipe thickness and design parameters

Implementation Plan

- Attachment IP1: NCHRP 12-74 Implementation Plan
  - New article presented recommended implementation plan to facilitate application of research results

Abbreviations and acronyms used without definitions in TRB publications:

AAAE	American Association of Airport Executives
AASHO	American Association of State Highway Officials
AASHTO	American Association of State Highway and Transportation Officials
ACI–NA	Airports Council International–North America
ACRP	Airport Cooperative Research Program
ADA	Americans with Disabilities Act
APTA	American Public Transportation Association
ASCE	American Society of Civil Engineers
ASME	American Society of Mechanical Engineers
ASTM	American Society for Testing and Materials
ATA	Air Transport Association
ATA	American Trucking Associations
CTAA	Community Transportation Association of America
CTBSSP	Commercial Truck and Bus Safety Synthesis Program
DHS	Department of Homeland Security
DOE	Department of Energy
EPA	Environmental Protection Agency
FAA	Federal Aviation Administration
FHWA	Federal Highway Administration
FMCSA	Federal Motor Carrier Safety Administration
FRA	Federal Railroad Administration
FTA	Federal Transit Administration
HMCRP	Hazardous Materials Cooperative Research Program
IEEE	Institute of Electrical and Electronics Engineers
ISTEA	Intermodal Surface Transportation Efficiency Act of 1991
ITE	Institute of Transportation Engineers
NASA	National Aeronautics and Space Administration
NASAO	National Association of State Aviation Officials
NCFRP	National Cooperative Freight Research Program
NCHRP	National Cooperative Highway Research Program
NHTSA	National Highway Traffic Safety Administration
NTSB	National Transportation Safety Board
PHMSA	Pipeline and Hazardous Materials Safety Administration
RITA	Research and Innovative Technology Administration
SAE	Society of Automotive Engineers
SAFETEA-LU	Safe, Accountable, Flexible, Efficient Transportation Equity Act: A Legacy for Users (2005)
TCRP	Transit Cooperative Research Program
TEA-21	Transportation Equity Act for the 21st Century (1998)
TRB	Transportation Research Board
TSA	Transportation Security Administration
U.S.DOT	United States Department of Transportation